Journal of Immunology Research

Role of Regulatory T-cells in Human Diseases: From Pathogenesis to Therapeutics

Lead Guest Editor: Mitesh Dwivedi
Guest Editors: E. Helen Kemp and Rasheedunnisa Begum

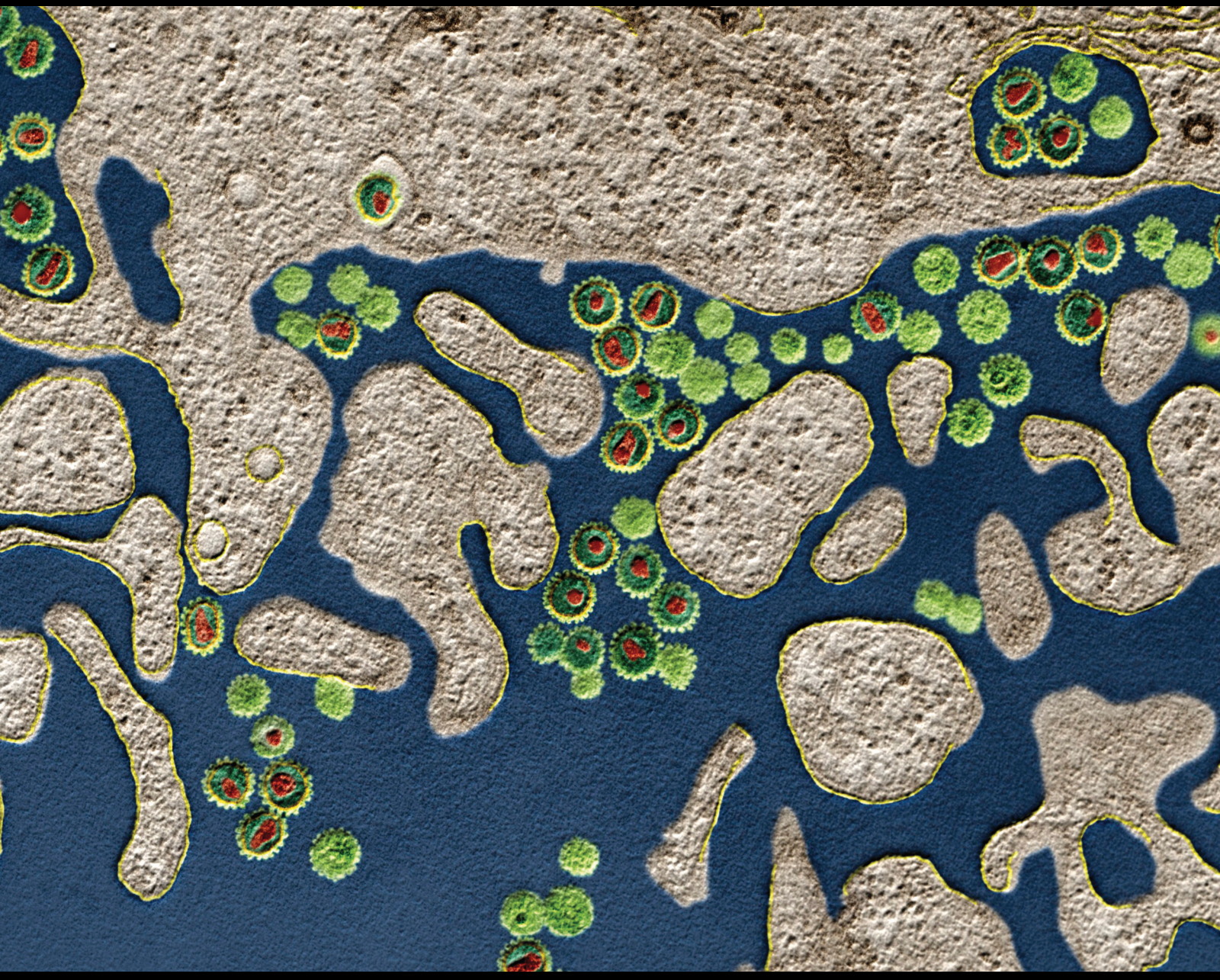

Role of Regulatory T-cells in Human Diseases: From Pathogenesis to Therapeutics

Journal of Immunology Research

Role of Regulatory T-cells in Human Diseases: From Pathogenesis to Therapeutics

Lead Guest Editor: Mitesh Dwivedi
Guest Editors: E. Helen Kemp and Rasheedunnisa Begum

Contents

Hindawi
Journal of Immunology Research
Volume 2022, Article ID 6952299, 16 pages
https://doi.org/10.1155/2022/6952299

Review Article

Meta-Analysis of Alterations in Regulatory T Cells' Frequency and Suppressive Capacity in Patients with Vitiligo

Prashant S. Giri, Jahanvi Mistry, and Mitesh Dwivedi

C. G. Bhakta Institute of Biotechnology, Faculty of Science, Uka Tarsadia University, Bardoli, Surat, 394 350 Gujarat, India

Correspondence should be addressed to Mitesh Dwivedi; mitesh_dwivedi@yahoo.com

Received 1 July 2022; Revised 6 August 2022; Accepted 18 August 2022; Published 16 September 2022

Academic Editor: Vladimir Jurisic

Vitiligo is a noncontagious autoimmune skin depigmenting disease. Regulatory T cells (Tregs) play a key role in maintaining peripheral tolerance; however, Tregs' number, suppressive function, and associated suppressive molecules (FOXP3, IL-10, and TGF-β) are found to be reduced in vitiligo patients. Although, the role of Tregs in vitiligo pathogenesis is well established, there are several contrary findings which suggest a controversial role of Tregs in vitiligo. Therefore, to clarify the role of Tregs in vitiligo pathogenesis, we aimed to study Tregs' frequency, suppressive capacity, and associated suppressive molecules (FOXP3, IL-10, and TGF-β) in vitiligo patients through meta-analysis approach. A total of 30 studies involving 1223 vitiligo patients and 1109 controls were included in the study. Pooled results from our meta-analysis suggested significantly reduced Treg cells' frequency in vitiligo patients ($p = 0.002$). Interestingly, Tregs' suppressive capacity was also significantly reduced in vitiligo patients ($p = 0.0002$); specifically, Treg-mediated suppression of $CD8^+$T cells was impaired in vitiligo patients ($p < 0.00001$). Moreover, FOXP3, a key Tregs' transcription factor, was significantly reduced in blood and skin of vitiligo patients ($p < 0.00001$). Intriguingly, the FOXP3 expression was significantly reduced in the lesional skin as compared to perilesional and nonlesional skin ($p = 0.007$ and $p = 0.04$). Furthermore, the expression of key Treg-associated suppressive cytokines IL-10 and TGF-β were significantly reduced in vitiligo patients ($p = 0.0005$ and $p = 0.01$). The disease activity-based analysis suggested for reduced Tregs' frequency and FOXP3 expression in active vitiligo patients ($p = 0.05$ and $p = 0.01$). We also studied the effect of microRNA-based treatment, narrow band–UVB phototherapy, and Treg-associated treatments on Tregs' frequency, FOXP3, and IL-10 expression. Interestingly, we found increased Tregs' frequency, FOXP3, and IL-10 expression after the treatment ($p = 0.007$, $p < 0.0001$, and $p = 0.002$). Overall, our meta-analysis suggests that the Tregs play a crucial role in pathogenesis and progression of vitiligo, and hence, Treg-based therapeutic interventions could be effective in vitiligo patients.

1. Introduction

Vitiligo is a skin depigmenting disease, characterized by the loss of pigment-producing cells, melanocytes, resulting in the production of white scaly lesion on the skin's peripheral layer [1]. Its prevalence is about 0.5-2% worldwide [1, 2]. Currently, there is no effective treatment for vitiligo [3]. The pathophysiology of vitiligo is complicated and involves genetic, environment, oxidative stress, and autoimmunity factors [4–7]. Candidate gene studies highlight the role of autoimmunity in vitiligo, as polymorphisms in *IL1B*, *IL4*, *PSMB8*, *NLRP1*, *NPY*, *FOXP3*, and *IFNG* genes were found to be associated with vitiligo [8–13].

Previous studies have shown the involvement of self-reactive $CD8^+$ T cells, in the destruction of melanocytes [6, 14, 15]. Regulatory T cells (Tregs) control such autoimmune response [16]; however, vitiligo patients exhibited a reduced number of Treg cells [8, 14, 17–21] and decreased Treg cell suppressive function [21, 22]. Forkhead box P3 (FOXP3) is a key transcription factor of Tregs; it regulates the production of Tregs' suppressive molecules such as TGF-β, CTLA-4, IL-10, and GITR [23]. However, FOXP3

expression has been found to be altered in vitiligo patients [5, 9, 17–20, 22, 24–26]. Additionally, IL-10 and TGF-β, the key immunosuppressive cytokines produced by Tregs, govern the development of iTreg cells and participate in peripheral tolerance preservation and peripheral Treg cell maintenance [27]. However, IL-10 [5, 21, 22, 28–30] and TGF-β [5, 20–22, 28, 29, 31, 32] have also been reduced in vitiligo patients.

Although the previous studies strongly suggest the key role of Treg cells in vitiligo pathogenesis [8, 14, 17–21], the role of Tregs in vitiligo patients' peripheral immunological tolerance is still being contested, as few findings suggest increased or unaltered Treg cells' frequency [33–35], Tregs' suppressive function [14], FOXP3 [14, 33], and TGF-β [24, 36, 37] expression in vitiligo patients. Therefore, to overcome such contradiction, our current meta-analysis assessed the role of Treg cells in vitiligo pathogenesis by (i) investigating Treg cells' frequency in vitiligo patients; (ii) assessing Treg cells' suppressive capacity in vitiligo patients; (iii) determining FOXP3 expression levels in blood and skin of vitiligo patients; (iv) determining the expression levels of Tregs' suppressive cytokines: IL-10 and TGF-β in blood and skin of vitiligo patients; (v) carrying out disease activity-based analysis for Treg cells' frequency, FOXP3, IL-10, and TGF-β expression in vitiligo patients; and (vi) evaluating the effect of different therapeutic interventions on Treg cells' frequency, FOXP3, and IL-10 expression in vitiligo mice model and vitiligo patients through meta-analysis.

2. Materials and Methods

2.1. Literature Search. PubMed, Google Scholar, and Web of Science databases were searched up to 01st July 2022 for identifying studies evaluating the role of Tregs in vitiligo pathogenesis. The main keywords were "Tregs vitiligo," "vitiligo," "regulatory T cells," "Treg," "Treg cells number," "Treg cells frequency," "suppressive function," "FOXP3," "Forkhead box P3," "IL-10," "interleukin 10," "transforming growth factor beta," and "TGF-β." The detailed search strategy is mentioned in Table S1. "The study protocol followed the Preferred Reporting Items for Systematic Reviews and Meta-Analyses (PRISMA) guidelines" (Table S2) [38, 39]. The studies were searched on the database for four different times independently by three investigators. All the reference lists in the relevant research papers were manually scanned.

2.2. Inclusion and Exclusion Criteria. The inclusion criteria included (1) original studies, (2) studies involving "vitiligo" and "regulatory T cells," (3) studies assessing the Tregs' frequency in the skin or blood of vitiligo patients, (4) studies assessing the Tregs' suppressive capacity, and (5) studies assessing Tregs' suppressive molecules like FOXP3, IL-10, and TGF-β.

The criteria for exclusion were (1) review articles; (2) duplicate research; (3) studies that do not conduct quantitative assessments of Treg levels, Tregs' suppressive function, and Tregs' suppressive molecules like FOXP3, IL-10, and TGF-β; (4) meta-analysis; (5) studies that lack original data; and (6) studies with no full text.

2.3. Data Extraction. Figure 1 depicts the detailed screening methodology. Information such as author details, year of publication, sample size, Tregs' characterization, Tregs' frequency, Tregs' suppressive capacity, FOXP3 levels, IL-10 levels, TGF-β levels, information regarding the above-mentioned parameters being studied in the skin, blood, serum, or plasma of vitiligo patients, and disease activity are mentioned in Table 1. Patients with a persistent increase in lesions in the previous six months were classified as active vitiligo (AV) patients, while those without such progression were classified as stable vitiligo (SV) patients [5].

2.4. Quality Assessment of Enrolled Studies. The quality of the enrolled studies was assessed by three independent investigators. Initially, based on sample size, inclusion criteria, and methodology, the studies were screened. After the initial screening, the Newcastle-Ottawa Scale (NOS) criteria were employed to evaluate the quality of enrolled studies. "The NOS criteria were graded on a scale of 0 to 9, and three important criteria were included: (1) evaluation, (2) selection, and (3) ascertaining the outcome. Studies with a NOS score of five or higher were deemed as high-quality studies, while those with a lower score were deemed low-quality studies" [39].

2.5. Assessment of Publication Bias. "Publication bias in the enrolled studies was assessed by Eggers linear regression methods and test for publication bias using the JASP 0.14.1.0 software" [39, 40].

2.6. Sensitivity Analysis. To study the effect of individual studies on the meta-analysis, sensitivity analysis was carried out. The influence of the individual studies on the standardized mean difference (SMD) was evaluated before and after exclusion of each study.

2.7. Statistical Analysis. The meta-analysis provided quantitative data of standardized mean difference (SMD) as forest plots for Tregs' frequency, Tregs' suppressive capacity, FOXP3 levels, IL-10 levels, and TGF-β levels in vitiligo patients minus controls and for Tregs' frequency, Tregs' suppressive capacity, FOXP3 levels, and IL-10 levels in vitiligo patients and mice models posttreatment minus pretreatment. The random-effects model was utilized in the study as there were differences in experimental methods and techniques among selected studies. Meta-analysis was carried out using Review Manager 5.4 (Cochrane Collaboration, Oxford, United Kingdom). $p \leq 0.05$ were considered statistically significant.

3. Results

3.1. Study Characteristics. 913 results were collected from PubMed, Google Scholar, and Web of Science databases. After initial screening, 913 studies were excluded as they contained duplicate records and did not involve assessment of Tregs' frequency, Tregs' suppressive capacity, FOXP3

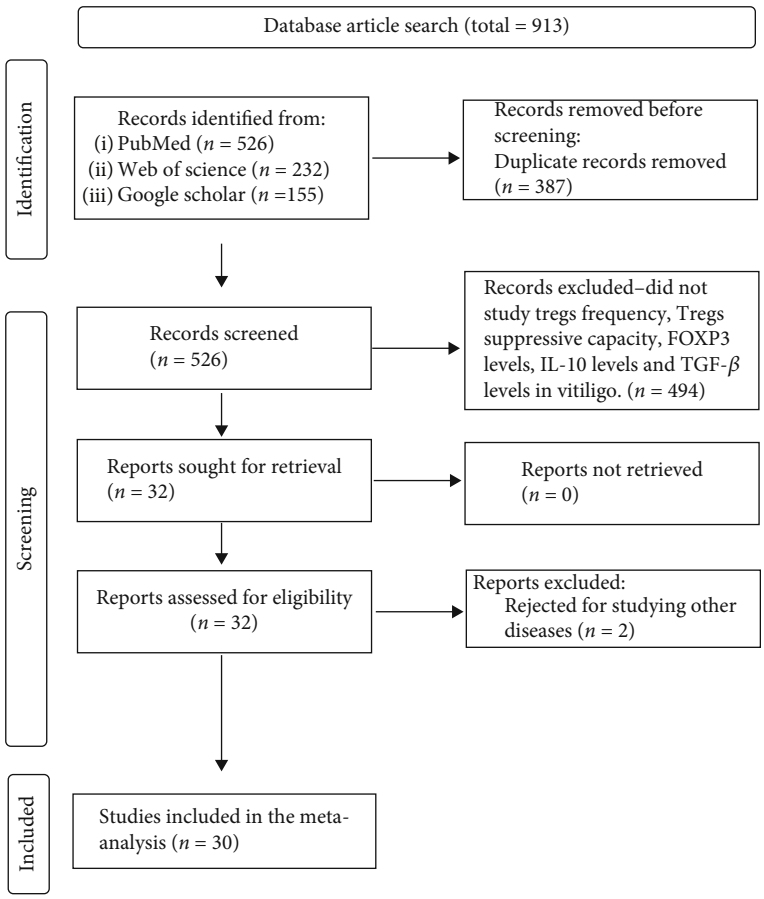

Figure 1: The flow chart of study selection for the meta-analysis. A total of 526 studies from PubMed, 232 studies from Web of Sciences, and 155 studies from Google Scholar databases were retrieved and processed for initial screening. After screening for the titles and abstracts, 387 duplicate records and 496 studies which did not study Tregs' frequency, Tregs' suppressive capacity, FOXP3 levels, IL-10 levels, and TGF-β levels in vitiligo were excluded. Finally, 30 studies consisting of total 1223 vitiligo patients and 1109 controls were included for the meta-analysis.

levels, IL-10 levels, and TGF-β levels in vitiligo. A total of 30 studies including 1223 vitiligo patients and 1109 controls were included in the meta-analysis. The study characteristics including author details, publication year, population size, Tregs' characterization, Tregs' frequency, Tregs' suppressive capacity, FOXP3 levels, IL-10 levels, TGF-β levels, information on the above-mentioned parameters investigated in the skin, blood, serum, or plasma of vitiligo patients, and disease activity are mentioned in Table 1. The studies included were in accordance with the quality assessment criteria, and the NOS score of 7 or 8 for the included studies suggests the high quality of these studies (Table S3).

3.2. Assessment of Publication Bias. The Eggers linear regression methods and test for publication bias suggested no significant publication bias for the meta-analysis ($p = 0.594$ and $p = 0.319$, respectively; Table S4), in vitiligo patients for the enrolled studies.

3.3. Treg Cells' Frequency in Vitiligo Patients. The proportion of Treg cells in vitiligo patients and controls were evaluated by calculating the standardized mean difference through meta-analysis. After initial screening, we found a total of 10 studies comprised of 478 vitiligo patients and 395 controls that assessed the Treg cells' frequency in vitiligo patients. Interestingly, we found significantly reduced Treg cells' frequency in vitiligo patients when compared to controls ($p = 0.002$, Figure 2(a)). The meta-analysis suggested that there was a 1.26 SMD decrease in Tregs' frequency in vitiligo patients (SMD: -1.26 [-2.04, -0.48], Figure 2(a)). Next, we carried out disease activity-based analysis for the frequency of Treg cells in vitiligo. However, only three studies comprised of 125 vitiligo patients and 61 controls carried out disease activity-based analysis for frequency of Treg cells. Our meta-analysis suggested a significant decrease in Treg cells' frequency in AV patients when compared to SV patients ($p = 0.05$, Figure 2(b)). Moreover, there was a difference of 3.08 SMD between AV patients and controls (SMD: -3.08 [-6.22, 0.06], Figure 2(b)). These findings from our meta-analysis suggested that the decrease in Treg cells numbers may lead to vitiligo pathogenesis and progression.

3.4. Treg Cells' Suppressive Capacity in Vitiligo Patients. As the proportion of Treg cells in vitiligo patients was decreased, we studied the suppressive capacity of Tregs in vitiligo patients by calculating the standardized mean

Table 1: Study characteristics.

Study	Year	Vitiligo patients/ controls	Skin/ blood	Treg characterization	Tregs' frequency	Tregs' suppressive capacity	FOXP3 levels	IL-10 levels	TGF-β levels	Disease activity-based analysis
Abdallah et al. [33]	2009	20/20	Blood	$CD4^+CD25$high $FoxP3^+$	Increased	NA	Increased	NA	NA	No
Ala et al.[30]	2015	130/150	Blood	NA	NA	NA	NA	Decreased	NA	No
Bhardwaj et al.[24]	2020	30/30	Skin	NA	NA	NA	Decreased	NA	Increased	No
Dwivedi et al.[8]	2013	82/50	Blood	$CD4^+CD25hiFOXP3^+$	Decreased	NA	Decreased	NA	NA	No
Eby et al.[50]	2015	7/6	Skin	$CD3^+FOXP3^+$	Increased after treatment	NA	NA	NA	NA	No
Abou Elela et al.[25]	2013	84/80	Blood	$CD4^+$ $CD25^+$ $FOXP3^+$	NA	NA	Decreased	NA	NA	Yes (VIDA)
El-Komy et al.[28]	2012	20/10	Skin	NA	NA	NA	NA	NA	Decreased	Yes (VIDA)
Ghanem et al.[36]	2017	38/40	Serum/ skin	NA	NA	NA	NA	NA	No difference	No
Giri et al.[5]	2020	55/45	Blood	$CD3^+CD25^+$ T cells	NA	NA	Decreased	Decreased	Decreased	Yes
Giri et al.[22]	2020	48/45	Blood	$CD3^+CD25^+$ T cells	NA	Decreased	Decreased	Decreased	Decreased	Yes
Giri et al.[9]	2021	96/90	Blood	$CD3^+CD25^+$ T cells	NA	NA	Decreased	NA	NA	Yes
Hegab et al.[17]	2015	80/60	Blood	$CD4^+CD25^+$	Decreased	NA	Decreased	NA	NA	Yes (VIDA)
Hegazy et al.[26]	2014	20/20	Skin	NA	NA	NA	Decreased	NA	NA	Yes (VIDA)
Huo et al.[19]	2021	15/15	Blood	$CD4^+CD25^+CD127^-$	Decreased	NA	Decreased	NA	NA	No
Kalaiselvi et al.[34]	2019	80/80	Blood	$CD4^+FOXP3^+$	No difference	NA	NA	NA	NA	Yes (VIDA)
Kidir et al.[29]	2017	30/30	Skin	NA	NA	NA	NA	Decreased	Decreased	No
Klarquist et al.[14]	2010	07/05	Skin	$CD4^+CD25^+CD127^-FOXP3^+$	Decreased	No difference	Increased	NA	NA	No
Lili et al.[18]	2012	50/20	Blood	$CD4^+CD25^+CD127^-$	Decreased	Decreased	Decreased	NA	NA	No
Lv et al.[49]	2019	1/1	Blood/ skin	$CD4^+$ $CD25^+$ $FOXP3^+$	Increased after treatment	NA	Increased after treatment	Increased after treatment	Increased after treatment	No
Miao et al.[51]	2018	8/9	Skin	$FOXP3^+CD3^+$	Increased after treatment	NA	NA	NA	NA	No
Mukhatayev et al.[47]	2020	11/12	Skin	$CD4^+$ $FOXP3^+$	Increased after treatment	NA	NA	Increased after treatment	NA	No

Table 1: Continued.

Study	Year	Vitiligo patients/ controls	Skin/ blood	Treg characterization	Tregs' frequency	Tregs' suppressive capacity	FOXP3 levels	IL-10 levels	TGF-β levels	Disease activity-based analysis
Osman et al.[31]	2015	42/43	Blood	NA	NA	NA	NA	NA	Decreased	No
Sohafy et al.[48]	2021	40/40	Blood	$CD4^+$ $CD25^+FOXP3^+$	Increased after treatment	NA	NA	NA	NA	No
Taher et al.[52]	2009	20/20	Skin	NA	NA	NA	NA	Increased after treatment	NA	No
Tembhre et al.[20]	2015	50/51	Skin	NA	Decreased	NA	Decreased	NA	Decreased	No
Tu et al.[32]	2017	46/25	Serum	$CD4^+$ $CD25^+$	NA	No difference	NA	NA	Decreased	No
Zhang et al.[21]	2018	51/51	Blood	$CD4^+CD25^{high}$	Decreased	Decreased	NA	Decreased	Decreased	No
Zhang et al.[53]	2021	3/3	Blood/ skin	$FOXP3^+$ $CD4^+$	NA	NA	NA	Increased after treatment	NA	No
Zhou et al.[35]	2012	43/43	Blood	$CD4^+$ $CD25^+$ $FOX3^+$	No difference	NA	NA	NA	NA	No
Zhou et al.[37]	2015	45/45	Serum	NA	NA	NA	NA	NA	Increased	No

Abbreviations: NA: not applicable; VIDA: vitiligo disease activity score; Treg: regulatory T cells; IL-10: interleukin 10; TGF-β: transforming growth factor beta.

Study or subgroup	Vitiligo patients Mean	SD	Total	Controls Mean	SD	Total	Weight	Std. mean difference IV, Random, 95% CI
Abdallah 2009	4.9	1.7	20	2.5	2.8	20	10.0%	1.02 (0.35, 1.68)
Dwivedi 2013	6.538	0.2863	82	8.122	0.5893	50	10.2%	−3.69 (−4.26,−3.12)
Hegab 2015	11.49	8.58	80	21.2	3.08	60	10.5%	−1.42 (−1.80,−1.05)
Huo 2021	6.5	1.8	15	11	1.2	15	9.0%	−2.86 (−3.92, −1.81)
Kalaiselvi 2019	8.65	3.37	80	8.13	5.84	80	10.6%	0.11 (−0.20, 0.42)
Klarquist 2010	2.6	3.5	7	46.2	37.8	5	8.0%	−1.67 (−3.08, −0.26)
Lili 2012	7.1	1.6	50	10.4	3.2	20	10.2%	−1.50 (−2.08, −0.93)
Tembhre 2015	1.98	0.88	50	3.12	1.36	51	10.5%	−0.99 (−1.40, −0.57)
Zhang 2018	5.9	0.6	51	6.9	0.5	51	10.4%	−1.80 (−2.26, −1.33)
Zhou 2012	3.69	2.26	43	3.85	1.62	43	10.5%	−0.08 (−0.50, 0.34)
Total (95% CI)			**478**			**395**	**100.0%**	**−1.26 (−2.04, −0.48)**

Heterogeneity: tau^2= 1.47; chi^2 = 218.86, df = 9 (P< 0.00001); I^2 = 96%
Test for overall effect: Z = 3.15 (P = 0.002)

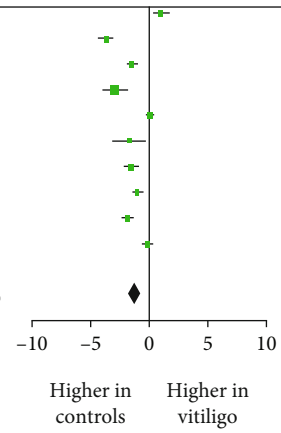

(a)

Study or subgroup	AV patients Mean	SD	Total	SV patients Mean	SD	Total	Weight	Std. mean difference IV, Random, 95% CI
Dwivedi 2013	6.04	0.41	56	7.731	0.43	29	33.6%	−4.02 (−4.78, −3.26)
Lili 2012	7.1	2.8	38	7.4	1.8	12	33.8%	−0.11 (−0.76, 0.54)
Zhang 2018	4.6	0.3	31	7.5	0.8	20	32.7%	−5.19 (−6.37, −4.00)
Total (95% CI)			**125**			**61**	**100.0%**	**−3.08 (−6.22, 0.06)**

Heterogeneity: tau^2 = 7.50; chi^2 = 85.60, df = 2 (P < 0.00001); I^2 = 98%
Test for overall effect: Z = 1.92 (P = 0.05)

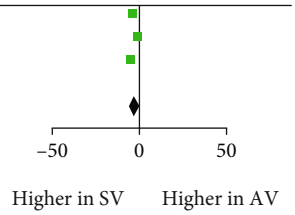

(b)

Figure 2: The forest plots for Treg cells' frequency in vitiligo patients and controls. (a) Treg cells' frequency in vitiligo patients vs. controls ($p = 0.002$; SMD: -1.26 [-2.04, -0.48]). (b) Treg cells' frequency in AV vs. SV patients ($p = 0.05$; SMD: -3.08[-6.22, 0.06]).

difference through meta-analysis. After screening we found that a total of 5 studies comprised of 186 vitiligo patients and 154 controls assessed the Treg cells' suppressive capacity in vitiligo. Interestingly, we found significant decrease in Treg cells' suppressive capacity between vitiligo patients and controls ($p = 0.0002$, Figure 3(a)). There was difference of 2.58 standardized mean between vitiligo patients and controls (SMD: -2.58 [-3.95, -1.21], Figure 3(a)). As there were 3 studies which accessed the Treg cells' suppressive capacity over CD4$^+$ T cells and 3 studies accessed the Treg cells' suppressive capacity over CD8$^+$ T cells, we carried out subgroup analysis to assess the Treg cells' suppressive capacity individually over CD4$^+$ and CD8$^+$ T cells. Our meta-analysis revealed significant decrease in Treg cells' suppressive capacity over CD8$^+$ T cells in vitiligo patients ($p < 0.00001$, SMD: -3.99 [-4.47, -3.51], Figure 3(a)). However, there was no significant difference observed in Treg cells' suppressive capacity over CD4$^+$ T cells in vitiligo patients when compared to controls ($p = 0.36$, Figure 3(a)). Although, the SMD of -1.27 suggests a trend of decreased Treg cells' suppressive capacity over CD4$^+$ T cells in vitiligo patients (SMD: 1.27 [-4.00, 1.45], Figure 3(a)). Unfortunately, we could not carry out disease activity-based analysis for Treg cells' suppressive capacity in vitiligo, as only one of the five studies assessed the disease activity-based analysis for Treg cells' suppressive capacity in vitiligo patients. These results suggest for the crucial role of impaired Tregs' suppressive capacity in vitiligo pathogenesis.

3.5. FOXP3 Expression Levels in Blood and Skin of GV Patients. As FOXP3 is a key molecule for Treg cells' frequency and suppressive function, we evaluated the FOXP3 levels in GV patients and controls by calculating the standardized mean difference through meta-analysis. After the initial screening, we found that a total of 14 studies, comprised of 831 vitiligo patients and 755 controls, assessed the FOXP3 levels in vitiligo. Our meta-analysis suggested a significant decrease in FOXP3 levels in vitiligo patients when compared to controls ($p < 0.00001$, Figure 3(b)). The meta-analysis suggested that there was difference of 5.43 standardized mean for FOXP3 levels between vitiligo patients and controls (SMD: -5.43 [-6.98, -3.88]), Figure 3(b)). As the previous studies assessed the FOXP3 protein levels in blood, skin, and *FOXP3* transcript levels in blood, we also carried out subgroup analysis for the FOXP3 expression. Interestingly, our meta-analysis suggested significant decrease in FOXP3 protein levels in blood ($p < 0.00001$, SMD: -4.94 [-6.96, -2.91]), Figure 3(b)) and skin ($p = 0.002$, SMD:

Study or subgroup	Vitiligo patients Mean	SD	Total	Controls Mean	SD	Total	Weight	Std. mean difference IV, Random, 95% CI
Suppression of CD4+ T cells								
Giri 2020b	61.2	3.69	55	73.9	2.97	45	18.4%	−3.72 (−4.38,-3.06)
Klarquist 2010	46.0	13.0	3	39.0	8.0	3	14.9%	0.52 (−1.16, 2.20)
Tu 2011	43.0	12.0	16	48.0	10.0	6	17.6%	−0.42 (−1.37, 0.53)
Sub total (95% CI)			**74**			**54**	**50.8%**	**−1.27 (−4.00, 1.45)**
Heterogeneity: tau² = 5.44; chi² = 43.95, df = 2 (*P* < 0.00001); I² = 95%								
Test for overall effect: Z = 0.92 (*P* = 0.36)								
Suppression of CD8+ T cells								
Giri 2020b	30.8	3.19	55	46.35	4.08	45	18.2%	−4.27 (−4.99, −3.55)
Lili 2012	27.76	5.71	6	49.03	5.8	4	12.6%	−3.34 (−5.61, −1.08)
Zhang 2018	3.8	2.0	51	12.5	2.5	51	18.4%	−3.81 (−4.47, −3.15)
Sub total (95% CI)			**112**			**100**	**49.2%**	**−3.99 (−4.47, −3.51)**
Heterogeneity: tau² = 0.00; chi² = 1.15, df = 2 (*P* = 0.56); I² = 0%								
Test for overall effect: Z = 16.44 (*P* < 0.00001)								
Total			**186**			**154**	**100.0%**	**−2.58 (−3.95, −1.21)**
Heterogeneity: tau² = 2.53; chi² = 66.14, df = 5 (*P* < 0.00001); I² = 92%								
Test for overall effect: Z = 3.70 (*P* = 0.0002)								
Test for subgroup differences: chi² = 3.71, df = 1 (*P* = 0.05), I² = 73.1%								

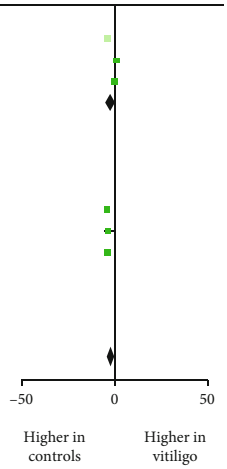

(a)

Study or subgroup	Vitiligo patients Mean	SD	Total	Controls Mean	SD	Total	Weight	Std. mean difference IV, Random, 95% CI
FOXP3 protein levels in blood								
Abdallah 2009	70.7	11.3	20	59.9	7.0	20	7.0%	1.13 (0.45, 1.80)
Dwivedi 2013	592.3	68.03	82	867.5	52.1	50	7.0%	−4.38 (−5.02, −3.74)
Giri 2020a	624.1	67.61	48	967.6	35.44	45	6.9%	−6.25 (−7.26, −5.25)
Giri 2020b	390.6	7.26	55	799.5	16.46	45	4.3%	−33.05 (−37.75, −28.36)
Giri 2021	524.7	62.43	90	1009	55.13	96	7.0%	−8.21 (−9.10, −7.32)
Hegab 2015	1.09	0.96	80	1.44	0.24	60	7.1%	−0.47 (−0.81, −0.13)
Kalaiselvi 2019	8.65	3.37	80	8.13	5.84	80	7.1%	0.11 (−0.20, 0.42)
Zhou 2012	5.68	2.87	43	5.87	3.97	43	7.1%	−0.05 (−0.48, 0.37)
Sub total (95% CI)			**498**			**439**	**53.6%**	**−4.94 (−6.96, −2.91)**
Heterogeneity: tau² = 8.01; chi² = 758.19, df = 7 (*P* < 0.00001); I² = 99%								
Test for overall effect: Z = 4.77 (*P* < 0.00001)								
FOXP3 Protein levels in Skin								
Bhardwaj 2020	0.2	0.1	30	24.0	2.0	30	5.5%	−16.59 (−19.70, −13.48)
Elela 2013	2.67	0.54	84	7.12	0.18	80	6.8%	−10.90 (−12.13, −9.67)
Hegazy 2014	4.04	1.14	20	17.14	2.81	20	6.7%	−5.99 (−7.50, −4.47)
Kidir 2017	0.0	0.73	20	2.0	0.79	10	6.9%	−2.60 (−3.63, −1.56)
Lili 2012	2.49	0.6	2	3.69	3.04	6	6.6%	−0.37 (−2.00, 1.25)
Sub total (95% CI)			**156**			**146**		**−7.16 (−11.73, −2.59)**
Heterogeneity: tau² = 26.31; chi² = 191.39, df = 4 (*P* < 0.00001); I² = 98%								
Test for overall effect: Z = 3.07 (*P* = 0.002)								
FOXP3 transcript in blood								
Bhardwaj 2020	0.27	0.0	30	1.0	0.0	30		Not estimable
Elela 2013	0.574	0.32	84	1.48	0.49	80	7.1%	−2.19 (−2.58, −1.80)
Giri 2020a	0.4	0.0	48	1.0	0.0	45		Not estimable
Huo 2021	0.24	0.1	15	1.0	0.2	15	6.7%	−4.68 (−6.13, −3.22)
Sub total (95% CI)			**177**			**170**		**−3.33 (−5.76, −0.90)**
Heterogeneity: tau² = 2.80; chi² = 10.44, df = 1 (*P* = 0.001); I² = 90%								
Test for overall effect: Z = 2.69 (*P* = 0.007)								
Total (95% CI)			**831**			**755**	**100.0%**	**−5.43 (−6.98, −3.88)**
Heterogeneity: tau² = 8.79; chi² = 1181.13, df = 14 (*P* < 0.00001); I² = 99%								
Test for subgroup differences: chi² = 2.36, df = 2 (*P* = 0.31), I² = 15.3%								
Test for overall effect: Z = 6.86 (P < 0.00001)								

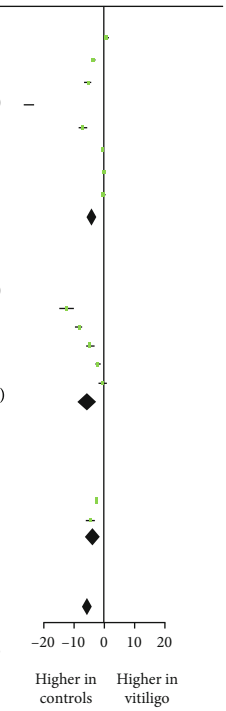

(b)

Figure 3: The forest plots for Tregs' suppressive capacity and FOXP3 expression in vitiligo patients and controls. (a) Tregs' suppressive capacity in vitiligo patients vs. controls ($p = 0.0002$; SMD: -2.58[-3.95, -1.21]). Treg-mediated suppression of $CD4^+$ T cells in vitiligo patients vs. controls ($p = 0.36$; SMD: -1.27[-4.00, 1.45]). Treg-mediated suppression of $CD8^+$ T cells in vitiligo patients vs. controls ($p < 0.00001$; SMD: -3.99[-4.47, -3.51]). (b) FOXP3 expression in skin and blood of vitiligo patients vs. controls ($p < 0.00001$; SMD: -5.43[-6.98, -3.88]). FOXP3 protein levels in blood of vitiligo patients vs. controls ($p < 0.00001$; SMD: -4.94 [-6.96, -2.91]). FOXP3 protein levels in skin of vitiligo patients vs. controls ($p = 0.002$, SMD: -7.16 [-11.73, -2.59]). *FOXP3* transcripts in blood of vitiligo patients vs. controls ($p = 0.007$, SMD: -3.33 [-5.76, -0.90]).

-7.16 [-11.73, -2.59]), Figure 3(b)) of vitiligo patients when compared to controls. Additionally, a significant decrease in *FOXP3* transcripts was observed in blood of vitiligo patients ($p = 0.007$, SMD: -3.33 [-5.76, -0.90]), Figure 3(b)). Next, we evaluated the FOXP3 expression in lesional, perilesional, and nonlesional skin. Interestingly, we found a significant decrease in FOXP3 levels in lesional skin when compared to perilesional skin ($p = 0.007$, SMD: -9.77

[-16.91, -2.62]) and nonlesional skin ($p = 0.04$, SMD: -1.01 [-1.95, -0.06]) in vitiligo patients (Figure S1a, b).

Further, we carried out disease activity-based analysis for FOXP3 expression in vitiligo. Previously, a total of four studies comprised of 179 vitiligo patients and 105 controls carried out disease activity-based analysis for FOXP3 expression. Our meta-analysis revealed significant decrease in FOXP3 protein expression in blood of AV patients when compared to SV patients ($p = 0.01$, Figure S1c). There was a difference of 2.99 SMD between AV and SV patients (SMD: -2.99 [-5.26, -0.71]), Figure S1c). These findings suggest the crucial role of FOXP3 in vitiligo pathogenesis and progression.

3.6. Expression of Treg-Associated Suppressive Cytokines (IL-10 and TGF-β) in Vitiligo. As our meta-analysis suggested impaired Tregs' suppressive capacity in vitiligo patients, we studied the expression levels of Treg-associated suppressive cytokines: IL-10 and TGF-β by calculating the standardized mean difference through meta-analysis. After the initial screening, we found that a total of 6 studies comprised of 334 vitiligo patients and 341 controls assessed the IL-10 levels in vitiligo. Interestingly, the meta-analysis revealed significant reduction in IL-10 protein levels in vitiligo patients when compared to controls ($p = 0.0005$, SMD: -3.62 [-5.65, -1.59]), Figure 4(a)). Further, to study the expression levels of IL-10 in blood and skin of vitiligo patients, we carried subgroup analysis. Interestingly, the meta-analysis showed significant decreased IL-10 protein levels in blood of vitiligo patients ($p = 0.004$, SMD: -5.48 [-9.20, -1.75] Figure 4(a)). However, there was no significant difference observed for IL-10 protein levels in skin of vitiligo patients (p = 0.79, SMD: -0.14 [-1.13, 0.85], Figure 4(a)). Next, to study the role of IL-10 on disease activity, we carried out disease activity-based analysis for IL-10 levels in vitiligo. However, we found only three studies comprised of 154 vitiligo patients and 79 controls and carried out the disease activity-based analysis for IL-10 expression. Our meta-analysis suggested that there was no significant decrease in IL-10 protein expression in AV patients when compared to SV patients ($p = 0.09$, SMD: -1.67 [-3.59, 0.25]) Figure S2a). Although, the SMD of -1.67 suggests for a trend of decreased TGF-β levels in AV patients (SMD: -1.67 [-3.59, 0.25]), Figure S2a).However, the SMD of -1.67 between AV and SV patients, suggested the trend for decreased TGF-β levels in AV patients (SMD: -1.67 [-3.59, 0.25]), Figure S2a). These findings suggest for the crucial role of IL-10 in vitiligo pathogenesis.

Furthermore, we studied the expression of TGF-β by calculating the standardized mean difference through meta-analysis in vitiligo patients and controls. After the initial screening, we found that a total of 8 studies comprised of 389 vitiligo patients and 333 controls assessed TGF-β levels in vitiligo. Our meta-analysis revealed a significant decrease in TGF-β protein levels in vitiligo patients when compared to controls ($p = 0.01$, SMD: -1.40 [-2.49, -0.30]), Figure 4(b)). In addition, we studied the expression of TGF-β in blood and skin of vitiligo patients by subgroup analysis. Interestingly, we found significant decrease in TGF-β protein levels in blood of vitiligo patients ($p = 0.01$, SMD: -1.77 [-3.14, -0.40]), Figure 4(b)). However, no significant difference was observed for TGF-β protein levels in skin of vitiligo patients ($p = 0.58$, SMD: -0.12 [-0.57, 0.32]), Figure 4(b)). Further, we carried out disease activity-based analysis to study the role of TGF-β on disease activity. However, only two studies comprised of 71 vitiligo patients and 32 controls carried out disease activity-based analysis for the TGF-β expression. There was no significant decrease observed in TGF-β protein expression in AV patients when compared to SV patients ($p = 0.06$, Figure S2b). Although, the SMD of -3.49 suggests for a trend of decreased TGF-β levels in AV patients (SMD: -3.49 [-7.08, 0.10]), Figure S2b). These findings suggest for the crucial role of TGF-β in GV pathogenesis.

3.7. Effect of Different Treatment on Tregs' Frequency, FOXP3, and IL-10 Levels in Vitiligo. To study the impact of microRNA-based treatment, narrow band–UVB phototherapy, and Treg-associated treatments on Tregs' frequency, FOXP3, and IL-10 levels in vitiligo, we assessed the Tregs' frequency, FOXP3, and IL-10 levels in vitiligo patients and mouse model of vitiligo, pre- and posttreatment by calculating the standardized mean difference through meta-analysis. There were a total of 7 studies comprised of 56 vitiligo patients (human studies) and 22 vitiligo mice (animal studies) that studied the Tregs' frequency, pre- and posttreatment. Interestingly, the meta-analysis revealed significant increase in Treg cells' frequency after the treatment ($p = 0.007$, SMD: 1.64 [0.45, 2.83]), Figure 5(a)). Furthermore, the subgroup analysis suggested significant increase in Treg cells' frequency after the treatment in mouse models of vitiligo ($p = 0.01$, 2.11 [0.43, 3.78]), Figure 5(a)). However, there was no significant difference found in Treg cells' frequency after the treatment, in human studies ($p = 0.21$, Figure 5(a)). However, the SMD of 1.16 between treatment groups, suggested the trend for increased Treg cells' frequency after treatment (SMD: 1.16 [-0.65, 2.96]), Figure 5(a)). Although, the SMD of 1.16 suggests a trend of increased Treg cells' frequency after the treatment (SMD: 1.16 [-0.65, 2.96]) Figure 5(a)).

Further, we evaluated FOXP3 expression posttreatment. A total of 8 studies comprised of 76 vitiligo patients (human studies) and 21 vitiligo mice (animal studies) studied the FOXP3 protein expression pre- and posttreatment. Our meta-analysis indicated a significant increase in FOXP3 protein expression after the treatment ($p < 0.0001$, SMD: 3.43 [1.90, 4.96]. Moreover, subgroup analysis revealed significant increase in FOXP3 expression after the treatment, in human studies ($p = 0.003$, 3.34 [1.13, 5.54]), Figure 5(b)) and vitiligo mice model studies ($p = 0.0008$, SMD: 3.43 [1.44, 5.43]), Figure 5(b)). Additionally, we assessed IL-10 expression posttreatment. A total of 5 studies comprised of 72 vitiligo patients (human studies) and 9 vitiligo mice (animal studies) studied the IL-10 protein levels pre- and posttreatment. Our meta-analysis revealed a significant increase in IL-10 protein levels after the treatment ($p = 0.002$, SMD: 1.32 [0.47, 2.17]), Figure 6(c)). Moreover, the subgroup analysis suggested significant increase in IL-10 protein levels after the treatment, in human studies ($p = 0.0006$, 0.82 [0.35, 1.29]), Figure 5(c)) and vitiligo mice model studies ($p = 0.0003$, SMD: 2.98 [1.37, 4.59]), Figure 5(c)).

Study or subgroup	Vitiligo patients Mean	SD	Total	Controls Mean	SD	Total	Weight	Std. mean difference IV, Random, 95% CI
IL-10 protein levels in blood								
Ala 2015	9.3	1.7	130	11.5	5.0	150	17.2%	−0.57 (−0.81, −0.33)
Giri 2020a	17.69	2.47	48	58.54	7.04	45	16.2%	−7.78 (−8.99, −6.57)
Giri 2020b	18.22	0.9	55	30.4	1.5	45	15.8%	−10.01 (−11.48, −8.54)
Zhang 2018	10.0	5.0	51	40.0	10.0	51	16.9%	−3.77 (−4.42, −3.11)
Subtotal (95% CI)			**284**			**291**	**66.1%**	**−5.48 (−9.20, −1.75)**
Heterogeneity: tau^2 = 14.18; chi^2 = 334.31, df = 3 (P < 0.00001); I^2 = 99%								
Test for overall effect: Z = 2.88 (P = 0.004)								
IL-10 protein levels in skin								
Kidir 2017	1.5	0.71	30	2.0	0.86	30	17.0%	−0.63 (−1.14, −0.11)
Taher 2009	37.8	15.9	20	31.9	14.2	20	16.9%	0.38 (−0.24, 1.01)
Sub Total (95% CI)			**50**			**50**	**33.9%**	**−0.14 (−1.13, 0.85)**
Heterogeneity: tau^2 = 0.42; chi^2 = 5.92, df = 1 (P = 0.01); I^2 = 83%								
Test for overall effect: Z = 0.27(P = 0.79)								
Total			**334**			**341**	**100.0%**	**−3.62 (−5.65, −1.59)**
Heterogeneity: tau^2 = 6.24; chi^2 = 365.03, df= 5 (P < 0.00001); I^2 = 99%								
Test for overall effect: Z = 3.49 (P = 0.0005)								
Test for subgroup differences: chi^2 = 7.38, df = 1 (P = 0.007), I^2 = 86.5%								

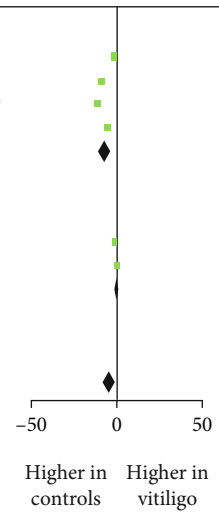

(a)

Study or subgroup	Vitiligo patients Mean	SD	Total	Controls Mean	SD	Total	Weight	Std. mean difference IV, Random, 95% CI
TGF-β Protein levels inblood								
EL-Komy 2012	13.97	3.61	20	23.15	7.49	0		Not estimable
Ghanem 2017	36.34	12.03	38	38.67	15.12	40	11.4%	−0.17 (−0.61, 0.28)
Giri 2020a	39.13	1.53	48	39.9	1.07	45	11.4%	−0.58 (−0.99, −0.16)
Giri 2020b	54.74	5.14	55	96.72	2.89	45	9.7%	−9.74 (−11.17, −8.30)
Osman 2015	0.042	0.032	42	0.047	0.036	43	11.4%	−0.15 (−0.57, 0.28)
Tu 2011	3495.89	3197.9	46	7607.0	4028.0	25	11.3%	−1.16 (−1.68, −0.63)
Zhang 2018	5000.0	800.0	51	7000.0	500.0	51	11.2%	−2.98 (−3.54, −2.41)
Zhou 2015	5.0	0.8	45	4.1	0.5	45	11.4%	1.34 (0.88, 1.80)
Sub total (95% CI)			**345**			**294**	**77.8%**	**−1.77 (−3.14, −0.40)**
Heterogeneity: tau^2 = 3.30; chi^2 = 304.08, df = 6 (P < 0.00001); I^2 = 98%								
Test for overall effect: Z = 2.54 (P = 0.01)								
TGF-β Protein levelsin skin								
EL-Komy 2012	1.28	0.47	20	3.06	8.2	10	11.0%	−0.37 (−1.14, 0.39)
Ghanem 2017	41.7	0.0	24	45.5	0.0	11		Not estimable
Kidir 2017	0.0	0.58	24	0.0	0.18	29	11.3%	0.00 (−0.54, 0.54)
Sub total (95% CI)			**68**			**50**	**22.2%**	**−0.12 (−0.57, 0.32)**
Heterogeneity: tau^2 = 0.00; chi^2 = 0.60, df = 1 (P = 0.44); I^2 = 0%								
Test for overall effect: Z = 0.55 (P = 0.58)								
Total (95% CI)			**413**			**344**	**100.0%**	**−1.40 (−2.49, −0.30)**
Heterogeneity: tau^2 = 2.70; chi^2 = 308.34, df = 8 (P < 0.00001); I^2 = 97%								
Test for overall effect: Z = 2.50 (P = 0.01)								
Test for subgroup differences: chi^2 = 5.05, df = 1 (P = 0.02), I^2 = 80.2%								

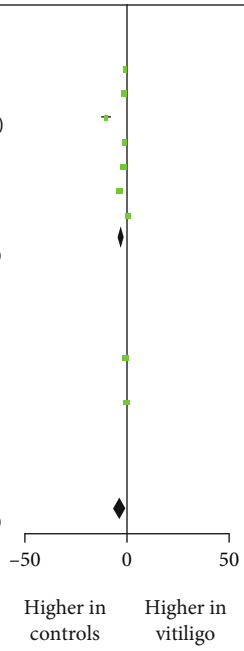

(b)

Figure 4: The forest plots for expression of Treg-associated suppressive cytokines (IL-10 and TGF-β) in vitiligo patients and controls. (a) IL-10 levels in blood and skin of vitiligo patients vs. controls (p = 0.0005; SMD: -3.62 [-5.65, -1.59]). IL-10 levels in blood of vitiligo patients vs. controls (p = 0.004; SMD: -5.48[-9.20, -1.75]). IL-10 expression levels in skin of vitiligo patients vs. controls (p = 0.79; SMD: -0.14 [-1.13, 0.85]). (b) TGF-β protein levels in blood and skin vitiligo patients vs. controls (p = 0.01, SMD: -1.40 [-2.49, -0.30]). TGF-β protein levels in blood of vitiligo patients vs. controls (p = 0.01, SMD: -1.77 [-3.14, -0.40]). TGF-β protein levels in skin of vitiligo patients vs. controls (p = 0.58, SMD: -0.12 [-0.57, 0.32]).

3.8. Sensitivity Analysis. We carried out sensitivity analysis to assess the influence of individual studies on the overall SMD. There were no outlying studies found to influence a significant change in the SMD (Table S5-S12).

4. Discussion

Treg cells maintain peripheral immune tolerance by actively suppressing self-reactive T cells [41]. Functional alteration in

Study or subgroup	Post-treatment Mean	SD	Total	Pre-treatment Mean	SD	Total	Weight	Std. Mean Difference IV, Random, 95% CI
Tregs frequency in vitiligo mice model studies								
Eby 2015	3.7	1.3	5	2.2	1.5	4	19.2%	0.96 (−0.48, 2.40)
Miao 2018	11.4	2.2	6	2.7	1.3	6	12.5%	4.44 (2.00, 6.89)
Mukhatayev 2020	6.1	4.0	3	0.0	0.0	6		Not estimable
Zhang 2021	5.2	2.0	6	1.9	1.5	6	19.4%	1.72 (0.31, 3.13)
Subtotal (95% CI)			**20**			**22**	**51.2%**	**2.11 (0.43, 3.78)**
Heterogeneity: tau² = 1.40; chi² = 5.80, df = 2 (*P* = 0.05); I² = 66%								
Test for overall effect: Z = 2.47 (*P* = 0.01)								
Tregs frequency in vitiligo Human studies								
Huo 2021	14.2	2.2	15	10.0	1.6	15	23.1%	2.12 (1.21, 3.04)
Lv 2019	55.0	3.0	1	48.0	2.0	1		Not estimable
Sohafy 2021	3.5	1.1	40	3.2	1.0	40	25.8%	0.28 (−0.16, 0.72)
Sub total (95% CI)			**56**			**56**	**48.8%**	**1.16 (−0.65, 2.96)**
Heterogeneity: tau² = 1.56; chi² = 12.54, df = 1 (*P* = 0.0004); I² = 92%								
Test for overall effect: Z = 1.26 (*P* = 0.21)								
Total			**76**			**78**	**100.0%**	**1.64 (0.45, 2.83)**
Heterogeneity: tau² = 1.38; chi² = 23.49, df = 4 *P*P = 0.0001); I² = 83%								
Test for overall effect: Z = 2.70 (*P* = 0.007)								
Test for subgroup differences: chi² = 0.57, df = 1 (*P* = 0.45), I² = 0%								

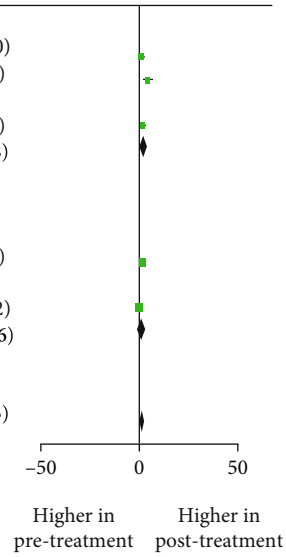

(a)

Study or subgroup	Post-treatment Mean	SD	Total	Pre-treatment Mean	SD	Total	Weight	Std. mean difference IV, Random, 95% CI
FOXP3 levels in vitiligo mice model studies								
Eby 2015	7.5	4.0	6	0.5	0.5	6	18.6%	2.27 (0.68, 3.85)
Miao 2018	11.4	2.2	6	2.7	1.3	6	14.6%	4.44 (2.00, 6.89)
Mukhatayev 2020	6.1	4.0	3	0.0	0.0	6		Not estimable
Zhang 2021	19.5	2.0	3	6.5	1.0	3	4.4%	6.58 (0.03, 13.13)
Sub total (95% CI)			**18**			**21**	**37.6%**	**3.43 (1.44, 5.43)**
Heterogeneity: tau² = 1.25; chi² = 3.30, df = 2 (*P* = 0.19); I² = 39%								
Test for overall effect: Z = 3.37 (*P* = 0.0008)								
FOXP3 levels in vitiligo Human studies								
Hegazy 2014	11.61	2.26	20	4.04	1.44	20	20.7%	3.92 (2.82, 5.01)
Huo 2021	2.0	0.2	15	1.0	0.2	15	19.0%	4.86 (3.36, 6.37)
Lv 2019	6.0	1.2	1	2.5	0.5	1		Not estimable
Sohafy 2021	1.8	0.6	40	1.1	0.3	40	22.7%	1.46 (0.97, 1.96)
Sub total (95% CI)			**76**			**76**	**62.4%**	**3.34 (1.13, 5.54)**
Heterogeneity: tau² = 3.49; chi² = 29.91, df = 2 (*P* < 0.00001); I² = 93%								
Test for overall effect: Z = 2.96 (*P* = 0.003)								
Total (95% CI)			**94**			**97**	**100.0%**	**3.43 (1.90, 4.96)**
Heterogeneity: tau² = 2.63; chi² = 34.97, df = 5 (*P* < 0.00001); I² = 86%								
Test for overall effect: Z = 4.38 (*P* < 0.0001)								
Test for subgroup differences: chi² = 0.00, df = 1 (*P* = 0.95), I² = 0%								

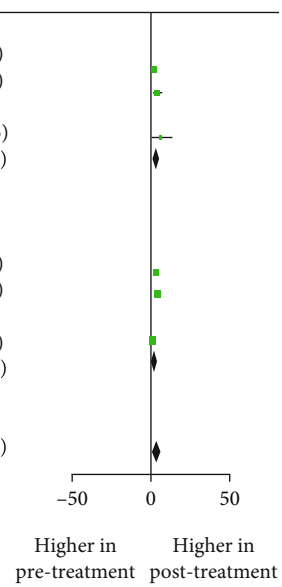

(b)

Figure 5: Continued.

Study or subgroup	Post-treatment Mean	SD	Total	Pre-treatment Mean	SD	Total	Weight	Std. Mean Difference IV, Random, 95% CI
IL-10 levels in vitiligo mice model studies								
Mukhatayev 2020	120.0	40.0	3	40.0	10.0	3	8.4%	2.20 (−0.46, 4.85)
Zhang 2021	15.0	3.0	6	7.0	0.5	6	12.9%	3.43 (1.41, 5.46)
Sub total (95% CI)			**9**			**9**	**21.3%**	**2.98 (1.37, 4.59)**
Heterogeneity: $tau^2 = 0.00$; $chi^2 = 0.53$, df = 1 ($P = 0.47$); $I^2 = 0\%$								
Test for overall effect: Z = 3.63 ($P = 0.0003$)								
IL-10 levels in vitiligo Human studies								
Lv 2019	37.0	2.0	1	28.0	1.0	1		Not estimable
Taher 2009	60.8	22.7	20	37.8	15.9	20	36.2%	1.15 (0.48, 1.82)
Zhang 2018	6.2	3.0	51	4.4	2.5	51	42.5%	0.65 (0.25, 1.05)
Sub total (95% CI)			**72**			**72**	**78.7%**	**0.82 (0.35, 1.29)**
Heterogeneity: $Tau^2 = 0.05$; $Chi^2 = 1.59$, df = 1 ($P = 0.21$); $I^2 = 37\%$								
Test for overall effect: Z = 3.43 ($P = 0.0006$)								
Total			**81**			**81**	**100.0%**	**1.32 (0.47, 2.17)**
Heterogeneity: $Tau^2 = 0.40$; $Chi^2 = 9.00$, df = 3 ($P = 0.03$); $I^2 = 67\%$								
Test for overall effect: Z = 3.03 ($P = 0.002$)								
Test for subgroup differences: $Chi^2 = 6.36$, df = 1 ($P = 0.01$), $I^2 = 84.3\%$								

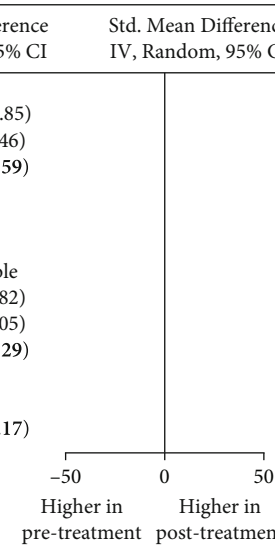

(c)

Figure 5: The forest plots for Tregs' frequency, FOXP3, and IL-10 levels in vitiligo pre- and posttreatment. (a) Tregs' frequency posttreatment vs. pretreatment ($p = 0.007$, SMD: 1.64 [0.45, 2.83]). Tregs' frequency posttreatment vs. pretreatment in mouse models of vitiligo ($p = 0.01$, SMD: 2.11 [0.43, 3.78]). Tregs' frequency post treatment vs. pretreatment in human studies for vitiligo ($p = 0.21$ SMD: 1.16 [-0.65, 2.96]). (b) FOXP3 protein levels posttreatment vs. pretreatment ($p < 0.0001$, SMD: 3.43 [1.90, 4.96]). FOXP3 protein levels posttreatment vs. pretreatment in vitiligo mice model study ($p = 0.0008$, SMD: 3.43 [1.44, 5.43]). FOXP3 protein levels posttreatment vs. pretreatment in human studies ($p = 0.003$, 3.34 [1.13, 5.54]). (c) IL-10 levels posttreatment vs. pretreatment in vitiligo patients ($p = 0.002$, SMD: 1.32 [0.47, 2.17]). IL-10 levels posttreatments vs. pretreatment in vitiligo mice models study ($p = 0.0003$, SMD: 2.98 [1.37, 4.59]). IL-10 levels post treatment vs. pretreatment in vitiligo human studies ($p = 0.0006$, 0.82 [0.35, 1.29]).

Treg cells lead to various autoimmune diseases [42]. Similarly, Treg cells have a critical role in vitiligo pathogenesis [5, 8, 14, 17–22, 24–26]. However, few contrary findings [14, 33–35] suggest a controversial role of Tregs in vitiligo pathogenesis. Therefore, we performed a meta-analysis to study Treg cells' frequency, Tregs' suppressive function, FOXP3, IL-10, and TGF-β expression in vitiligo patients. The pooled results of our meta-analysis suggested a significant decrease in Tregs' frequency in vitiligo patients (Figure 2(a)). Particularly, there was 1.26 SMD decrease in Treg cells' frequency in vitiligo patients (Figure 2(a)). Our results are strongly supported by previous studies suggesting significantly decreased Treg cells levels in vitiligo patients [8, 14, 17–21]. However, they contrast with few reports [33–35]. The conflicting results may be due to differences in sample size, difference in methodology used, and ethnicity differences. Additionally, difference in antibody clones used for flow cytometry studies could also account for differences in Tregs' number [8]. Moreover, the differences in the characterization of Tregs may also be responsible for the conflicting results [43], suggesting that future studies should use strict and consistent markers for Treg cell characterization in vitiligo. Interestingly, the disease activity-based analysis suggested the role of reduced Treg cells in vitiligo disease activity, which is in concordance to the previous studies [8, 18, 21]. Overall, our meta-analysis taking into consideration all the available data suggested that the decreased Treg cells' frequency might be involved in vitiligo pathogenesis and progression.

As we found decreased Tregs' frequency in vitiligo patients, it was pertinent to assess Tregs' suppressive capacity in vitiligo patients. Interestingly, our meta-analysis suggested significantly decreased Treg cells' suppressive capacity in vitiligo patients (Figure 3(a)). The results agreed with that of the previous studies [18, 21, 22]. Further, the subgroup analysis revealed a significant decrease in Treg-mediated suppression of $CD8^+$ T cells' proliferation in vitiligo patients (Figure 3(a)). These findings were in concordance with the previous studies [18, 21, 22]. The autoreactive $CD8^+$ T cells are the major culprits responsible for the destruction of melanocytes in vitiligo patients [6, 14, 15]. Our meta-analysis together with the previous studies suggest for the crucial role of Tregs and $CD8^+$ T cells in vitiligo pathogenesis [6, 14, 15]. Surprisingly, we did not find significant difference in Treg-mediated suppression of $CD4^+$ T cells in vitiligo patients (Figure 3(a)). This might be due to lower sample size in the available studies, difference in detection of effector cells proliferation, i.e., BrdU ELISA or [^{3}H] thymidine incorporation assay, and differences in activation of T cells, i.e., through antigen presenting cells or CD3/CD28 beads; hence, further studies with larger sample size and uniform detection methods are needed to confirm these findings. However, our meta-analysis suggested a trend for decreased Treg-mediated suppression of $CD4^+$ T cells in vitiligo patients as there was a 1.27 SMD decreased in Treg-mediated suppression of $CD4^+$ T cells in vitiligo patients (Figure 3(a)). Nevertheless, our meta-analysis suggested the crucial role of impaired Tregs' suppressive capacity in vitiligo pathogenesis.

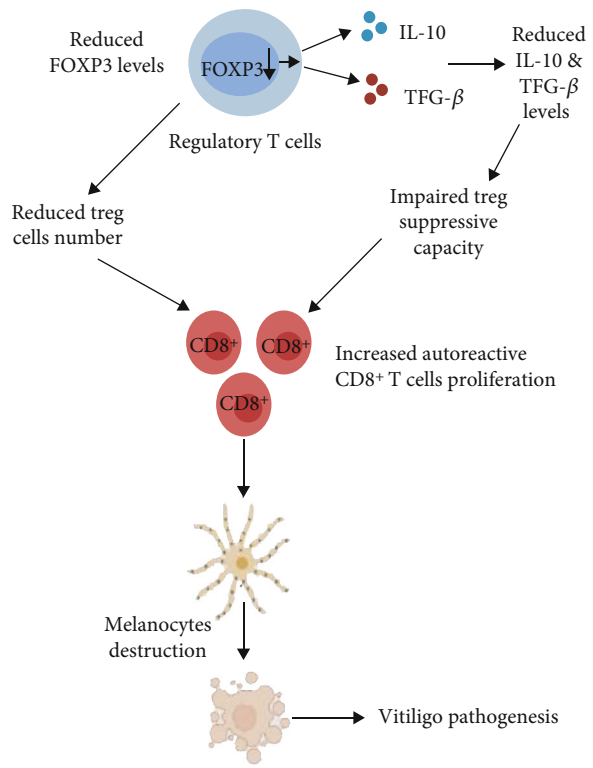

Figure 6: Role of regulatory T cells in vitiligo pathogenesis. The reduced expression of FOXP3, the key Tregs' transcription factors of Tregs, results in decreased expression of Tregs' suppressive cytokines (IL-10 and TGF-β) and impaired Tregs' suppressive capacity. Moreover, the reduced FOXP3 levels in the blood suggests reduced Tregs' number in vitiligo patients. Thus, the decreased Tregs' frequency and impaired Tregs' suppressive capacity lead to unchecked $CD8^+$ T proliferation, which results into melanocyte death and vitiligo pathogenesis.

As FOXP3 is an indispensable molecule for Tregs' number and suppressive function [44], next we assessed FOXP3 expression levels in blood and skin of vitiligo patients. Our meta-analysis suggested significantly decreased FOXP3 expression levels in blood and skin of vitiligo patients (Figure 3(b)). Additionally, our meta-analysis suggested the role of decreased FOXP3 expression in disease activity of vitiligo (Figure S1a). These results were in concordance with the previous studies [5, 9, 17–20, 22, 24–26]. The decreased FOXP3 protein and transcript levels in the blood may be due to the reduced Tregs' frequency in vitiligo patients; therefore, our meta-analysis further suggests for the role of decreased Tregs' frequency in vitiligo pathogenesis. Moreover, the FOXP3 expression was significantly reduced in lesional skin as compared to perilesional and nonlesional skin of vitiligo patients (Figure S1b, c), indicating that FOXP3 expressing Treg cells are indeed crucial for suppressing autoreactive melanocyte-specific $CD8^+$ T cells in lesional skin. Since FOXP3 plays a crucial role in phenotype and suppressive function of Tregs, our recent study also reported a positive correlation of FOXP3 levels with Treg cells' suppressive capacity in vitiligo [22]. Therefore, the decreased expression of FOXP3 in lesional skin, as suggested by our meta-analysis, further establishes the role of impaired Tregs' suppressive capacity in vitiligo pathogenesis.

Furthermore, FOXP3 governs the expression of downstream Tregs' suppressive cytokines such as IL-10 and TGF-β [23]. Apart from cell-to-cell contact, Treg cells maintain peripheral tolerance by secreting immunosuppressive cytokines such as IL-10 and TGF-β [45]. Moreover, IL-10 in presence of TGF-β also improves Treg cell expansion [45]. Hence, we further evaluated the role of IL-10 and TGF-β in vitiligo. Interestingly, our meta-analysis suggested a significant decrease in IL-10 expression levels in vitiligo patients more specifically in blood of vitiligo patients (Figure 4(a)). These findings were in concordance with the previous studies [5, 21, 22, 28–30] indicating the indispensable role of IL-10 in vitiligo pathogenesis. TGF-β is a pleotropic immunosuppressive cytokine, which regulates the immune response by suppressing T and B cells. Additionally, it plays a crucial role in proliferation and induction of Tregs [46]. Interestingly, the meta-analysis suggested significant decrease in TGF-β levels in vitiligo patients (Figure 4(b)). These results corroborate with the previous studies [5, 20–22, 28, 29, 31, 32]; however, these results contrast with few reports [24, 36, 37]. The contrasting results may be due to differences in sample size and methodology used for TGF-β detection, i.e., differences in ELISA kits with varying sensitivities and differences in antibodies used for detection of TGF-β. Moreover, there was no difference in IL-10 and TGF-β expression levels in skin of vitiligo patients, which might be due to lower sample size and differences in IL-10 and TGF-β detection techniques, i.e., ELISA and immunohistochemical staining. Furthermore, we could only find two studies assessing IL-10 and TGF-β expression levels in skin of vitiligo patients; hence, future studies with larger sample size are needed to confirm these findings. Additionally, we could not find significant difference in IL-10 and TGF-β levels between AV and SV patients (Figure S2a, b), which could be due to the less sample size and lower number of studies assessing disease activity-based analysis. However, we observed a trend of decreased IL-10 and TGF-β levels in AV patients, as there was a 1.67 and 3.49 SMD decrease in IL-10 and TGF-β levels, respectively (Figure S2a, b), indicating a likely role of IL-10 and TGF-β in vitiligo progression. Overall, our meta-analysis with the previously available studies suggests the crucial role of IL-10 and TGF-β in vitiligo pathogenesis.

Interestingly, our recent study has also suggested that the decreased expression of FOXP3 leads to impaired Tregs' suppressive capacity in vitiligo [22]. Therefore, our meta-analysis taking into consideration all the available data suggests that the reduced FOXP3 expression levels could lead to decreased downstream Tregs' suppressive cytokines IL-10 and TGF-β, thereby results into impaired Tregs' suppressive capacity. Moreover, the decreased Tregs' frequency and impaired Tregs' suppressive function could lead to widespread activation and expansion of $CD8^+$ T cells resulting into melanocytes destruction and vitiligo pathogenesis (Figure 6).

Furthermore, we evaluated Tregs' frequency, FOXP3, and IL-10 expression posttreatment in vitiligo. Interestingly,

out meta-analysis revealed increased Treg cells' frequency, FOXP3, and IL-10 expression after microRNA-based treatment, narrow band–UVB phototherapy, and Treg-associated treatments in vitiligo (Figures 5(a)–5(c)). The subgroup analysis suggested significant increase in Tregs' frequency, FOXP3, and IL-10 levels in vitiligo mice model studies (Figures 5(a)–5(c)). Additionally, we found significantly, increased FOXP3 and IL-10 levels in human studies (Figures 5(b) and 5(c)). However, we did not find significant increase in Tregs' frequency posttreatment in human studies (Figure 5(a)), which could be due to lower number of studies and less sample size. Nevertheless, our meta-analysis suggested a trend of increased Treg cells' frequency after treatment as there was 1.16 SMD increase in Tregs' frequency after treatment (Figure 5(a)). Moreover, our meta-analysis suggested improved Tregs' frequency, FOXP3, and IL-10 expression posttreatment in human and mice model studies, which is in concordance to the previous studies [47–53]. According to the studies included in the meta-analysis, treating vitiligo mouse models with antigen-specific CAR Tregs, PD-L1 fusion peptides, and CCL22 DNA reverses depigmentation by increasing the number of Tregs and FOXP3 expression in the skin [47, 50, 51]. Additionally, polymeric nanoparticles containing rapamycin and autoantigens induce antigen-specific immune tolerance, thereby inhibiting vitiligo in mouse models of vitiligo [53]. Furthermore, in human studies, tacrolimus, miR-155, and HO-1 increase the IL-10 expression in vitiligo lesions, whereas narrow band-UVB phototherapy, miR-21-5p, and miR-155 enhance the Tregs' frequency and FOXP3 levels, thereby suppressing the melanocyte destruction caused by unregulated Th1 pathways [19, 21, 48, 49, 52]. Therefore, such Treg-based therapeutics can control depigmentation and support immune tolerance in vitiligo. Additionally, our recent study has highlighted that calcium treatment significantly increases Treg cells' suppressive capacity in vitiligo pathogenesis [54]. Overall, our meta-analysis taking into consideration all the available data suggests that targeting Treg cells in vitiligo patients could lead to effective Treg-based therapeutics for vitiligo.

The limitations of the meta-analysis were inclusion of only the studies published in English language, interstudy heterogeneity, and analysis based on the type of vitiligo which could not be carried out due to scarcity of such studies involving type of vitiligo-based analysis. Moreover, the role of innate lymphoid cells subpopulations (ILC1, ILC2, ILC3, and ILCregs) in pathogenesis of various autoimmune and inflammatory diseases including Crohn's disease, atopic dermatitis, inflammatory bowel disease, psoriasis, multiple sclerosis, and colitis, has been suggested [55]. However, studies assessing the role of ILC in vitiligo are lacking; hence, it was not included in this meta-analysis. Nevertheless, the strengths of our meta-analysis were no publication bias for the enrolled studies and high statistical power due to population diversity. Additionally, sensitivity analysis suggested no influence of single study on overall SMD. Moreover, FOXP3, IL-10, and TGF-β levels in blood and skin were assessed by subgroup analysis, and disease activity-based analysis was also carried out.

5. Conclusions

This is the first meta-analysis conducted for confirming the role of Tregs in vitiligo pathogenesis. The pooled results of the meta-analysis suggested for crucial role of decreased Treg cells' frequency and FOXP3 expression in vitiligo pathogenesis and progression. The meta-analysis suggested an impaired Tregs' suppressive capacity in vitiligo patients; particularly the meta-analysis highlighted the reduced Treg-mediated suppression of $CD8^+$ T cells in vitiligo patients, which was also supported by decreased levels of key immunosuppressive cytokines (IL-10 and TGF-β). However, more number of studies is warranted with larger sample size for confirming the role of Tregs in vitiligo progression. This meta-analysis also revealed an increase in Tregs' frequency, FOXP3 expression, and IL-10 expression in vitiligo after microRNA-based treatment, narrow band–UVB phototherapy, and Treg-associated treatments, indicating that targeting Treg cells in vitiligo patients could lead to effective therapeutics.

Data Availability

Data will be available on request from the authors.

Conflicts of Interest

We wish to confirm that there are no known conflicts of interest associated with this publication and there has been no significant financial support for this work that could have influenced its outcome.

Authors' Contributions

Prashant S. Giri contributed to the investigation, methodology, validation, formal analysis, and writing-original draft preparation; Jahanvi Mistry contributed to the investigation, methodology, validation, and formal analysis; Mitesh Dwivedi contributed to the conceptualization, funding acquisition, investigation, methodology, analysis and validation, project administration, resources, supervision, and writing-reviewing and editing.

Acknowledgments

We thank the Science and Engineering Research Board, Department of Science and Technology (SERB-DST), New Delhi, India, for providing the research grant to Dr. Mitesh Dwivedi (ECR/2017/000858 and CRG/2021/002419). PSG thanks the SERB-DST, New Delhi, for awarding SRF. PSG thanks Knowledge Consortium of Gujarat, Department of Education Government of Gujarat, for Awarding SHoDH (ScHeme Of Developing High quality research) Fellowship. We are also thankful to Uka Tarsadia University, Gujarat, India, for providing necessary facilities to conduct the study.

Supplementary Materials

Supplementary 1. Table S1: search strategy for inclusion of studies in the meta-analysis. Table S2: PRISMA checklist. Table S3: Newcastle–Ottawa quality assessment scale for

selected studies. Table S4: test for publication bias. Table S5: sensitivity analysis: standardized mean difference for Tregs' frequency in vitiligo patients and controls. Table S6: sensitivity analysis: standardized mean difference for Tregs' suppressive capacity levels in vitiligo patients and controls. Table S7: sensitivity analysis: standardized mean difference for FOXP3 protein levels in vitiligo patients and controls. Table S8: sensitivity analysis: standardized mean difference for IL-10 protein levels in vitiligo patients and controls. Table S9: sensitivity analysis: standardized mean difference for TGF-β levels in vitiligo patients and controls. Table S10: sensitivity analysis: standardized mean difference for Treg levels in vitiligo posttreatment. Table S11: sensitivity analysis: standardized mean difference foxp3 levels in vitiligo post treatment. Table S12: sensitivity analysis: standardized mean difference for IL-10 levels in vitiligo post treatment.

Supplementary 2. Figure S1: the forest plots for FOXP3 expression levels in active vitiligo and stable vitiligo patients and lesional, perilesional, and nonlesional skin of vitiligo patients. (a) FOXP3 protein expression in active vitiligo patients vs. stable vitiligo patients ($p = 0.01$; SMD: -2.99 [-5.26, -0.71]). (b) FOXP3 levels in lesional skin vs. perilesional skin ($p = 0.007$, SMD: -9.77 [-16.91, -2.62]). (c) FOXP3 levels in lesional skin vs. nonlesional skin ($p = 0.04$, SMD: -1.01 [-1.95, -0.06]). Figure S2: the forest plots for IL-10 and TGF-β expression levels in active vitiligo and stable vitiligo patients. (a) IL-10 protein expression in active vitiligo patient's vs. stable vitiligo patients ($p = 0.09$, SMD: -1.67 [-3.59, 0.25]). (b) TGF-β levels in active vitiligo patient's vs. stable vitiligo patients ($p = 0.06$; SMD: -3.49 [-7.08, 0.10]).

References

[1] C. Bergqvist and K. Ezzedine, "Vitiligo: a review," *Dermatology*, vol. 236, no. 6, pp. 571–592, 2020.

[2] C. Kruger and K. U. Schallreuter, "A review of the worldwide prevalence of vitiligo in children/adolescents and adults," *International Journal of Dermatology*, vol. 51, no. 10, pp. 1206–1212, 2012.

[3] M. Dwivedi, N. C. Laddha, A. P. Weetman, R. Begum, and H. Kemp, "Vitiligo–a complex autoimmune skin depigmenting," *Autoimmunity: Pathogenesis, Clinical Aspects and Therapy of Specific Autoimmune Diseases*, vol. 153, 2015.

[4] R. A. Spritz and G. H. L. Andersen, "Genetics of vitiligo," *Dermatologic Clinics*, vol. 35, no. 2, pp. 245–255, 2017.

[5] P. S. Giri, M. Dwivedi, N. C. Laddha, R. Begum, and A. H. Bharti, "Altered expression of nuclear factor of activated T cells, forkhead box P3, and immune-suppressive genes in regulatory T cells of generalized vitiligo patients," *Pigment Cell & Melanoma Research*, vol. 33, no. 4, pp. 566–578, 2020.

[6] M. Dwivedi, E. H. Kemp, N. C. Laddha, M. S. Mansuri, A. P. Weetman, and R. Begum, "Regulatory T cells in vitiligo: implications for pathogenesis and therapeutics," *Autoimmunity Reviews*, vol. 14, no. 1, pp. 49–56, 2015.

[7] S. D. Jadeja, J. M. Mayatra, J. Vaishnav, N. Shukla, and R. Begum, "A concise review on the role of endoplasmic reticulum stress in the development of autoimmunity in vitiligo pathogenesis," *Frontiers in Immunology*, vol. 11, p. 3817, 2021.

[8] M. Dwivedi, N. C. Laddha, P. Arora, Y. S. Marfatia, and R. Begum, "Decreased regulatory T-cells and $CD4^+/CD8^+$ ratio correlate with disease onset and progression in patients with generalized vitiligo," *Pigment Cell & Melanoma Research*, vol. 26, no. 4, pp. 586–591, 2013.

[9] P. S. Giri, S. Patel, R. Begum, and M. Dwivedi, "Association of *FOXP3* and *GAGE10* promoter polymorphisms and decreased FOXP3 expression in regulatory T cells with susceptibility to generalized vitiligo in Gujarat population," *Gene*, vol. 768, article 145295, 2021.

[10] N. C. Laddha, M. Dwivedi, M. S. Mansuri et al., "Association of neuropeptide Y (*NPY*), interleukin-1B (*IL1B*) genetic variants and correlation of *IL1B* transcript levels with vitiligo susceptibility," *PLoS One*, vol. 9, no. 9, article e107020, 2014.

[11] S. D. Jadeja, M. S. Mansuri, M. Singh, M. Dwivedi, N. C. Laddha, and R. Begum, "A case-control study on association of proteasome subunit beta 8 (PSMB8) and transporter associated with antigen processing 1 (TAP1) polymorphisms and their transcript levels in vitiligo from Gujarat," *PLoS One*, vol. 12, no. 7, article e0180958, 2017.

[12] M. Imran, N. C. Laddha, M. Dwivedi et al., "Interleukin-4 genetic variants correlate with its transcript and protein levels in patients with vitiligo," *The British Journal of Dermatology*, vol. 167, no. 2, pp. 314–323, 2012.

[13] M. Dwivedi, N. C. Laddha, M. S. Mansuri, Y. S. Marfatia, and R. Begum, "Association of NLRP1 genetic variants and mRNA overexpression with generalized vitiligo and disease activity in a Gujarat population," *The British Journal of Dermatology*, vol. 169, no. 5, pp. 1114–1125, 2013.

[14] J. Klarquist, C. J. Denman, C. Hernandez et al., "Reduced skin homing by functional Treg in vitiligo," *Pigment Cell & Melanoma Research*, vol. 23, no. 2, pp. 276–286, 2010.

[15] R. L. Riding and J. E. Harris, "The role of memory $CD8^+$ T cells in vitiligo," *Journal of Immunology*, vol. 203, no. 1, pp. 11–19, 2019.

[16] S. Sakaguchi, "Naturally arising $CD4^+$ regulatory T cells for immunologic self-tolerance and negative control of immune responses," *Annual Review of Immunology*, vol. 22, no. 1, pp. 531–562, 2004.

[17] D. S. Hegab and M. A. S. Attia, "Decreased circulating T regulatory cells in Egyptian patients with nonsegmental vitiligo: correlation with disease activity," *Dermatology Research and Practice*, vol. 2015, Article ID 145409, 7 pages, 2015.

[18] Y. Lili, W. Yi, Y. Ji, S. Yue, S. Weimin, and L. Ming, "Global activation of $CD8^+$ cytotoxic T lymphocytes correlates with an impairment in regulatory T cells in patients with generalized vitiligo," *PLoS One*, vol. 7, no. 5, article e37513, 2012.

[19] J. Huo, T. Liu, F. Li, X. Song, and X. Hou, "MicroRNA-21-5p protects melanocytes via targeting STAT3 and modulating Treg/Teff balance to alleviate vitiligo," *Molecular Medicine Reports*, vol. 23, no. 1, p. 51, 2021.

[20] M. K. Tembhre, A. S. Parihar, V. K. Sharma, A. Sharma, P. Chattopadhyay, and S. Gupta, "Alteration in regulatory T cells and programmed cell death 1-expressing regulatory T cells in active generalized vitiligo and their clinical correlation," *The British Journal of Dermatology*, vol. 172, no. 4, pp. 940–950, 2015.

[21] Q. Zhang, T. Cui, Y. Chang et al., "HO-1 regulates the function of Treg: association with the immune intolerance in vitiligo," *Journal of Cellular and Molecular Medicine*, vol. 22, no. 9, pp. 4335–4343, 2018.

[22] P. S. Giri, M. Dwivedi, and R. Begum, "Decreased suppression of $CD8^+$ and $CD4^+$ T cells by peripheral regulatory T cells in generalized vitiligo due to reduced NFATC1 and FOXP3 proteins," *Experimental Dermatology*, vol. 29, no. 8, pp. 759–775, 2020.

[23] A. Corthay, "How do regulatory T cells work?," *Scandinavian Journal of Immunology*, vol. 70, no. 4, pp. 326–336, 2009.

[24] S. Bhardwaj, S. Rani, M. S. Kumaran, A. Bhatia, and D. Parsad, "Expression of Th17- and Treg-specific transcription factors in vitiligo patients," *International Journal of Dermatology*, vol. 59, no. 4, pp. 474–481, 2020.

[25] M. Abou Elela, R. A. Hegazy, M. M. Fawzy, L. A. Rashed, and H. Rasheed, "Interleukin 17, interleukin 22 and FoxP3 expression in tissue and serum of non-segmental vitiligo: a case-controlled study on eighty-four patients," *European Journal of Dermatology*, vol. 23, no. 3, pp. 350–355, 2013.

[26] R. A. Hegazy, M. M. Fawzy, H. I. Gawdat, N. Samir, and L. A. Rashed, "T helper 17 and Tregs: a novel proposed mechanism for NB-UVB in vitiligo," *Experimental Dermatology*, vol. 23, no. 4, pp. 283–286, 2014.

[27] M. Bettini and D. A. A. Vignali, "Regulatory T cells and inhibitory cytokines in autoimmunity," *Current Opinion in Immunology*, vol. 21, no. 6, pp. 612–618, 2009.

[28] M. H. EL-Komy, D. M. Kadry, I. Amin, O. M. Abu-Zeid, D. M. Abdel-Halim, and L. A. Rashed, "Serum and tissue transforming growth factor $\beta 1$ expression in vitiligo," *Journal of the Egyptian Women's Dermatologic Society*, vol. 9, no. 3, pp. 151–155, 2012.

[29] M. Kidir, A. A. Karabulut, M. E. Ercin, and P. Atasoy, "Regulatory T-cell cytokines in patients with nonsegmental vitiligo," *International Journal of Dermatology*, vol. 56, no. 5, pp. 581–588, 2017.

[30] Y. Ala, M. K. Pasha, R. N. Rao, P. L. Komaravalli, and P. Jahan, "Association of IFN-γ : IL-10 cytokine ratio with nonsegmental vitiligo pathogenesis," *Autoimmune Diseases*, vol. 2015, Article ID 423490, 8 pages, 2015.

[31] A. M. Osman, M. M. Mukhtar, K. H. Bakheit, and H. Z. Hamdan, "Plasma levels of interleukin-17, interleukin-23, and transforming growth factor-β in Sudanese patients with vitiligo: a case-control study," *Indian Journal of Dermatology*, vol. 60, no. 6, p. 635, 2015.

[32] C.-X. Tu, W.-W. Jin, M. Lin, Z. H. Wang, and M. Q. Man, "Levels of TGF-β_1 in serum and culture supernatants of $CD4^{+-}$ $CD25^+$ T cells from patients with non-segmental vitiligo," *Archives of Dermatological Research*, vol. 303, no. 9, pp. 685–689, 2011.

[33] M. Abdallah and A. Saad, "Evaluation of circulating CD4+ CD25highFoxP3+ T lymphocytes in active non-segmental vitiligo," *Journal of Pan-Arab League of Dermatologists*, vol. 20, p. 1, 2009.

[34] R. Kalaiselvi, M. Rajappa, L. Chandrasekhar, D. Thappa, and P. Munisamy, "Immunophenotype of circulatory T-helper cells in patients with non-segmental vitiligo," *Advances in Dermatology and Allergology/Postępy Dermatologii i Alergologii*, vol. 36, no. 4, pp. 449–454, 2019.

[35] L. Zhou, K. Li, Y.-L. Shi et al., "Systemic analyses of immunophenotypes of peripheral T cells in non-segmental vitiligo: implication of defective natural killer T cells," *Pigment Cell & Melanoma Research*, vol. 25, no. 5, pp. 602–611, 2012.

[36] B. M. Ghanem, M. E.-S. Sallam, K. A. El-Hawary, D. EL-Tantawy, R-A. Ahmed, and M. Darwish, "Transforming growth factor-$\beta 1$ in the skin and serum of patients with non-segmental vitiligo," *Asian Journal of Dermatology*, vol. 9, pp. 1–6, 2016.

[37] L. Zhou, Y.-L. Shi, K. Li et al., "Increased circulating Th17 cells and elevated serum levels of TGF-beta and IL-21 are correlated with human non-segmental vitiligo development," *Pigment Cell & Melanoma Research*, vol. 28, no. 3, pp. 324–329, 2015.

[38] A. Liberati, D. G. Altman, J. Tetzlaff et al., "The PRISMA statement for reporting systematic reviews and meta-analyses of studies that evaluate healthcare interventions: explanation and elaboration," *BMJ*, vol. 339, p. b2700, 2009.

[39] P. S. Giri, R. Begum, and M. Dwivedi, "Meta-analysis for association of TNFA-308 (G> A) SNP with vitiligo susceptibility," *Gene*, vol. 809, p. 146027, 2022.

[40] H. Han and K. J. Dawson, *JASP (software)*, 2020.

[41] S. Sakaguchi, N. Sakaguchi, M. Asano, M. Itoh, and M. Toda, "Immunologic self-tolerance maintained by activated T cells expressing IL-2 receptor alpha-chains (CD25). Breakdown of a single mechanism of self-tolerance causes various autoimmune diseases," *Journal of Immunology*, vol. 155, pp. 1151–1164, 1995.

[42] M. Dominguez-Villar and D. A. Hafler, "Regulatory T cells in autoimmune disease," *Nature Immunology*, vol. 19, no. 7, pp. 665–673, 2018.

[43] T. Morita, Y. Shima, J. B. Wing, S. Sakaguchi, A. Ogata, and A. Kumanogoh, "The proportion of regulatory T cells in patients with rheumatoid arthritis: a meta-analysis," *PLoS One*, vol. 11, no. 9, article e0162306, 2016.

[44] E. M. Shevach, "Mechanisms of $foxp3^+$ T regulatory cell-mediated suppression," *Immunity*, vol. 30, no. 5, pp. 636–645, 2009.

[45] P. Hsu, B. Santner-Nanan, M. Hu et al., "IL-10 potentiates differentiation of human induced regulatory T cells via STAT3 and Foxo1," *Journal of Immunology*, vol. 195, no. 8, pp. 3665–3674, 2015.

[46] Y. Y. Wan and R. A. Flavell, "'Yin–Yang' functions of transforming growth factor-β and T regulatory cells in immune regulation," *Immunological Reviews*, vol. 220, no. 1, pp. 199–213, 2007.

[47] Z. Mukhatayev, E. R. Dellacecca, C. Cosgrove et al., "Antigen specificity enhances disease control by Tregs in vitiligo," *Frontiers in Immunology*, vol. 11, 2020.

[48] E. Sohafy, M. A. Mageed, B. M. Ghanem, S. S. Mitwally, and R. A. Elshawaf, "Effect of narrow band–UVB phototherapy on circulating T-regulatory cells and serum IL-17 level in Egyptian patients with non-segmental vitiligo," *Egyptian Journal of Hospital Medicine*, vol. 85, no. 1, pp. 3098–3103, 2021.

[49] M. Lv, Z. Li, J. Liu et al., "MicroRNA-155 inhibits the proliferation of CD8+ T-cells via upregulating regulatory T cells in vitiligo," *Molecular Medicine Reports*, vol. 20, pp. 3617–3624, 2019.

[50] J. M. Eby, H.-K. Kang, S. T. Tully et al., "CCL22 to activate Treg migration and suppress depigmentation in vitiligo," *The Journal of Investigative Dermatology*, vol. 135, no. 6, pp. 1574–1580, 2015.

[51] X. Miao, R. Xu, B. Fan et al., "PD-L1 reverses depigmentation in Pmel-1 vitiligo mice by increasing the abundance of Tregs in the skin," *Scientific Reports*, vol. 8, no. 1, p. 1605, 2018.

[52] Z. A. Taher, G. Lauzon, S. Maguiness, and M. T. Dytoc, "Analysis of interleukin-10 levels in lesions of vitiligo following

treatment with topical tacrolimus," *The British Journal of Dermatology*, vol. 161, no. 3, pp. 654–659, 2009.

[53] X. Zhang, D. Liu, M. He, M. Lin, C. Tu, and B. Zhang, "Polymeric nanoparticles containing rapamycin and autoantigen induce antigen-specific immunological tolerance for preventing vitiligo in mice," *Human Vaccines & Immunotherapeutics*, vol. 17, no. 7, pp. 1923–1929, 2021.

[54] P. S. Giri, A. H. Bharti, R. Begum, and M. Dwivedi, "Calcium controlled NFATc1 activation enhances suppressive capacity of regulatory T cells isolated from generalized vitiligo patients," *Immunology*, 2022.

[55] T. Dzopalić, B. Božić-Nedeljković, and V. Jurišić, "Function of innate lymphoid cells in the immune-related disorders," *Human Cell*, vol. 32, no. 3, pp. 231–239, 2019.

Hindawi
Journal of Immunology Research
Volume 2022, Article ID 3426717, 17 pages
https://doi.org/10.1155/2022/3426717

Research Article

Decreased *GZMB*, *NRP1*, *ITPR1*, and *SERPINB9* Transcripts Lead to Reduced Regulatory T Cells Suppressive Capacity in Generalized Vitiligo Patients

Prashant S. Giri,[1] **Ankit H. Bharti**,[2] **and Mitesh Dwivedi**[1]

[1]*C. G. Bhakta Institute of Biotechnology, Faculty of Science, Uka Tarsadia University, Bardoli, Surat, 394 350 Gujarat, India*
[2]*Independent Researcher, Vyara, Gujarat, India*

Correspondence should be addressed to Mitesh Dwivedi; mitesh_dwivedi@yahoo.com

Received 28 April 2022; Revised 24 June 2022; Accepted 24 August 2022; Published 15 September 2022

Academic Editor: Hector Mora-Montes

Generalized vitiligo (GV) is an autoimmune skin disease characterized by bilateral white patches over the entire body. Regulatory T cells (Tregs) maintain peripheral tolerance; however, they are found to be reduced in numbers and function in vitiligo patients. The exact mechanism for reduced Treg suppressive capacity is unknown. Therefore, we aimed to assess transcript levels of Tregs-associated immunosuppressive genes (*GZMB*, *NRP1*, *PDCD1*, *FASLG*, and *TNFRS18*), regulatory molecules of Tregs suppressive function (*SERPINB9*, *ITPR1*, and *UBASH3A*), and Treg-associated transcription factors (*GATA2*, *GATA3*, *RUNX1*, *STAT3*, and *STAT5*) in 52 GV patients and 48 controls by real-time PCR (qPCR). We found significantly reduced *GZMB*, *NRP1*, *SERPINB9*, and *ITPR1* transcripts in GV Tregs compared to controls ($p = 0.03$, $p = 0.023$, $p = 0.0045$, and $p < 0.0001$, respectively). There were 0.44-, 0.45-, 0.32-, and 0.54-fold decrease in *GZMB*, *NRP1*, *SERPINB9*, and *ITPR1* transcripts in GV Tregs. Additionally, disease activity and severity-based analyses revealed significantly decreased *GZMB* ($p = 0.019$ and 0.034), *SERPINB9* ($p = 0.031$ and $p = 0.035$), and *ITPR1* ($p = 0.0003$ and $p = 0.034$) transcripts in active vitiligo and severe GV patients' Tregs. Interestingly, we found a positive correlation for *ITPR1* with *GZMB* ($r = 0.45$, $p = 0.0009$) and *SERPINB9* ($r = 0.52$, $p = 0.001$) transcripts in GV Tregs. Moreover, we found positive correlation for percentage Treg mediated suppression of $CD4^+$ and $CD8^+$T cells with *ITPR1* ($r = 0.54$; $r = 0.49$), *GZMB* ($r = 0.61$; $r = 0.58$), *NRP1* ($r = 0.55$; $r = 0.52$), and *SERPINB9* ($r = 0.56$; $r = 0.48$) in GV Tregs. Further, calcium treatment of Tregs resulted into significantly increased *ITPR1*, *SERPINB9*, and *GZMB* transcripts in GV Tregs ($p = 0.023$, $p = 0.0345$, $p = 0.02$). Overall, our results for the first time revealed the crucial role of *GZMB*, *NRP1*, *SERPINB9*, and *ITPR1* transcripts in decreased Treg suppressive capacity leading to GV pathogenesis, progression, and severity. In addition, our study highlighted that *ITPR1* might be linked with decreased *GZMB* and *NRP1* expression in GV Tregs. Moreover, our study for the first time suggest that increased *SERPINB9* transcripts may lead to endogenous granzyme B-mediated Tregs apoptosis, and calcium treatment of Tregs may improve the Treg suppressive capacity. These findings may further aid in development of Treg-based therapeutics for GV.

1. Introduction

Generalized vitiligo (GV) is an autoimmune disease characterized by symmetrical white patches on the entire body [1]. Its prevalence is about 0.5 to 2% worldwide [2]. The key role of autoimmunity in GV has been suggested by the presence of autoantibodies and autoreactive $CD4^+$ and $CD8^+$ T cells in vitiligo skin lesions [3]. Furthermore, if they remain unchecked, these autoreactive T cells can lead to granzyme and FAS-FASL-mediated melanocyte destruction, leading to GV pathogenesis [4–8]. Additionally, our previous studies have found the role of inflammatory cytokines IFN-γ and TNF-α in melanocyte destruction [6, 9–11].

Regulatory T cells (Tregs) are crucial role in controlling such self-reactive T cells [12, 13]. However, previous studies have found altered Tregs number and function in vitiligo [6,

14, 15]. Moreover, our previous studies suggested impaired levels of the transcription factors of Tregs, such as nuclear factors of activated T cells (NFATs) and Forkhead box P3 (FOXP3) that led to reduced downstream immunosuppressive genes (IL-10, TGF-β, and CTLA-4), resulting in impaired Treg-mediated suppression of $CD4^+$ and $CD8^+$ T cells [6, 15, 16]. Thus, the impaired Treg suppressive capacity leads to widespread $CD8^+$ and $CD4^+$ T cells activation, proliferation, and IFN-γ production, which results in melanocyte destruction in GV patients [6, 15, 16].

In Tregs, the key immunosuppressive molecules such as granzyme B (*GZMB*), neuropilin-1 (*NRP1*), PDCD1 (programmed cell death protein 1 (PD-1) or CD279), FASLG (Fas ligand (FasL) or CD95L or CD178), and TNFRS18 (glucocorticoid-induced TNFR-related protein (GITR) or CD357) maintain Treg suppressive function [17–20]. Additionally, SERPINB9 (Serpin family B member 9) endogenous inhibitor of granzyme B protects Tregs from self-inflicted granzyme B-mediated apoptosis [21]. Moreover, inositol 1,4,5-trisphosphate receptor type 1 (ITPR1) regulates calcium entry in T cells. Furthermore, UBASH3A (ubiquitin associated and SH3 domain-containing A) governs T cells' function by regulating the TCR-CD3 complex [22]. Nevertheless, transcription factors such as GATA-binding factor 2 (GATA2), GATA3, runt-related transcription factor 1 (RUNX1), signal transducer and activator of transcription 3 (STAT3), and STAT5 also play a critical role in Treg cells' function [23–27]. Although the role of NFATs and FOXP3 in Treg dysfunction has been suggested previously, the role of Tregs-associated immunosuppressive genes (*GZMB*, *NRP1*, *PDCD1*, *FASLG*, and *TNFRS18*), regulatory molecules of Tregs function (*SERPINB9*, *ITPR1*, and *UBASH3A*), and Treg-associated transcription factors (*GATA2*, *GATA3*, *RUNX1*, *STAT3*, and *STAT5*) is unknown in GV.

Therefore, to delineate the exact pathway of Treg cells dysfunction, the current study aimed to study the mRNA expression levels of (i) Tregs-associated immunosuppressive genes (*GZMB*, *NRP1*, *PDCD1*, *FASLG*, and *TNFRS18*), (ii) regulatory molecules of Tregs function (*SERPINB9*, *ITPR1*, and *UBASH3A*), and (iii) Treg associated transcription factors (*GATA2*, *GATA3*, *RUNX1*, *STAT3*, and *STAT5*) in GV pathogenesis, progression, and severity. Additionally, we carried out the age of onset and gender-based analysis for these genes to study their effect on age of onset and gender biasness for GV pathogenesis.

2. Materials and Methods

2.1. Study Population. A total of 52 GV patients and 48 healthy controls were included in the study. Table 1 depicts the demographic details for the enrolled participants. Vitiligo was diagnosed by a dermatologist from Aura skin care clinic, Vyara, India, by observing symmetrical white color lesions on skin under woods lamps. Newborn babies, pregnant/lactating women, patients on treatment, and patients with other autoimmune diseases were excluded from the study. Controls were free from any signs of vitiligo and other autoimmune diseases. The study protocol was per the Institutional Human Research Ethics Committee (IHREC), Maliba Pharmacy College, UKA Tarsadia University, India. The study protocol followed the Helsinki Declaration of 1964 and its successful amendments. The GV patients were divided into active vitiligo (AV) patients and stable vitiligo (SV) patients as mentioned previously [15]. The patients were categorized as AV, if they developed any increase in lesions size or number within the past six months; otherwise, they were categorized as SV [28]. Moreover, patients were categorized based on the disease severity measured by the vitiligo area scoring index (VASI) as described by Bhor and Pande [29]. GV patients were divided into three groups: (i) 10%-25% VASI: mild GV; (ii) 25%-50% VASI: moderate GV; and (iii) 50%-75%: severe GV, as mentioned previously [6].

2.2. Isolation of $CD4^+CD25^+$ Treg Cells and $CD4^+$ T Cells. $CD4^+CD25^+$ Treg cells and $CD4^+$ T cells were isolated from three-milliliter peripheral blood of 52 GV patients and 48 controls using MACSxpress® whole blood Treg isolation kit (Miltenyi Biotec, Auburn, CA) as mentioned previously [15]. In the first step, all the non-$CD4^+$ cells were removed from the whole blood using MACSxpress beads by negative selection. In the second step, through positive selection, the $CD4^+CD25^+$ Treg cells were enriched from $CD4^+$ T cells using microbeads and LS columns under a strong magnetic field. Flow cytometry was carried out to confirm the purity of isolated Treg cells (Figure 1), the purity of isolated $CD3^{+-}$ $CD4^+CD25^+FOXP3^+$ Treg cells was found to be 94.22%. The isolated Treg cells were immediately processed for the downstream experiments.

2.3. Isolation of $CD8^+$ T Cells. $CD8^+$ T cells were isolated from two-milliliter blood sample of GV patients and controls using MACSxpress® whole blood CD8 T cell isolation kit human (Miltenyi Biotec, Auburn, CA) according to the manufacturer's instructions and as mentioned previously [6]. All the non-CD8 T cells were immunomagnetically depleted with MACSxpress beads. The isolated $CD8^+$ T cells were immediately processed for *in vitro* Treg suppression assay.

2.4. Total RNA Isolation and cDNA Synthesis. The total RNA was extracted from $CD4^+CD25^+$ Treg cells using TRIzol reagent (Invitrogen, Carlsbad, CA, USA) as mentioned previously [15]. RNA integrity, yield, and purity were determined by 1.5% gel electrophoresis and spectrophotometrically at 260/280 nm. The cDNA was synthesized from 1 μg of total RNA by iScript™ cDNA Synthesis Kit (Bio-Rad, CA, USA) as per the manufacturer's instructions.

2.5. Quantitative Real-Time PCR. The mRNA expression levels of Treg-associated genes *GZMB*, *NRP1*, *ITPR1*, *SERPINB9*, *PDCD1*, *FASLG*, *UBASH3A*, *IKZF4*, *GATA2*, *GATA3*, *TNFRSF18*, *RUNX1*, *STAT3*, and *STAT5* were measured with qPCR. Glyceraldehyde 3-phosphate dehydrogenase (*GAPDH*) gene expression levels were used as a reference gene. Gene-specific primers for the expression study are mentioned in Table S1. mRNA expression

Table 1: Demographic characteristics of generalized vitiligo (GV) patients and controls.

	GV patients ($n = 52$)	Controls ($n = 48$)
Average age (mean age ± SD)	37.04 ± 11.22 years	32.18 ± 3.18 years
Gender		
Male	28 (53.84%)	26 (54.16%)
Female	24 (46.16%)	22 (45.83%)
Age of onset (mean age ± SD)	18.23 ± 4.21 years	NA
Duration of disease (mean ± SD)	7.22 ± 4.24 years	NA
Extent of disease		
VASI score (mean ± SD)	58.12% ± 22.58%	NA
10–25% VASI (mild GV)	12 (23.07%)	
25–50% VASI (moderate GV)	18 (34.61%)	
50–75% VASI (severe GV)	22 (42.30%)	
Disease activity		
Active vitiligo	28 (54.00%)	NA
Stable vitiligo	24 (46.00%)	
Family history	20 (34.61%)	NA

analysis was carried out using iTaq Universal SYBR Green Supermix (Bio-Rad, CA, USA) as per the manufacturer's instructions. The qPCR conditions for the gene expressions study are mentioned in Table S1. The specificity of the qPCR products was checked by dissociation curve analysis (Figures S1 and S2). The fluorescence data were collected during the extension step and the cycle at which the fluorescence intensity raised above the background was termed as cycle threshold (C_T). The difference between the target and reference genes C_T was considered as ΔC_T value. The $\Delta\Delta C_T$ value was determined as the difference between the ΔC_T value of controls and patients. The fold change value in gene expression was calculated using $2^{-\Delta\Delta CT}$ formula.

2.6. In Vitro Calcium Treatment of Treg Cells. Treg cells were subjected to calcium treatment by dissolving 750 μM calcium (Cayman, MI, USA) in RPMI media. The dissolved calcium level in the medium was confirmed using calcium assay kit (Cayman, MI, USA). Treg cells were seeded in 24-well plate at density of 5×10^4 cells, in 1 ml RPMI medium supplemented with 5% FBS containing desired calcium concentration at 37°C at 5% CO_2 for 24 hours. The calcium-treated Treg cells were immediately processed for downstream *in vitro* functional assays. The standard curve for the estimation of calcium is presented in Figure S3.

2.7. In Vitro Treg Suppression Assay. $CD4^+CD25^+$ Treg cells (5000 cells) were co-cultured with $CD8^+$ T cells and $CD4^+$ T cells (10,000 cells) at a ratio of 1 : 2 individually, as mentioned previously [6]. The cells were activated with 200 IU rIL2 (PeproTech, NJ, USA) and anti-CD3/CD28 dynabeads Gibco; Thermo Fisher Scientific, Inc., Waltham, MA, USA) at a 1 : 1 (bead:cells) ratio in 200 μl RPMI supplemented with 10% fetal bovine serum for 5 days at 37°C and 5% CO_2 in 96 well U-bottom plate. On 4th day, the cells were labelled with 10 μM BrdU (Sigma-Aldrich, MO, USA) and incubated for 18 hrs and then further processed for BrdU cell proliferation assay as mentioned previously [6, 30, 31].

2.8. BrdU Cell Proliferation Assay. Incorporation of BrdU in proliferating cells was measured by BrdU cell proliferation enzyme-linked immunosorbent assay kit (Sigma-Aldrich, Missouri, USA) according to the manufacturer's instructions. Percentage suppression was calculated using the following formula: [(proliferation of Tconv cells alone – proliferation of Tconv cells treated with Treg)/proliferation of Tconv cells alone] x 100 [6, 31].

2.9. Correlation of ITPR1, GZMB, NRP1, and SERPINB9 Transcripts with In Vitro Treg Suppressive Capacity. The isolated Tregs population was divided into two fractions. The inherent levels of *ITPR1*, *GZMB*, *NRP1*, and *SERPINB9* transcripts were assessed from the first fraction, whereas *in vitro* Treg suppression assay was carried out from the second Treg fraction. Further, the inherent levels of *ITPR1*, *GZMB*, *NRP1*, and *SERPINB9* transcripts in Tregs of GV were correlated with the Treg suppressive capacity by Spearman's rank correlation analysis.

2.10. Statistical Analysis. The comparison of mean ΔC_T values in GV patients and controls for relative mRNA expression analysis, disease activity analysis, disease severity analysis, age of onset analysis, and gender-based analysis was carried out using nonparametric Mann–Whitney *U* test. The $2^{-\Delta\Delta CT}$ analysis was carried out to calculate the fold difference in gene expression. The statistical analysis was carried out using GraphPad prism software (Graphpad software

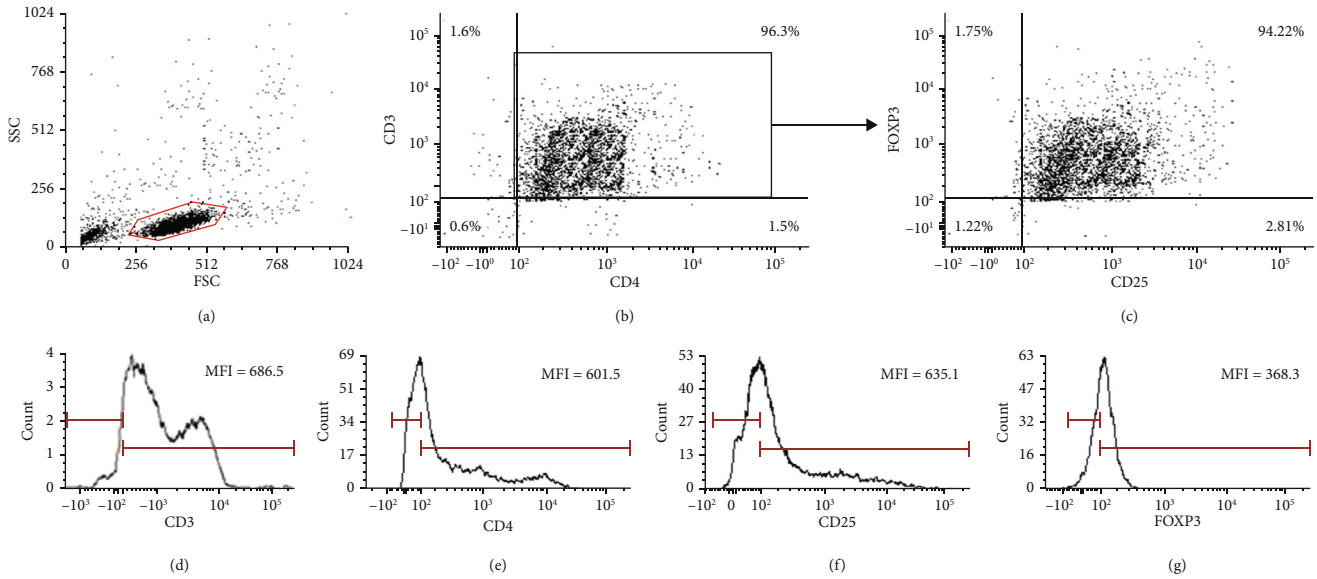

Figure 1: Gating strategy for $CD4^+CD25^+FOXP3^+$ Treg cells. Estimation of protein levels of CD4, and CD25. (a) Lymphocytes were gated on the basis of size and morphology. (b) $CD3^+CD4^+$T cells were gated on the basis of CD3 and CD4 expression.(c) Treg cells were gated on the basis of CD3, CD4, CD25, and FOXP3 expression. The purity of isolated $CD3^+CD4^+CD25^+FOXP3^+$ Treg cells was found to be 94.22%. (d) Expression of CD3 in T cells. Representative graph shows the amount of CD3 in the T cells as mean fluorescence intensity (MFI). (e) Expression of CD4 in T cells. Representative graph shows amount of CD4 in the T cells as mean fluorescence intensity (MFI). (f) Expression of CD25 in T cells. Representative graph shows amount of CD25 in the T cells as mean fluorescence intensity (MFI). (g) Expression of FOXP3 in T cells. Representative graph shows amount of intracellular FOXP3 in the T cells as mean fluorescence intensity (MFI).

Inc.; San Diego, CA, USA, 2003). $p \leq 0.05$ was considered statistically significant.

3. Results

3.1. Transcript Levels of Tregs Associated Immunosuppressive Genes (GZMB, NRP1, PDCD1, FASLG, and TNFRS18) in GV Patients and Controls. The transcript levels of Tregs-associated immunosuppressive genes (*GZMB*, *NRP1*, *PDCD1*, *FASLG*, and *TNFRS18*) were assessed in 52 GV patients and 48 controls using nonparametric Mann–Whitney *U* test after normalization with *GAPDH* expression. We found significantly reduced transcript levels for *GZMB* and *NRP1* expression in GV Tregs compared to control Tregs ($p = 0.03$ and $p = 0.023$; Figures 2(a) and 2(d)). The $2^{-\Delta\Delta CT}$ analysis suggested a 0.44- and 0.45-fold difference in mRNA expression levels of *GZMB* and *NRP1* in GV Tregs compared to control Tregs (Figures 2(c) and 2(e)). Further, the disease activity and disease severity-based analysis suggested significantly reduced mRNA expression levels of *GZMB* in AV and severe GV Tregs compared to SV and mild GV Tregs ($p = 0.019$ and $p = 0.034$, respectively; Figures 2(a) and 2(b)). However, there was no significant difference in mRNA expression levels of *NRP1* in AV and severe GV Tregs compared to SV and mild GV Tregs ($p = 0.453$ and $p = 0.2642$; Figures 2(d) and 2(e)). Additionally, we did not find any significant difference in transcripts levels of *PDCD1*, *FASLG*, and *TNFRS18* in GV Tregs compared to control Tregs ($p > 0.05$; Figure S4). Moreover, the disease activity and disease severity-based analysis suggested no significant difference in transcripts levels of *PDCD1*, *FASLG*, and *TNFRS18* in AV and severe GV Tregs compared to SV and mild GV Tregs ($p > 0.05$; Figure S4).

3.2. Transcript Levels of SERPINB9, ITPR1, and UBASH3A (Regulatory Molecules of Treg Function) in GV Patients and Controls. The transcript levels for regulatory molecules of Treg function (*SERPINB9*, *ITPR1*, and *UBASH3A*) were assessed in 52 GV patients and 48 controls using nonparametric Mann–Whitney *U* test after normalization with *GAPDH* expression. Our study suggested significant decrease in transcript levels of *SERPINB9* and *ITPR1* for GV Tregs compared to controls' Tregs ($p = 0.045$ and $p < 0.0001$; Figures 3(a) and 3(d)). According to the $2^{-\Delta\Delta CT}$ analysis, there was a 0.32- and 0.54-fold difference in transcript levels of *SERPINB9* and *ITPR1* in GV Tregs compared to controls' Tregs (Figures 3(c) and 3(f)). Moreover, the disease activity and severity-based analysis suggested a significantly decreased mRNA expression levels of *SERPINB9* and *ITPR1* in AV Tregs ($p = 0.031$ and $p = 0.0003$; Figures 3(a) and 3(d)) and severe GV Tregs ($p = 0.035$ and $p = 0.034$; Figures 3(b) and 3(e)) as compared to SV and mild GV Tregs. However, we could not find any significant difference in transcript levels of *UBASH3A* for GV Tregs as compared to controls' Tregs ($p = 0.145$; Figure S5). The disease activity and severity-based analysis also suggested no significant difference in mRNA expression levels of *UBASH3A* in AV and severe GV Tregs compared to SV and mild GV Tregs ($p = 0.487$; Figure S5).

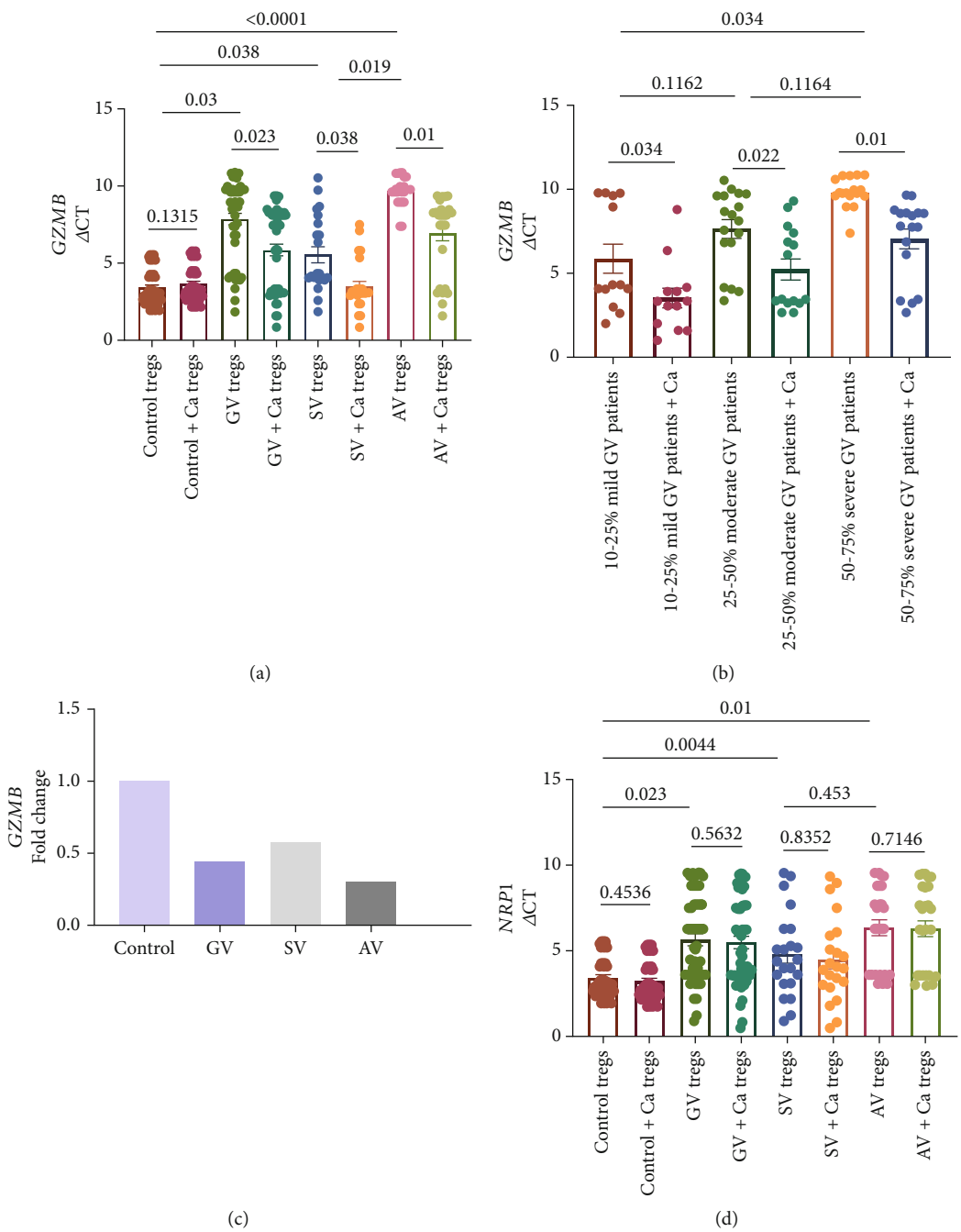

Figure 2: Continued.

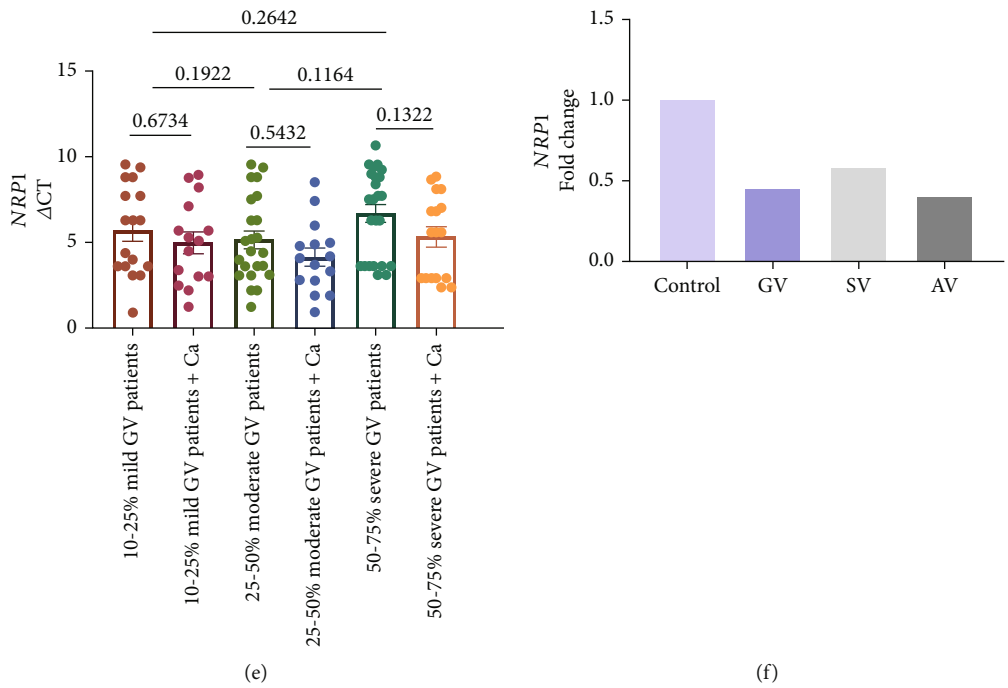

Figure 2: *GZMB* and *NRP1* transcripts in Tregs of GV patients and controls. *GZMB* and *NRP1* transcripts in Tregs of 52 GV patients and 48 controls were analyzed by Nonparametric Mann–Whitney *U* test. (a) *GZMB* transcripts in GV, SV, and AV vs controls' Tregs ($p = 0.03$, $p = 0.038$, and $p < 0.0001$, respectively). *GZMB* transcripts in AV vs SV Tregs ($p = 0.019$). *GZMB* transcripts in GV, SV, and AV Tregs before and after calcium treatment ($p = 0.023$, $p = 0.0328$, and $p = 0.01$). (b) *GZMB* transcripts in 50-75% severe GV vs 10-25% mild GV Tregs ($p = 0.034$). *GZMB* transcripts in moderate GV (25-50% VASI) vs mild GV (10-25% VASI) and severe GV (50-75% VASI) Tregs ($p = 0.1162$ and $p = 0.1164$, respectively). *GZMB* transcripts in mild GV, moderate GV, and severe GV Tregs before and after calcium treatment ($p = 0.034$, $p = 0.022$, and $p = 0.01$). (c) There was a 0.44-, 0.58-, and 0.30-fold changes in *GZMB* transcripts for GV, SV, and AV Tregs as compared to controls. (d) *NRP1* transcripts in GV, SV, and AV vs controls' Tregs ($p = 0.023$, $p = 0.044$, and $p = 0.001$, respectively). *NRP1* transcripts in AV vs SV Tregs ($p = 0.453$). *NRP1* transcripts in GV, SV, and AV Tregs before and after calcium treatment ($p = 0.5632$, $p = 0.8352$, and $p = 0.7146$). (e) *NRP1* transcripts in severe GV (50-75% VASI) vs mild GV (10-25% VASI) Tregs ($p = 0.2642$). *NRP1* transcripts in moderate GV (25-50% VASI) vs mild GV (10-25% VASI) and severe GV (50-75% VASI) Tregs ($p = 0.1922$ and $p = 0.1164$, respectively). *NRP1* transcripts in mild GV, moderate GV, and severe GV Tregs before and after calcium treatment ($p = 0.6734$, $p = 0.5432$, and $p = 0.1322$). (f) There was a 0.45-, 0.58-, and 0.40-fold changes in *NRP1* transcripts for GV, SV, and AV Tregs when compared to controls.

3.3. Transcripts Levels of Treg Associated Transcription Factors (GATA2, GATA3, RUNX1, STAT3, and STAT5) in GV Patients and Controls. The transcript levels for Treg-associated transcription factors (*GATA2*, *GATA3*, *RUNX1*, *STAT3*, and *STAT5*) were assessed in 52 GV patients and 48 controls using nonparametric Mann–Whitney *U* test after normalization with *GAPDH* expression. We did not find any significant difference for transcript levels of *GATA2*, *GATA3*, *RUNX1*, *STAT3*, and *STAT5* in GV Tregs when compared to controls' Tregs ($p > 0.05$; Figures S5 and S6). Moreover, the disease activity and severity-based analysis also suggested no significant difference in mRNA expression levels of *GATA2*, *GATA3*, *RUNX1*, *STAT3*, and *STAT5* in AV and severe GV Tregs as compared to SV and mild GV Tregs ($p > 0.05$; Figures S5 and S6).

3.4. Effect of Calcium Treatment on ITPR1, GZMB, NRP1, and SERPINB9 Transcripts in GV Patients' and Controls' Tregs. Previously, we have found that calcium treatment enhances the calcium uptake in Tregs resulting in increased NFATc1 activity which leads to enhanced Treg suppressive capacity in GV [32]. As *ITPR1*governs the release of calcium in Tregs and *GZMB*, *NRP1*, and *SERPINB9* are crucial for Treg cells activity, we studied the effect of calcium treatment on *ITPR1*, *GZMB*, *NRP1*, and *SERPINB9* transcripts in Tregs of GV patients and controls. Upon calcium treatment, we found significantly increased *ITPR1* transcripts in Tregs of GV, SV, and AV patients compared to controls ($p = 0.02$, $p = 0.0327$, and $p = 0.01$; Figure 3(d)). Interestingly, the calcium treatment led to an increased *SERPINB9* ($p = 0.0345$, $p = 0.0432$, and $p = 0.02$; Figure 3(a)) and *GZMB* ($p = 0.023$, $p = 0.038$, and $p = 0.01$; Figure 2(a)) transcripts in calcium-treated Tregs of GV, SV, and AV patients, respectively, compared to untreated Tregs of GV, SV, and AV patients, respectively. Moreover, the calcium treatment led to increased *ITPR1* ($p = 0.033$, $p = 0.021$, and $p = 0.01$; Figure 3(e)), *GZMB* ($p = 0.034$, $p = 0.022$, and $p = 0.01$; Figure 2(b)), and *SERPINB9* ($p = 0.034$, $p = 0.02$, and $p = 0.001$; Figure 3(b)) transcripts in mild GV, moderate GV and severe GV Tregs. We did not find any significant

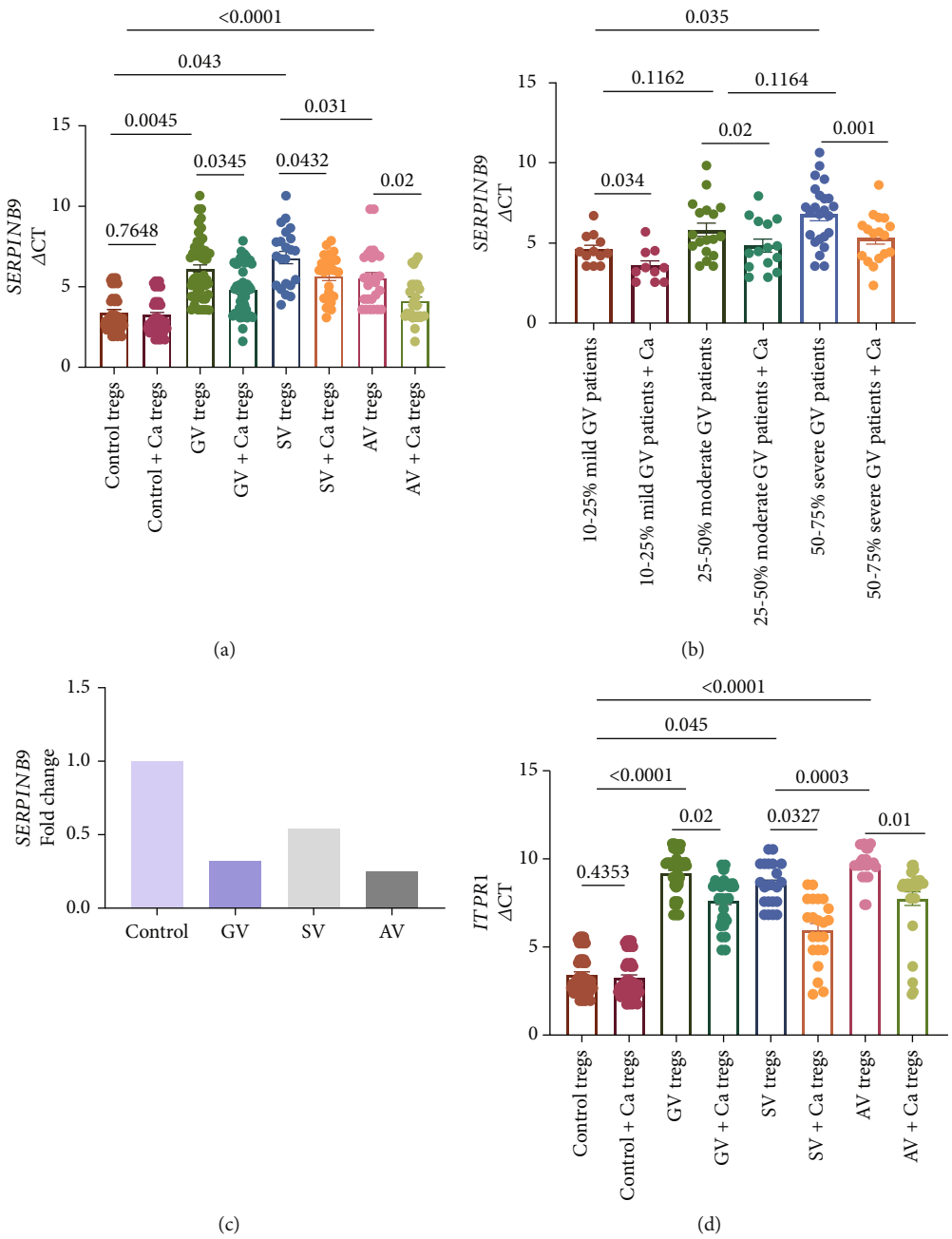

Figure 3: Continued.

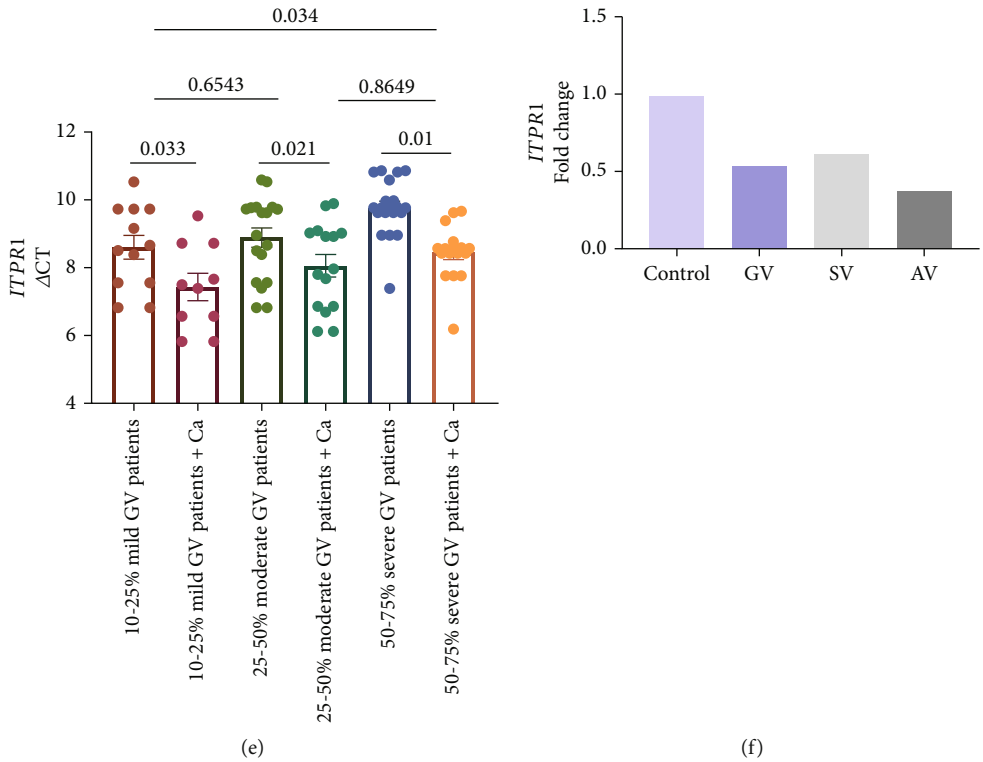

Figure 3: *SERPINB9* and *ITPR1* transcripts in Tregs of GV patients and controls. *SERPINB9* and *ITPR1* transcripts in Tregs of 52 GV patients and 48 controls were analyzed by nonparametric Mann–Whitney *U* test. (a) *SERPINB9* transcripts in GV, SV, and AV vs controls' Tregs ($p = 0.0045$, $p = 0.043$, and $p < 0.0001$, respectively). *SERPINB9* transcripts in AV vs SV Tregs ($p = 0.031$). *SERPINB9* transcripts in GV, SV, and AV Tregs before and after calcium treatment ($p = 0.0345$, $p = 0.0432$, and $p = 0.02$). (b) *SERPINB9* transcripts in severe GV (50-75% VASI) vs mild GV (10-25% VASI) Tregs ($p = 0.035$). *SERPINB9* transcripts in moderate GV (25-50% VASI) vs mild GV (10-25% VASI) and severe GV (50-75% VASI) Tregs ($p = 0.1162$ and $p = 0.1164$, respectively). *SERPINB9* transcripts in mild GV, moderate GV, and severe GV Tregs before and after calcium treatment ($p = 0.034$, $p = 0.02$, and $p = 0.001$, respectively). (c) There was a 0.32-, 0.54-, and 0.25-fold changes in *SERPINB9* transcripts for GV, SV, and AV Tregs when compared to controls. (d) *ITPR1* transcripts in GV, SV, and AV vs controls' Tregs ($p < 0.0001$, $p = 0.045$, and $p < 0.0001$, respectively). *ITPR1* transcripts in AV vs SV Tregs ($p = 0.0003$). *ITPR1* transcripts in GV, SV, and AV Tregs before and after calcium treatment ($p = 0.02$, $p = 0.0327$, and $p = 0.01$). (e) *ITPR1* transcripts in severe GV (50-75% VASI) vs mild GV (10-25% VASI) Tregs ($p = 0.034$). *ITPR1* transcripts in moderate GV (25-50% VASI) vs mild GV (10-25% VASI) and severe GV (50-75% VASI) Tregs ($p = 0.6543$ and $p = 0.8649$, respectively). *ITPR1* transcripts in mild GV, moderate GV, and severe GV Tregs before and after calcium treatment ($p = 0.033$, $p = 0.021$, and $p = 0.01$). (f) There was a 0.54-, 0.62-, and 0.28-fold changes in *ITPR1* transcripts for GV, SV, and AV Tregs when compared to controls.

difference in *NRP1* transcripts in calcium-treated Tregs of GV, SV, AV, mild GV, moderate GV, and severe GV patients ($p > 0.05$; Figures 2(d) and 2(e)).

3.5. Correlation of ITPR1 Transcripts with GZMB, NRP1, and SERPINB9 Transcripts in Tregs and Correlation of In Vitro Treg Suppression Assay with of ITPR1, GZMB, NRP1, and SERPINB9 Transcripts in Tregs of GV Patients. Interestingly, we found a positive correlation for *ITPR1* transcripts with GZMB ($r = 0.45$; $p = 0.0009$) and *NRP1* ($r = 0.52$; $p = 0.001$) transcripts in Tregs of GV patients (Figures 4(a) and 4(b)). However, we could not find any correlation between *ITPR1* and *SERPINB9* transcripts in Tregs of GV patients ($r = 0.22$; $p = 0.2473$; Figure 4(c)). Further, we correlated *in vitro* Treg suppression assay with *GZMB*, *NRP1*, *SERPINB9*, and *ITPR1* transcripts in Tregs of GV patients. We found a positive correlation for percentage Treg-mediated suppression of $CD4^+$ T cells with *GZMB* ($r = 0.61$; $p = 0.0012$), *NRP1* ($r = 0.55$; $p = 0.021$), *SERPINB9* ($r = 0.56$; $p = 0.002$), and *ITPR1* ($r = 0.54$; $p = 0.001$) and percentage Treg-mediated suppression of $CD8^+$ T cells with *GZMB* ($r = 0.58$; $p = 0.004$), *NRP1* ($r = 0.52$; $p = 0.022$), *SERPINB9* ($r = 0.48$; $p = 0.024$), and *ITPR1* ($r = 0.49$; $p = 0.032$) in GV patients (Figures 5(a)–5(h)).

3.6. Age of Onset and Gender-Based Analyses for Transcripts Levels of Treg-Associated Genes (GZMB, NRP1, ITPR1, SERPINB9, PDCD1, FASLG, UBASH3A, IKZF4, GATA2, GATA3, TNFRSF18, RUNX1, STAT3, and STAT5) in GV Patients. Further, the expression of *GZMB*, *NRP1*, *ITPR1*, *SERPINB9*, *PDCD1*, *FASLG*, *UBASH3A*, *IKZF4*, *GATA2*, *GATA3*, *TNFRSF18*, *RUNX1*, *STAT3*, and *STAT5* transcripts was monitored in different age at onset groups of GV patients. We did not find any significant difference in the

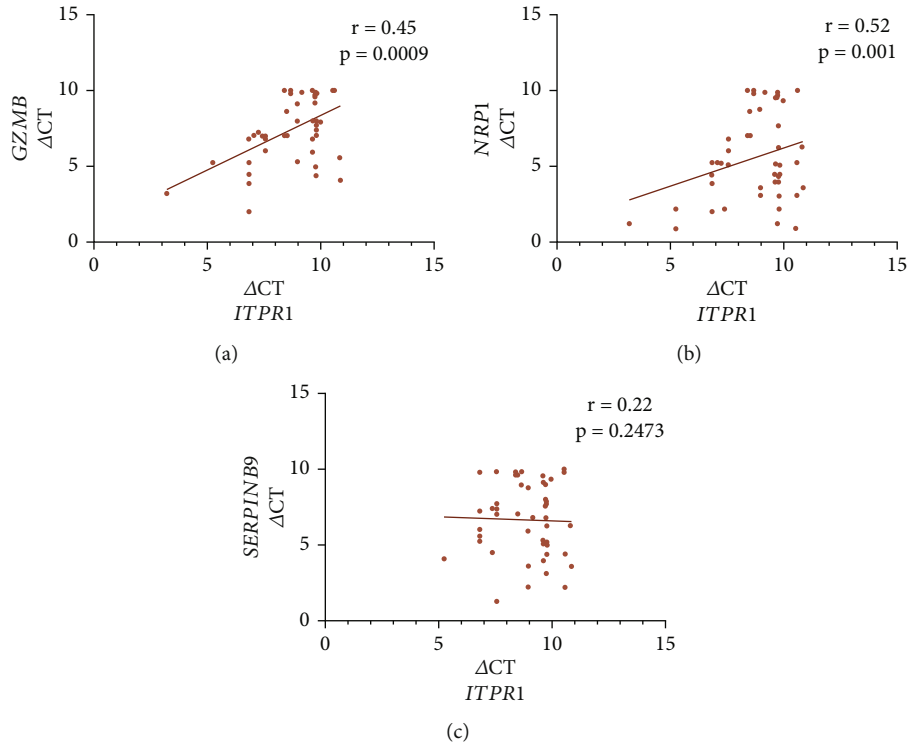

Figure 4: Correlation of *ITPR1* transcripts with *GZMB*, *NRP1*, and *SERPINB9* transcripts in GV patients. The correlation of *ITPR1* transcripts with *GZMB*, *NRP1*, and *SERPINB9* transcripts were analyzed by Spearman's correlation analysis. (a) *ITPR1* transcripts positively correlated with *GZMB* transcripts in GV patients' Tregs ($r = 0.45$, $p = 0.0009$). (b) *ITPR1* transcripts positively correlated with *NRP1* transcripts in GV patients' Tregs ($r = 0.52$, $p = 0.001$). (c) No correlation was observed between *ITPR1* transcripts and *SERPINB9* transcripts in GV patients' Tregs ($r = 0.22$, $p = 0.2473$).

expression of *GZMB*, *NRP1*, *ITPR1*, *SERPINB9*, *PDCD1*, *FASLG*, *UBASH3A*, *IKZF4*, *GATA2*, *GATA3*, *TNFRSF18*, *RUNX1*, *STAT3*, and *STAT5* transcripts in Tregs between 1–20, 21-40, and 41-60 years age of onset groups ($p > 0.05$; Figures S7 and S8).

Next, we carried out gender-based analysis for expression of *GZMB*, *NRP1*, *ITPR1*, *SERPINB9*, *PDCD1*, *FASLG*, *UBASH3A*, *IKZF4*, *GATA2*, *GATA3*, *TNFRSF18*, *RUNX1*, *STAT3*, and *STAT5* transcripts. We did not find any significant difference in expression of *GZMB*, *NRP1*, *ITPR1*, *SERPINB9*, *PDCD1*, *FASLG*, *UBASH3A*, *IKZF4*, *GATA2*, *GATA3*, *TNFRSF18*, *RUNX1*, *STAT3*, and *STAT5* transcripts between male and female GV Tregs ($p > 0.05$; Figures S9 and S10).

4. Discussion

Autoimmunity has been strongly implicated in GV pathogenesis by the presence of autoantibodies and autoreactive $CD4^+$ and $CD8^+$ T cells in GV patients [3–8]. Additionally, studies have implicated the role of cytotoxic T cells in melanocyte death in vitiligo patients [7, 8, 15]. Tregs control such autoimmune responses against melanocytes by actively suppressing self-reactive T cells activation and expansion [13, 14]. However, studies have suggested impaired Tregs' number and Tregs suppressive function in GV patients [6, 14, 15]. Moreover, our recent study has suggested the role of altered expression of NFATs and FOXP3 in impaired Treg suppressive function [6]. Thus, impaired Tregs fail to control the ongoing autoimmune response leading to widespread self-reactive T cells activation, resulting in GV pathogenesis [6]. Overall, these studies highlight that Tregs and their suppressive molecules may represent a potential therapeutic target for developing Treg-based therapeutics for GV.

Inositol 1,4,5-trisphosphate receptor type 1 (ITPR1) governs the release of calcium from the endoplasmic reticulum [22]. The exact role of ITPR1 in Treg function in GV is unknown. However, upon TCR stimulations in T cells, ITPR1 controls the release of stored calcium from the endoplasmic reticulum [33]. Our previous study has suggested that optimal calcium levels in Tregs are a prerequisite for NFATc1 activation in Treg of GV patients [32]. In current study, we found significantly reduced *ITPR1* transcripts in GV patients. Moreover, our study suggested the role of decreased *ITPR1* transcripts in GV progression and disease severity. Thus, the reduced *ITPR1* expression in Tregs may lead to reduced intracellular Treg calcium levels, resulting in impaired NFAT signalling pathway (Figure 6). Finally, the impaired NFAT signalling pathway may lead to decreased downstream immunosuppressive molecules leading to impaired Treg suppressive function.

As altered *ITPR1* transcripts may lead to impaired Treg activation and suppressive function, we assessed the mRNA expression of Treg-associated suppressive molecules *GZMB*,

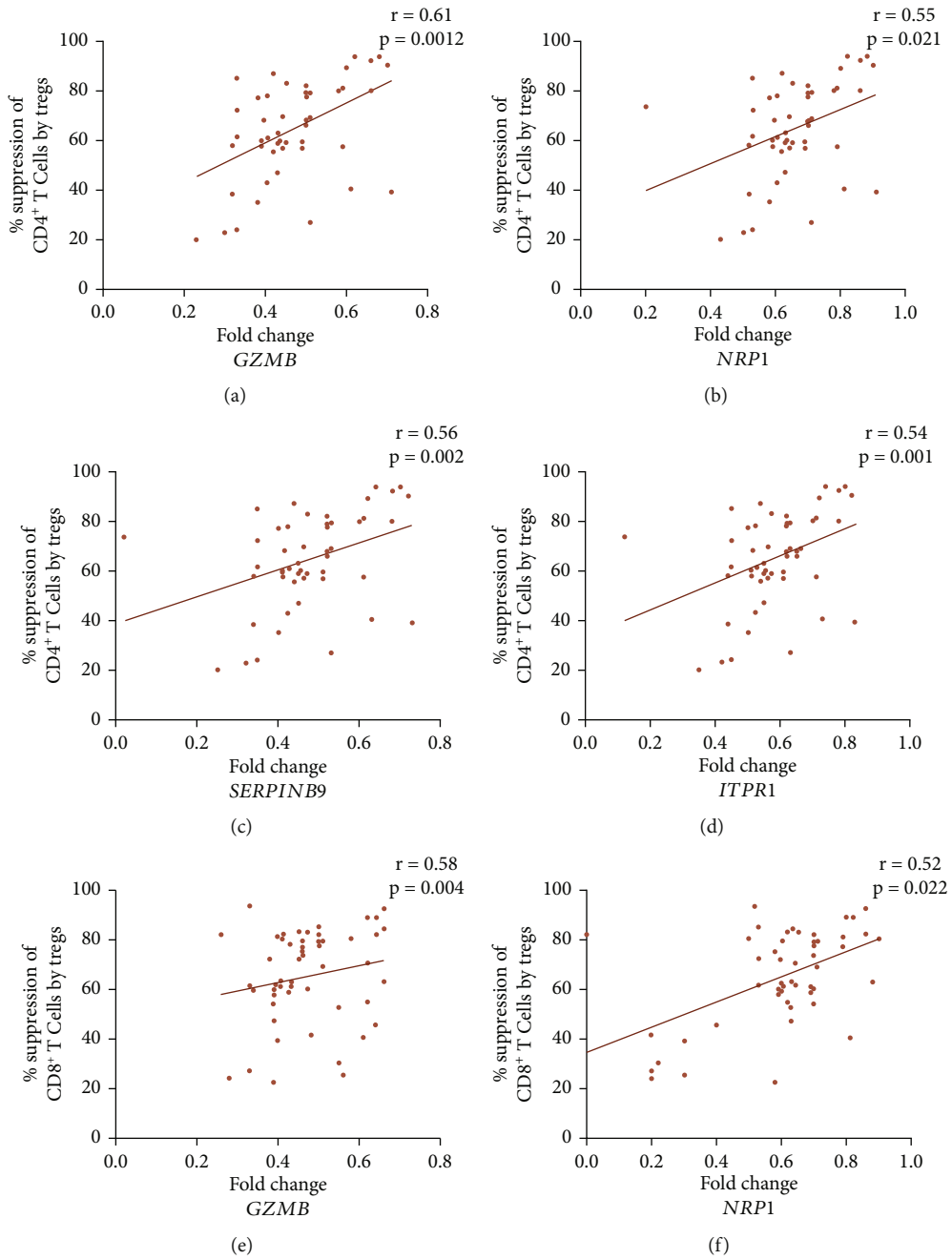

Figure 5: Continued.

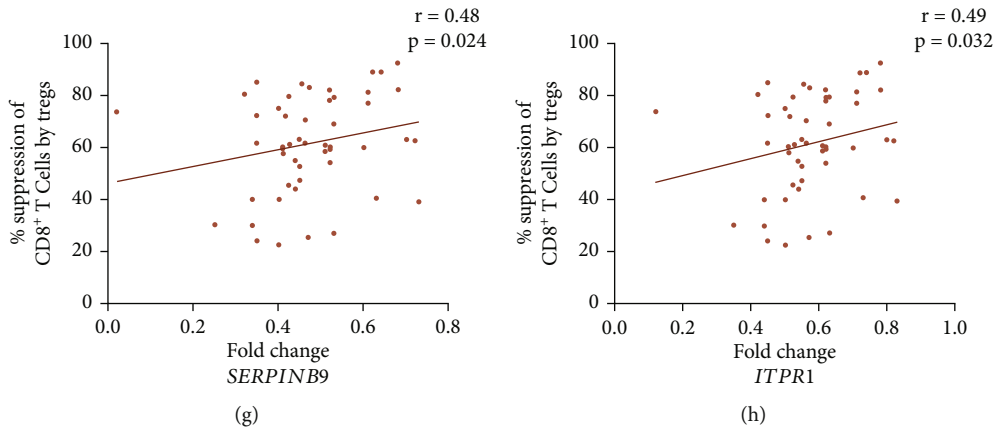

Figure 5: Correlation of *in vitro* Treg suppression assay with *ITPR1*, *GZMB*, *NRP1*, and *SERPINB9* transcripts in Tregs of GV patients. The correlation of *in vitro* Treg suppression assay with *ITPR1*, *GZMB*, *NRP1*, and *SERPINB9* was analyzed by Spearman's correlation analysis. (a) *GZMB* transcripts were positively correlated with *in vitro* Treg mediated suppression of $CD4^+$ T cells in GV patients' Tregs ($r = 0.61$; $p = 0.0012$). (b) *NRP1* transcripts were positively correlated with *in vitro* Treg-mediated suppression of $CD4^+$ T cells in GV patients' Tregs ($r = 0.55$; $p = 0.021$). (c) *SERPINB9* transcripts were positively correlated with *in vitro* Treg-mediated suppression of $CD4^+$ T cells in GV patients' Tregs ($r = 0.56$; $p = 0.002$). (d) *ITPR1* transcripts were positively correlated with *in vitro* Treg-mediated suppression of $CD4^+$ T cells in GV patients' Tregs ($r = 0.54$; $p = 0.001$). (e) *GZMB* transcripts positively correlated with *in vitro* Treg-mediated suppression of $CD8^+$ T cells in GV patients' Tregs ($r = 0.58$; $p = 0.004$). (f) *NRP1* transcripts positively correlated with *in vitro* Treg-mediated suppression of $CD8^+$ T cells in GV patients' Tregs ($r = 0.52$; $p = 0.0022$). (g) *SERPINB9* transcripts positively correlated with *in vitro* Treg-mediated suppression of $CD8^+$ T cells in GV patients' Tregs ($r = 0.48$; $p = 0.024$). (h) *ITPR1* transcripts positively correlated with *in vitro* Treg-mediated suppression of $CD8^+$ T cells in GV patients' Tregs ($r = 0.49$; $p = 0.032$).

NRP1, *PDCD1*, *FASLG*, and *TNFRS18* in GV patients. Studies have suggested that Tregs control the immune response by granzyme B-dependent cytotoxicity [34]. Upon TCR stimulation and receptor activation, Treg cells produce granzyme B, and previous studies have found increased CD107a expression upon Treg activation, suggesting extracellular degranulation of granzyme B [21, 35]. However, our study revealed significantly reduced *GZMB* transcripts in GV patients. Moreover, we found that the reduced *GZMB* transcripts were associated with GV disease severity and disease progression, suggesting the crucial role of *GZMB* expression in Tregs function. Furthermore, we found a positive correlation between *GZMB* transcripts and *ITPR1* transcripts. Therefore, our study suggests that impaired *ITPR1* transcripts might lead to reduced Treg intracellular calcium levels leading to impaired NFAT signalling pathway in GV (Figure 6). Additionally, our previous study has suggested altered calcium NFAT signalling pathway in GV Tregs [36]. Although the role of NFAT signalling pathway in granzyme B production is unknown, interestingly, studies have suggested for NFAT-binding sites on *GZMB* promoter [36]. Therefore, the decreased *ITPR1* transcripts could further lead to impaired calcium-NFAT signalling pathway, resulting in decreased *GZMB* transcripts, and thus lead to impaired Tregs suppressive function in GV (Figure 6). However, future studies must explore the role of *ITPR1* and NFAT signalling pathway in granzyme B expression. Furthermore, single-nucleotide polymorphisms (SNPs) and epigenetic changes in *GZMB* promoter must be explored as they might be responsible for the decreased *GZMB* expression.

Next, we evaluated the expression levels of Treg suppressive molecule neuropolin 1 (NRP-1). NRP-1 is constitutively expressed on the surface of Tregs and mediates prolonged binding with immature dendritic cells [19, 37]. Anti-NRP-1 antibodies have been shown to abrogate Treg immunosuppressive function [38]. Additionally, lack of NRP-1 on surface of Tregs has been linked with impaired Treg suppressive function and worsening of experimental autoimmune encephalomyelitis severity [38]. However, the role of NRP-1 in GV is unknown. Interestingly, we found significantly reduced *NRP1* transcripts in GV patients, suggesting for the crucial role of *NRP1* in reduced Treg suppressive function leading to GV pathogenesis. Moreover, we found a positive correlation of *NRP1* with *ITPR1* transcripts. Although the link between *ITPR1*-calcium-NFAT signalling pathway and *NRP1* is unknown, previous studies suggest that *NRP1* expression is accompanied with high levels of NFATc1 transcript expression [39]. Additionally, NRP-1 expression is controlled by T cells activation, and inhibition of NFATs has shown to suppress NRP-1 expression in Tregs [39]. Overall, our results suggest that the altered *ITPR1*-calcium-NFAT signalling pathway might be involved in reduced *NRP1* transcripts which led to impaired Treg suppressive function in GV patients (Figure 6). However, future studies must explore the involvement of *ITPR1*-calcium-NFAT signalling pathway, promoter SNPs, and epigenetic changes in *NRP1* promoter, as they might be responsible for decreased *NRP1* expression.

Furthermore, we assessed the expression levels of *SERPINB9* in GV Tregs. *SERPINB9* is an endogenous granzyme B inhibitor [21, 40]. After Treg activation, there is an increase in the production of granzyme B and its

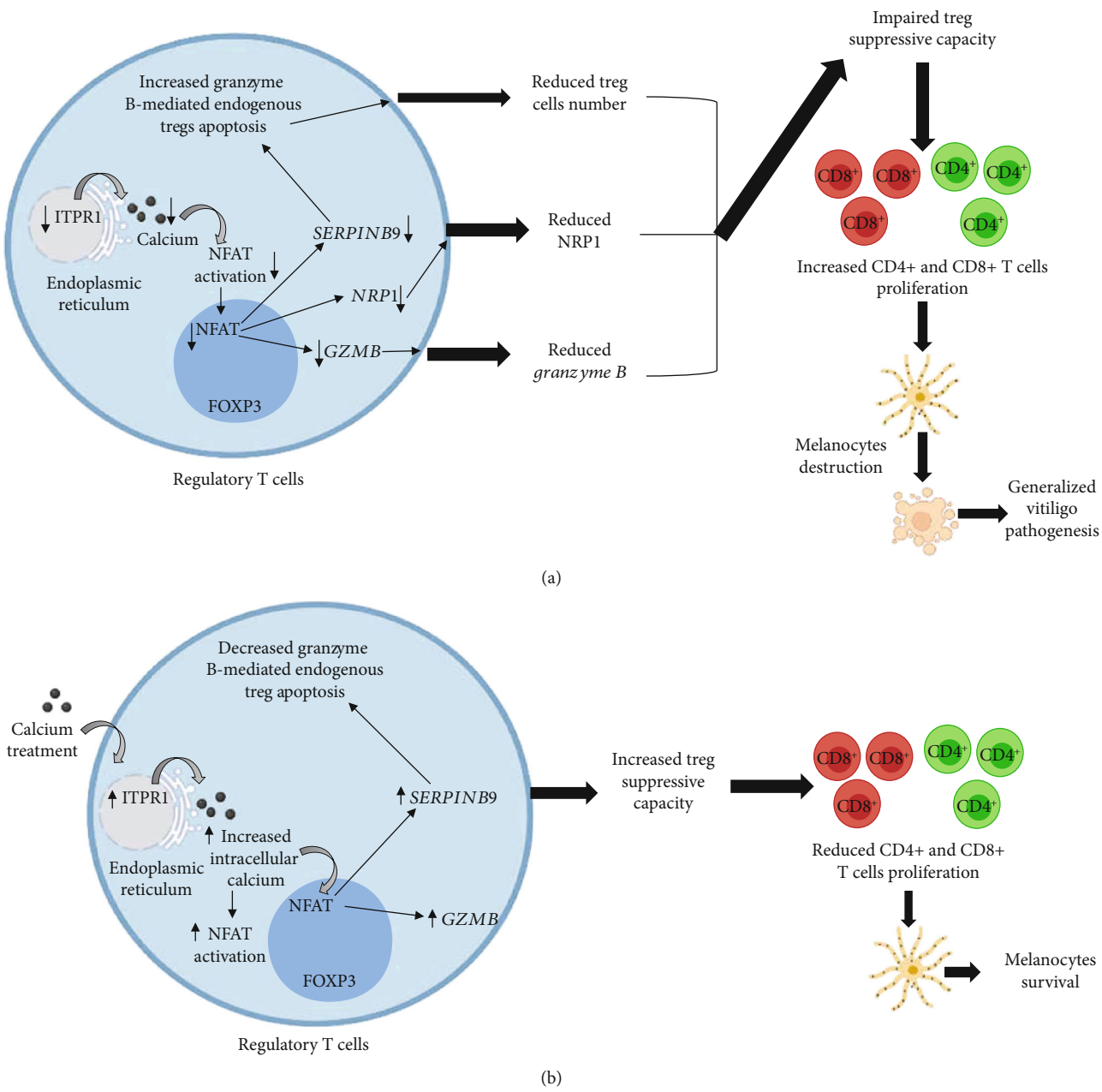

Figure 6: Role of *GZMB*, *NRP1*, *SERPINB9*, and *ITPR1* transcripts in GV pathogenesis. (a) The decreased *ITPR1* transcripts could lead to impaired calcium-NFAT signalling pathway, which might result in decreased *GZMB* and NRP1 transcripts. Further, the decreased *SERPINB9* transcripts may result in increased granzyme B-mediated endogenous apoptosis of Tregs. Overall, the decreased *GZMB*, *NRP1*, *SERPINB9*, and *ITPR1* transcripts result into decreased Treg suppressive capacity, which could lead to unchecked $CD4^+$ and $CD8^+$ T cells and thereby results into melanocytes' destruction contributing to GV pathogenesis, progression, and severity. (b) Upon calcium treatment, *ITPR1* mRNA expression is increased which may lead to intracellular Treg calcium influx and calcium-NFAT signalling pathway, thereby results into increased *GZMB* and *SERPINB9* transcripts, leading to increased Treg suppressive capacity. The increased Treg suppressive capacity controls the $CD8^+$ and $CD4^+$ T cells proliferation and IFN-γ production and thereby contributes to melanocytes survival.

endogenous inhibitor *SERPINB9* [21]. Previous studies have shown an increase in granzyme B-mediated apoptosis in SERPINB9 knockout mice, suggesting that Tregs upon activation can undergo self-inflicted apoptosis mediated by granzyme B in absence of SERPINB9 [21]. Interestingly, our study suggested significantly reduced *SERPINB9* transcripts in GV Tregs. Moreover, we found a significant association of *SERPINB9* transcripts with GV disease severity and disease progression. Additionally, previous studies have suggested significantly decreased Treg cells in vitiligo patients [6, 14, 15], suggesting that the increased *SERPINB9* transcripts can lead to Treg cells apoptosis, resulting into decreased Tregs number, thereby contributing to GV pathogenesis, progression, and severity.

However, future studies must confirm these findings by studying granzyme caspases-mediated apoptosis pathway in Tregs of GV patients.

Next, we aimed to study the key Treg-associated transcription factors (*GATA2*, *GATA3*, *RUNX1*, *STAT3*, and *STAT5)* in GV patients. The GATA transcription factors are zinc finger motif DNA-binding proteins, and they have a crucial role in Treg function [26, 27]. Genetic ablation in GATA3 has been associated with inflammatory disorder in mice [26]. Additionally, mutations in GATA2 have been associated with autoimmune hepatitis [27]. Additionally, *RUNX1* is a runt-related transcription factor, and it plays a crucial role in generation and function of Treg cells [25]. Moreover, STAT transcription factors, i.e., signal transducers of activation of transcription, control Treg cells development [24, 41]. Genetic knockdown of *STAT3* decreases the Tregs generation [24]. Moreover, *STAT5* plays a crucial role in sustaining FOXP3 expression in Tregs [41]. However, we did not find an association for Treg-associated transcription factors (*GATA2*, *GATA3*, *RUNX1*, *STAT3*, and *STAT5*) with GV pathogenesis, progression, and severity.

Previously, we had studied the *in vitro* Treg suppression assay in GV patients [6]. Our study had revealed significantly decreased *in vitro* Treg-mediated suppression of $CD4^+$ and $CD8^+$ T cells in GV patients [6]. To study the role of *ITPR1*, *GZMB*, *NRP1*, and *SERPINB9* on *in vitro* Treg suppressive capacity, we carried out correlation analysis. Interestingly, we found a positive correlation for Treg-mediated suppression of $CD4^+$ and $CD8^+$ T cells with *ITPR1*, *GZMB*, *NRP1*, and *SERPINB9* transcripts in GV patients' Tregs. Therefore, our results suggest that decreased *ITPR1*, *GZMB*, *NRP1*, and *SERPINB9* transcripts might impair Treg suppressive function, resulting in widespread activation of $CD4^+$ and $CD8^+$ T cells, which could lead to GV pathogenesis (Figure 6).

Our previous study suggested that calcium treatment of Tregs increased the intracellular calcium influx in Tregs of GV patients, due to increased expression of calcium ion channel gene *ORAI1* after calcium treatment [42]. Moreover, the optimum calcium influx enhanced the calcineurin and NFATc1 activity in calcium treated Tregs, which led to increased Treg suppressive capacity [32]. As *ITPR1* is crucial for the release of calcium in Tregs, we studied the transcript levels of *ITPR1* in calcium-treated Tregs of GV patients and controls. Interestingly, our study suggested an increase in mRNA expression of *ITPR1* in Tregs after the calcium treatment (Figure 3(d)). As the increased expression of *ITPR1* after the calcium treatment may further lead to enhanced Treg suppressive activity, we accessed the transcript levels of *GZMB* and *SERPINB9* in calcium-treated Tregs of GV patients. Our study suggested that the calcium treatment increased the expression levels of *GZMB* and *SERPINB9* in GV Tregs (Figures 2(a) and 3(a)). Our results are in line with the previous findings which suggest that calcium signalling modulates cytolytic T lymphocyte function [42]. Overall, our study suggests that calcium treatment may improve Treg suppressive capacity, and targeting the Ca^{2+}-calmodulin-calcineurin-NFAT signalling pathway may be a potent therapeutic target for GV.

5. Conclusions

Overall, our results for the first time suggest the crucial involvement of *GZMB*, *NRP1*, *SERPINB9*, and *ITPR1* transcripts in reduced Treg-mediated suppression of $CD4^+$ and $CD8^+$ T cells which lead to GV pathogenesis, progression, and severity. Moreover, our study highlighted that *ITPR1* might be responsible for decreased *GZMB* and *NRP1* transcripts in GV Tregs. Furthermore, our study revealed that the increased *SERPINB9* transcripts might result in endogenous granzyme B-mediated Tregs apoptosis, and the Treg suppressive capacity can be enhanced after calcium treatment in Tregs. These findings may aid in development of Treg-based therapeutics for GV; however, *in vivo* studies must be carried out to validate the role of *GZMB*, *NRP1*, *SERPINB9*, and *ITPR1* in Treg-mediated GV pathogenesis.

Data Availability

Data available on request.

Ethical Approval

All procedures performed in this study involving human participants were in accordance with the ethical standards of the Institutional-Human Research Ethical Committee (IHREC), Maliba Pharmacy College, Uka Tarsadia University, Bardoli, Gujarat, India, and with the 1964 Helsinki Declaration and its later amendments or comparable ethical standards. All patients and healthy control subjects signed informed consent.

Consent

Informed consent was obtained from all patients and control participants of the study.

Conflicts of Interest

We wish to confirm that there are no known conflicts of interest associated with this publication, and there has been no significant financial support for this work that could have influenced its outcome.

Authors' Contributions

Prashant S. Giri has contributed to the investigation, methodology, validation, analysis, and writing-original draft preparation. Ankit H Bhart has contributed to the resources (patients' samples), clinical information, and analysis. Mitesh Dwivedi has contributed to the conceptualization, funding acquisition, investigation, methodology, resources, supervision, visualization, and writing-reviewing and editing.

Acknowledgments

We are thankful to vitiligo patients and control participants for donating blood samples for this study. We thank Science and Engineering Research Board, Department of Science and Technology (SERB-DST), New Delhi, India, for providing the research grant to Dr. Mitesh Dwivedi {ECR/2017/000858} and {CRG/2021/002419}. PSG thanks the SERB-DST, New Delhi, for awarding SRF and Knowledge Consortium of Gujarat, Education Department, Government of Gujarat, India, for awarding SHODH (Scheme of Developing High Quality Research) fellowship. This work was supported by grants to Dr. Mitesh Dwivedi {ECR/2017/000858} and {CRG/2021/002419} Science and Engineering Research Board, Department of Science and Technology (SERB-DST), New Delhi, India.

Supplementary Materials

Supplementary 1. Table S1. Primer sequence for transcript analysis of GZMB, NRP1, ITPR1, SERPINB9, PDCD1, FASLG, UBASH3A, IKZF4, GATA2, GATA3, TNFRSF18, RUNX1, STAT3, and STAT5 genes by qPCR.

Supplementary 2. Figure S1. Melt curve analysis for *GZMB*, *NRP1*, *ITPR1*, *SERPINB9*, *PDCD1*, *FASLG*, *UBASH3A*, and *IKZF4* transcripts. (a) Representative image for melt curve analysis for *GZMB* transcripts. (b) Representative image for melt curve analysis for *NRP1* transcripts. (c) Representative image for melt curve analysis for *ITPR1* transcripts. (d) Representative image for melt curve analysis for *SERPINB9* transcripts. (e) Representative image for melt curve analysis for *PDCD1* transcripts. (f) Representative image for melt curve analysis for *FASLG* transcripts. (g) Representative image for melt curve analysis for *UBASH3A* transcripts and (h) Representative image for melt curve analysis for *IKZF4* transcripts. Figure S2: Melt curve analysis for *GATA2*, *GATA3*, *TNFRSF18*, *RUNX1*, *STAT3*, *STAT5*, and *GAPDH* transcripts. (a) Representative image for melt curve analysis for *GATA2* transcripts. (b) Representative image for melt curve analysis for *GATA3* transcripts. (c) Representative image for melt curve analysis for *TNFRSF18* transcripts. (d) Representative image for melt curve analysis for *RUNX1* transcripts. (e) Representative image for melt curve analysis for *STAT3* transcripts. (f) Representative image for melt curve analysis for *STAT5* transcripts. (g) Representative image for melt curve analysis for *GAPDH* transcripts. Figure S3. Standard curve for estimation of calcium levels: standard curve for calcium ELISA. Figure S4. *PDCD1*, *FASLG*, and *TNFRS18* transcripts in Tregs of GV patients and controls. *PDCD1*, *FASLG*, and *TNFRS18* transcripts in Tregs of 52 GV patients and 48 controls were analyzed by nonparametric Mann–Whitney *U* test. (a) *PDCD1* transcripts in GV, SV, and AV vs controls' Tregs ($p = 0.4625$, $p = 0.2563$, and $p = 0.3627$, respectively). *PDCD1* transcripts in AV vs SV Tregs ($p = 0.1273$). (b) *PDCD1* transcripts in severe GV (50-75% VASI) vs mild GV (10-25% VASI) Tregs ($p = 0.2427$). *PDCD1* transcripts in moderate GV (25-50% VASI) vs mild GV (10-25% VASI) and severe GV (50-75% VASI) Tregs ($p = 0.1225$ and $p = 0.1423$, respectively). (c) There were 0.88-, 0.87-, and 0.98-fold changes in *PDCD1* transcripts for GV, SV, and AV Tregs when compared to controls. (d) *FASLG* transcripts in GV, SV, and AV vs controls' Tregs ($p = 0.753$, $p = 0.999$, and $p = 0.213$, respectively). *FASLG* transcripts in AV vs SV Tregs ($p = 0.521$). (e) *FASLG* transcripts in severe GV (50-75% VASI) vs mild GV (10-25% VASI) Tregs ($p = 0.113$). *FASLG* transcripts in moderate GV (25-50% VASI) vs mild GV (10-25% VASI) and severe GV (50-75% VASI) Tregs ($p = 0.7123$ and $p = 0.2321$, respectively). (f) There were 0.72-, 0.65-, and 0.77-fold changes in *FASLG* transcripts for GV, SV, and AV Tregs as compared to controls. (g) *TNFRS18* transcripts in GV, SV, and AV vs controls' Tregs ($p = 0.3362$, $p = 0.1272$, and $p = 0.3627$, respectively). *TNFRS18* transcripts in AV vs SV Tregs ($p = 0.1265$). (h) *TNFRS18* transcripts in severe GV (50-75% VASI) vs mild GV (10-25% VASI) Tregs ($p = 0.4653$). *TNFRS18* transcripts in moderate GV (25-50% VASI) vs mild GV (10-25% VASI) and severe GV (50-75% VASI) Tregs ($p = 0.1263$ and $p = 0.7625$, respectively). (i) There were 0.86-, 0.87-, and 0.85-fold changes in *TNFRS18* transcripts for GV, SV, and AV Tregs as compared to controls. Figure S5. *UBASH3A*, *GATA2*, and *GATA3* transcripts in Tregs of GV patients and controls. *UBASH3A*, *GATA2*, and *GATA3* transcripts in Tregs of 52 GV patients and 48 controls were analyzed by nonparametric Mann–Whitney *U* test. (a) *UBASH3A* transcripts in GV, SV, and AV vs controls' Tregs ($p = 0.145$, $p = 0.127$, and $p = 0.647$, respectively). *UBASH3A* transcripts in AV vs SV Tregs ($p = 0.487$). (b) *UBASH3A* transcripts in severe GV (50-75% VASI) vs mild GV (10-25% VASI) Tregs ($p = 0.2347$). *UBASH3A* transcripts in moderate GV (25-50% VASI) vs mild GV (10-25% VASI) and severe GV (50-75% VASI) Tregs ($p = 0.1252$ and $p = 0.1625$, respectively). (c) There was a 0.92-, 0.89-, and 1.1-fold changes in *UBASH3A* transcripts for GV, SV, and AV Tregs as compared to controls. (d) *GATA2* transcripts in GV, SV, and AV vs controls' Tregs ($p = 0.1537$, $p = 0.1922$, and $p = 0.1189$, respectively). *GATA2* transcripts in AV vs SV Tregs ($p = 0.7891$). (e) *GATA2* transcripts in severe GV (50-75% VASI) vs mild GV (10-25% VASI) Tregs ($p = 0.1922$). *GATA2* transcripts in moderate GV (25-50% VASI) vs mild GV (10-25% VASI) and severe GV (50-75% VASI) Tregs ($p = 0.7654$ and $p = 0.1165$, respectively). (f) There was a 0.89-, 0.86-, and 0.84-fold changes in *GATA2* transcripts for GV, SV, and AV Tregs as compared to controls. (g) *GATA3* transcripts in GV, SV, and AV vs controls' Tregs ($p = 0.2224$, $p = 0.86322$, and $p = 0.1152$, respectively). *GATA3* transcripts in AV vs SV Tregs ($p = 0.3641$). (h) *GATA3* transcripts in severe GV (50-75% VASI) vs mild GV (10-25% VASI) Tregs ($p = 0.8742$). *GATA3* transcripts in moderate GV (25-50% VASI) vs mild GV (10-25% VASI) and severe GV (50-75% VASI) Tregs ($p = 0.1645$ and $p = 0.8873$, respectively). (i) There was a 0.89-, 0.92-, and 0.97-fold changes in *GATA3* transcripts for GV, SV, and AV Tregs as compared to controls. Figure S6. *RUNX1*, *STAT3*, and *STAT5* transcripts in Tregs of GV patients and controls. *RUNX1*, *STAT3*, and *STAT5* transcripts in Tregs of 52 GV patients and 48 controls were analyzed by nonparametric Mann–Whitney *U* test. (a) *RUNX1* transcripts in GV, SV,

and AV vs controls' Tregs ($p = 0.1152$, $p = 0.1254$, and $p = 0.1455$, respectively). *RUNX1* transcripts in AV vs SV Tregs ($p = 0.2235$). (b) *RUNX1* transcripts in severe GV (50-75% VASI) vs mild GV (10-25% VASI) Tregs ($p = 0.1455$). *RUNX1* transcripts in moderate GV (25-50% VASI) vs mild GV (10-25% VASI) and severe GV (50-75% VASI) Tregs ($p = 0.1152$ and $p = 0.1164$, respectively). (c) There was a 0.1.1-, 1.2-, and 0.97-fold changes in *RUNX1* transcripts for GV, SV, and AV Tregs when compared to controls. (d) *STAT3* transcripts in GV, SV, and AV vs controls' Tregs ($p = 0.2333$, $p = 0.2143$, and $p = 0.3541$, respectively). *STAT3* transcripts in AV vs SV Tregs ($p = 0.3436$). (e) *STAT3* transcripts in 50-75% severe GV vs 10-25% mild GV Tregs ($p = 0.4222$). *STAT3* transcripts in moderate GV (25-50% VASI) vs mild GV (10-25% VASI) and severe GV (50-75% VASI) Tregs ($p = 0.1455$ and $p = 0.8423$, respectively). (f) There was a 1.01-, 1.3-, and 1.0-fold changes in *STAT3* transcripts for GV, SV, and AV Tregs as compared to controls. (g) *STAT5* transcripts in GV, SV, and AV vs controls' Tregs ($p = 0.1454$, $p = 0.2241$, and $p = 0.1535$, respectively). *STAT5* transcripts in AV vs SV Tregs ($p = 0.4535$). (h) *STAT5* transcripts in severe GV (50-75% VASI) vs mild GV (10-25% VASI) Tregs ($p = 0.2532$). *STAT5* transcripts in moderate GV (25-50% VASI) vs mild GV (10-25% VASI) and severe GV (50-75% VASI) Tregs ($p = 0.1432$ and $p = 0.1484$, respectively). (i) There was a 0.99-, 1.1-, and 0.94-fold changes in *STAT5* transcripts for GV, SV, and AV Tregs as compared to controls. Figure S7. Age of onset analysis for *GZMB*, *NRP1*, P*DCD1*, *FASLG*, *TNFRS18*, *SERPINB9*, and *ITPR1* transcripts in GV Tregs and control Tregs. (a) *GZMB* transcript levels in Tregs of different age of onset groups (1-20 vs 21-40 years: $p = 0.1263$; 1-20 vs 41-60 years: $p = 0.6532$; 21-40 vs 41-60 years: $p = 0.9836$). (b) *NRP1* transcript levels in Tregs of different age of onset groups (1-20 vs 21-40 years: $p = 0.1563$; 1-20 vs 41-60 years: $p = 0.8832$; 21-40 vs 41-60 years: $p = 0.6863$). (c) *PDCD1* transcript levels in Tregs of different age of onset groups (1-20 vs 21-40 years: $p = 0.1348$; 1-20 vs 41-60 years: $p = 0.2842$; 21-40 vs 41-60 years: $p = 0.4923$). (d) *FASLG* transcript levels in Tregs of different age of onset groups (1-20 vs 21-40 years: $p = 0.1323$; 1-20 vs 41-60 years: $p = 0.2932$; 21-40 vs 41-60 years: $p = 0.1937$). (e) *TNFRS18* transcript levels in Tregs of different age of onset groups (1-20 vs 21-40 years: $p = 0.4627$; 1-20 vs 41-60 years: $p = 0.2847$, 21-40 vs 41-60 years: $p = 0.2948$). (f) *SERPINB9* transcript levels in Tregs of different age of onset groups (1-20 vs 21-40 years: $p = 0.3533$; 1-20 vs 41-60 years: $p = 0.4242$; 21-40 vs 41-60 years: $p = 0.4363$). (g) *ITPR1* transcript levels in Tregs of different age of onset groups (1-20 vs 21-40 years: $p = 0.2648$; 1-20 vs 41-60 years: $p = 0.3762$; 21-40 vs 41-60 years: $p = 0.2635$). Figure S8. Age of onset analysis for *UBASH3A*, *GATA2*, *GATA3*, *RUNX1*, *STAT3*, and *STAT5* transcripts in GV Tregs and control Tregs. (a) *UBASH3A* transcript levels in Tregs of different age of onset groups (1-20 vs 21-40 years: $p = 0.4836$; 1-20 vs 41-60 years: $p = 0.5247$; 21-40 vs 41-60 years: $p = 0.1938$). (b) *GATA2* transcript levels in Tregs of different age of onset groups (1-20 vs 21-40 years: $p = 0.1321$; 1-20 vs 41-60 years: $p = 0.1380$; 21-40 vs 41-60 years: $p = 0.5221$). (c) *GATA3* transcript levels in Tregs of different age of onset groups (1-20 vs 21-40 years: $p = 0.1241$; 1-20 vs 41-60 years: $p = 0.5384$; 21-40 vs 41-60: $p = 0.2411$). (d) *RUNX1* transcript levels in Tregs of different age of onset groups (1-20 vs 21-40 years: $p = 0.1434$; 1-20 vs 41-60 years: $p = 0.3210$; 21-40 vs 41-60 years: $p = 0.1281$). (e) *STAT3* transcript levels in Tregs of different age of onset groups (1-20 vs 21-40 years: $p = 0.4826$; 1-20 vs 41-60 years: $p = 0.3292$; 21-40 vs 41-60 years: $p = 0.1196$). (f) *STAT5* transcript levels in Tregs of different age of onset groups (1-20 vs 21-40 years: $p = 0.1284$; 1-20 vs 41-60 years: $p = 0.3421$; 21-40 vs 41-60 years: $p = 0.1248$). Figure S9. Gender-based analysis for *GZMB*, *NRP1*, *PDCD1*, *FASLG*, *TNFRS18*, *SERPINB9*, and *ITPR1* transcripts in GV Tregs and control Tregs. (a) *GZMB* transcript levels in Tregs of male and female GV patients ($p = 0.2462$). (b) *NRP1* transcript levels in Tregs of male and female GV patients ($p = 0.1739$). (c) *PDCD1* transcript levels in Tregs of male and female GV patients ($p = 0.5642$). (d) *FASLG* transcript levels in Tregs of male and female GV patients ($p = 0.4852$). (e) *TNFRS18* transcript levels in Tregs of male and female GV patients ($p = 0.6737$). (f) *SERPINB9* transcript levels in Tregs of male and female GV patients ($p = 0.5742$). (g) *ITPR1* transcript levels in Tregs of male and female GV patients ($p = 0.4513$). Figure S10. Gender-based analysis for *UBASH3A*, *GATA2*, *GATA3*, *RUNX1*, *STAT3*, and *STAT5* transcripts in GV Tregs and control Tregs. (a) *UBASH3A* transcript levels in Tregs of male and female GV patients ($p = 0.4547$). (b) *GATA2* transcript levels in Tregs of male and female GV patients ($p = 0.6780$). (c) *GATA3* transcript levels in Tregs of male and female GV patients ($p = 0.6734$). (d) *RUNX1* transcript levels in Tregs of male and female GV patients ($p = 0.6797$). (e) *STAT3* transcript levels in Tregs of male and female GV patients ($p = 0.6792$). (f) *STAT5* transcript levels in Tregs of male and female GV patients ($p = 0.7621$).

References

[1] J. J. Nordlund, R. E. Boissy, V. J. Hearing, R. A. King, W. S. Oetting, and J. P. Ortonne, *The pigmentary system: physiology and pathophysiology*, John Wiley & Sons, Second edition, 2007.

[2] C. Kruger and K. U. Schallreuter, "A review of the worldwide prevalence of vitiligo in children/adolescents and adults," *International Journal of Dermatology*, vol. 51, no. 10, pp. 1206–1212, 2012.

[3] K. Ongenae, N. Van Geel, and J. M. Naeyaert, "Evidence for an autoimmune pathogenesis of vitiligo," *Pigment Cell Research*, vol. 16, no. 2, pp. 90–100, 2003.

[4] T. Lambe, J. C. H. Leung, T. Bouriez-Jones et al., "CD4 T cell-dependent autoimmunity against a melanocyte neoantigen induces spontaneous vitiligo and depends upon Fas-Fas ligand interactions," *The Journal of Immunology*, vol. 177, no. 5, pp. 3055–3062, 2006.

[5] M. Dwivedi, E. H. Kemp, N. C. Laddha, M. S. Mansuri, A. P. Weetman, and R. Begum, "Regulatory T cells in vitiligo: implications for pathogenesis and therapeutics," *Autoimmunity Reviews*, vol. 14, no. 1, pp. 49–56, 2015.

[6] P. S. Giri, M. Dwivedi, and R. Begum, "Decreased suppression of CD8+ and CD4+ T cells by peripheral regulatory T cells in generalized vitiligo due to reduced NFATC1 and FOXP3

proteins," *Experimental Dermatology*, vol. 29, no. 8, pp. 759–775, 2020.

[7] A. Wankowicz-Kalinska, C. Le Poole, R. van den Wijngaard, W. J. Storkus, and P. K. Das, "Melanocyte-specific immune response in melanoma and vitiligo: two faces of the same coin?," *Pigment Cell Research*, vol. 16, no. 3, pp. 254–260, 2003.

[8] J. Wu, M. Zhou, Y. Wan, and A. Xu, "CD8+ T cells from vitiligo perilesional margins induce autologous melanocyte apoptosis," *Molecular Medicine Reports*, vol. 7, no. 1, pp. 237–241, 2013.

[9] M. Dwivedi, N. C. Laddha, K. Shah, B. J. Shah, and R. Begum, "Involvement of interferon-gamma genetic variants and intercellular adhesion molecule-1 in onset and progression of generalized vitiligo," *Journal of Interferon & Cytokine Research*, vol. 33, no. 11, pp. 646–659, 2013.

[10] N. C. Laddha, M. Dwivedi, and R. Begum, "Increased Tumor Necrosis Factor (TNF)-α and Its Promoter Polymorphisms Correlate with Disease Progression and Higher Susceptibility towards Vitiligo," *PLoS ONE*, vol. 7, no. 12, p. e52298, 2012.

[11] P. S. Giri, R. Begum, and M. Dwivedi, "Meta-analysis for association of TNFA -308 G>A polymorphism with vitiligo susceptibility," *Gene*, vol. 809, article 146027, 2022.

[12] M. Dwivedi, P. Kumar, N. C. Laddha, and E. H. Kemp, "Induction of regulatory T cells: a role for probiotics and prebiotics to suppress autoimmunity," *Autoimmunity Reviews*, vol. 15, no. 4, pp. 379–392, 2016.

[13] A. Corthay, "How do regulatory T cells work?," *Scandinavian Journal of Immunology*, vol. 70, no. 4, pp. 326–336, 2009.

[14] M. Dwivedi, N. C. Laddha, P. Arora, Y. S. Marfatia, and R. Begum, "Decreased regulatory T-cells and CD4(+) /CD8(+) ratio correlate with disease onset and progression in patients with generalized vitiligo," *Pigment Cell & Melanoma Research*, vol. 26, no. 4, pp. 586–591, 2013.

[15] P. S. Giri, M. Dwivedi, N. C. Laddha, R. Begum, and A. H. Bharti, "Altered expression of nuclear factor of activated T cells, forkhead box P3, and immune-suppressive genes in regulatory T cells of generalized vitiligo patients," *Pigment Cell & Melanoma Research*, vol. 33, no. 4, pp. 566–578, 2020.

[16] P. S. Giri, S. Patel, R. Begum, and M. Dwivedi, "Association of *FOXP3* and *GAGE10* promoter polymorphisms and decreased FOXP3 expression in regulatory T cells with susceptibility to generalized vitiligo in Gujarat population," *Gene*, vol. 768, p. 145295, 2021.

[17] E. Gianchecchi and A. Fierabracci, "Inhibitory receptors and pathways of lymphocytes: the role of PD-1 in Treg development and their involvement in autoimmunity onset and cancer progression," *Frontiers in Immunology*, vol. 9, 2018.

[18] C. M. Paluskievicz, X. Cao, R. Abdi, P. Zheng, Y. Liu, and J. S. Bromberg, "T regulatory cells and priming the suppressive tumor microenvironment," *Frontiers in Immunology*, vol. 10, 2019.

[19] M. Sarris, K. G. Andersen, F. Randow, L. Mayr, and A. G. Betz, "Neuropilin-1 expression on regulatory T cells enhances their interactions with dendritic cells during antigen recognition," *Immunity*, vol. 28, no. 3, pp. 402–413, 2008.

[20] A. Schmidt, N. Oberle, and P. Krammer, "Molecular mechanisms of Treg-mediated T cell suppression," *Frontiers in Immunology*, vol. 3, 2012.

[21] J. Azzi, N. Skartsis, M. Mounayar et al., "Serine protease inhibitor 6 plays a critical role in protecting murine granzyme B-producing regulatory T cells," *Journal of Immunology*, vol. 191, no. 5, pp. 2319–2327, 2013.

[22] T. Jayaraman, E. Ondriasová, K. Ondrias, D. J. Harnick, and A. R. Marks, "The inositol 1,4,5-trisphosphate receptor is essential for T-cell receptor signaling," *Proceedings of the National Academy of Sciences of the United States of America*, vol. 92, no. 13, pp. 6007–6011, 1995.

[23] S. A. Mahmud, L. S. Manlove, and M. A. Farrar, "Interleukin-2 and STAT5 in regulatory T cell development and function," *Jak-Stat*, vol. 2, no. 1, article e23154, 2013.

[24] J.-R. Pallandre, E. Brillard, G. Créhange et al., "Role of STAT3 in regulatory lymphocyte generation: implications in graft-versus-host disease and antitumor immunity," *Frontiers in Immunology*, vol. 179, pp. 7593–7604, 2007.

[25] L. Li, N. Patsoukis, V. Petkova, and V. A. Boussiotis, "Runx1 and Runx3 are involved in the generation and function of highly suppressive IL-17-producing T regulatory cells," *PLoS One*, vol. 7, no. 9, pp. e45115–e45115, 2012.

[26] Y. Wang, M. A. Su, and Y. Y. Wan, "An essential role of the transcription factor GATA-3 for the function of regulatory T cells," *Immunity*, vol. 35, no. 3, pp. 337–348, 2011.

[27] G. Webb, Y.-Y. Chen, K.-K. Li et al., "Single-gene association between *GATA-2* and autoimmune hepatitis: a novel genetic insight highlighting immunologic pathways to disease," *Journal of Hepatology*, vol. 64, no. 5, pp. 1190–1193, 2016.

[28] H. Uda, M. Takei, and Y. Mishima, "Immunopathology of vitiligo vulgaris, Sutton's leukoderma and melanoma-associated vitiligo in relation to steroid effects: II the IgG and C3 deposits in the skin," *Journal of Cutaneous Pathology*, vol. 11, no. 2, pp. 114–124, 1984.

[29] U. Bhor and S. Pande, "Scoring systems in dermatology," *Indian Journal of Dermatology, Venereology and Leprology*, vol. 72, no. 4, p. 315, 2006.

[30] C. E. Avalos-Martínez, J. C. Rodríguez-Alba, L. Berrón-Ruiz et al., "Measurement of suppressor activity of T $CD4^{+-}$ $CD25^{+}$ T reg cells using bromodeoxyuridine incorporation assay," *Immunological Investigations*, vol. 42, no. 4, pp. 369–381, 2013.

[31] L. W. Collison and D. A. A. Vignali, "In vitro Treg suppression assays," *Methods in Molecular Biology*, vol. 707, pp. 21–37, 2011.

[32] P. S. Giri, A. H. Bharti, R. Begum, and M. Dwivedi, "Calcium controlled NFATc1 activation enhances suppressive capacity of regulatory T cells isolated from generalized vitiligo patients," *Immunology*, 2022.

[33] J.-H. Izquierdo, F. Bonilla-Abadía, C. A. Cañas, and G. J. Tobón, "Calcium, channels, intracellular signaling and autoimmunity," *Reumatología Clínica*, vol. 10, no. 1, pp. 43–47, 2014.

[34] X. Cao, S. F. Cai, T. A. Fehniger et al., "Granzyme B and perforin are important for regulatory T cell-mediated suppression of tumor clearance," *Immunity*, vol. 27, no. 4, pp. 635–646, 2007.

[35] J. Loebbermann, H. Thornton, L. Durant et al., "Regulatory T cells expressing granzyme B play a critical role in controlling lung inflammation during acute viral infection," *Mucosal Immunology*, vol. 5, no. 2, pp. 161–172, 2012.

[36] A. Wargnier, S. Legros-Maida, R. Bosselut et al., "Identification of human granzyme B promoter regulatory elements interacting with activated T-cell-specific proteins: implication of Ikaros and CBF binding sites in promoter activation,"

Proceedings of the National Academy of Sciences of the United States of America, vol. 92, no. 15, pp. 6930–6934, 1995.

[37] D. Bruder, M. Probst-Kepper, A. M. Westendorf et al., "Frontline: neuropilin-1: a surface marker of regulatory T cells," *European Journal of Immunology*, vol. 34, no. 3, pp. 623–630, 2004.

[38] E. Szurek, A. Cebula, L. Wojciech et al., "Differences in expression level of helios and neuropilin-1 do not distinguish thymus-derived from extrathymically-induced CD4+Foxp3+ regulatory T cells," *PLoS One*, vol. 10, no. 10, article e0141161, 2015.

[39] M. Leclerc, E. Voilin, G. Gros et al., "Regulation of antitumour CD8 T-cell immunity and checkpoint blockade immunotherapy by Neuropilin-1," *Nature Communications*, vol. 10, no. 1, p. 3345, 2019.

[40] C. H. Bird, M. E. Christensen, M. S. J. Mangan et al., "The granzyme B-Serpinb9 axis controls the fate of lymphocytes after lysosomal stress," *Cell Death and Differentiation*, vol. 21, no. 6, pp. 876–887, 2014.

[41] E. Zorn, E. A. Nelson, M. Mohseni et al., "IL-2 regulates FOXP3 expression in human CD4+CD25+ regulatory T cells through a STAT-dependent mechanism and induces the expansion of these cells in vivo," *Blood*, vol. 108, no. 5, pp. 1571–1579, 2006.

[42] M. T. Esser, D. M. Haverstick, C. L. Fuller, C. A. Gullo, and V. L. Braciale, "Ca2+ signaling modulates cytolytic T lymphocyte effector functions," *The Journal of Experimental Medicine*, vol. 187, no. 7, pp. 1057–1067, 1998.

Hindawi
Journal of Immunology Research
Volume 2022, Article ID 6789055, 19 pages
https://doi.org/10.1155/2022/6789055

Research Article

BACH2 in TRegs Limits the Number of Adipose Tissue Regulatory T Cells and Restrains Type 2 Immunity to Fungal Allergens

Amanda Contreras,[1] Darin L. Wiesner,[2] Brock Kingstad-Bakke,[1] Woojong Lee,[1] John P. Svaren,[3] Bruce S. Klein,[2] and M. Suresh[1]

[1]*Department of Pathobiological Sciences, University of Wisconsin-Madison, Madison, 53706 WI, USA*
[2]*Department of Medical Microbiology and Immunology, University of Wisconsin-Madison, Madison, 53706 WI, USA*
[3]*Department of Comparative Biosciences, University of Wisconsin-Madison, Madison, 53706 WI, USA*

Correspondence should be addressed to M. Suresh; sureshm@vetmed.wisc.edu

Received 21 June 2022; Accepted 19 July 2022; Published 5 August 2022

Academic Editor: Mitesh Dwivedi

FoxP3+ regulatory T cells (Tregs) are essential for self-tolerance and moderating tissue-damaging inflammation. Tregs that develop and mature in the thymus are classified as central Tregs or effector Tregs based on whether Tregs predominately inhabit secondary lymphoid organs (central Tregs) or tissues (effector Tregs). By generating mice that are conditionally deficient for Bach2 in peripheral Tregs, we have examined the role of Bach2 in regulating Treg homeostasis and effector functions. Unlike global and T cell-specific Bach2-deficient mice, Treg-specific Bach2 ablation did not result in unprovoked T_H2 inflammation in the lungs. However, Bach2 deficiency in Tregs led to augmented expressions of IRF4, BATF, and GATA3 and a significant increase in the accumulation of ST2 (IL-33R)$^{+ve}$ effector Tregs in the spleen and visceral adipose tissue (VAT) but not in the lungs. Enhanced Bach2-deficient Treg numbers in VAT was not linked to hyperresponsiveness to exogenous IL-33 in vivo. Most strikingly, Treg-specific Bach2 deficiency resulted in enhanced fungal protease-induced Type 2 allergic inflammation in the lungs, with no detectable effects on Type 1 responses to systemic or respiratory viral infections. In summary, we ascribe vital roles for Bach2 in peripheral Tregs: as a transcriptional checkpoint to limit precocious differentiation into effector Tregs in lymphoid tissues and as a regulator of the functional program that restrains Type 2 but not Type 1 inflammation in lungs. Results presented in this manuscript implicate dysregulated Tregs in the pathogenesis of airway hypersensitivities, asthma, and other allergic disorders.

1. Introduction

Foxp3+ regulatory T (Treg) cells are a vital T-cell subset that enforce self-tolerance and mitigate inflammatory pathology during immune responses to foreign antigens [1]. Peripheral Treg cells are divided into two distinct subtypes based on their anatomical distribution and function: central (cTregs) and effector Tregs (eTregs) [2, 3]. The majority of Treg cells in the secondary lymphoid tissues are cTregs that express high levels of lymphoid homing receptors CD62L and CCR7 and have trafficking patterns similar to naïve conventional T cells. By contrast, eTregs constitute a small fraction of Tregs in the lymphoid tissues, but the majority of Tregs in the peripheral tissues. Unlike cTregs, the eTregs display an activated effector phenotype (e.g., low expression levels of CD62L and CCR7, but high levels of CD44, inducible T cell costimulatory [ICOS], glucocorticoid-induced tumor necrosis factor receptor [GITR], and KLRG-1) with trafficking patterns similar to conventional effector T cells (i.e., traffic between blood and peripheral non-lymphoid tissues) [4, 5]. These Foxp3+ eTregs have been further classified into T_H1-Tregs, T_H2-Tregs, and T_H17-Tregs depending upon their polarity and co-opted expression of T-bet, GATA-3, and STAT-3 transcription factors, respectively [6]. This pattern of polarized differentiation endows each eTreg subset with distinct migratory and functional properties tailored to specifically balance inflammatory

responses driven by T_H1, T_H2, or T_H17 effector T cells. While IL-2R signaling is clearly necessary for eTreg cell differentiation [7–9], activation and polarization of cTregs into eTreg cell subsets are driven by TCR signaling and the inflammatory milieu in the peripheral tissues [10–13].

Tissue Tregs are a specialized subset of effector Tregs that reside in non-lymphoid tissues [14] and display characteristics including expression of transcription factors and homing or effector molecules that allow them to specialize for their specific tissue environment [14]. The IL-33 receptor ST2 thus far appears to be a universal feature of tissue Tregs that distinguishes them from classical lymphoid-organ Tregs [14]. While it is known that BATF and IRF4 are required for the induction of key components of the effector Treg transcriptional program, it has recently been demonstrated that BATF and IRF4 are required for the maintenance of tissue Tregs and expression of ST2 [15]. Furthermore, IL-33 induces GATA-3 phosphorylation, which subsequently binds to the ST2 locus to promote ST2 gene expression [16].

The transcriptional mechanisms that actively maintain the "quiescence" of cTregs or oppose the premature differentiation of eTregs or tissue Tregs from cTregs are not well understood. Bach2 is a transcription repressor that plays an integral role in the maintenance of T cell quiescence, differentiation, and generation of memory T cells [17–19]. Using global Bach2-deficient mice, we and others have shown that Bach2 plays crucial roles in the differentiation and competitive fitness of Tregs and protects against fatal T_H2-driven eosinophilic crystalline pneumonia [20, 21]. Further, it has been reported that ablation of Bach2 in all T cells leads to dysregulated T_H2 immunity and pulmonary inflammation in mice [22–24]. Until recently, Treg-specific role of Bach2 in maintaining the homeostasis of peripheral Tregs or suppressing T_H1/T_H2 immunity was unknown. Two reports have since shown that Bach2 restrains the differentiation of eTregs by repressing genes regulated by transcription factors such as IRF-4 [25–27]. Here, we report that ablation of Bach2 in peripheral Tregs leads to enhanced differentiation of effector/tissue Tregs in the lymphoid tissues, increased numbers of visceral adipose tissue (VAT) Tregs, and increased activation of T cells in response to normal homeostatic cues. Further, we show that loss of Bach2 in Tregs does not affect the development of T_C1/T_H1 cells during mucosal or systemic viral infections but instead augments the differentiation of IL-5 and IL-13-producing T_H2 cells during fungal allergen-induced inflammation in the lungs. These findings provide new insights into the Treg-specific roles for Bach2 in (i) regulating the homeostasis of splenic and VAT eTregs and (ii) restraining fungal protease-induced Type 2 immunity but not virus-induced Type 1 immunity.

2. Materials and Methods

2.1. Mice. Mice with a FoxP3+ Treg-specific deletion of Bach2 were generated by breeding floxed Bach2 mice [19] with B6.129(Cg)-*Foxp3*$^{tm4(YFP/icre)Ayr}$/J mice [28] to create Bach2$^{loxp/loxp}$FoxP3-Cre mice. Either littermate WT or C57BL/6 J mice were used as controls. The mice used in these studies were housed in specific-pathogen-free conditions in University of Wisconsin-Madison animal facilities. All animal experiments were conducted in accordance with approved protocols of the institutional animal care committee.

2.2. Viral Infections and Protease Treatment. The Armstrong strain of lymphocytic choriomeningitis virus (LCMV) was administered intraperitoneally at 2×10^5 plaque-forming units (PFU) per mouse to six- to eight-week-old mice; virus-specific T cell responses in spleen were quantified at day 8 after LCMV infection. The influenza virus strain A/PR/8/34 H1N1 (PR8) was administered intranasally at 100 PFU per mouse. Mice were euthanized, and lungs were harvested 10 days after PR8 infection. For fungal protease treatment, 10-week-old mice were anesthetized to receive intratracheal doses of 25 ug of fungal protease from *Aspergillus melleus* (Sigma #P4032) on days 1, 2, 7, and 14. On day 15 after the initial treatment, mice were injected with 3 ug of anti-CD45 antibody intravenously immediately prior to euthanasia and lung harvest.

2.3. IL-33 In Vivo Administration. Mice received intraperitoneal injections of 0.5 ug of recombinant murine IL-33 (Peprotech) or PBS on days 0, 2, 4, and 6 [29]. On the 8th day of IL-33 treatment, mice were euthanized to harvest lungs, VAT, and spleens.

2.4. IL-33 In Vitro Treatment. Spleens from naïve Bach2$^{loxp/loxp}$FoxP3-Cre and WT mice were processed into single cell suspensions and were plated at a concentration of 5×10^5 cells/well in a 96-well plate. Prior to plating cells, wells were coated with 1ug/mL anti-CD3. Cells were cultured for 72 hours with IL-2 (10 ng/mL) (BD Biosciences) and anti-CD28 (2ug/mL) in either the presence or absence of 1 ng/mL IL-33. Cells were then collected and processed for flow cytometry.

2.5. Flow Cytometry. Single-cell suspensions of mononuclear cells from lung, VAT, and spleen were prepared using standard procedures. Lung and VAT were digested in 2 mg/mL Collagenase D (Sigma) for 30 minutes while rotating at 37 °C. The digested tissues were then homogenized using the GentleMACS Dissociator (Miltenyi). Single-cell suspensions were first stained for viability with a LiveDead stain (eBioscience). Cells were then resuspended and stained with antibodies diluted in a staining buffer of either 2% BSA in PBS or in Brilliant Stain Buffer (BD Biosciences), depending on the combination of antibodies used. The fluorochrome-labeled antibodies that were used against cell-surface antigens include the following: CD8, CD4, CD25, CD44, CD62L, CD127, CD69, GITR, CTLA-4, KLRG-1, CCR7, CD103, CXCR3, ST2, CD27, CD11b, CD90.2, CD64, Siglec-F, PD-L1, CD19, CD11c, Ly6G, $\gamma\delta$ TCR, and TCR-β. Fluorochrome-labeled antibodies that were used against intracellular antigens include the following: IFN-γ, IL-4, IL-5, IL-13, IL-17A, BATF, IRF4, GATA3, Foxp3, Ki-67, Eomes, Tbet, and Helios. These antibodies were purchased from BD Biosciences (San Jose, CA), Biolegend (San Diego, CA), or eBioscience (San Diego, CA). Fluorochrome-conjugated tetramers for LCMV epitopes (D^b/NP396, D^b/GP33, I-A^b/GP66) and for PR8/H1N1 epitopes (D^b/NP366, D^b/PA224, I-A^b/NP311) were provided by the NIH Tetramer Core Facility (Emory University, Atlanta, GA). Samples were acquired with a BD LSRFortessa (BD Biosciences), and

resulting data was analyzed with FlowJo software (TreeStar, Ashland, OR).

2.6. Intracellular Cytokine Staining. To induce cytokine production in cells for intracellular cytokine staining, cells were stimulated directly ex vivo with human recombinant IL-2 (10 U/well) (BD Biosciences) and the epitope peptide at 0.1ug/mL. Depending on the experiment, cells were either stimulated with PMA/Ionomycin (Tonbo Biosciences) or LCMV peptides (NP396, GP33, and GP276) or PR8/H1N1 peptides (NP366, PA224, and NP311) (thinkpeptides, ProImmune Ltd.). Cells undergo 5 hours of stimulation at 37 °C in the presence of brefeldin A (1ug/mL, GolgiPlug, BD Biosciences). After stimulation, cells were stained for cell surface antigens, fixed, and permeabilized using the Cytofix/Cytoperm kit (BD Sciences). After fixation/permeabilization, cells were incubated with fluorochrome-labeled antibodies targeted against cytokines. For the fungal protease studies, cells extracted from the lungs were restimulated directly ex vivo with 100 ug/well of heat inactivated fungal protease for 6 hours. Brefeldin A was added for the last 4 hours of the restimulation. The cells were then fixed, permeabilized, and stained for intracellular cytokine expression as described above.

2.7. Intracellular Staining for Transcription Factors and Ki-67. To stain for intracellular proteins such as transcription factors and Ki-67, cells were fixed and permeabilized with the FoxP3 Staining Kit (eBioscience) using the manufacture's protocol. After fixation/permeabilization, cells were incubated with fluorochrome-labeled antibodies targeted against transcription factors and Ki-67. After staining, cells were analyzed with a BD LSRFortessa flow cytometer.

2.8. Statistical Analyses. Data statistics were calculated with Prism software (GraphPad Software, La Jolla, California, USA). Student's two-tailed *t*-test and one-way ANOVA analyses were used to calculate the statistical significance of differences between groups, and significance was defined at $p < 0.05$.

3. Results

3.1. Bach2 Restrains the Activation and Differentiation of Effector Tregs and Maintains Homeostasis of Naïve and Activated/Memory T Cells. We and others have previously reported that global Bach2 deficiency leads to aberrant differentiation of Tregs and activated/memory phenotype of peripheral T cells [20, 21]. To investigate the effect of conditional Bach2 deficiency in mature Tregs, we bred floxed Bach2 mice with Rudensky's Foxp3-Cre mice to generate the Bach2$^{loxp/loxp}$FoxP3-Cre mice. Loss of Bach2 in Tregs did not alter the frequency or total numbers of foxp3^{+ve} Tregs in spleen, which suggested that Bach2 is not required for the development and/or maintenance of these cells (Figures 1(a) and 1(b)). Next, we assessed whether Treg-specific Bach2 deficiency dysregulated the homeostasis of naïve and activated/effector Tregs. Notably, Bach2-deficient Tregs exhibited enhanced expression of CD44, CD127, CD69, and GITR, which was strongly suggestive of skewed differentiation favoring an effector Treg phenotype (Figure 1(c)) [4, 5]. Clearly, there was a significant increase in the percentages and numbers of the activated/effector (CD44^{HI}/CD62L^{LO}/CCR7^{LO}) Bach2-deficient Tregs, as compared to their WT counterparts (Figure 1(d)). Further, there were increased frequencies and total numbers of Bach2-deficient Tregs that expressed high levels of KLRG1, CD127, and CD69.

Next, we investigated whether loss of Bach2 in Tregs affected the homeostasis of classical naïve and activated/memory T cells in *trans*. We found an increase in the percentages of CD4 and CD8 T cells with an activated/effector phenotype (CD44^{HI}/CD62L^{LO}) in the spleens of Bach2$^{loxp/loxp}$FoxP3-Cre mice compared to WT counterparts (Figure 1(e)). In addition, we observed a decrease in the percentages of CD4 T cells with a naïve phenotype (CD44^{LO}/CD62L^{HI}) (Figure 1(e)). Next, we were interested in whether Bach2-deficient Tregs altered the production of cytokines from conventional T cells. Splenic CD8 and CD4 T cells had a substantial increase in the percentages and total numbers of cells that produced IFNγ in the Bach2$^{loxp/loxp}$FoxP3-Cre mice compared to WT mice. Additionally, CD4 T cells from Bach2$^{loxp/loxp}$FoxP3-Cre mice displayed higher frequencies of IL-13 and IL-17A-producing cells as well as total cells that produced IL-17A (Figures 1(f) and 1(g)). These augmented levels of cytokine-producing cells suggest that Bach2-deficient Tregs are unable to repress the activation and differentiation of T_H1 (IFNγ), T_H2 (IL-13), and T_H17 (IL-17A) effector CD4 T cells. Taken together, these data suggested that Bach2 plays an essential role in maintaining quiescence/naivety by restraining the differentiation of naïve Tregs into effector Tregs. Furthermore, loss of Bach2 expression in Tregs led to the development of activated/memory T cells, which suggests that the ability of Tregs to limit activation of classical T cells requires Bach2 expression in Tregs.

3.2. Bach2 Represses Tissue Treg-like Cell Differentiation in Secondary Lymphoid Tissues. Apart from the well-defined subsets of naïve and effector Tregs in secondary lymphoid tissues, recent work has identified a distinct subset of Tregs termed as tissue Tregs that can be found in non-lymphoid tissues such as lungs, skeletal muscle, and lamina propria [14]. While these tissue Tregs display the prototypical effector surface phenotype markers such as CXCR3 and CD103 and express transcription factors BATF, IRF4, and GATA3, they possess certain properties that make each tissue Treg population unique. However, tissue Tregs possess a distinguishing surface marker that has been found on all tissue-residing Tregs populations currently examined: ST2. ST2 is a receptor for IL-33 and is expressed on Tregs that preferentially accumulate in non-lymphoid tissues [30, 31]. It was of interest to determine whether Bach2 deficiency dysregulated the differentiation of tissue Tregs in lymphoid tissues. As expected, a modest fraction of Tregs expressed CD103, CXCR3, and ST2 in spleens of WT mice. Surprisingly, however, we found that Bach2 deficiency in Tregs led to a substantive increase in the frequencies of CD103^{+ve}, CXCR3^{+ve}, and ST2^{+ve} Tregs in spleen, as compared to their WT counterparts. The total numbers of CD103^{+ve} and ST2^{+ve} Tregs were significantly higher in the spleens of Treg-specific Bach2-deficient mice than in WT mice

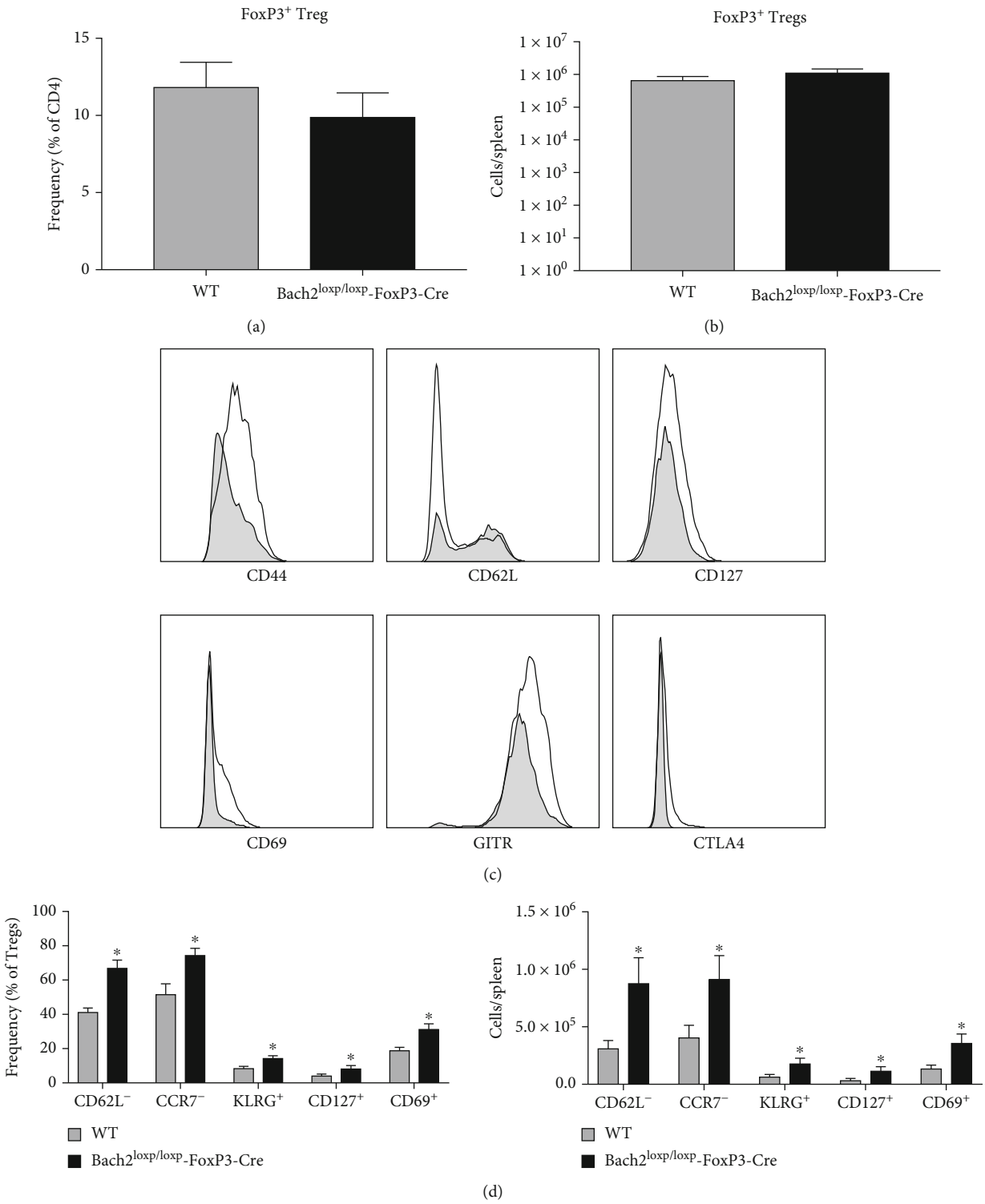

Figure 1: Continued.

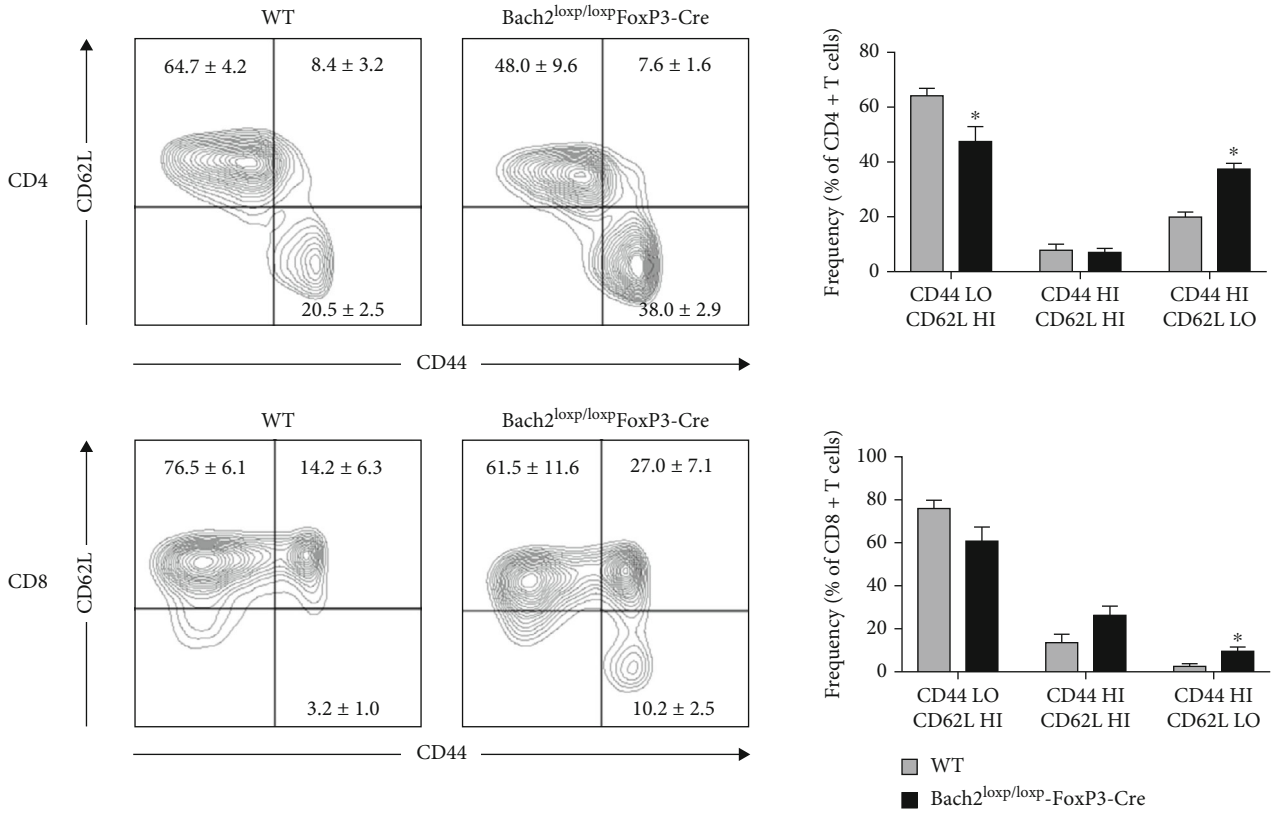

(e)

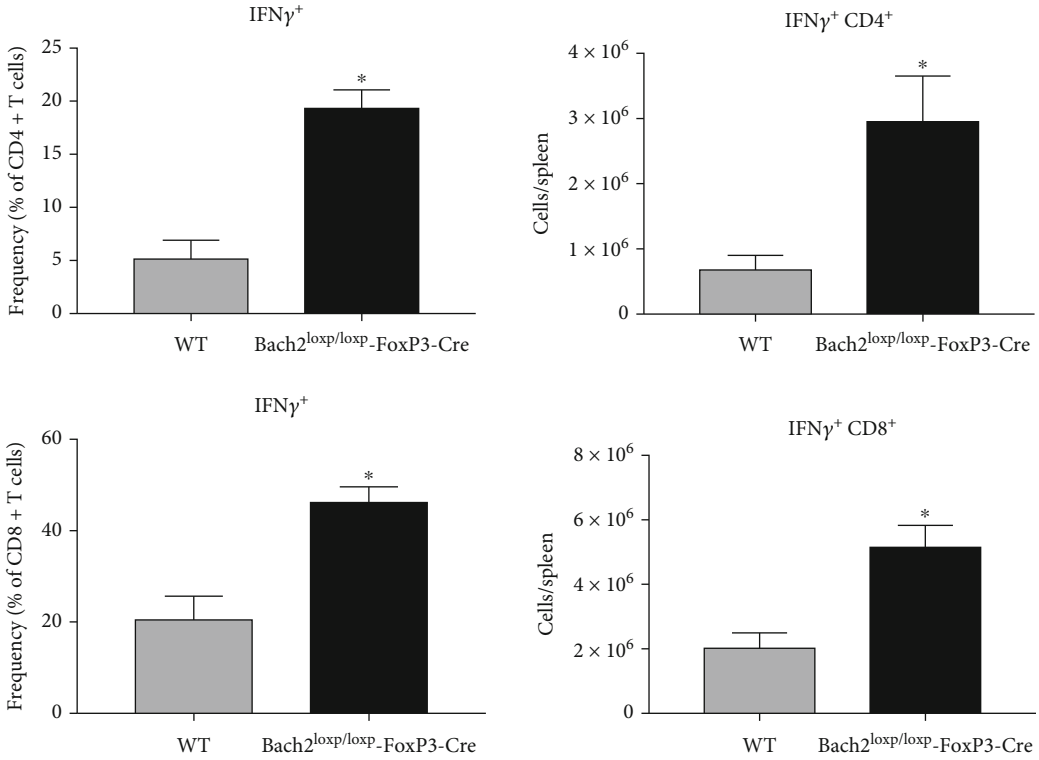

(f)

Figure 1: Continued.

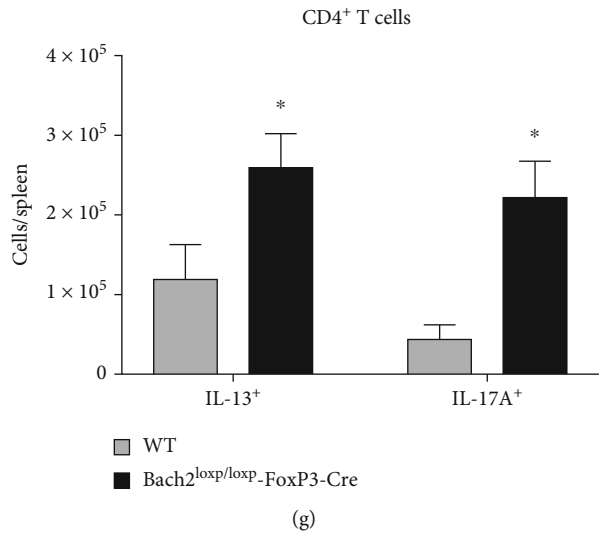

Figure 1: Bach2 regulates classical and regulatory T cell homeostasis. Splenocytes from naïve WT and Bach2$^{loxp/loxp}$FoxP3-Cre mice were stained for intracellular and extracellular antigens and analyzed by flow cytometry. (a) Frequency and (b) number of Foxp3^{+ve} Treg cells. (c) Histograms are gated on Foxp3^{+ve} Treg cells and show staining for the indicated markers in WT (shaded) and Bach2$^{loxp/loxp}$FoxP3-Cre mice (line) mice. (d) Frequency and numbers of Tregs expressing the indicated molecules. (e) Activation of classical T cells was analyzed by staining with anti-CD44 and anti-CD62L; contour plots are gated on CD4 or CD8 T cells. (f), (g) Splenocytes were stimulated for 5 hrs in vitro with PMA and ionomycin in the presence of Brefeldin A, and cytokine production by CD4 and CD8 T cells was measured by intracellular staining for (f) IFN-γ and (g) IL-13 and IL-17A. This experiment was repeated three times with similar results, 4-5 mice per group. $*p < 0.05$.

(Figure 2(a)). It is possible that the increased numbers of tissue Treg-like cells in the spleen of Treg-specific Bach2-deficient mice could result from defects in trafficking of these cells to non-lymphoid tissues. To address this possibility, we quantified Tregs in lungs and liver of Treg-specific Bach2-deficient mice. Data in Figure 2 show that the percentages and numbers of Tregs in lungs and liver (data not shown) of Treg-specific Bach2-deficient mice were comparable to those in WT mice. Therefore, it is likely that tissue Tregs are accumulating in spleen of Treg-specific Bach2-deficient mice due to increased differentiation and not driven by defective trafficking of these cells from spleen to non-lymphoid tissues.

We next investigated whether Bach2 deficiency-induced enhancement in the development of ST2^{+ve} tissue Tregs was associated with altered expression of tissue Treg fate determining transcription factors BATF, IRF4, and GATA3. Indeed, we found statistically significant increases of BATF, IRF4, and GATA3 expression in Bach2-deficient Tregs compared to their WT counterparts only in spleen, but not in lungs (Figure 2(b)). Overall, our studies have revealed an unexpected increase in the ST2^{+} CD103^{+} CXCR3^{+} tissue Treg-like cells in the spleen of mice harboring a Treg-specific Bach2 deletion. These data suggest that Bach2 exerts a transcriptional block in the differentiation of tissue Treg-like cells in the lymphoid tissues.

3.3. Bach2 Limits the Numbers of Visceral Adipose Tissue Tregs. Tissue Tregs have been most thoroughly characterized in the VAT, and transcription factors BATF and IRF-4 bind to the ST2 promoter and promote ST2 expression [15]. Since Bach2-deficient Tregs express elevated levels of ST2, BATF, and IRF-4 (Figure 2), it was of interest to investigate whether Bach2 regulated the homeostasis of VAT Tregs. Analysis of Tregs in VAT showed that Bach2 deficiency led to a significant increase in the numbers of CD103^{+ve} and CXCR3^{+ve} Tregs in VAT (Figure 3(b)); the numbers of ST2^{+ve} Tregs were not significantly altered in VAT of Treg-specific Bach2 deficient mice. Next, we examined whether Bach2 deficiency-induced increased numbers of VAT Tregs was associated with elevated expression of transcription factors that drive the VAT Treg program. We found that Bach2-deficient VAT Tregs exhibited significantly higher levels of GATA3 and IRF4 compared to WT Tregs (Figure 3(c)).

ST2 is the cellular receptor for IL-33, and it is known that ST2 and IL-33 are required for the development of VAT Tregs [15]. Mechanistically, IL-33 enhances ST2 expression by inducing GATA-3 phosphorylation and subsequent recruitment of GATA-3 to the ST2 locus. Because Bach2-deficient Tregs have higher expression of ST2 in the spleen and express elevated levels of GATA3 and IRF4, we explored whether Bach2-deficient Tregs are more poised to the effects of IL-33 and therefore more readily differentiate into tissue Tregs. As expected, in vitro exposure of WT splenic Tregs to IL-33 induced ST2 expression in a fraction of Tregs (Figure 3(d)). While the percentages of ST2-expressing Tregs were already higher among untreated Bach2-deficient Tregs, IL-33 treatment further increased the percentages of ST2^{+ve} Tregs (Figure 3(d)). The magnitude of ST2 induction was comparable in WT and Bach2-deficient Tregs, but the IL-33-induced expressions of GATA3, IRF4, and BATF were greater in Bach2-deficient Tregs, as compared to those in WT Tregs (Figure 3(d)), which suggest that Bach2 restrains IL-33-induced expression of these transcription factors in Tregs.

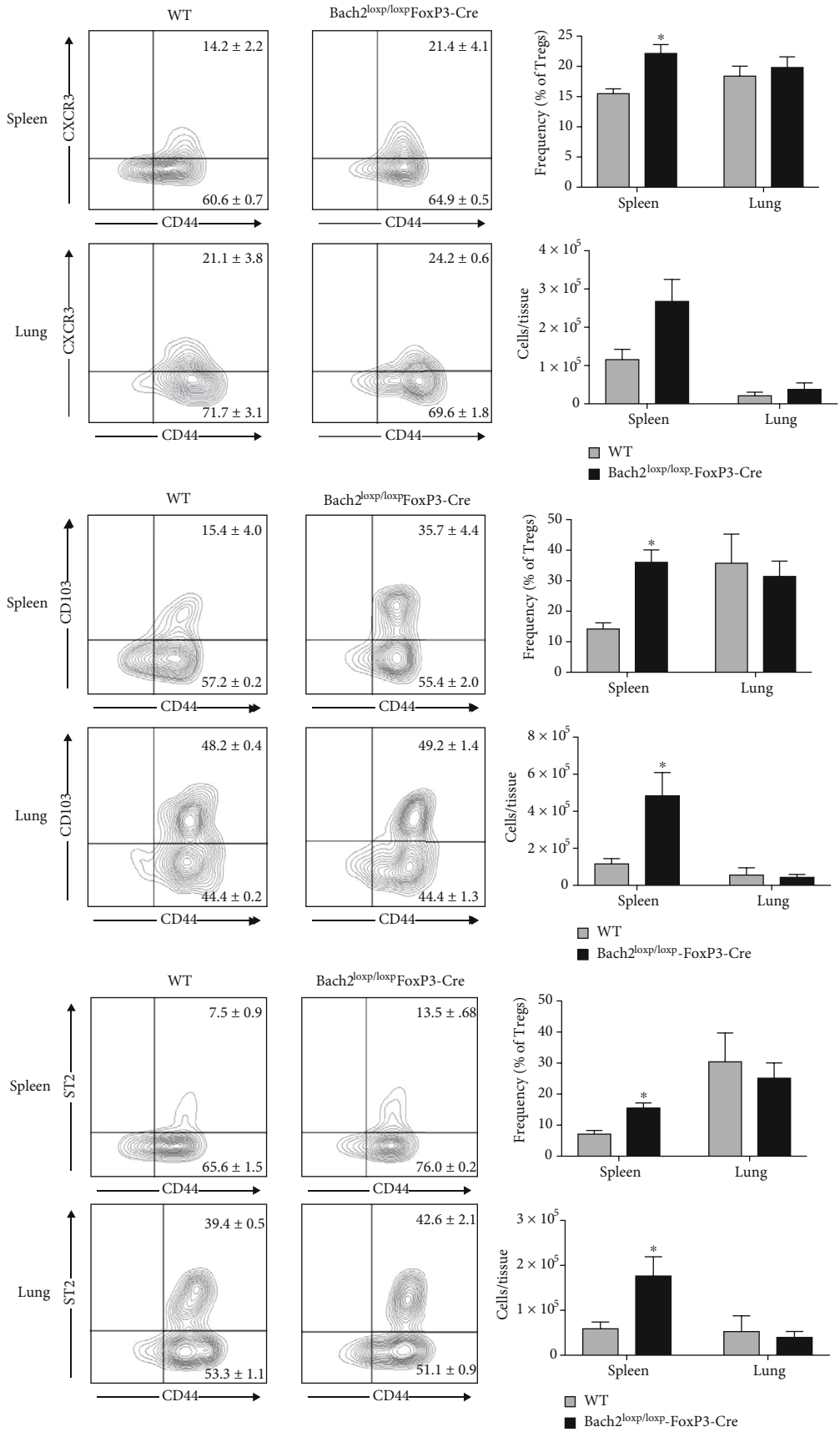

(a)

Figure 2: Continued.

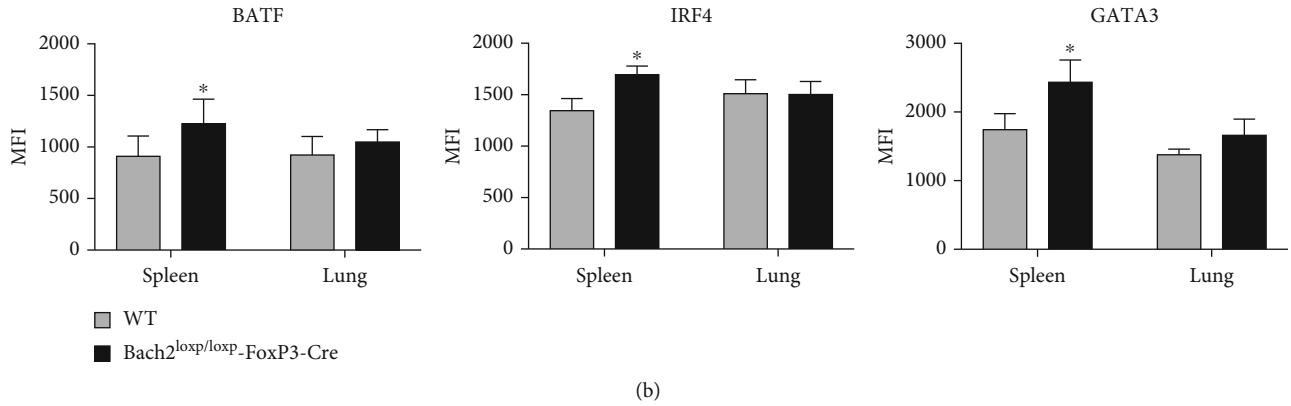

Figure 2: Bach2 restrains tissue regulatory T cell differentiation in the spleen. Spleens and lungs were collected from naïve WT and Bach2$^{loxp/loxp}$FoxP3-Cre mice and Tregs were analyzed by flow cytometry. (a) Frequency and number of Foxp3^{+ve} Tregs in lung and splenic Treg cells that expressed CXCR3, CD103, or ST2. (b) Data shows MFI levels for BATF, IRF4, and GATA3 staining in Foxp3^{+ve} Tregs. This experiment was repeated three times with similar results, 4-5 mice per group. $*p < 0.05$.

Exogenous IL-33 administration has been reported to drive the expansion of VAT Tregs in vivo [15]. Here, we investigated whether Tregs from WT or Bach2-deficient Tregs mice respond differently to IL-33 treatment in vivo. IL-33 treatment significantly augmented the numbers of Tregs only in the VAT, but not in the spleen or lungs (Figure 3(e)) of both WT and Bach2$^{loxp/loxp}$FoxP3-Cre mice. The IL-33-responsive population of Tregs included CD103^{+ve}, CXCR3^{+ve}, and ST2^{+ve} Tregs in both groups of mice (Figure 3(f)). Mechanistically, IL-33-driven expansion of Tregs in VAT was associated with elevated percentages of proliferating Ki67^{+ve} Tregs (not shown) in both WT and Bach2$^{loxp/loxp}$FoxP3-Cre mice. As compared to PBS-treated controls, the magnitude of increase in the number of Tregs was similar for WT and Bach2$^{loxp/loxp}$-FoxP3-Cre mice. Taken together, data in Figure 3 strongly suggest that Bach2 deficiency did not alter the IL-33-driven proliferative expansion of VAT Tregs.

3.4. Bach2-Deficiency in Tregs Does Not Alter the Development of T_H1 or T_C1 Cells during an Acute Viral Infection. Viral infections typically trigger Type 1 immune responses and Tregs play a crucial role in restraining the effector phase of T cell responses to mitigate inflammation and the associated tissue damage. Data in Figure 1 showed that conventional CD8 and CD4 T cells from Bach2$^{loxp/loxp}$FoxP3-Cre mice displayed greater activated/effector phenotypic and functional properties, as compared to conventional T cells from WT mice. The elevated levels of IFNγ production in CD4 T cells of Bach2$^{loxp/loxp}$FoxP3-Cre mice suggested that deficiency for Bach2 in Tregs might lead to dysregulated Type 1 immunity. Therefore, it was of interest to determine whether (1) dysregulated Treg homeostasis in Bach2$^{loxp/loxp}$FoxP3-Cre mice is altered by viral infections and (2) Bach2 deficiency in Tregs affects the development of T_H1 and T_C1 type T cells during an acute viral infection. First, we infected cohorts of WT and Bach2$^{loxp/loxp}$FoxP3-Cre mice with lymphocytic choriomeningitis virus (LCMV) and assessed Tregs in spleen at day 8 after infection. The percentages and total number of Foxp3^{+ve} Tregs in spleens of LCMV-infected Bach2$^{loxp/loxp}$FoxP3-Cre mice were similar to those in WT mice (Figure 4(a)). Next, we evaluated the expression of surface markers associated with an activated/effector Treg phenotype in LCMV-infected WT and Bach2$^{loxp/loxp}$FoxP3-Cre mice. There were no significant changes in the percentages of CD44, CD62L, CXCR3, CD27, CD127, and KLRG-1-expressing Tregs in spleens of Bach2$^{loxp/loxp}$FoxP3-Cre mice. However, greater percentages of Bach2-deficient Tregs expressed CD69 and GITR, as compared to WT Tregs (Figure 4(b)). Thus, overall, as compared to Tregs in uninfected mice (Figure 1), LCMV infection led to activation of WT Tregs, and the levels were similar to those in LCMV-infected Bach2$^{loxp/loxp}$FoxP3-Cre mice.

Next, we assessed the effect of Treg-specific Bach2 deficiency on CD4 and CD8 T cell responses to LCMV infection. The frequency and numbers of LCMV-specific CD8 T cells in Bach2$^{loxp/loxp}$FoxP3-Cre mice were similar to those in WT mice. Likewise, the numbers of CD4 T cells specific to the LCMV GP66 epitope in WT mice were comparable to those in Bach2$^{loxp/loxp}$FoxP3-Cre mice (Figure 4(c)). To investigate if Bach2 deficiency altered cytokine production by LCMV-specific CD4 and CD8 T cells, we measured antigen-induced IFN-γ production ex vivo. We did not find differences in the percentages of LCMV-specific IFN-γ-producing CD8 and CD4 T cells in spleens between WT and Bach2$^{loxp/loxp}$FoxP3-Cre mice (Figure 4(d)). Taken together, data in Figure 4 suggest that Treg-specific Bach2 deficiency had no detectable effect on the development of CD4 and CD8 T cell responses during an acute LCMV infection.

Next, we assessed the effect of Treg-specific Bach2 deficiency on T_H1/T_C1 responses to a mucosal infection with influenza A virus (IAV). First, we infected Bach2$^{loxp/loxp}$-FoxP3-Cre and WT mice with PR8 strain of IAV and analyzed Tregs in the lung on day 10 post-infection. We did not find significant differences in the number of Tregs between the Bach2$^{loxp/loxp}$FoxP3-Cre and WT mice in the lung (Figure 4(e)). Likewise, there were no changes in the percentages of CD44, CD62L, CXCR3, CD103, CD27, CD69, CD127, and KLRG-1-expressing Tregs in the lung or BAL of influenza virus-infected Bach2$^{loxp/loxp}$FoxP3-Cre mice (Figure 4(f)).

Next, we investigated whether Bach2-deficiency in regulatory T cells altered the activation and expansion of effector

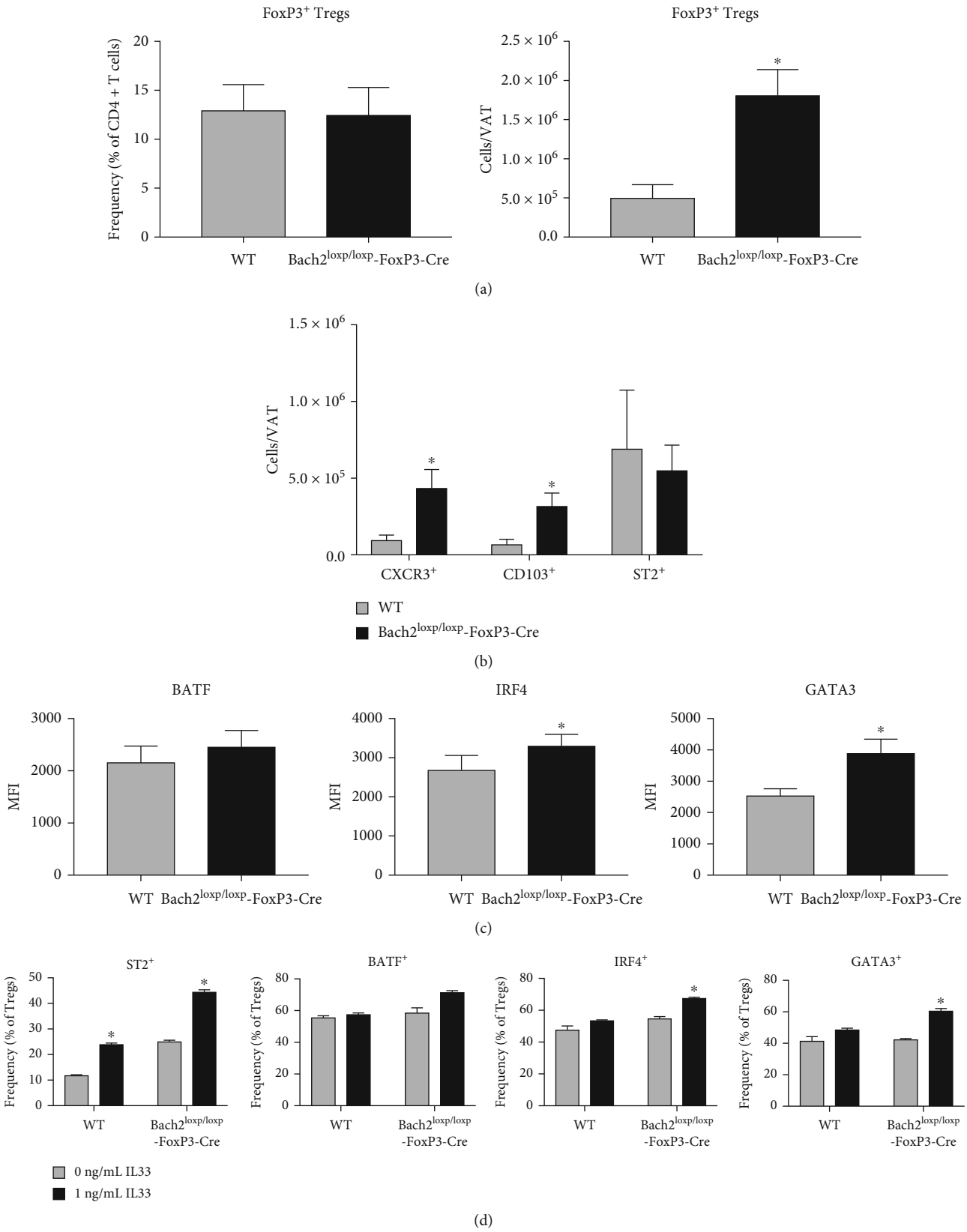

Figure 3: Continued.

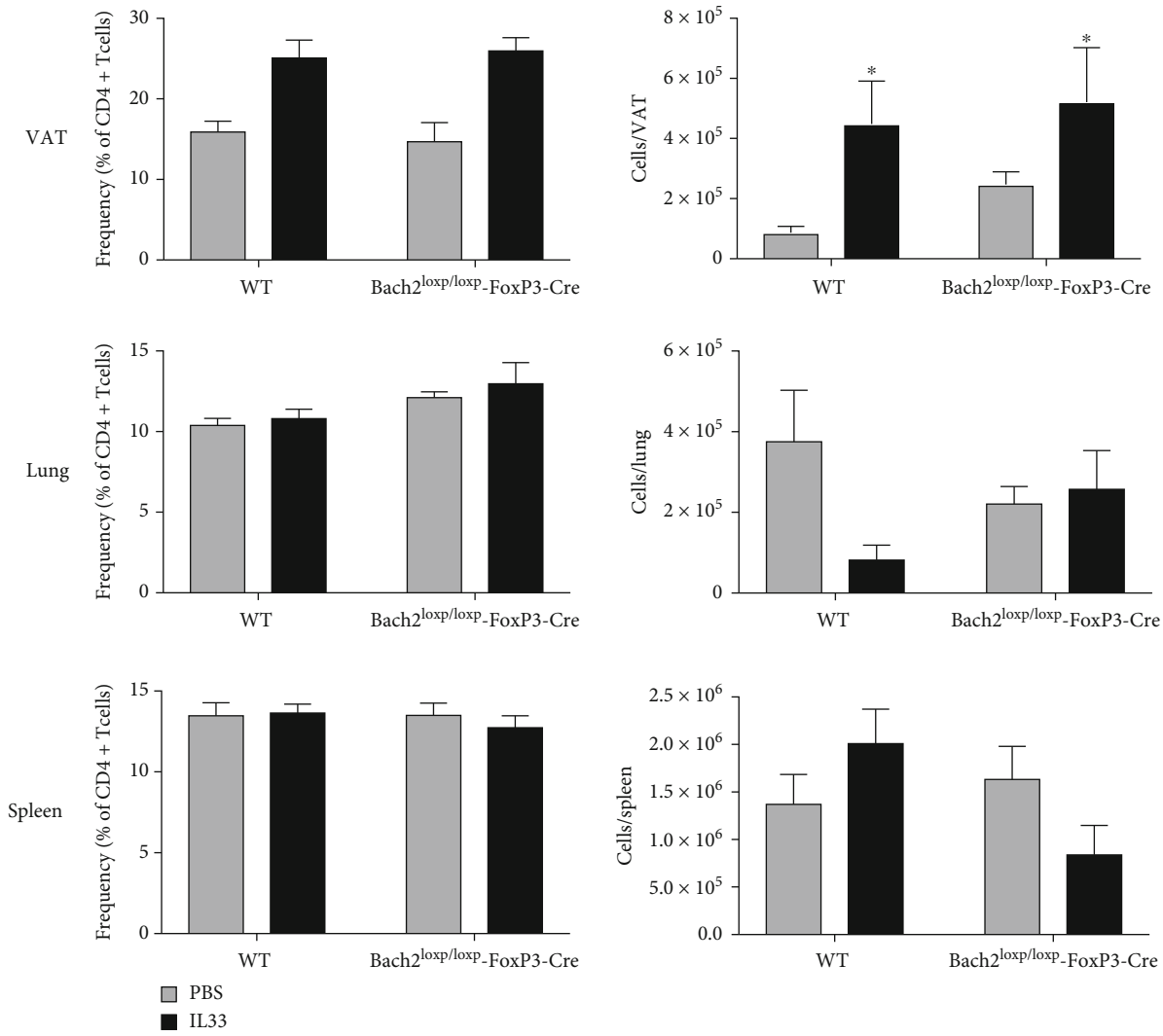

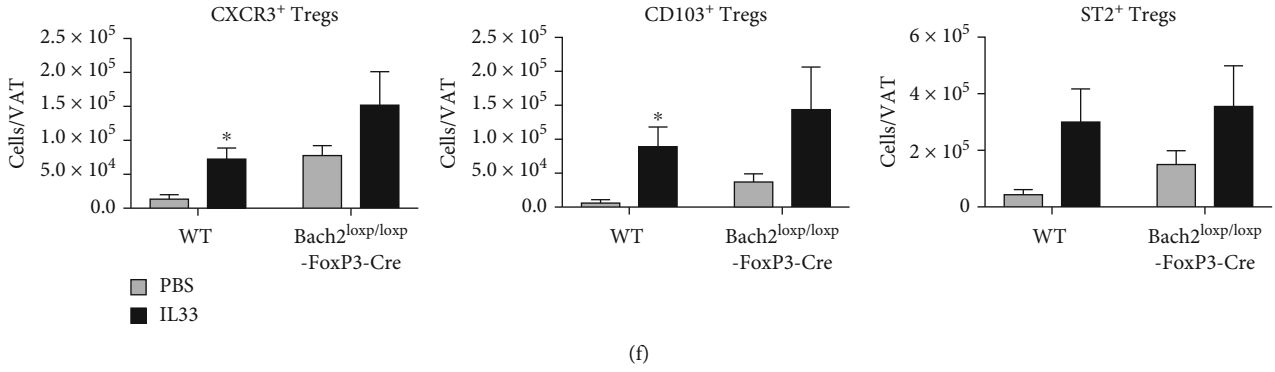

Figure 3: Bach2 limits the size of tissue regulatory T cell population in the VAT. Mononuclear cells isolated from the VAT of WT and Bach2$^{loxp/loxp}$FoxP3-Cre mice were analyzed by flow cytometry. Tregs in the VAT of naïve WT and Bach2$^{loxp/loxp}$FoxP3-Cre mice were analyzed for (a) their frequency and numbers, (b) tissue Treg marker expression, and (c) MFI levels for BATF, IRF4, and GATA3. (d) Splenocytes from naïve WT and Bach2$^{loxp/loxp}$FoxP3-Cre mice were stimulated in vitro with anti-CD3, anti-CD28, and IL-2 in the presence of absence of IL-33 for 72 hrs. Bar graphs display frequencies of ST2^{+ve} and BATF^{+ve}, IRF4^{+ve}, or GATA3^{+ve} Tregs. (E-H) WT and Bach2$^{loxp/loxp}$FoxP3-Cre mice received four injections of IL-33, and the indicated tissues were analyzed on day 8. (e) Frequency and number of Treg cells in the VAT, lungs, and spleen. (f) Number of CXCR3-, CD103-, and ST2-positive Tregs in the VAT. This experiment was repeated two times with similar results, 5 mice per group. $*p < 0.05$.

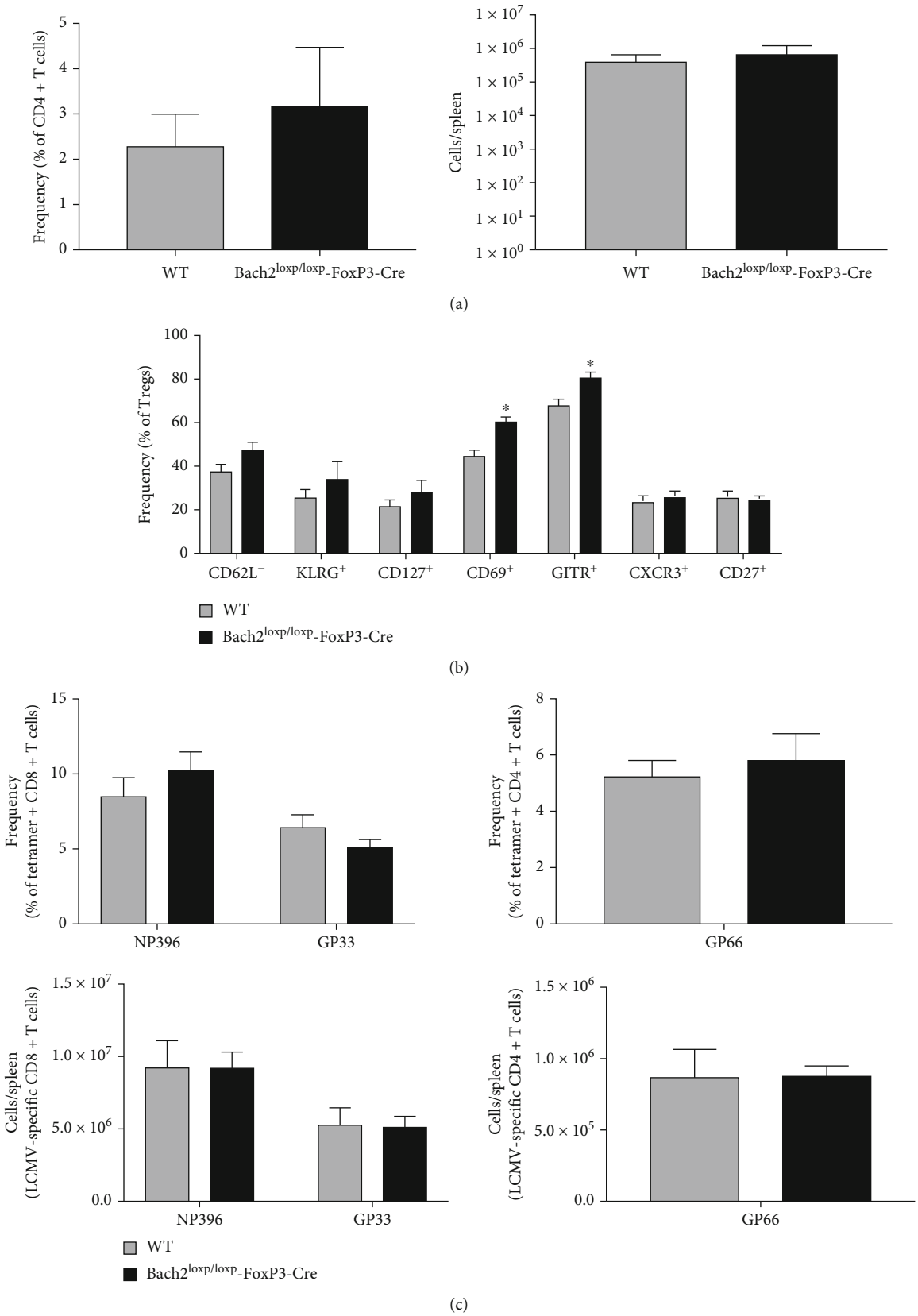

Figure 4: Continued.

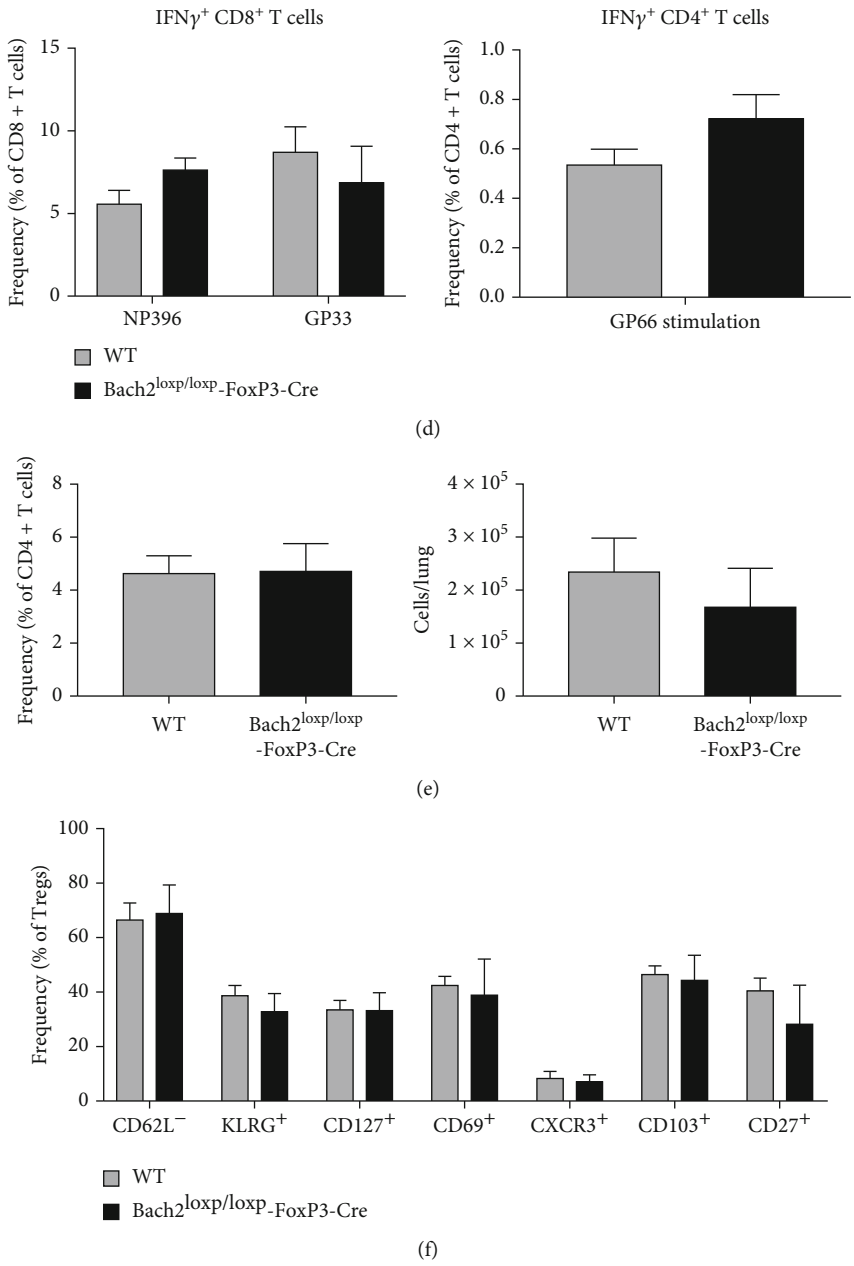

Figure 4: Continued.

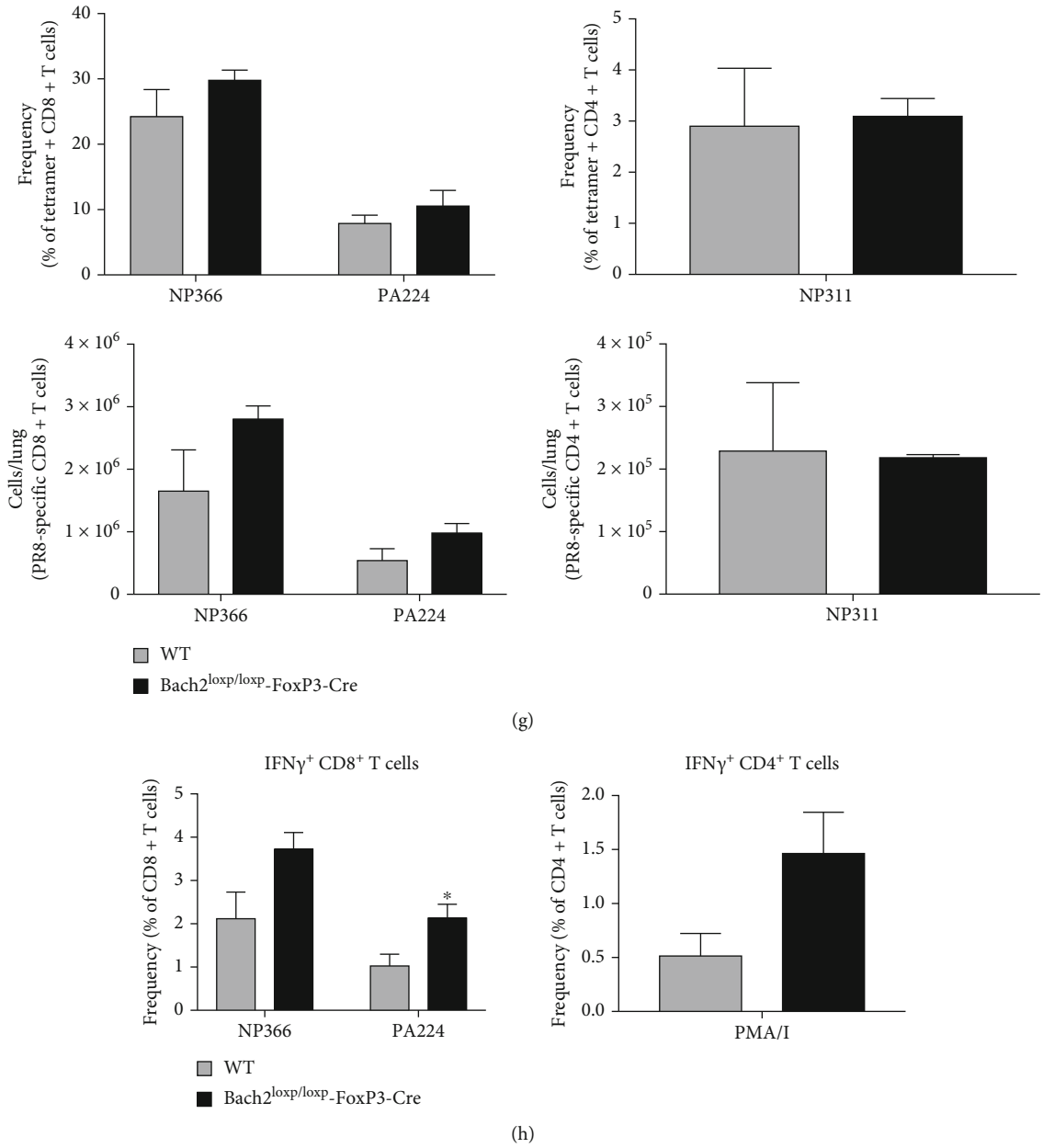

Figure 4: Bach2-deficiency in Tregs does not affect systemic or mucosal Type 1 immunity. WT and Bach2$^{loxp/loxp}$FoxP3-Cre mice were infected with (a-d) LCMV-Armstrong or (e-h) PR8/H1N1 influenza virus, and Tregs were analyzed by flow cytometry. (a) Frequency and numbers of splenic Tregs in LCMV-infected mice. (b) Frequency of effector Treg subsets in the spleen. (c) Frequency and numbers of tetramer binding CD8 (specific to NP396 or GP33 epitopes) and CD4 (specific for GP66 epitope) T cells in the spleen. (d) Splenocytes were stimulated for 5 hrs in vitro with LCMV peptides in the presence of Brefeldin A, and cytokine production was measure by intracellular staining for IFNγ in CD8 and CD4 T cells from the spleen. (e) Frequency and numbers of Tregs in the lung of influenza virus-infected mice. (f) Frequency of effector Treg subsets in the lung. (g) Frequency and numbers of influenza virus-specific CD8 (specific to NP66 and PA224 epitopes) and CD4 (specific to NP311 epitope) T cells in the lung. (h) Mononuclear cells from the lung were stimulated for 5 hrs in vitro with PR8 peptides or PMA and ionomycin in the presence of Brefeldin A, and cytokine production was measured by intracellular staining of IFNγ in CD8 and CD4 T cells from the lung. This experiment was repeated three times with similar results, 4-5 mice per group. $*p < 0.05$.

CD8 and CD4 T cells during an influenza infection. No significant differences in the frequencies or total number of influenza-specific CD8 or CD4 T cells were seen in the lung and BAL of Bach2$^{loxp/loxp}$FoxP3-Cre mice (Figure 4(g)). To determine if there were any changes in the production of IFN-γ by influenza-specific CD4 and CD8 T cells, we stimulated lymphocytes in the lung with corresponding influenza peptides and measured IFN-γ production. Although stimulation with the PA224 peptide elicited greater percentages of IFN-γ-producing CD8 T cells in Bach2$^{loxp/loxp}$FoxP3-

Cre mice (Figure 4(h)), Bach2-deficiency in Tregs had minimal effects on the activation or cytokine production of CD8 or CD4 T cells, during a mucosal T_H1/T_C1 response to influenza virus.

3.5. Bach2 Deficiency in Tregs Exacerbates Fungal Protease-Induced T_H2 Immunity. Genome-wide association studies have linked variations in Bach2 gene to asthma in humans, and global Bach2 deficiency in mice leads to unprovoked T_H2 immunity and fatal eosinophilic crystalline pneumonia [20, 32, 33]. Additionally, Bach2 deficiency in all T cells leads to spontaneous development of T_H2-driven lung disease [24]. We observed that Treg-specific Bach2 deficiency did not result in overt lung pathology, which suggested that Bach2 expression in conventional T cells is sufficient to protect against spontaneous T_H2 lung disease. However, it was unknown whether Bach2 deficiency in Tregs affected (1) their responses to allergic inflammation and (2) T_H2 responses and susceptibility of mice to allergen-provoked inflammation in the lungs. To investigate the effect of Treg-specific Bach2 deficiency on T_H2 immunity, we utilized a model of allergic inflammation that is induced by administration of alkaline protease 1 of *Aspergillus melleus*; *Aspergillus* protease has been known to elicit a potent T_H2 response in the lungs [34]. The immunological response of Bach2$^{loxp/loxp}$FoxP3-Cre and WT mice to *Aspergillus* protease administration is shown in Figure 5. As shown in Figure 5(a), protease administration induced substantial increases in the numbers of Tregs in the lungs of WT mice, and protease-induced Treg accumulation was markedly accentuated in lungs of Bach2$^{loxp/loxp}$FoxP3-Cre mice. The increased numbers of Tregs in lungs of protease-treated Bach2$^{loxp/loxp}$FoxP3-Cre mice included CXCR3^{+ve}, CD103^{+ve}, ST2^{+ve}, and KLRG-1^{+ve} Tregs (Figure 5(b)), and this was associated with elevated levels of IRF4 and GATA3 (Figure 5(c)). We also compared the accumulation of inflammatory cells in the lungs of protease-treated WT and Bach2$^{loxp/loxp}$FoxP3-Cre mice (Figure 5(d)). Overall, lungs of protease-treated Bach2$^{loxp/loxp}$FoxP3-Cre mice contained higher numbers of monocytes, monocyte-derived DCs, CD103^{+ve} DCs, inflammatory DCs, alveolar macrophages, neutrophils, and eosinophils, as compared to protease-treated WT mice. Next, we assessed whether Treg-specific Bach2 ablation affected the $T_H1/T_H2/T_H17$ polarization of protease-reactive CD4 T cells in the lungs. Significantly more IL-5- and IL-13-producing CD4 T cells were detected in the lungs of protease-treated Bach2$^{loxp/loxp}$FoxP3-Cre mice than in WT mice (Figure 5(e)). Taken together, data in Figure 5 strongly suggest that Bach2 plays a critical role in promoting the ability of Tregs to limit T_H2 immunity and allergic inflammation in the lungs.

4. Discussion

It has been established that ST2^{+ve} tissue Tregs are a specialized subset of effector Tregs that reside primarily in non-lymphoid tissues [14, 15], but not in the spleen [15, 16, 35, 36]. In this study, we report a surprising finding that a substantive proportion of Bach2-deficient Tregs in spleen expressed conventional activation markers and elevated levels of tissue Treg markers CXCR3, CD103, and ST2. The increase in the numbers of effector/tissue Tregs in spleen of Treg-specific Bach2-deficient mice cannot be explained by defective homing to the peripheral tissues because lungs and VAT contained normal or greater numbers of Tregs. Apart from IL-2R and TCR signaling, development of eTregs is driven by inflammatory milieu in the peripheral tissues [7–13]. Governed by extracellular cues, transcription factors BATF and IRF4 maintain tissue Tregs, orchestrate the effector Treg transcriptional program, and promote expression of ST2 [15]. Subsequently, IL-33 induces GATA-3 phosphorylation, which binds to the ST2 locus to enhance ST2 gene expression [16]. The expression of ST2 in T_H2 [37, 38] and tissue Tregs [16, 39] is reliant on a positive feedback loop where IL-33 induces GATA3 recruitment to the ST2 locus, *IL1rl1*. Studies by Vasanthakumar et al. demonstrated that IRF4 and BATF binding to the *IL1rl1* loci is required for maintaining VAT Treg identity, and administration of IL-33 amplifies the number of Tregs in the VAT [15]. Our discovery of ST2^{+ve}GATA3^{+ve} Bach2-deficient Tregs in the spleen prompted us to further investigate whether Bach2-deficient splenic Tregs are hypersensitive to IL-33, as compared to their WT counterparts. We find that IL-33 exposure in vitro further increased the expression of ST2 in splenic Bach2-deficient Tregs. This increase is impressive considering that Bach2-deficient Tregs already express elevated basal levels of ST2 compared to WT Tregs. This increase of ST2 expression was associated with increased frequencies of GATA3-, BATF-, and IRF4-expressing cells, which suggest that Bach2 might repress GATA3/BATF/IRF4-driven expression of ST2 and subsequent differentiation of tissue Tregs in the spleen. Furthermore, Bach2 restrains differentiation of eTregs by competing with, or directly repressing BATF, IRF4, and GATA3 expression in response to extracellular cues [21, 24–27], which in turn can limit ST2 expression and eTreg development.

Most notably, Treg phenotypes were largely normal in non-lymphoid tissues such as lungs, but Bach2-deficiency in Tregs resulted in substantive increase in the numbers of CXCR3+ and CD103+ Tregs in the VAT. Although there was not any detectable change of ST2 expression, Bach2-deficient Tregs exhibited higher levels of GATA3 and IRF4, overall suggesting that Bach2 is needed to repress tissue Treg differentiation in the VAT. In the present study, we found that in vivo IL-33 treatment increased the numbers of Tregs in VAT of Bach2$^{loxp/loxp}$FoxP3-Cre and WT mice and that these IL-33-responsive cells were CD103^{+ve}, CXCR3^{+ve}, and ST2^{+ve} Tregs. Notably, WT Treg levels of GATA3, BATF, and IRF4 were induced to levels that were comparable to those of IL-33-treated Bach2-deficient Tregs. In contrast to our in vitro experiment with splenic Tregs, IL-33 treatment did not induce significant in vivo changes in the splenic Treg population in Bach2-deficient mice. This difference could be attributed to the fact that Bach2-deficient Tregs already demonstrate a higher basal level of expression of tissue Treg phenotype compared to WT and, in vivo, it could take a higher concentration to exacerbate this phenotype than the regimen that we used. Alternatively, IL-33-induced Tregs in spleen might have already relocalized to VAT.

Despite displaying a robust effector phenotype, Bach2-deficient Tregs seemed to be incapable of restraining the

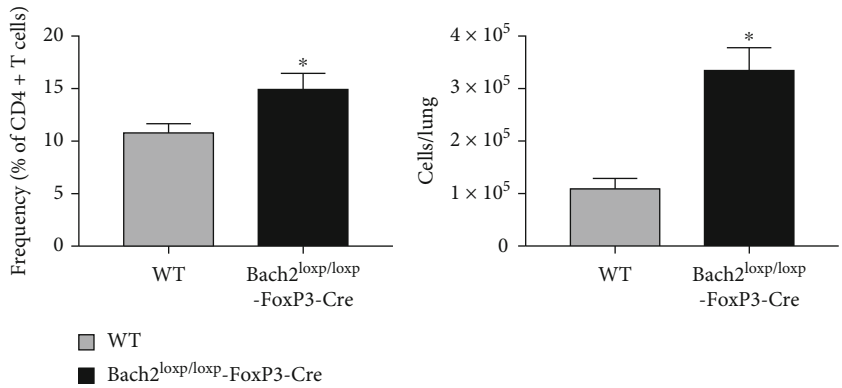

(a)

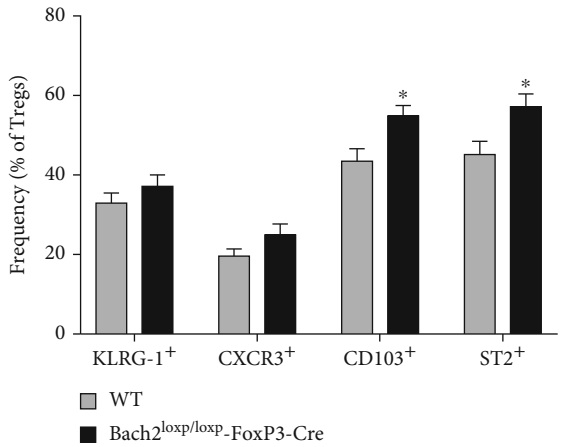

(b)

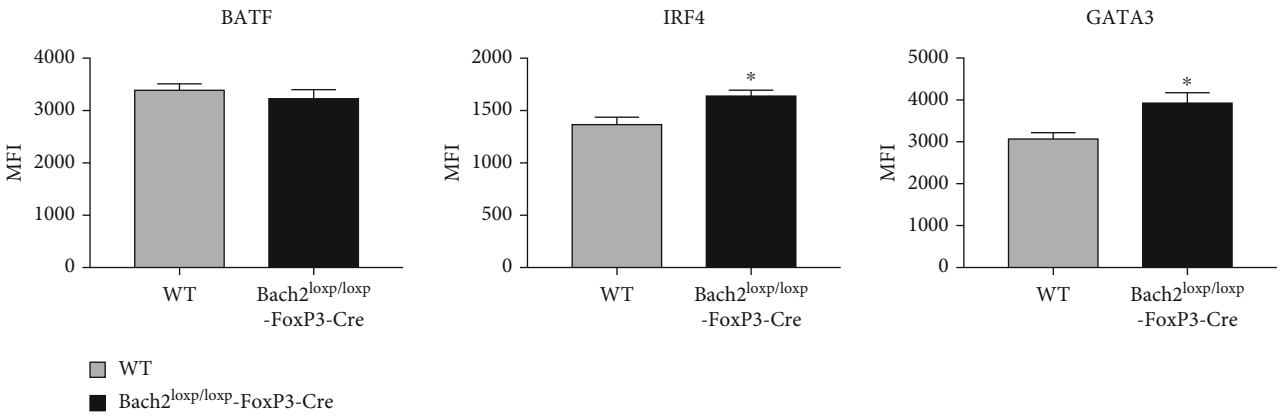

(c)

Figure 5: Continued.

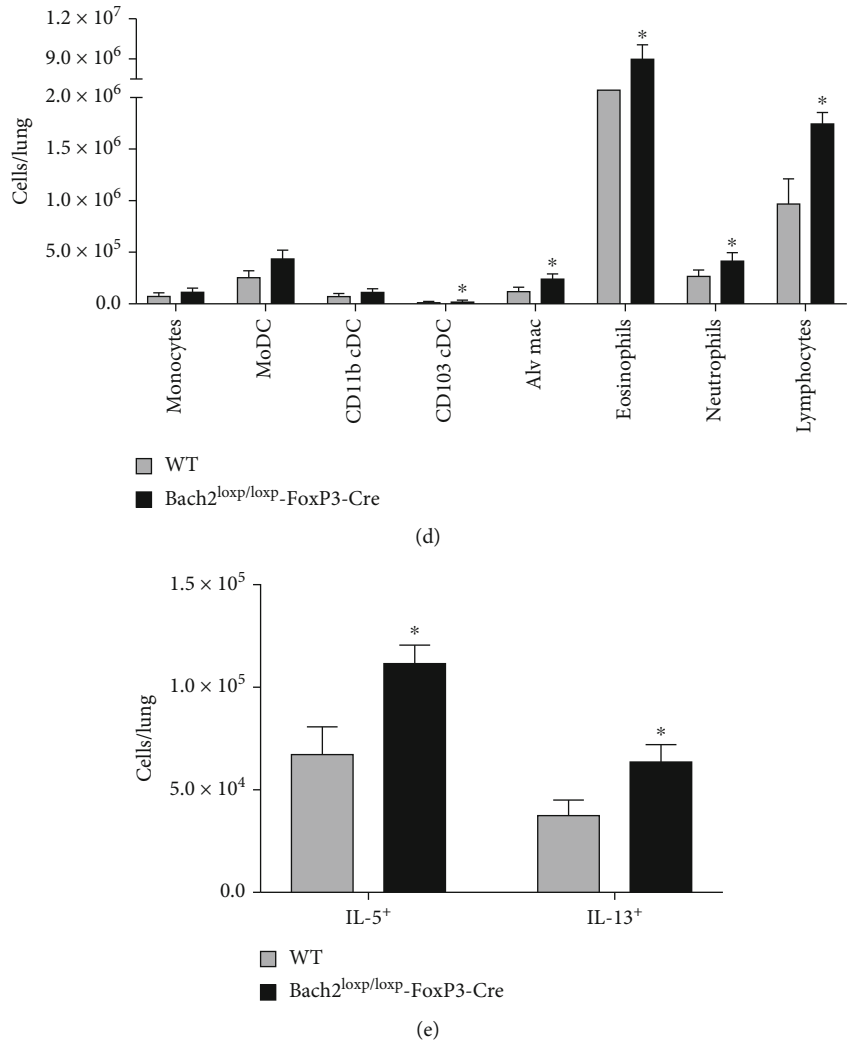

Figure 5: Bach2 is required for Tregs to control T_H2 immunity in lungs. WT and Bach2$^{loxp/loxp}$FoxP3-Cre mice were administered *Aspergillus melleus* fungal protease intratracheally and lungs were harvested on day 15; mononuclear cells from lungs were analyzed by flow cytometry. (a) Frequency and numbers of Foxp3^{+ve} Tregs in the lungs. (b) Frequency of KLRG-1-, CXCR3-, CD103-, and ST2-positive Tregs in lungs. (c) MFI levels for BATF, IRF4, and GATA3 staining in Foxp3^{+ve} Tregs. (d) Numbers of inflammatory cell subsets in the lungs. (e) Cells from the lung were stimulated for 6 hrs in vitro with heat-inactivated fungal protease in the presence of Brefeldin A during the last 4 hrs, and cytokine production was measure by intracellular staining of IFNγ, IL-5, IL-13, and IL17 in CD4 T cells. This experiment was repeated two times with similar results, 4-6 mice per group. $*p < 0.05$.

activation of conventional T cells. Higher numbers of CD8 and CD4 T cells in Treg-specific Bach2-deficient mice exhibited an activated/effector phenotype as determined by CD44 and CD62L expression. Further, these CD8 and CD4 T cells secreted substantial amounts of pro-inflammatory cytokines. Specifically, higher percentages of CD4 T cells from Treg-specific Bach2-deficient mice secrete IFNγ, IL-13, and IL-17A, suggesting that Tregs require Bach2 expression to repress the activation and differentiation of T_H1, T_H2, and T_H17 cells, respectively. These findings led us to explore whether Bach2-deficient Tregs are unable to control Type 1 and Type 2 responses in vivo. Acute viral infections typically induce Type 1 responses, and it was of interest to assess whether Bach2 deficiency altered the effect of LCMV infection on Tregs and whether Treg-specific Bach2 deficiency led to enhanced T cell responses to an LCMV infection. Surprisingly, Treg-specific Bach2 deficiency has no detectable effect on the numbers of Tregs or the magnitude of virus-specific CD8/CD4 T cell response or the cytokine-producing ability of virus-specific CD8/CD4 T cells. Unlike in an LCMV infection, Treg-specific Bach2 deficiency limits the expansion of Tregs in mice infected with *Plasmodium chabaudi* [26]. Thus, Bach2 regulation of Tregs depends on the infection type. We also found that Treg-specific Bach2 deficiency had minimal effects on mucosal T cell responses in the lungs during an acute influenza virus infection. Notably, in a model of chemically-induced colitis, loss of Bach2 in Tregs protected against colitis [26]. An emerging theme from our studies is that loss of Bach2 expression in Tregs does not affect T_H1 responses to systemic or mucosal viral infections.

We have previously reported that global knockout of Bach2 leads to the development of Type 2 cytokine-driven

fatal eosinophilic crystalline pneumonia [20]. Further, loss of Bach2 in all T cells also leads to aberrant T_H2 immunity and lung disease [24]. Treg-specific Bach2 deficiency did not lead to the unprovoked development of eosinophilic crystalline pneumonia or T_H2-driven lung disease for at least until 8-9 months of age. Thus, Bach2 deficiency in Tregs is not sufficient to cause unprovoked T_H2-driven lung inflammation. Since variations in the Bach2 gene have been linked to asthma in humans and Bach2 deficiency led to eosinophilic crystalline pneumonia in mice [20, 32, 33], we assessed whether Treg-specific Bach2 deficiency affected the development of fungal protease-induced allergic inflammation in the lungs. Recent work has shown that some allergen proteases possess the ability to cleave and potentiate IL-33 [40, 41]. IL-33 is then capable of driving an ST2-dependent type 2 inflammatory response. Remarkably, despite expressing high basal levels of GATA3 and ST2, Bach2-deficient Tregs appeared to be unable to suppress *Aspergillus* protease-induced allergic inflammation. Bach2-deficient Tregs expressed a more activated phenotype with protease treatment, and these increases were paralleled by increases of effector phenotypes in WT counterparts as well. Overall, these data suggest that Bach2 is required for Tregs to restrain T_H2 inflammation. Mechanistically, the absence of Bach2 leads to increased levels of GATA3, BATF, and IRF4, and subsequently more ST2 expression. The inherently higher basal level of an activated/effector tissue Treg phenotype in Bach2-deficient Tregs makes it difficult to detect further activation or display of effector characteristics; however, it should be noted that WT Tregs need to be stimulated in order to reach the basal level of magnitude that Bach2-deficient Tregs express.

5. Conclusions

Maintenance of Treg homeostasis and effector function in lymphoid and nonlymphoid tissues is critical for mitigating autoimmunity and inflammatory diseases. In this manuscript, we ascribe vital roles for Bach2 in regulating the numbers and functions of effector Tregs in lymphoid and non-lymphoid tissues. First, we confirm previous findings [25–27] that Treg-specific Bach2 deficiency leads to unprovoked precocious differentiation of effector Tregs in lymphoid tissues. Second, we document that Bach2 restrains the development of CXCR3 + CD103 + ST2+ tissue Tregs in secondary lymphoid tissues. Third, we show that Bach2 in Tregs limits the number of CXCR3 + CD103+ Tregs in VAT. Fourth, loss of Bach2 in Tregs does not affect Type 1 immunity to systemic and mucosal viral infections. Fifth, we show that Treg-specific Bach2 deficiency does not result in unprovoked T_H2-driven inflammation, but restrains aggressive fungus protease-induced Type 2 inflammation in lungs by functioning as a transcriptional checkpoint in both Tregs and conventional effector cells. In summary, findings presented in this manuscript provide mechanistic insights into the role of Bach2 in regulating Treg homeostasis and protecting humans against Type 2 immunity such as asthma and other allergic disorders.

Data Availability

All data presented in this manuscript is archived in secure computers at the University of Wisconsin-Madison.

Conflicts of Interest

Authors have no conflicts of interest with data published in this manuscript.

Authors' Contributions

AC, DW, JS, BK, and MS. designed, performed, analyzed experiments, and provided conceptual input for the manuscript. WL and BK performed experiments. AC and MS wrote the manuscript, which was proofread by all authors.

Acknowledgments

This work was supported by PHS grants (U01 AI124299 R21 AI149793-01A1) from National Institutes of Health and John E. Butler professorship to M. Suresh. AC was supported by a predoctoral fellowship from the National Institutes of Health (T32AI055397). We gratefully acknowledge Emory NIH Tetramer Core Facility for providing MHC-I and MHC-II tetramers. We would also like to thank genuine appreciation for the efforts of the veterinary and animal care staff at UW-Madison.

References

[1] S. Z. Josefowicz, L. F. Lu, and A. Y. Rudensky, "Regulatory T cells: mechanisms of differentiation and function," *Annual Review of Immunology*, vol. 30, no. 1, pp. 531–564, 2012.

[2] K. S. Smigiel, E. Richards, S. Srivastava et al., "CCR7 provides localized access to IL-2 and defines homeostatically distinct regulatory T cell subsets," *The Journal of Experimental Medicine*, vol. 211, no. 1, pp. 121–136, 2014.

[3] A. Liston and D. H. Gray, "Homeostatic control of regulatory T cell diversity," *Nature Reviews. Immunology*, vol. 14, no. 3, pp. 154–165, 2014.

[4] E. Cretney, A. Xin, W. Shi et al., "The transcription factors Blimp-1 and IRF4 jointly control the differentiation and function of effector regulatory T cells," *Nature Immunology*, vol. 12, no. 4, pp. 304–311, 2011.

[5] E. Cretney, A. Kallies, and S. L. Nutt, "Differentiation and function of Foxp3$^+$ effector regulatory T cells," *Trends in Immunology*, vol. 34, no. 2, pp. 74–80, 2013.

[6] D. J. Campbell and M. A. Koch, "Phenotypical and functional specialization of FOXP3$^+$ regulatory T cells," *Nature Reviews. Immunology*, vol. 11, no. 2, pp. 119–130, 2011.

[7] K. E. Webster, S. Walters, R. E. Kohler et al., "In vivo expansion of T reg cells with IL-2-mAb complexes: induction of resistance to EAE and long-term acceptance of islet allografts without immunosuppression," *The Journal of Experimental Medicine*, vol. 206, no. 4, pp. 751–760, 2009.

[8] G. Cheng, A. Yu, M. J. Dee, and T. R. Malek, "IL-2R signaling is essential for functional maturation of regulatory T cells during thymic development," *Journal of Immunology*, vol. 190, no. 4, pp. 1567–1575, 2013.

[9] A. Yu, L. Zhu, N. H. Altman, and T. R. Malek, "A low interleukin-2 receptor signaling threshold supports the development and homeostasis of T regulatory cells," *Immunity*, vol. 30, no. 2, pp. 204–217, 2009.

[10] J. H. Lee, S. G. Kang, and C. H. Kim, "FoxP3+ T cells undergo conventional first switch to lymphoid tissue homing receptors in thymus but accelerated second switch to nonlymphoid tissue homing receptors in secondary lymphoid tissues," *Journal of Immunology*, vol. 178, no. 1, pp. 301–311, 2007.

[11] M. Feuerer, J. A. Hill, K. Kretschmer, H. von Boehmer, D. Mathis, and C. Benoist, "Genomic definition of multiple ex vivo regulatory T cell subphenotypes," *Proceedings of the National Academy of Sciences of the United States of America*, vol. 107, no. 13, pp. 5919–5924, 2010.

[12] B. D. Sather, P. Treuting, N. Perdue et al., "Altering the distribution of Foxp3(+) regulatory T cells results in tissue-specific inflammatory disease," *The Journal of Experimental Medicine*, vol. 204, no. 6, pp. 1335–1347, 2007.

[13] A. M. Sanchez, J. Zhu, X. Huang, and Y. Yang, "The development and function of memory regulatory T cells after acute viral infections," *Journal of Immunology*, vol. 189, no. 6, pp. 2805–2814, 2012.

[14] M. Panduro, C. Benoist, and D. Mathis, "Tissue Tregs," *Annual Review of Immunology*, vol. 34, no. 1, pp. 609–633, 2016.

[15] A. Vasanthakumar, K. Moro, A. Xin et al., "The transcriptional regulators IRF4, BATF and IL-33 orchestrate development and maintenance of adipose tissue-resident regulatory T cells," *Nature Immunology*, vol. 16, no. 3, pp. 276–285, 2015.

[16] C. Schiering, T. Krausgruber, A. Chomka et al., "The alarmin IL-33 promotes regulatory T-cell function in the intestine," *Nature*, vol. 513, no. 7519, pp. 564–568, 2014.

[17] B. Afzali, J. Gronholm, J. Vandrovcova et al., "BACH2 immunodeficiency illustrates an association between super-enhancers and haploinsufficiency," *Nature Immunology*, vol. 18, no. 7, pp. 813–823, 2017.

[18] R. Roychoudhuri, D. Clever, P. Li et al., "BACH2 regulates $CD8^+$ T cell differentiation by controlling access of AP-1 factors to enhancers," *Nature Immunology*, vol. 17, no. 7, pp. 851–860, 2016.

[19] S. Tsukumo, M. Unno, A. Muto et al., "Bach2 maintains T cells in a naive state by suppressing effector memory-related genes," *Proceedings of the National Academy of Sciences of the United States of America*, vol. 110, no. 26, pp. 10735–10740, 2013.

[20] E. H. Kim, D. J. Gasper, S. H. Lee, E. H. Plisch, J. Svaren, and M. Suresh, "Bach2 regulates homeostasis of Foxp3+ regulatory T cells and protects against fatal lung disease in mice," *Journal of Immunology*, vol. 192, no. 3, pp. 985–995, 2014.

[21] R. Roychoudhuri, K. Hirahara, K. Mousavi et al., "BACH2 represses effector programs to stabilize T(reg)-mediated immune homeostasis," *Nature*, vol. 498, no. 7455, pp. 506–510, 2013.

[22] L. Yang, S. Chen, Q. Zhao, Y. Sun, and H. Nie, "The critical role of Bach2 in shaping the balance between CD4+ T cell subsets in immune-mediated diseases," *Mediators of Inflammation*, vol. 2019, Article ID 2609737, 9 pages, 2019.

[23] M. Yamashita and M. Kuwahara, "The critical role of Bach2 in regulating type 2 chronic airway inflammation," *International Immunology*, vol. 30, no. 9, pp. 397–402, 2018.

[24] M. Kuwahara, W. Ise, M. Ochi et al., "Bach2-Batf interactions control Th2-type immune response by regulating the IL-4 amplification loop," *Nature Communications*, vol. 7, no. 1, article 12596, 2016.

[25] F. M. Grant, J. Yang, R. Nasrallah et al., "BACH2 drives quiescence and maintenance of resting Treg cells to promote homeostasis and cancer immunosuppression," *The Journal of Experimental Medicine*, vol. 217, no. 9, 2020.

[26] T. Sidwell, Y. Liao, A. L. Garnham et al., "Attenuation of TCR-induced transcription by Bach2 controls regulatory T cell differentiation and homeostasis," *Nature Communications*, vol. 11, no. 1, p. 252, 2020.

[27] H. Zhang, D. Dai, Q. Hu et al., "Bach2 attenuates IL-2R signaling to control Treg homeostasis and Tfr development," *Cell Reports*, vol. 35, no. 6, article 109096, 2021.

[28] Y. P. Rubtsov, J. P. Rasmussen, E. Y. Chi et al., "Regulatory T cell-derived interleukin-10 limits inflammation at environmental interfaces," *Immunity*, vol. 28, no. 4, pp. 546–558, 2008.

[29] B. M. Matta and H. R. Turnquist, "Expansion of regulatory T cells in vitro and in vivo by IL-33," *Methods in Molecular Biology*, vol. 1371, pp. 29–41, 2016.

[30] M. Delacher, C. D. Imbusch, A. Hotz-Wagenblatt et al., "Precursors for nonlymphoid-tissue Treg cells reside in secondary lymphoid organs and are programmed by the transcription factor BATF," *Immunity*, vol. 52, no. 2, pp. 295–312.e11, 2020.

[31] M. Delacher, C. D. Imbusch, D. Weichenhan et al., "Genome-wide DNA-methylation landscape defines specialization of regulatory T cells in tissues," *Nature Immunology*, vol. 18, no. 10, pp. 1160–1172, 2017.

[32] E. Kreiner, J. Waage, M. Standl et al., "Shared genetic variants suggest common pathways in allergy and autoimmune diseases," *The Journal of Allergy and Clinical Immunology*, vol. 140, no. 3, pp. 771–781, 2017.

[33] Y. Huo and H. Y. Zhang, "Genetic mechanisms of asthma and the implications for drug repositioning," *Genes (Basel)*, vol. 9, no. 5, p. 237, 2018.

[34] D. L. Wiesner, R. M. Merkhofer, C. Ober et al., "Club cell TRPV4 serves as a damage sensor driving lung allergic inflammation," *Cell Host & Microbe*, vol. 27, no. 4, pp. 614–628.e6, 2020.

[35] B. Popovic, M. Golemac, J. Podlech et al., "IL-33/ST2 pathway drives regulatory T cell dependent suppression of liver damage upon cytomegalovirus infection," *PLoS Pathogens*, vol. 13, no. 4, article e1006345, 2017.

[36] A. Vasanthakumar and A. Kallies, "Interleukin (IL)-33 and the IL-1 family of cytokines-regulators of inflammation and tissue homeostasis," *Cold Spring Harbor Perspectives in Biology*, vol. 11, no. 3, article a028506, 2019.

[37] L. Guo, G. Wei, J. Zhu et al., "IL-1 family members and STAT activators induce cytokine production by Th2, Th17, and Th1 cells," *Proceedings of the National Academy of Sciences of the United States of America*, vol. 106, no. 32, pp. 13463–13468, 2009.

[38] Z. Guo, J. Wu, J. Zhao et al., "IL-33 promotes airway remodeling and is a marker of asthma disease severity," *The Journal of Asthma*, vol. 51, no. 8, pp. 863–869, 2014.

[39] B. M. Matta, J. M. Lott, L. R. Mathews et al., "IL-33 is an unconventional Alarmin that stimulates IL-2 secretion by dendritic cells to selectively expand IL-33R/ST2+ regulatory T cells," *Journal of Immunology*, vol. 193, no. 8, pp. 4010–4020, 2014.

[40] Y. Hiraishi, S. Yamaguchi, T. Yoshizaki et al., "IL-33, IL-25 and TSLP contribute to development of fungal-associated protease-induced innate-type airway inflammation," *Scientific Reports*, vol. 8, no. 1, article 18052, 2018.

[41] I. C. Scott, J. B. Majithiya, C. Sanden et al., "Interleukin-33 is activated by allergen- and necrosis-associated proteolytic activities to regulate its alarmin activity during epithelial damage," *Scientific Reports*, vol. 8, no. 1, p. 3363, 2018.

Hindawi
Journal of Immunology Research
Volume 2022, Article ID 5545319, 13 pages
https://doi.org/10.1155/2022/5545319

Review Article

Role of T Regulatory Cells and Myeloid-Derived Suppressor Cells in COVID-19

Alhasan Alsalman,[1] **Mohammad A. Al-Mterin**,[1] **and Eyad Elkord**[1,2]

[1]*Natural and Medical Sciences Research Center, University of Nizwa, Nizwa, Oman*
[2]*Biomedical Research Center, School of Science, Engineering and Environment, University of Salford, Manchester, UK*

Correspondence should be addressed to Eyad Elkord; e.elkord@salford.ac.uk

Received 25 January 2022; Revised 13 March 2022; Accepted 28 March 2022; Published 19 April 2022

Academic Editor: Mitesh Dwivedi

Coronavirus disease 2019 (COVID-19) has been raised as a pandemic disease since December 2019. Immunosuppressive cells including T regulatory cells (Tregs) and myeloid-derived suppressor cells (MDSCs) are key players in immunological tolerance and immunoregulation; however, they contribute to the pathogenesis of different diseases including infections. Tregs have been shown to impair the protective role of $CD8^+$ T lymphocytes against viral infections. In COVID-19 patients, most studies reported reduction, while few other studies found elevation in Treg levels. Moreover, Tregs have a dual role, depending on the different stages of COVID-19 disease. At early stages of COVID-19, Tregs have a critical role in decreasing antiviral immune responses, and consequently reducing the viral clearance. On the other side, during late stages, Tregs reduce inflammation-induced organ damage. Therefore, inhibition of Tregs in early stages and their expansion in late stages have potentials to improve clinical outcomes. In viral infections, MDSC levels are highly increased, and they have the potential to suppress T cell proliferation and reduce viral clearance. Some subsets of MDSCs are expanded in the blood of COVID-19 patients; however, there is a controversy whether this expansion has pathogenic or protective effects in COVID-19 patients. In conclusion, further studies are required to investigate the role and function of immunosuppressive cells and their potentials as prognostic biomarkers and therapeutic targets in COVID-19 patients.

1. Introduction

Coronavirus disease 2019 (COVID-19) is caused by SARS-CoV-2. In December 2019, the first cases were reported in China, and the virus quickly spread to other countries around the world [1, 2]. In less than three years, SARS-CoV-2 has infected hundreds of millions. There are a wide variety of clinical symptoms, ranging from asymptomatic to severe symptoms, with acute respiratory distress syndrome (ARDS) and multiorgan dysfunction in fewer than 10% of patients [3, 4]. Several factors increase the risk of COVID-19 disease, including aging, high blood pressure, cardiovascular disease, diabetes, and obesity [5]. The virus causes early immunological suppression through unknown mechanisms. Lymphocyte subsets, particularly $CD4^+$ and $CD8^+$ T cells, were altered in COVID-19 patients, and lymphopenia has been reported as the primary symptom in most cases of COVID-19 patients [6]. It has been shown that lymphopenia was worsened with the progression of disease to respiratory distress syndrome [7].

T regulatory cells (Tregs) play critical roles in immunological tolerance, but they also contribute to the pathogenesis of different diseases, including cancer, autoimmune diseases, transplantation, and infections. Myeloid-derived suppressor cells (MDSCs) are immature myeloid cells that strongly suppress the immune system by inhibiting different immune cells, including T cells, natural killer cells (NK), and dendritic cells [8–11]. COVID-19 pathogenesis and severity could be linked to dysregulation of immunosuppressive cells to SARS-CoV-2 [8]. In this review, we present the available data describing the role of Tregs and MDSCs in viral infections and COVID-19 patients.

2. T Regulatory Cells

Tregs have important roles in the modulation of immune responses by maintaining self-tolerance and immunological homeostasis. They contribute to the regulation of immune responses to many diseases [12]. They can suppress various immune cells, including $CD4^+$ and $CD8^+$ T cells, monocytes, dendritic cells, B cells, and NK cells, to reduce unwanted immune responses in different immune diseases such as allergy, autoimmunity, and transplant rejection [13–15]. Generally, Tregs are classified into two types based on their origin: thymus-derived Tregs (tTreg) and peripherally induced Tregs (pTreg) [16, 17]. tTregs originate in the thymus and migrate to the periphery to control peripheral immunological tolerance [18]. pTregs are induced in peripheral tissues, and they differentiate by contact with nonself-antigens in the presence of transforming growth factor β and IL-2 [19, 20]. Tregs express different molecules essential for their function such as CD25, cytotoxic T lymphocyte associated antigen-4 (CTLA-4), and forkhead box P3 (FoxP3) [12]. The FoxP3 is a transcriptional factor, which is essential for Treg development and function. Immunosuppressive activities of FoxP3+superscript Tregs could be determined by the level of FoxP3 expression [21]. Tregs were classified into three subgroups based on FoxP3 and CD45RA expression; these include activated Tregs ($CD45RA^-FoxP3^{high}$), resting Tregs ($CD45RA^+FoxP3^{low}$), and non-Tregs ($CD45RA^-FoxP3^{low}$). Activated Tregs strongly inhibit immune responses, compared with resting Tregs. However, non-Tregs secrete different effector cytokines such as interferon (IFN)-γ, interleukin (IL)-2, and IL-17 but without any inhibitory function [22, 23].

2.1. Role of Tregs in Viral Infection. Herein, we briefly discuss some studies investigated Tregs in viral infections in human. It has been demonstrated that the presence of Tregs impaired the protective function of $CD8^+$ T cells against viral infection [24, 25]. There has been a variety of explanations for Treg suppressive ability in viral infections, including a decrease in the quantity of the protective T cell responses, a reduction in the antiviral cytokine secretion by effector cells, and preventing the migration of protective T cells to the infected region [26]. According to Raiden et al., Tregs were reduced in the peripheral blood of infected infants with severe respiratory syncytial virus (RSV), this could be explained by elevated levels of Tregs in lung and lymph nodes and increased apoptosis [27]. Another study reported that Tregs, TGF-β, and IL-10 were decreased in infants with RSV bronchiolitis infection, compared with healthy infants [28]. Additionally, Qin et al., reported that bronchial epithelial cells of infected humans with RSV inhibited the differentiation of Treg subsets and induced the differentiation of Th2 and Th17 cells [29]. Some studies reported that $CD4^+CD25^+$ T cells were increased in chronic hepatitis C virus (HCV) disease, compared with recovered or normal patients [30–32]. These data indicated that the inhibition of virus-specific $CD8^+$ T cells was increased in patients with chronic HCV disease; this could be associated with elevated levels of Tregs in HCV patients [32]. Also, some researchers indicated that Tregs were increased in liver and peripheral blood of HCV patients [33]. Other studies reported that Tregs and Th17 were increased in infected patients with chronic hepatitis B virus (HBV) [34–36]. Additionally, elevated Tregs in peripheral blood were associated with HBV replication in chronic disease, and it was less common in the early stages of acute HBV infection [37]. Another study showed that frequency of Tregs was significantly increased in chronic active HBV and asymptomatic HBV carriers, in comparison to resolved and controlled patients [38, 39]. However, Prendergast et al. found that the count of Tregs was decreased in human immunodeficiency virus (HIV) patients [40]. Interestingly, the count of Tregs was decreased in the blood of HIV patients, but the proportion of Tregs was increased in chronic infection, which could be associated with HIV progression [41]. Milman et al. reported that the count of Tregs was significantly high in herpes simplex virus type 2 (HSV-2), compared with control biopsy from unaffected skin [42].

2.2. Role of Tregs in COVID-19. There have been different findings for investigating Tregs in COVID-19 patients. Firstly, Tregs and the transcription factor FoxP3 were elevated in severe COVID-19 patients, which was associated with worse outcomes [43]. These data indicate that Tregs could play negative roles in COVID-19 by inhibiting antiviral T cell responses in the severe phases of illness (Figure 1(a)). Moreover, in critical COVID-19 patients, the activity and frequency of Tregs were increased, compared with other respiratory diseases such as influenza and respiratory syncytial virus (RSV) (Table 1) [44]. Interestingly, IL-10-secreting Tregs, a lineage known to possess anti-inflammatory properties in the lung, were elevated in severe COVID-19 patients, compared to mild/moderate diseases [45]. These results indicate that the increase in IL-10-secreting Tregs could contribute to more severe COVID-19 symptoms. In addition, in mechanically ventilated COVID-19 patients, the percentage of Tregs and Th17 cells was highly increased in the lung, compared with blood [46]. Some studies indicated that activated $CD4^+CD25^+CD127^{low}$ Tregs were highly increased in moderate and severe COVID-19 patients, compared with healthy controls [47, 48]. De Biasi et al. reported that Tregs and IL-10 were elevated in the blood of COVID-19 patients [49]. A potential explanation for such increase of Tregs in circulation is that SARS-CoV-2 impeded the transit of Tregs from circulation to the respiratory tract, resulting in Treg accumulation in circulation and lung damage due to excessive inflammatory response in the lung [44].

Secondly, Rezaei et al. reported that the total counts of white blood cells, T cells, $CD38^+$, and $CD3^+HLA\text{-}DR^+$ lymphocytes were significantly elevated in hospitalized COVID-19 patients [50]. Also, they found that $CD4^+/CD8^+$ ratio, B cells, $FoxP3^+$ Tregs, and FoxP3 median fluorescence did not show any significant difference between early and late responders of hospitalized COVID-19 patients (Table 1) [50].

Thirdly, Kratzer et al. showed that $CD4^+$ and $CD8^+$ T effector memory cells, plasma blast, and transitional B cells were elevated in convalescent COVID-19 patients. However,

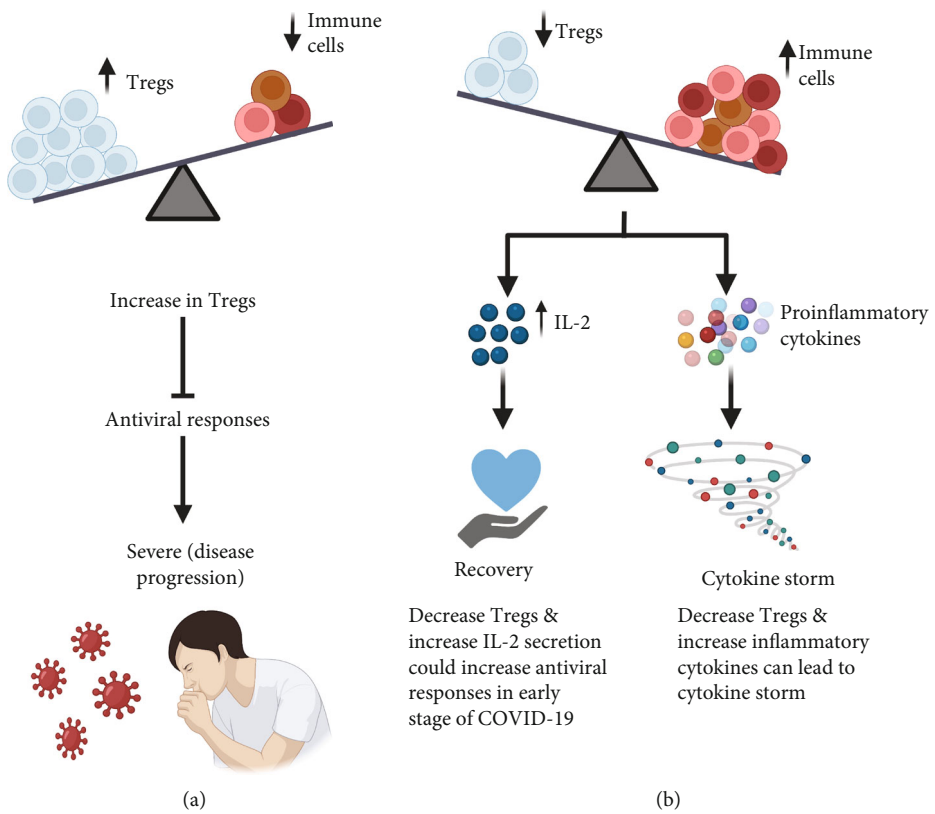

Figure 1: Role of Tregs in COVID-19 patients: An increase in level of Tregs could play a negative role in COVID-19 patients by inhibiting antiviral T cell responses, resulting in the progression of COVID-19 disease (a). A decrease in level of Tregs could result in cytokine storm or recovery depending on the response of proinflammatory cytokines. Firstly, early increase in IL-2 could be associated with faster viral clearance and early immune response in asymptomatic COVID-19 patients. Secondly, the significant increase in T helper cells such as Th17 could be related to hyperinflammation and progression of COVID-19 disease (b).

$CD25^+FoxP3^+$ Tregs were significantly decreased in convalescent COVID-19 patients, compared with healthy donors [51]. In line with these findings, Sadeghi et al. found that the count of Tregs and the expression level of FoxP3, TGF-β, and IL-10 were decreased in critical COVID-19 patients, compared with healthy controls [52]. In contrast, patients had a significant increase in Th17 cells and associated cytokines IL-17 and IL-23 in COVID-19 patients [52]. These data indicate that the increased and decreased responses of Th17 and Tregs, respectively, could be strongly correlated with hyperinflammation and pathogenesis of the disease (Figure 1(b)). Additionally, Patterson et al. reported that T cells expressing PD-1 and Tregs were highly reduced in COVID-19 patients, compared with healthy controls [53]. A recent study reported that asymptomatic COVID-19 patients have a reduction in Tregs and anti-inflammatory cytokine IL-10 [54]. Also, they found that the early increase in inflammatory cytokine IL-2 was associated with faster viral clearance and early immune responses in asymptomatic COVID-19 patients (Figure 1(b)) [54]. According to Meckiff et al. the cytotoxic follicular helper cells and cytotoxic T helper cells were increased in hospitalized COVID-19 patients [55]. They also reported that Tregs were decreased in hospitalized compared to nonhospitalized patients [55]. These data indicate that immunosuppressive Tregs were impaired in hospitalized COVID-19 patients [55]. Another study reported that T lymphocytes and Tregs were significantly decreased in critical COVID-19 patients with ARDS, compared with severe illness [56]. However, they also found that the percentage of $CD45RO^+CD95^+$ Tregs, among other Treg subsets, was increased in critical COVID-19 patients, compared with severe patients (Table 1) [56]. Additionally, it has been reported that expression level of $CD4^+FoxP3^+CD25^+$ was significantly decreased in COVID-19 patients, compared with healthy controls [57]. Other studies reported that Tregs were decreased in moderate adult and pediatric patients, and Tregs were more reduced in severe COVID-19 patients [58, 59]. Furthermore, Tregs and activated T cells were decreased in hospitalized COVID-19 patients, compared to healthy controls [8]. Moreover, COVID-19 patients have lower levels of Tregs ($CD4^+CD25^+CD127^{low}$), especially in severe cases of the disease [59]. Levels of Tregs were significantly decreased in severe COVID-19 patients, compared with moderate and mild illness [60, 61]. Interestingly, levels of Tregs were increased through the progression from mild to severe patients but then decreased through the progression to critical illness (Table 1) [62]. Moreover, activated $CD4^+$ T cells in severe COVID-19 patients expressed higher levels of CD25, while suppressing the expression of FoxP3,

Table 1: Summary of Tregs in COVID-19 patients with different severities.

	Study groups (number of patients)	Change in Treg levels	Cell phenotype	Notes	Reference no.
Xie et al.	Asymptomatic disease	Decrease	NA	In asymptomatic patients, IL-2 was associated with faster viral clearance and early immune responses.	[54]
Kratzer et al.	Convalescent patients (109) vs. healthy (98)	Decrease	$CD25^+FoxP3^+$	Acute SARS-CoV-2 infection is beneficial by activation of T cells or harmful by reduction of neutrophils.	[51]
Chen et al.	Mild (80)/severe (22) vs. healthy (67)	Increase	$CD4^+CD25^+CD127^{low}$	$CD4^+$ T cells, B cells, IL-6, and IL-10 are indicators of COVID-19 severity.	[47]
Sadeghi et al.	Critical (40) vs. healthy (40)	Decrease	$CD4^+CD25^+CD127^-$	Imbalanced ratios of Th17/Tregs could play an important role in inflammatory responses and the pathogenesis of the disease.	[52]
Jiménez-Cortegana et al.	Hospitalized (20) vs. healthy (20)	Decrease	$CD4^+CD25^{high}CD127^-$	M-MDSCs, but not Tregs, could play a role in the immunosuppression shown in COVID-19 patients.	[8]
Patterson et al.	Different severity (224)	Decrease	NA	Decreased Tregs in COVID-19 compared with healthy controls.	[53]
Mohebbi et al.	Different severity (30)	Decrease	$CD4^+FoxP3^+CD25^+$	Decreased Tregs in COVID-19 patients compared with healthy controls.	[57]
Galván-Peña et al.	Different severity (57)	Increase	$CD25^+FoxP3^+$	Increased Tregs in severe patients is associated with worse outcome.	[43]
Kalfaoglu et al.	Severe	Decrease	NA	In the lung, T cells highly expressed immune-regulatory receptors and CD25, while suppressing expression of FoxP3.	[63]
Qin et al.	Severe (286) vs. non-severe (166)	Decrease	$CD4^+CD25^+CD127^{low}$		[59]
Neumann et al.	Severe (20) vs. mild/moderate (23)	Increase	IL-10-secreting Tregs		[45]
Wang et al.	Extremely severe (15) vs. severe (20) vs. mild (30)	Decrease	$CD45RA^+$ cells	The percentage of natural Tregs was decreased in extremely severe patients.	[61]
Wang et al.	Critical (3) vs. severe (5) vs. mild (4)	Decrease	$CD4^+CD25^+CD127^-$	Tregs increase during progression from mild to severe then decreased through the progression to critical disease.	[62]
Meckiff et al.	Hospitalized (critical) vs. non hospitalized (mild)	Decrease	NA		[55]
Chen et al.	Severe (11) vs. moderate (10)	Decrease	$CD4^+CD25^+CD127^{low}$ and $CD45RA^+$		[60]
Rezaei et al.	Critical (8) vs. severe (27) vs. Moderate (17)	No change	$CD4^+CD25^+FOXP3^+$		[50]
Rutkowska et al.	Critical (18) vs. severe (23)	Decrease	NA	Percentage of $CD45RO^+CD95^+$ Tregs, among other Treg subsets, was higher in critical compared to severe.	[56]
Ronit et al.	Mechanically ventilated patients (4) with moderate-to-severe COVID-19 ARDS	Increase	$FoxP3^+CTLA\text{-}4^+$ Tregs	Increased Tregs with activation markers in the lung.	[46]
Vicket et al.	SARS-CoV-2 (24) vs. RSV (10) vs. Flu (9) vs. Healthy donors (23)	Immune landscape in SARS cov-2 similar to flu or RSV patients	$CD25^+$ $CD127^-Foxp3^+$	Only in critical patients, the levels of $CD25^+CD127^-$ $FoxP3^+$ cells were increased.	[44]

NA: not available.

resulting in a disrupted FoxP3-mediated mechanism in the lung [63].

In severe COVID-19 patients, lower levels of Tregs could be one of the explanations for the hyperactivated immune system and injured lungs. These reductions in Tregs in COVID-19 patients could be explained by some potential mechanisms. Kalfaoglu et al. reported that IL-2 transcripts were decreased in severe COVID-19 patients, compared with mild illness [63]. Therefore, decreased IL-2 could enhance the apoptosis of Tregs. Moreover, levels of soluble IL-2R (CD25) were increased in severe COVID-19 patients, which could lead to binding of IL-2 with its receptor (IL-2R) and enhance apoptosis of Tregs [59, 61].

2.3. Role of Tregs in COVID-19 Elderly Patients. Old age is one of the most important risk factors in COVID-19, and the majority of COVID-19-related deaths are in elderly patients [64]. The severity of COVID-19 in elderly patients could be associated with age-related thymic involutions and consequent T cell changes [65]. In the elderly, increased ratio of thymic Tregs (tTregs) to thymic T conventional cells (tTcon) [66] results in exacerbated age-related accumulation of peripheral Tregs (pTreg) [67–69]. Accumulation of pTregs in the elderly impairs immunological balance and inhibits antiviral immune responses [65]. In COVID-19, early inflammatory response is crucial for host protection. Therefore, older patients are probably not capable of mounting strong antiviral immune responses in the early stages, which leads to increased viral load and damage associated with inflammation. Overall, a weak early inflammatory response is associated with severe symptoms in older age, while a robust early inflammatory response is associated with asymptomatic or mild illness [54].

3. Myeloid-Derived Suppressor Cells (MDSCs)

Generally, MDSCs in human are defined as $CD33^{+}CD11b^{+-}$ $HLA\text{-}DR^{low}$ cells and are classified into two primary subgroups based on differences in cell morphology and cell-surface markers: granulocytic (polymorphonuclear) $CD33^{+-}$ $CD11b^{+}HLA\text{-}DR^{low}CD15^{+}$ cells (G-MDSCs) and monocytic $CD33^{+}CD11b^{+}HLA\text{-}DR^{low}CD14^{+}$ cells (M-MDSCs) [70–73]. More recently, an additional subgroup has been identified as $CD33^{+}CD11b^{+}$ $HLA\text{-}DR^{low}CD14^{-}CD15^{-}$, and they are named immature or early-stage MDSCs (e-MDSCs) [72, 74, 75].

MDSCs present at very low levels in healthy individuals because of the rapid differentiation into mature myeloid cells. However, in the presence of pathological conditions, such as malignancies, infections, bone marrow transplantation, or some autoimmune diseases, MDSC levels are highly increased due to inhibition of their differentiation into mature myeloid cells [76, 77]. Interestingly, when activated in a pathogenic situation, these cells overexpress immune inhibitory factors such as nitric oxide synthase (NOS), arginase 1 (ARG1), and peroxynitrite ($ONOO^{-}$) [76, 78]. Additionally, MDSCs have the ability to increase the number of $FoxP3^{+}$ Tregs [76, 79].

MDSCs have been shown to expand in the peripheral blood of individuals suffering from a variety of malignant and nonmalignant illnesses [80]. Indeed, MDSC levels in cancer patients are considered to have prognostic and predictive value [81]. MDSC subpopulations of monocytic and granulocytic cells have been identified and characterized in different human cancers [82–85]. They inhibit antitumor immune responses [85–87], and as a result, cancer cells continue to evolve [75].

3.1. MDSCs in Viral Infections. Levels of MDSCs are elevated in viral diseases, and they could potently suppress T cell proliferation and decrease viral clearance [9, 88, 89]. MDSCs were found to be significantly higher in the blood of chronic hepatitis C (CHC) patients, compared with healthy controls [88]. Interestingly, they found that HCV-RNA levels in plasma were related to the amount of MDSCs in CHC patients [88]. Furthermore, Tacke et al. showed that hepatitis C virus (HCV) enhanced the accumulation of MDSCs, resulting in a decrease in T cell responses [90]. Specifically, Ren et al. observed an expansion in M-MDSCs, but not G-MDSCs, in chronic HCV-infected patients [91]. Garg et al. found that MDSC levels were elevated in activated and non-activated HIV-infected patients [92]. Moreover, Vollbrecht et al. observed a higher level of G-MDSC in chronic HIV-1 patients, compared with healthy controls. Also, they found a positive relationship between MDSC frequencies and viral load and a negative relationship with $CD4^{+}$ amount in HIV-1 patients [93]. In addition, Pal et al. showed that MDSCs have been linked to T cell dysfunction in infected patients with chronic hepatitis B virus (HBV) [94]. However, Pallett et al. observed that G-MDSCs have a protective mechanism by expressing arginase I to effectively inhibit HBV-specific T cell responses in hepatitis B virus-(HBV-) infected patients [95].

3.2. MDSCs in COVID-19

3.2.1. Pathogenic Roles. In COVID-19 patients, different studies observed that alteration in MDSC levels in the blood has been associated with disease severity (Figure 2(a)) [96, 97]. Furthermore, Reizine et al. found that expansion of MDSCs in response to COVID-19 was shown to be significantly linked to lymphopenia and increased arginase activity [98]. Also, they found that frequency of MDSCs in severe COVID-19 patients was higher in hospitalized patients than patients with moderate COVID-19 [98]. Accordingly, it has been reported that SARS-CoV-2 patient plasma inhibited human leukocyte antigen D related (HLA-DR) expression [99]. Therefore, decreasing levels of HLA-DR on monocytes have been observed in severe COVID-19, considering an increase in M-MDSC levels [99, 100]. Clearly, further investigations are necessary to determine the underlying mechanisms of elevated MDSC levels in COVID-19 patients.

Importantly, Atanackovic et al. found that severe COVID-19 patients had a larger amount of MDSCs and higher concentrations of TGF-β, compared with mild patients. This might result in an undesirable suppression of SARS–CoV-2–specific T cell responses, which can contribute to poor outcomes in these patients (Figure 2(a)) [101]. Therefore, both MDSC and TGF-β should be studied further as possible

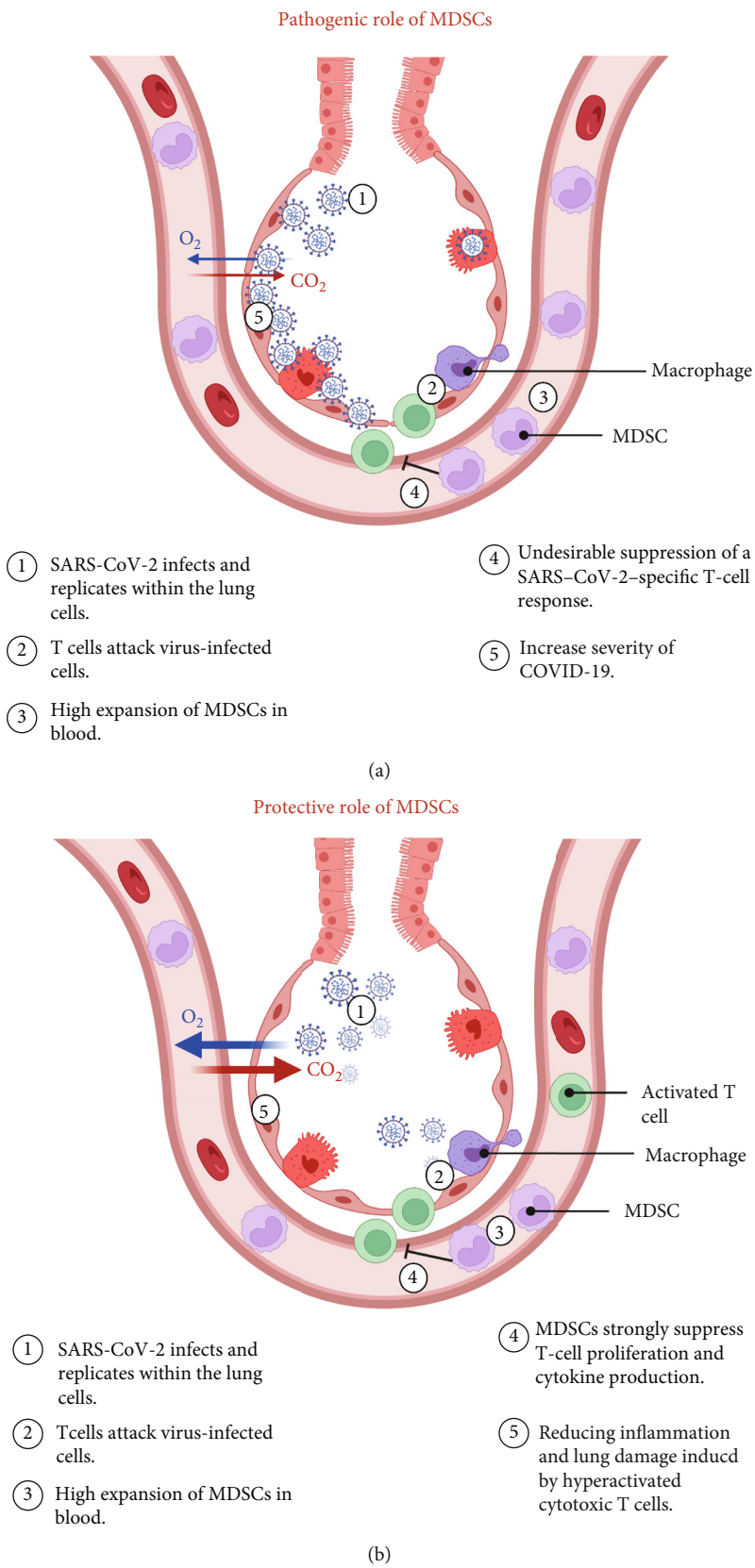

Figure 2: Pathogenic and protective roles of MDSCs in COVID-19 patients: Severe COVID-19 patients had higher levels of MDSCs. This might result in an undesirable suppression of SARS-CoV-2-specific T cell responses, which can contribute to worse outcomes in these patients (a). MDSC expansion may help to limit an overly aggressive and possibly damaging immune responses by decreasing inflammation caused by hyperactivated T cells (b).

pathogenic/prognostic variables and therapeutic targets in COVID-19 [101]. Moreover, it has been reported that M-MDSC level in the blood was considerably higher in COVID-19 patients, compared with healthy controls [102]. Additionally, it was observed that patients with more severe illnesses had considerably higher peak of M-MDSC frequencies in their blood, compared with mild and healthy controls [102]. Similarly, Kvedaraite et al. found that there were high frequencies of M-MDSC in blood samples from severe COVID-19 patients, compared with moderate patients [97]. Equally important, Jiménez-Cortegana et al. found that the amount of peripheral M-MDSC in COVID-19 patients was significantly increased, compared with healthy controls [8]. They also reported a negative correlation between levels of M-MDSC and activated T cells, implying that M-MDSCs suppress T cell activation [8]. Another study found an association between M-MDSC level and sex and age [103]. Men had significantly higher levels of M-MDSCs, and there was a significant positive correlation between age and M-MDSC level [103]. Moreover, Xue et al. found a strong negative correlation between M-MDSC frequency and lymphocyte levels and serum albumin and a positive correlation with oropharyngeal viral loads and length of hospitalization in severe COVID-19 patients, suggesting that M-MDSC might be used to predict the severity and prognosis of COVID-19 [104]. Additionally, Emsen et al. found that patients with COVID-19 had substantially higher levels of total MDSCs, PMN-MDSCs, and M-MDSCs, when compared to healthy controls [105]. Furthermore, they found that severe COVID-19 patients had much higher PMN-MDSC levels than mild COVID-19 patients [105]. However, another study observed that levels of G-MDSC and M-MDSC were higher in COVID-19 patients, compared with healthy controls, with no difference between COVID-19 severity or ventilator status [106]. Schulte-Schrepping et al. found a large proportion of preneutrophil and immature neutrophil cells in peripheral blood of severe COVID-19 patients, compared with mild patients, demonstrating that a dysregulated myeloid cell component contributes to severe COVID-19 [96]. Moreover, other studies showed that the frequency of PMN-MDSCs in severe COVID-19 patients was higher compared with mild disease or healthy controls [107–109]. Recent studies indicated that PMN-MDSCs played a novel function in platelet activation by decreasing L-arginine concentration in COVID-19 patients, indicating a novel role of MDSCs in the pathogenesis of COVID-19 [110].

3.2.2. Protective Roles. MDSCs have been characterized as a response to inflammatory processes that help to limit overly aggressive and possibly damaging immune responses by inhibiting the function of several immune cells including NK cell and T lymphocytes in severe COVID-19 patients (Figure 2(b)) [111]. It has been reported that the expansion of MDSCs was found to be significantly linked to lymphopenia and increased arginase activity in response to COVID-19 [98]. Surprisingly, *in vitro*, arginine was found to be essential in the lifecycle of several DNA and RNA viruses [112]. Therefore, therapeutic depletion of arginine may inhibit SARS-CoV-2 replication [112]. Accordingly, MDSCs may have a protective role against SARS-CoV-2 by producing ARG1. In addition, Agrati et al. demonstrated that patients with severe COVID-19 had a massive expansion of MDSCs, accounting for up to 90% of the total number of circulating mononuclear cells in the blood, indicating that immunological suppression, potentially mediated by expanded MDSCs, might be useful in decreasing inflammation and lung damage caused by hyperactivated cytotoxic T cells (Figure 2(b)) [113]. Interestingly, Takano *et al.* reported that G-MDSCs, but not other MDSC subgroups, exhibited temporary expansion in severe COVID-19, but not in mild or moderate diseases [114]. This temporary expansion of G-MDSCs was seen among survivors of severe COVID-19, but not among nonsurvivors, suggesting a beneficial effect of the G-MDSCs subgroup, which has the ability to reduce excessive inflammation during severe COVID-19 recovery [114].

In vaccination settings, a study reported that frequency of PMN-MDSCs and M-MDSCs increased dramatically after the first COVID-19 vaccination dose, which was reduced at further periods of time, approaching but not reaching prevaccination values, which may have reduced postvaccination responses [115].

4. Targeting Tregs and MDSCs in COVID-19

The primary causes of morbidity and death in COVID-19 patients are cytokine storm and defective haemostasis [2]. Function of Tregs in COVID-19 patients should be evaluated depending on their physiological location and illness stage. If there are more Tregs in the lungs during inflammatory cytokine storm, this could reduce the excessive immune responses [116, 117]. Therefore, expanding Tregs or increasing their activity could be beneficial in this context. There are some potential strategies to expand Tregs or enhance their activity. Tregs cord infusions were associated with recovery in two critical COVID-19 patients; this could be due to increase in Tregs and reduction in hyperinflammation [118]. In type 1 diabetes and autoimmune diseases, low-dose IL-2 has been utilized to induce Treg expansion. There is only one clinical trial investigated the administration of low-dose IL-2 in hospitalized COVID-19 patients with ARDS [119]. This trial has been completed, and results are awaited (trial NCT04357444 registered at ClinicalTrials.gov). Additionally, abatacept (recombinant Fc-fused CTLA-4 protein) could potentially influence innate cell activation, such as monocytes and dendritic cells, and increase Tregs, although research on Treg activity is limited and contradictory [116, 120]. Moreover, abatacept could be an attractive drug to reduce the hyperinflammation condition of severe COVID-19 patients [121].

On the other hand, some studies showed that increased Tregs are associated with inhibiting antiviral T cell responses in the severe stages of COVID-19 [43]. Therefore, reducing Treg levels or suppressing their activity could provide some benefits to COVID-19 patients. In this context, there are some potential strategies to reduce Treg levels or activities. These include the use of monoclonal antibodies targeting Tregs (e.g., anti-CD25 (LMB-2)), immune checkpoint inhibitors

(e.g., anti-PD-1, anti-CTLA-4), TGF-β blockers to suppress induced Tregs, and denileukin diftitox (DAB-IL-2, ONTAK).

There are some potential strategies to reduce MDSC activity. IL-6 blocker can partially elevate HLA-DR expression, leading to decrease levels of M-MDSC in severe COVID-19 patients [99]. Moreover, expression of vitamin D receptor correlates with the immunosuppressive activity of MDSCs [122]. The active form of vitamin D, 1,25(OH)2D, decreases the suppressive action of MDSCs [122, 123]. Moreover, a clinical trial reported that in hospitalized COVID-19 patients with acute respiratory distress syndrome, administration of L-citrulline, an endogenous precursor of arginine, for one week, decreases the possibility of organ failure, compared to the placebo group (trial NCT04404426 registered at ClinicalTrials.gov).

5. Perspective

It is evident that Tregs are different in patients with different disease severities. Treg increase in the early stages of COVID-19 could be one of the viral evasion mechanisms to inhibit antiviral immune responses. Therefore, approaches to target Tregs and reducing their suppressive activity could be useful to restore antiviral immune responses, especially in old patients with immune-compromised immunity. When the disease progresses, Tregs are beneficial to inhibit inflammation; however, Tregs are either reduced or nonfunctional in the periphery or lung of severe COVID-19 patients; unfortunately, this is part of the hard battle between the virus and the immune system. It is important to exploit approaches inducing or expanding Tregs in these patients to reduce hyperinflammation and tissue damage.

Mechanisms of Treg reduction in peripheral blood of severe COVID-19 patients are largely unknown, but migration of Tregs to the lung to inhibit inflammation and protect tissue damage could be a potential mechanism. Another mechanism could be Treg apoptosis because of deficiency in Treg growth cytokines such as IL-2. There are no enough strong studies with large number of patients reported on the level and function of Tregs in the lung. One study found that Tregs in the lung of severe COVID-19 patients downregulated FoxP3 expression, and they were of a more activated rather than a suppressive phenotype, which could induce hyperinflammation and tissue damage [63].

Most available studies reported elevated levels of MDSCs in severe COVID-19 patients. Identification of MDSC's subpopulations in severe versus mild or asymptomatic COVID-19 patients is essential for prognosis and therapeutic targeting. MDSCs, by releasing ARG1, are a double-edged sword, which inhibit T cell proliferation through decreasing L-arginine, but also reduce SARS-CoV-2 replication. Further studies are needed to investigate MDSC subpopulations and the effect of targeting them in severe COVID-19 patients.

6. Conclusions

Studies investigating Tregs in COVID-19 patients have reported different results. Some studies reported that Tregs were increased in COVID-19 patients and played a negative role in the progression of the disease. Other studies reported that the decreased levels of Tregs and increased response of proinflammatory cytokines in COVID-19 could be associated with hyperinflammation and severe disease. However, an early increase in inflammatory cytokines could be associated with faster viral clearance and early immune responses. The balance between anti-inflammatory cells such as Tregs and proinflammatory cells such as Th17 is critical to determine the clinical outcome in COVID-19 patients. Understanding the relationship between Tregs and inflammatory cytokines could lead to discovering novel therapeutic approaches in COVID-19 disease.

Different studies observed that alteration in MDSC levels in the blood has been associated with disease severity. Furthermore, there is a strong negative correlation between M-MDSC frequency and lymphocyte levels in severe COVID-19 patients, suggesting that M-MDSC might be used to predict the severity and prognosis of COVID-19. Moreover, different studies observed that the frequency of G-MDSCs was higher in severe COVID-19 and might be associated with lymphopenia and severity of the disease. However, some studies found that MDSCs were expanded as a response to inflammatory processes, which helped to limit an overly aggressive and possibly damaging immune responses by inhibiting several immune cells. In addition, some researchers found that G-MDSCs, but not other MDSC subgroups, exhibited temporary expansion in severe COVID-19, which can reduce excessive inflammation during severe COVID-19.

In conclusion, immune cells, including Tregs and MDSCs, should be further studied as potential prognostic biomarkers and therapeutic targets in COVID-19. Further studies, including higher numbers of patients with mild and severe diseases and validated protocols for identification and measuring levels of Tregs and MDSCs, are required to make stronger conclusions. Additionally, investigations on patients receiving different types of COVID-19 vaccinations are urgently needed to determine any changes in Treg and MDSC levels in circulation following vaccinations, and how these changes can correlate with the protective roles of vaccines.

Abbreviations

ARG:	Arginase
ARDS:	Acute respiratory distress syndrome
COVID-19:	Coronavirus disease 2019
CTLA-4:	Cytotoxic T lymphocyte associated antigen-4
E-MDSCs:	Early stage myeloid- derived suppressor cells
FoxP3:	Forkhead box P3
G-MDSCs:	Granulocytic myeloid- derived suppressor cells
HCV:	Hepatitis C virus
HBV:	Hepatitis B virus
HIV:	Human immunodeficiency virus
HSV-2:	Herpes simplex virus type 2
IL:	Interleukin
MDSCs:	Myeloid-derived suppressor cells

M-MDSCs: Monocytic myeloid- derived suppressor cells
NOS: Nitric oxide synthase
NK: Natural killer
$ONOO^-$: Peroxynitrite
PD-1: Programmed cell death protein 1
PMN-MDSCs: Polymorphonuclear myeloid-derived suppressor cells
RSV: Respiratory syncytial virus
SARS-CoV-2: Severe acute respiratory syndrome coronavirus 2
TGF-β: Transforming growth factor –Beta 1
Th2: T helper 2
Th17: T helper 17
tTreg: Thymus-derived Tregs
Tregs: T regulatory cells
pTreg: Peripherally-T regulatory cells
WBCs: White blood cells.

Conflicts of Interest

The authors declare no conflict of interest.

References

[1] J. F.-W. Chan, S. Yuan, K. H. Kok et al., "A familial cluster of pneumonia associated with the 2019 novel coronavirus indicating person-to-person transmission: a study of a family cluster," *The Lancet*, vol. 395, no. 10223, pp. 514–523, 2020.

[2] C. Huang, Y. Wang, X. Li et al., "Clinical features of patients infected with 2019 novel coronavirus in Wuhan, China," *The Lancet*, vol. 395, no. 10223, pp. 497–506, 2020.

[3] R. T. Gandhi, J. B. Lynch, and C. Del Rio, "Mild or moderate Covid-19," *New England Journal of Medicine*, vol. 383, no. 18, pp. 1757–1766, 2020.

[4] D. A. Berlin, R. M. Gulick, and F. J. Martinez, "Severe COVID-19," *New England Journal of Medicine*, vol. 383, no. 25, pp. 2451–2460, 2020.

[5] B. Thakur, P. Dubey, J. Benitez et al., "A systematic review and meta-analysis of geographic differences in comorbidities and associated severity and mortality among individuals with COVID-19," *Scientific Reports*, vol. 11, no. 1, pp. 1–13, 2021.

[6] D. Liao, F. Zhou, L. Luo et al., "Haematological characteristics and risk factors in the classification and prognosis evaluation of COVID-19: a retrospective cohort study," *The Lancet Haematology*, vol. 7, no. 9, pp. e671–e678, 2020.

[7] H. K. Siddiqi and M. R. Mehra, "COVID-19 illness in native and immunosuppressed states: a clinical-therapeutic staging proposal," *The Journal of Heart and Lung Transplantation*, vol. 39, no. 5, pp. 405–407, 2020.

[8] C. Jiménez-Cortegana, J. Liró, N. Palazón-Carrión et al., "Increased blood monocytic myeloid derived suppressor cells but low regulatory T lymphocytes in patients with mild COVID-19," *Viral Immunology*, vol. 34, no. 9, pp. 639–645, 2021.

[9] M. A. O'Connor, J. L. Rastad, and W. R. Green, "The role of myeloid-derived suppressor cells in viral infection," *Viral Immunology*, vol. 30, no. 2, pp. 82–97, 2017.

[10] N. L. Bowers, E. S. Helton, R. P. H. Huijbregts, P. A. Goepfert, S. L. Heath, and Z. Hel, "Immune suppression by neutrophils in HIV-1 infection: role of PD-L1/PD-1 pathway," *PLoS Pathogens*, vol. 10, no. 3, article e1003993, 2014.

[11] B. K. C. Thakuri, J. Zhang, J. Zhao et al., "LncRNA HOTAIRM1 promotes MDSC expansion and suppressive functions through the HOXA1-miR124 axis during HCV infection," *Scientific Reports*, vol. 10, no. 1, p. 22033, 2020.

[12] S. Sakaguchi, M. Miyara, C. M. Costantino, and D. A. Hafler, "$FOXP3^+$ regulatory T cells in the human immune system," *Nature Reviews Immunology*, vol. 10, no. 7, pp. 490–500, 2010.

[13] Q. Tang and J. A. Bluestone, "Regulatory T-cell therapy in transplantation: moving to the clinic," *Cold Spring Harbor Perspectives in Medicine*, vol. 3, no. 11, article a015552, 2013.

[14] A. Xu, Y. Liu, W. Chen et al., "TGF-β–induced regulatory T cells directly suppress B cell responses through a noncytotoxic mechanism," *The Journal of Immunology*, vol. 196, no. 9, pp. 3631–3641, 2016.

[15] S. G. Zheng, J. H. Wang, J. D. Gray, H. Soucier, and D. A. Horwitz, "Natural and induced CD4+ CD25+ cells educate CD4+ CD25− cells to develop suppressive activity: the role of IL-2, TGF-β, and IL-10," *The Journal of Immunology*, vol. 172, no. 9, pp. 5213–5221, 2004.

[16] C.-S. Hsieh, Y. Liang, A. J. Tyznik, S. G. Self, D. Liggitt, and A. Y. Rudensky, "Recognition of the peripheral self by naturally arising $CD25^+$ $CD4^+$ T cell receptors," *Immunity*, vol. 21, no. 2, pp. 267–277, 2004.

[17] N. M. Tsuji, K. Mizumachi, and J. I. Kurisaki, "Antigen-specific, CD4+ CD25+ regulatory T cell clones induced in Peyer's patches," *International Immunology*, vol. 15, no. 4, pp. 525–534, 2003.

[18] A. K. Abbas, C. Benoist, J. A. Bluestone et al., "Regulatory T cells: recommendations to simplify the nomenclature," *Nature Immunology*, vol. 14, no. 4, pp. 307-308, 2013.

[19] S. Z. Josefowicz, L.-F. Lu, and A. Y. Rudensky, "Regulatory T cells: mechanisms of differentiation and function," *Annual Review of Immunology*, vol. 30, no. 1, pp. 531–564, 2012.

[20] J. A. Bluestone and A. K. Abbas, "Natural versus adaptive regulatory T cells," *Nature Reviews Immunology*, vol. 3, no. 3, pp. 253–257, 2003.

[21] Y. Y. Wan and R. A. Flavell, "Regulatory T-cell functions are subverted and converted owing to attenuated Foxp3 expression," *Nature*, vol. 445, no. 7129, pp. 766–770, 2007.

[22] M. Miyara, Y. Yoshioka, A. Kitoh et al., "Functional delineation and differentiation dynamics of human $CD4^+$ T cells expressing the FoxP3 transcription factor," *Immunity*, vol. 30, no. 6, pp. 899–911, 2009.

[23] J. Zhao, J. Zhao, and S. Perlman, "Differential effects of IL-12 on Tregs and non-Treg T cells: roles of IFN-γ, IL-2 and IL-2R," *PLoS One*, vol. 7, no. 9, article e46241, 2012.

[24] U. Dittmer, H. He, R. J. Messer et al., "Functional impairment of $CD8^+$ T cells by regulatory T cells during persistent retroviral infection," *Immunity*, vol. 20, no. 3, pp. 293–303, 2004.

[25] S. Suvas, U. Kumaraguru, C. D. Pack, S. Lee, and B. T. Rouse, "CD4+ CD25+ T cells regulate virus-specific primary and memory CD8+ T cell responses," *The Journal of Experimental Medicine*, vol. 198, no. 6, pp. 889–901, 2003.

[26] T. Veiga-Parga, S. Sehrawat, and B. T. Rouse, "Role of regulatory T cells during virus infection," *Immunological Reviews*, vol. 255, no. 1, pp. 182–196, 2013.

[27] S. Raiden, J. Pandolfi, F. Payasliàn et al., "Depletion of circulating regulatory T cells during severe respiratory syncytial

virus infection in young children," *American Journal of Respiratory and Critical Care Medicine*, vol. 189, no. 7, pp. 865–868, 2014.

[28] B. Li, F. L. Wu, X. B. Feng, D. K. Sun, Q. Q. Cui, and Z. X. Zhao, "Changes and the clinical significance of CD4+ CD25+ regulatory T cells and Th17 cells in peripheral blood of infants with respiratory syncytial virus bronchiolitis," *Chinese Journal of Cellular and Molecular Immunology*, vol. 28, no. 4, pp. 426–428, 2012.

[29] L. Qin, C. P. Hu, J. T. Feng, and Q. Xia, "Activation of lymphocytes induced by bronchial epithelial cells with prolonged RSV infection," *PLoS One*, vol. 6, no. 12, article e27113, 2011.

[30] K. Sugimoto, F. Ikeda, J. Stadanlick, F. A. Nunes, H. J. Alter, and K. M. Chang, "Suppression of HCV-specific T cells without differential hierarchy demonstrated _ex vivo_ in persistent HCV infection," *Hepatology*, vol. 38, no. 6, pp. 1437–1448, 2003.

[31] R. Cabrera, Z. Tu, Y. Xu et al., "An immunomodulatory role for CD4+ CD25+ regulatory T lymphocytes in hepatitis C virus infection," *Hepatology*, vol. 40, no. 5, pp. 1062–1071, 2004.

[32] T. Boettler, H. C. Spangenberg, C. Neumann-Haefelin et al., "T cells with a CD4+ CD25+ regulatory phenotype suppress in vitro proliferation of virus-specific CD8+ T cells during chronic hepatitis C virus infection," *Journal of Virology*, vol. 79, no. 12, pp. 7860–7867, 2005.

[33] M. A. Claassen, R. J. de Knegt, H. W. Tilanus, H. L. A. Janssen, and A. Boonstra, "Abundant numbers of regulatory T cells localize to the liver of chronic hepatitis C infected patients and limit the extent of fibrosis," *Journal of Hepatology*, vol. 52, no. 3, pp. 315–321, 2010.

[34] Z. Wan, Z. Zhou, Y. Liu et al., "Regulatory T cells and T helper 17 cells in viral infection," *Scandinavian Journal of Immunology*, vol. 91, no. 5, article e12873, 2020.

[35] W. Wu, J. Li, F. Chen, H. Zhu, G. Peng, and Z. Chen, "Circulating Th17 cells frequency is associated with the disease progression in HBV infected patients," *Journal of Gastroenterology and Hepatology*, vol. 25, no. 4, pp. 750–757, 2010.

[36] H. Feng, J. Yin, Y. P. Han et al., "Regulatory T cells and IL-17+ T helper cells enhanced in patients with chronic hepatitis B virus infection," *International Journal of Clinical and Experimental Medicine*, vol. 8, no. 6, pp. 8674–8685, 2015.

[37] J. Fu, D. P. Xu, P. Zhao et al., "The characterization of regulatory T cells in peripheral blood of HBV-infected patients," *Zhonghua Yi Xue Za Zhi*, vol. 86, no. 22, pp. 1522–1525, 2006.

[38] G. Yang, A. Liu, Q. Xie et al., "Association of CD4+ CD25+ Foxp3+ regulatory T cells with chronic activity and viral clearance in patients with hepatitis B," *International Immunology*, vol. 19, no. 2, pp. 133–140, 2007.

[39] J. N. Stoop, R. G. van der Molen, C. C. Baan et al., "Regulatory T cells contribute to the impaired immune response in patients with chronic hepatitis B virus infection," *Hepatology*, vol. 41, no. 4, pp. 771–778, 2005.

[40] A. Prendergast, J. G. Prado, Y. H. Kang et al., "HIV-1 infection is characterized by profound depletion of CD161+ Th17 cells and gradual decline in regulatory T cells," *AIDS*, vol. 24, no. 4, pp. 491–502, 2010.

[41] W. H. Wang, L. Ming, Y. Wang, Q. C. Kan, and X. Y. Zhang, "High frequency of regulatory T cells among HIV type 1-infected men who have sex with men correlates with disease progression," *Chinese Medical Journal*, vol. 126, no. 11, pp. 2054–2061, 2013.

[42] N. Milman, J. Zhu, C. Johnston et al., "In situ detection of regulatory T cells in human genital herpes simplex virus type 2 (HSV-2) reactivation and their influence on spontaneous HSV-2 reactivation," *The Journal of Infectious Diseases*, vol. 214, no. 1, pp. 23–31, 2016.

[43] S. Galván-Peña, J. Leon, K. Chowdhary et al., "Profound Treg perturbations correlate with COVID-19 severity," *Proceedings of the National Academy of Sciences*, vol. 118, no. 37, 2021.

[44] S. C. Vick, M. Frutoso, F. Mair et al., "A regulatory T cell signature distinguishes the immune landscape of COVID-19 patients from those with other respiratory infections," *Science Advances*, vol. 7, no. 46, article eabj0274, 2021.

[45] J. Neumann, T. Prezzemolo, L. Vanderbeke et al., "Increased IL-10-producing regulatory T cells are characteristic of severe cases of COVID-19," *Clinical & translational immunology*, vol. 9, no. 11, article e1204, 2020.

[46] A. Ronit, R. M. G. Berg, J. T. Bay et al., "Compartmental immunophenotyping in COVID-19 ARDS: a case series," *Journal of Allergy and Clinical Immunology*, vol. 147, no. 1, pp. 81–91, 2021.

[47] X. Chen, J. Huang, Y. Huang et al., "Characteristics of immune cells and cytokines in patients with coronavirus disease 2019 in Guangzhou, China," *Human Immunology*, vol. 81, no. 12, pp. 702–708, 2020.

[48] J. Yang, E. Zhang, M. Zhong et al., "Impaired T cell functions along with elevated activated Tregs at the early stage of asymptomatic SARS-CoV-2 infection," *SSRN Electronic Journal*, 2020.

[49] S. De Biasi, M. Meschiari, L. Gibellini et al., "Marked T cell activation, senescence, exhaustion and skewing towards TH17 in patients with COVID-19 pneumonia," *Nature Communications*, vol. 11, no. 1, article 3434, 2020.

[50] M. Rezaei, M. Marjani, S. Mahmoudi, E. Mortaz, and D. Mansouri, "Dynamic changes of lymphocyte subsets in the course of covid-19," *International Archives of Allergy and Immunology*, vol. 182, no. 3, pp. 254–262, 2021.

[51] B. Kratzer, D. Trapin, P. Ettel et al., "Immunological imprint of COVID-19 on human peripheral blood leukocyte populations," *Allergy*, vol. 76, no. 3, pp. 751–765, 2021.

[52] A. Sadeghi, S. Tahmasebi, A. Mahmood et al., "Th17 and Treg cells function in SARS-CoV2 patients compared with healthy controls," *Journal of Cellular Physiology*, vol. 236, no. 4, pp. 2829–2839, 2021.

[53] B. K. Patterson, J. Guevara-Coto, R. Yogendra et al., "Immune-based prediction of COVID-19 severity and chronicity decoded using machine learning," *Frontiers in Immunology*, vol. 12, p. 2520, 2021.

[54] C. Xie, Q. Li, L. Li et al., "Association of early inflammation with age and asymptomatic disease in COVID-19," *Journal of Inflammation Research*, vol. 14, pp. 1207–1216, 2021.

[55] B. J. Meckiff, C. Ramírez-Suástegui, V. Fajardo et al., "Imbalance of regulatory and cytotoxic SARS-CoV-2-reactive $CD4^+$ T cells in COVID-19," *Cell*, vol. 183, no. 5, pp. 1340–1353.e16, 2020.

[56] E. Rutkowska, I. Kwiecień, M. Żabicka et al., "Cytokines and leukocytes subpopulations profile in SARS-CoV-2 patients depending on the CT score severity," *Viruses*, vol. 13, no. 5, p. 880, 2021.

[57] S. R. Mohebbi, K. Baghaei, M. Rostami-Nejad et al., "Significant changes of CD4, FOXP3, CD25, and IL6 expression level in Iranian COVID-19 patients," *Gastroenterology and Hepatology From Bed to Bench*, vol. 13, no. 4, p. 388, 2020.

[58] R. Jia, X. Wang, P. Liu et al., "Mild cytokine elevation, moderate CD4+ T cell response and abundant antibody production in children with COVID-19," *Virologica Sinica*, vol. 35, no. 6, pp. 734–743, 2020.

[59] C. Qin, L. Zhou, Z. Hu et al., "Dysregulation of immune response in patients with coronavirus 2019 (COVID-19) in Wuhan, China," *Clinical Infectious Diseases*, vol. 71, no. 15, pp. 762–768, 2020.

[60] G. Chen, D. Wu, W. Guo et al., "Clinical and immunological features of severe and moderate coronavirus disease 2019," *The Journal of Clinical Investigation*, vol. 130, no. 5, pp. 2620–2629, 2020.

[61] F. Wang, H. Hou, Y. Luo et al., "The laboratory tests and host immunity of COVID-19 patients with different severity of illness," *JCI Insight*, vol. 5, no. 10, 2020.

[62] W. Wang, B. Su, L. Pang et al., "High-dimensional immune profiling by mass cytometry revealed immunosuppression and dysfunction of immunity in COVID-19 patients," *Cellular & Molecular Immunology*, vol. 17, no. 6, pp. 650–652, 2020.

[63] B. Kalfaoglu, J. Almeida-Santos, C. A. Tye, Y. Satou, and M. Ono, "T-cell hyperactivation and paralysis in severe COVID-19 infection revealed by single-cell analysis," *Frontiers in Immunology*, vol. 11, article 589380, 2020.

[64] X. Yang, Y. Yu, J. Xu et al., "Clinical course and outcomes of critically ill patients with SARS-CoV-2 pneumonia in Wuhan, China: a single-centered, retrospective, observational study," *The Lancet Respiratory Medicine*, vol. 8, no. 5, pp. 475–481, 2020.

[65] W. Wang, R. Thomas, J. Oh, and D. M. Su, "Thymic aging may be associated with COVID-19 pathophysiology in the elderly," *Cell*, vol. 10, no. 3, p. 628, 2021.

[66] J. Oh, W. Wang, R. Thomas, and D. M. Su, "Capacity of tTreg generation is not impaired in the atrophied thymus," *PLoS Biology*, vol. 15, no. 11, article e2003352, 2017.

[67] J. Raynor, C. S. Lages, H. Shehata, D. A. Hildeman, and C. A. Chougnet, "Homeostasis and function of regulatory T cells in aging," *Current Opinion in Immunology*, vol. 24, no. 4, pp. 482–487, 2012.

[68] H. Tsukamoto, K. Clise-Dwyer, G. E. Huston et al., "Age-associated increase in lifespan of naive CD4 T cells contributes to T-cell homeostasis but facilitates development of functional defects," *Proceedings of the National Academy of Sciences*, vol. 106, no. 43, pp. 18333–18338, 2009.

[69] C. A. Chougnet, P. Tripathi, C. S. Lages et al., "A major role for Bim in regulatory T cell homeostasis," *The Journal of Immunology*, vol. 186, no. 1, pp. 156–163, 2011.

[70] A. Sacchi, G. Grassi, V. Bordoni et al., "Early expansion of myeloid-derived suppressor cells inhibits SARS-CoV-2 specific T-cell response and may predict fatal COVID-19 outcome," *Cell Death & Disease*, vol. 11, no. 10, p. 921, 2020.

[71] J. E. Talmadge and D. I. Gabrilovich, "History of myeloid-derived suppressor cells," *Nature Reviews. Cancer*, vol. 13, no. 10, pp. 739–752, 2013.

[72] D. I. Gabrilovich, "Myeloid-derived suppressor cells," *Cancer Immunology Research*, vol. 5, no. 1, pp. 3–8, 2017.

[73] M. Rajabinejad, F. Salari, A. Gorgin Karaji, and A. Rezaiemanesh, "The role of myeloid-derived suppressor cells in the pathogenesis of rheumatoid arthritis; anti- or pro-inflammatory cells?," *Artificial Cells, Nanomedicine, and Biotechnology*, vol. 47, no. 1, pp. 4149–4158, 2019.

[74] V. Kumar, S. Patel, E. Tcyganov, and D. I. Gabrilovich, "The nature of myeloid-derived suppressor cells in the tumor microenvironment," *Trends in Immunology*, vol. 37, no. 3, pp. 208–220, 2016.

[75] S. M. Toor, S. Khalaf, K. Murshed, M. Abu Nada, and E. Elkord, "Myeloid cells in circulation and tumor microenvironment of colorectal cancer patients with early and advanced disease stages," *Journal of Immunology Research*, vol. 2020, Article ID 9678168, 2020.

[76] D. I. Gabrilovich and S. Nagaraj, "Myeloid-derived suppressor cells as regulators of the immune system," *Nature Reviews Immunology*, vol. 9, no. 3, pp. 162–174, 2009.

[77] K. Koushki, M. Salemi, S. M. Miri, Y. Arjeini, M. Keshavarz, and A. Ghaemi, "Role of myeloid-derived suppressor cells in viral respiratory infections; hints for discovering therapeutic targets for COVID-19," *Biomedicine & Pharmacotherapy*, vol. 144, article 112346, 2021.

[78] T. Condamine and D. I. Gabrilovich, "Molecular mechanisms regulating myeloid-derived suppressor cell differentiation and function," *Trends in Immunology*, vol. 32, no. 1, pp. 19–25, 2011.

[79] B. Huang, P. Y. Pan, Q. Li et al., "Gr-1+CD115+ immature myeloid suppressor cells mediate the development of tumor-induced T regulatory cells and T-cell anergy in tumor-bearing host," *Cancer Research*, vol. 66, no. 2, pp. 1123–1131, 2006.

[80] L. Cassetta, K. Bruderek, J. Skrzeczynska-Moncznik et al., "Differential expansion of circulating human MDSC subsets in patients with cancer, infection and inflammation," *Journal for Immunotherapy of Cancer*, vol. 8, no. 2, p. e001223, 2020.

[81] L. Wang, E. W. Y. Chang, S. C. Wong, S. M. Ong, D. Q. Y. Chong, and K. L. Ling, "Increased myeloid-derived suppressor cells in gastric cancer correlate with cancer stage and plasma S100A8/A9 proinflammatory proteins," *Journal of Immunology*, vol. 190, no. 2, pp. 794–804, 2013.

[82] S. Mandruzzato, S. Solito, E. Falisi et al., "IL4Rα+myeloid-derived suppressor cell expansion in cancer patients," *Journal of Immunology*, vol. 182, no. 10, pp. 6562–6568, 2009.

[83] C. Y. Liu, Y. M. Wang, C. L. Wang et al., "Population alterations of L-arginase- and inducible nitric oxide synthase-expressed CD11b+/CD14$^-$/CD15+/CD33+ myeloid-derived suppressor cells and CD8+ T lymphocytes in patients with advanced-stage non-small cell lung cancer," *Journal of Cancer Research and Clinical Oncology*, vol. 136, no. 1, pp. 35–45, 2010.

[84] S. Vuk-Pavlović, P. A. Bulur, Y. Lin et al., "Immunosuppressive CD14+HLA-DRlow/− monocytes in prostate cancer," *Prostate*, vol. 70, no. 4, pp. 443–455, 2010.

[85] Y. S. Khaled, B. J. Ammori, and E. Elkord, "Increased levels of granulocytic myeloid-derived suppressor cells in peripheral blood and tumour tissue of pancreatic cancer patients," *Journal of Immunology Research*, vol. 2014, Article ID 879897, 2014.

[86] D. Lindau, P. Gielen, M. Kroesen, P. Wesseling, and G. J. Adema, "The immunosuppressive tumour network: myeloid-derived suppressor cells, regulatory T cells and natural killer T cells," *Immunology*, vol. 138, no. 2, pp. 105–115, 2013.

[87] M. Motallebnezhad, F. Jadidi-Niaragh, E. S. Qamsari, S. Bagheri, T. Gharibi, and M. Yousefi, "The immunobiology of myeloid-derived suppressor cells in cancer," *Tumour Biology*, vol. 37, no. 2, pp. 1387–1406, 2016.

[88] W. Cai, A. Qin, P. Guo et al., "Clinical significance and functional studies of myeloid-derived suppressor cells in chronic hepatitis C patients," *Journal of Clinical Immunology*, vol. 33, no. 4, pp. 798–808, 2013.

[89] B. A. Norris, L. S. Uebelhoer, H. I. Nakaya, A. A. Price, A. Grakoui, and B. Pulendran, "Chronic but not acute virus infection induces sustained expansion of myeloid suppressor cell numbers that inhibit viral-specific T cell immunity," *Immunity*, vol. 38, no. 2, pp. 309–321, 2013.

[90] R. S. Tacke, H. C. Lee, C. Goh et al., "Myeloid suppressor cells induced by hepatitis C virus suppress T-cell responses through the production of reactive oxygen species," *Hepatology*, vol. 55, no. 2, pp. 343–353, 2012.

[91] J. P. Ren, J. Zhao, J. Dai et al., "Hepatitis C virus-induced myeloid-derived suppressor cells regulate T-cell differentiation and function via the signal transducer and activator of transcription 3 pathway," *Immunology*, vol. 148, no. 4, pp. 377–386, 2016.

[92] A. Garg and S. A. Spector, "HIV type 1 gp120-induced expansion of myeloid derived suppressor cells is dependent on interleukin 6 and suppresses immunity," *The Journal of Infectious Diseases*, vol. 209, no. 3, pp. 441–451, 2014.

[93] T. Vollbrecht, R. Stirner, A. Tufman et al., "Chronic progressive HIV-1 infection is associated with elevated levels of myeloid-derived suppressor cells," *AIDS*, vol. 26, no. 12, pp. F31–F37, 2012.

[94] S. Pal, M. Nandi, D. Dey et al., "Myeloid-derived suppressor cells induce regulatory T cells in chronically HBV infected patients with high levels of hepatitis B surface antigen and persist after antiviral therapy," *Alimentary Pharmacology & Therapeutics*, vol. 49, no. 10, pp. 1346–1359, 2019.

[95] L. J. Pallett, U. S. Gill, A. Quaglia et al., "Metabolic regulation of hepatitis B immunopathology by myeloid-derived suppressor cells," *Nature Medicine*, vol. 21, no. 6, pp. 591–600, 2015.

[96] J. Schulte-Schrepping, N. Reusch, D. Paclik et al., *Suppressive myeloid cells are a hallmark of severe COVID-19*, no. article 2020.06.03.20119818, 2020medRxiv, 2020.

[97] E. Kvedaraite, L. Hertwig, I. Sinha et al., *Perturbations in the mononuclear phagocyte landscape associated with COVID-19 disease severity*, no. article 2020.08.25.20181404, 2020medRxiv, 2020.

[98] F. Reizine, M. Lesouhaitier, M. Gregoire et al., "SARS-CoV-2-induced ARDS associates with MDSC expansion, lymphocyte dysfunction, and arginine shortage," *Journal of Clinical Immunology*, vol. 41, no. 3, pp. 515–525, 2021.

[99] E. J. Giamarellos-Bourboulis, M. G. Netea, N. Rovina et al., "Complex immune dysregulation in COVID-19 patients with severe respiratory failure," *Cell Host & Microbe*, vol. 27, no. 6, pp. 992–1000.e3, 2020.

[100] F. Veglia, E. Sanseviero, and D. I. Gabrilovich, "Myeloid-derived suppressor cells in the era of increasing myeloid cell diversity," *Nature Reviews. Immunology*, vol. 21, no. 8, pp. 485–498, 2021.

[101] D. Atanackovic, S. V. Avila, F. Lutfi et al., "Deep dissection of the antiviral immune profile of patients with COVID-19," *Communications Biology*, vol. 4, no. 1, p. 1389, 2021.

[102] S. Falck-Jones, S. Vangeti, M. Yu et al., *Functional myeloid-derived suppressor cells expand in blood but not airways of COVID-19 patients and predict disease severity*, no. article 2020.09.08.20190272, 2020medRxiv, 2020.

[103] S. Falck-Jones, S. Vangeti, M. Yu et al., "Functional monocytic myeloid-derived suppressor cells increase in blood but not airways and predict COVID-19 severity," *The Journal of Clinical Investigation*, vol. 131, no. 6, 2021.

[104] G. Xue, M. Jiang, R. Zhao, A. P. le, and J. M. Li, "Elevated frequencies of CD14+HLA-DRlo/neg MDSCs in COVID-19 patients," *Aging (Albany NY)*, vol. 13, no. 5, pp. 6236–6246, 2021.

[105] A. Emsen, S. Sumer, B. Tulek et al., "Correlation of myeloid-derived suppressor cells with C-reactive protein, ferritin and lactate dehydrogenase levels in patients with severe COVID-19," *Scandinavian Journal of Immunology*, vol. 95, no. 1, article e13108, 2022.

[106] E. Mortaz, N. K. Dezfuli, N. D. Roofchayee, and I. Adcock, "Myeloid-derived suppressor cells in the blood of COVID-19 patients," *European Respiratory Journal*, vol. 58, article PA2318, suppl 65, 2021.

[107] H. F. Peñaloza, J. S. Lee, and P. Ray, "Neutrophils and lymphopenia, an unknown axis in severe COVID-19 disease," *PLoS Pathogens*, vol. 17, no. 9, article e1009850, 2021.

[108] L. E. Cabrera, P. T. Pekkarinen, M. Alander et al., "Characterization of low-density granulocytes in COVID-19," *PLoS Pathogens*, vol. 17, no. 7, article e1009721, 2021.

[109] E. A. Thompson, K. Cascino, A. A. Ordonez et al., "Metabolic programs define dysfunctional immune responses in severe COVID-19 patients," *Cell Reports*, vol. 34, no. 11, article 108863, 2021.

[110] A. Sacchi, G. Grassi, S. Notari et al., "Expansion of myeloid derived suppressor cells contributes to platelet activation by L-arginine deprivation during SARS-CoV-2 infection," *Cell*, vol. 10, no. 8, p. 2111, 2021.

[111] V. Bordoni, A. Sacchi, E. Cimini et al., "An inflammatory profile correlates with decreased frequency of cytotoxic cells in coronavirus disease 2019," *Clinical Infectious Diseases*, vol. 71, no. 16, pp. 2272–2275, 2020.

[112] J. M. Grimes, S. Khan, M. Badeaux, R. M. Rao, S. W. Rowlinson, and R. D. Carvajal, "Arginine depletion as a therapeutic approach for patients with COVID-19," *International Journal of Infectious Diseases*, vol. 102, pp. 566–570, 2021.

[113] C. Agrati, A. Sacchi, V. Bordoni et al., "Expansion of myeloid-derived suppressor cells in patients with severe coronavirus disease (COVID-19)," *Cell Death and Differentiation*, vol. 27, no. 11, pp. 3196–3207, 2020.

[114] T. Takano, T. Matsumura, Y. Adachi et al., "Myeloid cell dynamics correlating with clinical outcomes of severe COVID-19 in Japan," *International Immunology*, vol. 33, no. 4, pp. 241–247, 2021.

[115] R. Sindhi, C. Ashokkumar, V. Singh et al., *Cellular and Antibody Immunity after COVID-19 Vaccination at >4-Month Follow Up in Immunocompetent and Immunocompromised Subjects*, no. article 2021.10.07.21257459, 2021medRxiv, 2021.

[116] K. Langdon and N. Haleagrahara, "Regulatory T-cell dynamics with abatacept treatment in rheumatoid arthritis," *International Reviews of Immunology*, vol. 37, no. 4, pp. 206–214, 2018.

[117] X. Michelena, H. Borrell, M. López-Corbeto et al., "Incidence of COVID-19 in a cohort of adult and paediatric patients

with rheumatic diseases treated with targeted biologic and synthetic disease-modifying anti-rheumatic drugs," in *Seminars in Arthritis and Rheumatism*, vol. 50, no. 4pp. 564–570, Elsevier, 2020.

[118] D. E. Gladstone, B. S. Kim, K. Mooney, A. H. Karaba, and F. R. D'Alessio, "Regulatory T cells for treating patients with COVID-19 and acute respiratory distress syndrome: two case reports," *Annals of Internal Medicine*, vol. 173, no. 10, pp. 852-853, 2020.

[119] A. Hartemann, G. Bensimon, C. A. Payan et al., "Low-dose interleukin 2 in patients with type 1 diabetes: a phase 1/2 randomised, double-blind, placebo-controlled trial," *The Lancet Diabetes & Endocrinology*, vol. 1, no. 4, pp. 295–305, 2013.

[120] M. Bonelli, L. Göschl, S. Blüml et al., "Abatacept (CTLA-4Ig) treatment reduces T cell apoptosis and regulatory T cell suppression in patients with rheumatoid arthritis," *Rheumatology*, vol. 55, no. 4, pp. 710–720, 2016.

[121] E. Stephen-Victor, M. Das, A. Karnam, B. Pitard, J. F. Gautier, and J. Bayry, "Potential of regulatory T-cell-based therapies in the management of severe COVID-19," *European Respiratory Journal*, vol. 56, no. 3, p. 2002182, 2020.

[122] M. Kloc, R. M. Ghobrial, A. Lipińska-Opałka et al., "Effects of vitamin D on macrophages and myeloid-derived suppressor cells (MDSCs) hyperinflammatory response in the lungs of COVID-19 patients," *Cellular Immunology*, vol. 360, article 104259, 2021.

[123] J. C. Fleet, G. N. Burcham, R. D. Calvert, B. D. Elzey, and T. L. Ratliff, "1α, 25 Dihydroxyvitamin D (1,25$(OH)_2$D) inhibits the T cell suppressive function of myeloid derived suppressor cells (MDSC)," *The Journal of Steroid Biochemistry and Molecular Biology*, vol. 198, article 105557, 2020.

Hindawi
Journal of Immunology Research
Volume 2022, Article ID 8720438, 15 pages
https://doi.org/10.1155/2022/8720438

Research Article

The Association between Regulatory T Cell Subpopulations and Severe Pneumonia Post Renal Transplantation

Quan Zhuang,[1,2] Haozheng Cai,[1] Min Yang,[1] Bo Peng,[1,2] Yulin Luo,[1] Ying Zhang,[1] and Yingzi Ming[1,2]

[1]*Transplantation Center, The 3rd Xiangya Hospital, Central South University, Changsha 410013, China*
[2]*Research Center of National Health Ministry on Transplantation Medicine, Changsha 410013, China*

Correspondence should be addressed to Yingzi Ming; myz_china@aliyun.com

Received 24 October 2021; Revised 5 March 2022; Accepted 10 March 2022; Published 9 April 2022

Academic Editor: Mitesh Dwivedi

Severe pneumonia accounts for the majority of morbidity and mortality in renal allograft recipients due to immunosuppressant maintenance. Regulatory T cells (Tregs), which are involved in tackling infections under immunosuppressive conditions, are rarely uncovered. We aimed to investigate the relationship between various Treg subpopulations and severe pneumonia after kidney transplantation (KTx). KTx recipients with pneumonia were divided into severe pneumonia and mild pneumonia groups. The frequencies and absolute numbers (Ab No.) of total Tregs ($CD4^+CD25^+FoxP3^+$), six subsets of Tregs ($Helios^{+/-}$, $CD39^{+/-}$, and $CD45RA^{+/-}$), and T cells, B cells, and NK cells were assessed from peripheral blood via flow cytometry using the *t* or Mann-Whitney test and receiver operating curve analysis. We also determined the median fluorescence intensity (MFI) of human leukocyte antigen- (HLA-) DR on monocytes and CD64 on neutrophils. Logistic regression was used to identify the risk factors of disease progression, and Pearson's correlation analysis was performed to identify relationships between the measured immune indices and patients' clinical information. Our research indicated that Treg subpopulations were strongly associated with severe pneumonia progression post KTx. Based on the monitoring of Treg subpopulations, better-individualized prevention and therapy might be achieved for patients with severe pneumonia post KTx.

1. Introduction

Kidney transplantation (KTx) has been considered as the most effective therapeutic method for end-stage renal disease (ESRD). Although this surgery provides a new lease of life for many ESRD patients, a series of postoperative complications can have a severe effect on patients' survival [1]. Among them, pneumonia is a frequent infectious complication after KTx, which is considered to be a chief cause of morbidity and mortality in renal allograft recipients due to the continued use of immunosuppressants [2, 3].

The long-term application of immunosuppressants has a significant impact on immunity for renal allograft recipients; thus; it is crucial to monitor the immune function of these patients. Recently, regular immune biomarkers have been applied and carried out in clinical practice, including the distribution and absolute counts of $CD3^+$, $CD4^+$, and $CD8^+$ T cells, B cells, natural killer (NK) cells, the CD4/CD8 ratio as well as human leukocyte antigen- (HLA-) DR expression on monocytes, and CD64 expression on neutrophils [4], which have become increasingly useful for diagnosis and treatment in immunosuppressive patients.

Moreover, regulatory T cells (Tregs) are a minor subpopulation (5%–10%) of peripheral T cells (most of which are CD4 positive) [5], and the existence of Tregs is important for self-tolerance. Generally, Tregs are categorized as thymus-derived (natural) and peripheral inducible. In the presence of some anti-inflammatory factors, like transforming growth factor-β (TGF-β) and interleukin- (IL-) 2, inducible Tregs can be kindled from naïve $CD4^+CD25^-$ cells upon T cell receptor stimulation [6]. Tregs are usually defined as having a high expression of the α-subunit of the IL-2 receptor (CD25) and transcription factor FoxP3, as well as a low expression of the IL-7 receptor α-subunit (CD127) in both

mice and humans [7]. Furthermore, the expression of FoxP3 is necessary for Treg development [8]. Tregs play a crucial role in upholding immune homeostasis and providing protection from autoimmune diseases or allograft rejection [9]. Importantly, KTx patients with chronic rejection have a lower level of peripheral $CD4^+CD25^+FoxP3^+$ T cells (total Treg) than operationally tolerant and immune-stable patients [10]. *Pneumocystis jirovecii* pneumonia is an opportunistic infection in patients with KTx [11]. Previous studies have shown that in immunocompetent mice with *Pneumocystis* infection, total Tregs are recruited to the lung, and their loss leads to increased pulmonary injury with high levels of T helper (Th) 2 cells and proinflammatory cytokines [12]. However, there are currently no studies elucidating Treg distribution in KTx patients with pneumonia.

Helios (Ikzf2) is one of the important members of the Ikaros transcription factor family, which is detected on 60%–70% of Tregs, and has been proposed as a marker to distinguish natural from peripheral inducible Tregs [13]. Helios can enhance the suppressive capacity of $FoxP3^+$ Tregs but not $FoxP3^-$ Tregs [14] because Helios upregulates FoxP3 by binding to the FoxP3 promoter [15]. Furthermore, an increased percentage of $FoxP3^+Helios^+$ Treg has been shown to be significantly related to decreased acute graft-versus-host disease in allogeneic bone marrow transplant patients [16]. $FoxP3^+Helios^+$ Tregs were not only correlated to the improvement of graft-versus-host disease but also influenced the prognosis of bacterial pneumonia. A study showed that adoptive transfer of $FoxP3^+Helios^+$ Treg to CBA/Ca mice, prior to *Pneumococcal* infection, prolonged survival and decreased bacterial dissemination from lung to blood [17].

CD39 (ENTPD1) could turn adenosine triphosphate (ATP) to adenosine diphosphate (ADP) and subsequently to adenosine monophosphate (AMP) [18], which is constantly expressed in FoxP3 Tregs in mice. However, CD39 expression in humans is confined to a subset of FoxP3 regulatory effector/memory-like T (TREM) cells [19]. $FoxP3^{+-}$ $CD39^+$ Tregs mainly abrogate the inflammasome-mediated induction of proinflammatory responses by hydrolyzing ATP. Recently, several studies demonstrated that there were remarkably decreased numbers of $CD39^+$ Tregs in blood in multiple sclerosis, type 2 diabetes [20, 21]. Compared to wild-type mice, Tregs from CD39-deficient mice could not have enough ability to avert rejection in allogeneic skin grafts [22]. $CD39^+$ Tregs were more stable and functional than $CD39^-$ Tregs. A previous study has been reported that when adoptively transferring $CD39^+$ Tregs to the murine xeno-graft-versus-host model, the survival of mice was longer than that of $CD39^-$ Tregs [23]. Furthermore, increased proportions of circulating $CD39^+$ Tregs were observed to suppress the replica of human immunodeficiency virus (HIV) and hepatitis B virus (HBV) [24, 25].

In 2006, Hoffmann et al. first defined a naive Treg subpopulation ($CD4^+CD25^+FoxP3^+CD45RA^+$) [26], which homogeneously expressed CD62L, CCR7, and CTLA-4 and produced no proinflammatory cytokines. However, under stimulation by alloantigen and IL-12, $CD45RA^+$ Treg acquired memory phenotypes, antigen-specific potent suppressive properties, and conversion to an active phenotype ($CD25^+FoxP3^+CD45RA^-$) [27]. Compared to $CD45RA^+$ Tregs, $CD45RA^-$ Tregs have robust immunosuppression [28]. Recently, several studies have shown that patients with high levels of $CD45RA^-$ Treg have a low rate of transplant rejection [29, 30]. However, elevated $CD45RA^-$ Treg may lead to poor prognosis in patients with chronic hepatitis C and HIV infection [31, 32]. Conversely, high levels of $CD45RA^+$ Tregs were correlated with low HIV load and replication [31].

Our study was designed to observe the distribution and absolute numbers (Ab No.) of total Treg ($CD4^+CD25^{+-}$ $FoxP3^+$), six subsets of Tregs ($Helios^{+/-}$, $CD39^{+/-}$, and $CD45RA^{+/-}$), and T cells, B cells, and NK cells (TBNK) between patients with mild and severe pneumonia after KTx. Ours is the first study to investigate different Treg subpopulations in patients with severe pneumonia after KTx and could provide new insights into the monitoring, individualized prevention, and therapy for patients with severe pneumonia post KTx.

2. Materials and Methods

2.1. Patient Recruitment and Blood Specimen Collection. In this retrospective case-control study, patients diagnosed with pneumonia after KTx were enrolled from June 1, 2019, to October 1, 2020, in our transplant center. Kidney transplant recipients with pneumonia were divided into severe pneumonia (SP) and mild pneumonia (MP) groups. The exclusion criteria included the following: (1) individuals < 18 or >65 years old; (2) other transplant patients (liver, pancreas, bone marrow, etc.); (3) multiorgan transplant recipients; (4) time after transplantation ≤ 3 months post KTx; (5) rejection, tumor, or other site infections; and (6) rituximab treatment. All recipients signed an informed consent form. The study decorum had been assessed and accepted by the Institutional Review Board (Ethics Committee) of the 3rd Xiangya Hospital, Central South University (No. 2018-S347).

Kidney allografts were obtained from donations after circulatory death (DCD) or from close relatives. All surgeries were achieved and were authorized by the DCD Ethics Committee of our hospital. The allocation scheme for the organs was decided by the China Organ Transplant Response System. The induction regimen was made up of antithymocyte globulin (1.00 mg/kg daily for 3 days) or basiliximab (20 mg on days 0 and 4). The maintenance immunosuppressants included calcineurin inhibitors (CNIs), mycophenolate mofetil, and corticosteroids. This regimen was used to maintain a weak immune state and reduce the probability of rejection. Clinical manifestations, meaningful laboratory test results, and prominent radiological examinations were used to diagnose pneumonia patients. Diagnostic criteria of severe pneumonia were based on the American Thoracic Society criteria. The major criteria contained the following: (1) requirement for mechanical ventilation and (2) septic shock. The minor criteria comprised the following: (1) an aspiratory rate > 30 per min, (2) an arterial oxygen pressure/fraction of inspired oxygen ratio < 250, (3) a blood urea nitrogen level > 20 mg/dL, (4) leukopenia $< 4 \times 10^9$/L,

Table 1: Overview of the Treg subset panel dedicated to a specific cell type which is indicated by individual colors.

Excitation (nm)	Blue: 488				Red: 633		Violet: 405
Emission peak (nm)	523	575	692	760	665	783	455
Fluorochrome	FITC	PE	PC5.5	PC7	A647	APC-A750	PB
Treg subset panel	CD45RA	CD25	CD39	CD4	FoxP3	CD3	Helios
Compensation control	CD4	CD4	CD39	CD4	FoxP3	CD3	CD4

FITC: fluorescein isothiocyanate; PE: phycoerythrin; PC5.5/7: phycoerythrin cyanine 5.5/7; A647: Alexa Fluor 647; APC-A750: allophycocyanin Alexa Fluor 750; PB: Pacific Blue.

(5) thrombocytopenia, (6) hypothermia, and (7) hypotension requiring aggressive fluid resuscitation. The major criteria ≥ 1 or the minor criteria ≥ 3 [33]. After admission, the patient stopped immunosuppressive treatment. Patients with pneumonia underwent Treg subpopulation tests at the time of pneumonia diagnosis. Most of these patients underwent regular immune monitoring tests. The test was performed at the same time after the patients were admitted to the hospital. Although some patients received multiple tests, only the results of the first test were included. Ethylenediaminetetraacetic acid-K2 anticoagulant tubes were used to collect peripheral blood samples from the patients. Samples were stored and transported at 4°C. Flow cytometry was used to analyze all samples on the day of blood collection.

2.2. Regular Immune Status Panel. There are 2 sections in our regular immune status panel. In the first part, BD 6-color TBNK reagent and BD Trucount tubes were used to count the distribution and absolute numbers of leukocytes from peripheral blood. These leukocytes included $CD3^+CD4^+$ T cells, $CD3^+CD8^+$ T cells, NK cells, and $CD19^+$ B cells. BD FACSCanto clinical software (BD Biosciences, San Jose, CA, USA) was used to investigate the collected flow results. The median fluorescence intensity (MFI) of HLA-DR on monocytes, and CD64 on neutrophils, was detected by another panel. Fluorochrome-conjugated monoclonal antibodies were used in this study, including anti-CD45-PerCP, anti-CD14-APC-Cy7, anti-HLA-DR-APC, and anti-CD64-PE. Briefly, 50 μL of whole blood was stained with fluorescent antibodies for 15 minutes in the dark (room temperature). The specific steps have been described in the previous study [34]. All samples were analyzed using BD FACSDiva software. BD FACSCanto II was used to perform two panels. Every tube was stopped for testing when 10000 cells were collected.

2.3. Treg Subpopulation Test Panel. DuraClone IM Treg tubes were obtained from Beckman Coulter. The details of each fluorochrome-conjugated antibody, the schemes of each fluorochrome channel, and the compensation controls (each of a single color) are shown in Table 1. Briefly, 50 μL of fresh whole blood was added to DuraClone IM Treg Tube 1 and incubated for 15 min (room temperature). Thereafter, phosphate-buffered saline was added to wash the cells. After centrifuging the mixed liquor and aspirating the supernatant, the cell pellet in Tube 1 was resuspended with 50 μL of 100% fetal calf serum. Thereafter, 5 μL of PerFix reagent Buffer 1 was added to Tube 1 and incubated for 15 min in the dark (RT). Subsequently, 400 μL of PerFix nc reagent Buffer 2 (permeabilizing reagent) was added to Tube 1. The contents of DuraClone IM Treg Tube 1 were transferred to Tube 2 and incubated for 60 min in the dark (room temperature). The cells were then rinsed twice and resuspended in 1x PerFix nc Buffer 3. A 13-Color CytoFlex Flow Cytometer (Beckman Coulter, Brea, CA, USA) was used to analyze the samples. The flow cytometer was calibrated using Flow-Set Pro Beads (Beckman Coulter, Brea, CA, USA) daily before use. The Kaluza software (version 1.2; Beckman Coulter, Brea, CA, USA) was carried out to investigate the collected flow cytometric information. We performed compensation by following the AutoSetup Scheduler Application Note "Compensation Setup for High Content DuraClone reagents," which could be obtained from the Beckman Coulter official weblink. The gating strategies for Treg subpopulations are presented in Figure 1.

2.4. Data and Statistical Analysis. Continuous data are presented as the mean ± standard deviation and were compared using the unpaired t-test. Variables that do not follow a normal distribution are presented as the median ± interquartile range and were compared using the Mann-Whitney U test. Pearson's chi-squared (χ^2) test or Fisher's exact test was used to compare categorical data, where appropriate. The optimal cut-off values of the lymphocytes, $CD3^+CD4^+$ T cells, $CD4^+CD25^+$ T cells, total, $Helios^+$, $CD39^+$, and $CD45RA^-$ Tregs were calculated by applying the receiver operating curve (ROC) analysis. The optimal cut-off values were calculated by "sensitivity + specificity − 1," and the maximum values were considered as the optimal cut-off values.

Univariate and multivariate logistic regression analyses were applied to screen for risk factors of disease progression. In this section, the indicators which have statistical significance in Tables 2 and 3 were firstly selected to do the univariate logistic analysis. According to the results of the univariate logistic analysis, the variables which have statistical significance were retained to do the next analysis. Then, a forward stepwise multivariate logistic regression analysis was done to select the combination of success factors that have diagnostic value for the occurrence of SP. Improvement of the model was determined from changes in the −2LogLikelihood (−2LL) value. When the model did not improve anymore, no more factors were added. The variables calculated in this part were all numeric variables.

GraphPad Prism 9.0 was used for statistical analysis. Statistical significance was set at $P < 0.05$. Pearson's correlation analysis was performed to identify relationships between the Treg subsets and the clinical information of the patients

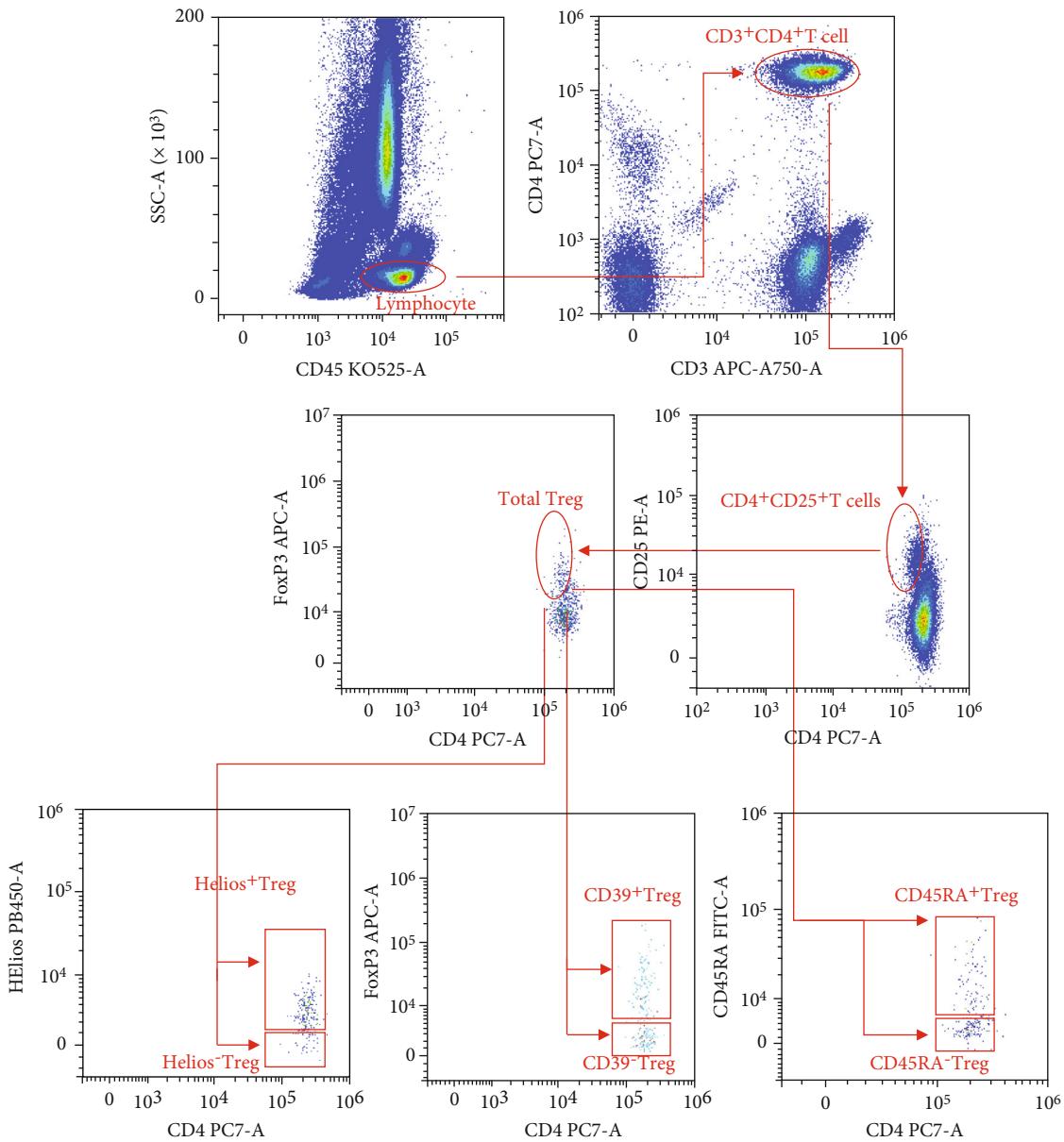

Figure 1: Gating strategies for Treg subpopulations. The first gate was on lymphocytes based on CD45 and SSC-A, and then, CD3 and CD4 were used to gate $CD3^+CD4^+$ T cells. CD25 and FoxP3 together were used to identify total Treg. Helios, CD39, and CD45RA were used to define six subpopulations of Treg: $Helios^{+/-}$ Treg, $CD39^{+/-}$ Treg, and $CD45RA^{+/-}$ Treg.

(with the Pearson $R > 0.4$ (moderate correlation), and $P < 0.05$). The correlation between the results of the regular immune monitoring and Treg subpopulation tests was also calculated and displayed.

3. Results

3.1. Clinical Characteristics. In total, 27 MP and 13 SP patients were joined. The study flowchart is exhibited in Figure 2. All patients with pneumonia experienced the Treg subpopulation test during the first week after admission. Among these patients, 29 recipients received a regular immune monitoring test at the same time as the Treg test. The clinical characteristics between the MP and SP groups showed no significant difference in the age, sex, body mass index, donor source, time since transplantation, CNI regimen, CRP (C reactive protein), Ca^+, and white blood cell or platelet counts. The procalcitonin levels were lower in the MP group, compared to the SP group. Patients in the MP group had better allograft function than those in the SP group. Additionally, the creatinine (Cr) and blood urea nitrogen (BUN) levels in the MP group were lower than those in the SP group, and the survival rate in the SP group was 69.23%, which was significantly lower than that in the MP group (100%). The albumin levels in the MP group were higher than those in the SP group. Additionally, the hospital

Table 2: Clinical characteristics of the patients.

Characteristics	All ($n = 40$)	Mild ($n = 27$)	Severe ($n = 13$)	P
Age (years), mean ± SD	43.93 ± 2.09	45.04 ± 2.56	41.62 ± 3.67	0.4492
Male, n (%)	22 (55.00%)	15 (55.56%)	7 (53.85%)	0.99*
BMI (kg/m^2)	20.32 ± 0.47	20.53 ± 0.56	19.9 ± 0.88	0.5314
Donor, n (%)				0.1540*
DCD	35 (87.50)	22 (81.48)	13 (100.00)	
Relative	5 (12.50)	5 (18.52)	0 (0.00)	
Time since transplantation (months), median ± IQR	8.07 ± 22.45	10.93 ± 25.08	7.20 ± 5.50	0.1140#
CNI, n (%)				0.99*
FK506	38 (95.00)	26 (96.30)	12 (92.31)	
CSA	2 (5.00)	1 (3.70)	1 (7.69)	
Survival, n (%)	36 (90.00)	27 (100)	9 (69.23)	0.0078*
Hospital stay period (days), median ± IQR	16 ± 17.50	13 ± 13.50	34 ± 25	0.0078#
WBC (10^9/L), median ± IQR	7.52 ± 4.45	7.69 ± 3.37	6.95 ± 6.57	0.2865#
PLT (10^9/L), median ± IQR	201 ± 96.25	202 ± 80.5	198 ± 138	0.6430#
BUN (mmol/L), median ± IQR	9.21 ± 10.81	7.12 ± 5.79	17.26 ± 8.76	0.0002#
Cr admission (μmol/L), median ± IQR	123 ± 68.25	119 ± 63	155 ± 255	0.0242#
CRP (mg/L), median ± IQR	37.45 ± 54.59	36.72 ± 53.04	41.13 ± 97.08	0.3423#
Procalcitonin (ng/mL), median ± IQR	0.10 ± 0.33	0.06 ± 0.16	0.24 ± 7.34	0.0030#
Albumin (g/L)	37.0 ± 6.23	39.3 ± 5.46	32.38 ± 5.09	0.0005
Ca^+ (mmol/L), median ± IQR	2.40 ± 0.24	2.45 ± 0.13	2.26 ± 0.33	0.1324#

SD: standard deviation; IQR: interquartile range; DCD: donation after citizens' death; CNI: calcineurin inhibitor; CsA: cyclosporine A; BUN: blood urea nitrogen; Cr: serum creatinine; CRP: C reactive protein; *tested by Fisher's exact test; #tested by Mann-Whitney U test.

Table 3: Regular immune monitoring panel of the patients.

Parameters	All ($n = 30$)	MP ($n = 19$)	SP ($n = 11$)	P
Monocyte HLA-DR, MFI ± SD	1335 ± 205.0	1671.00 ± 285.80	783.60 ± 184.60	0.0329
Neutrophil CD64, MFI ± SD	595.4 ± 86.70	522.10 ± 112.20	715.5 ± 134.80	0.2872
$CD3^+$ T cells/TBNK, mean ± SD (%)	77.72 ± 1.82	76.09 ± 2.41	80.38 ± 2.65	0.2583
$CD3^+$ T cells, mean ± SD (/μL)	707.38 ± 77.05	819.2 ± 96.83	524.5 ± 111.1	0.0621
$CD8^+$ T cells/TBNK, mean ± SD (%)	34.12 ± 1.80	32.45 ± 1.79	37.06 ± 3.69	0.2207
$CD8^+$ T cells, median ± IQR (/μL)	313 ± 245	335.50 ± 204.75	189 ± 241.50	0.2038#
$CD4^+$ T cells/TBNK, mean ± SD (%)	39.75 ± 1.87	41.60 ± 2.60	36.73 ± 2.33	0.2111
$CD4^+$ T cells, mean ± SD (/μL)	367.14 ± 44.49	451.4 ± 58.41	229.2 ± 45.33	0.0125
NK cells/TBNK, mean ± SD (%)	11.23 ± 1.44	12.99 ± 1.90	8.475 ± 1.98	0.1301
NK cells, median ± IQR (/μL)	80 ± 112	110.50 ± 125.75	45 ± 53.50	0.0249#
B cells/TBNK, median ± IQR (%)	7.78 ± 8.84	7.03 ± 10.38	8.46 ± 6.20	0.5801#
B cells, median ± IQR (/μL)	77 ± 102	93 ± 92.25	41 ± 112	0.5724#
CD4/CD8 ratio, median ± IQR	1.11 ± 0.83	1.45 ± 1.01	0.99 ± 0.29	0.2906#

#Tested by the Mann-Whitney U test; others were tested by the unpaired t-test. HLA-DR: human leukocyte antigen-DR; MFI: median fluorescence intensity; SD: standard deviation; IQR: interquartile range; TBNK: T, B, and NK cells; NK cells: natural killer cells.

stay (HS) period in the SP group was much longer than that in the MP group. The details of these clinical characteristics are presented in Table 2.

3.2. Regular Immune Status. Among the 29 patients who underwent regular immune monitoring tests, 18 were MP patients and 11 were SP patients. Compared to the MP group, the SP group was characterized by significantly lower cell counts of $CD4^+$ T cells (451.4 ± 58.41/μL vs. 229.2 ± 45.33/μL, $P = 0.0125$) and NK cells (110.50 ± 125.75/μL vs. 45 ± 53.50/μL, $P = 0.0249$). The MFI of HLA-DR on monocytes was significantly lower in the SP group than that

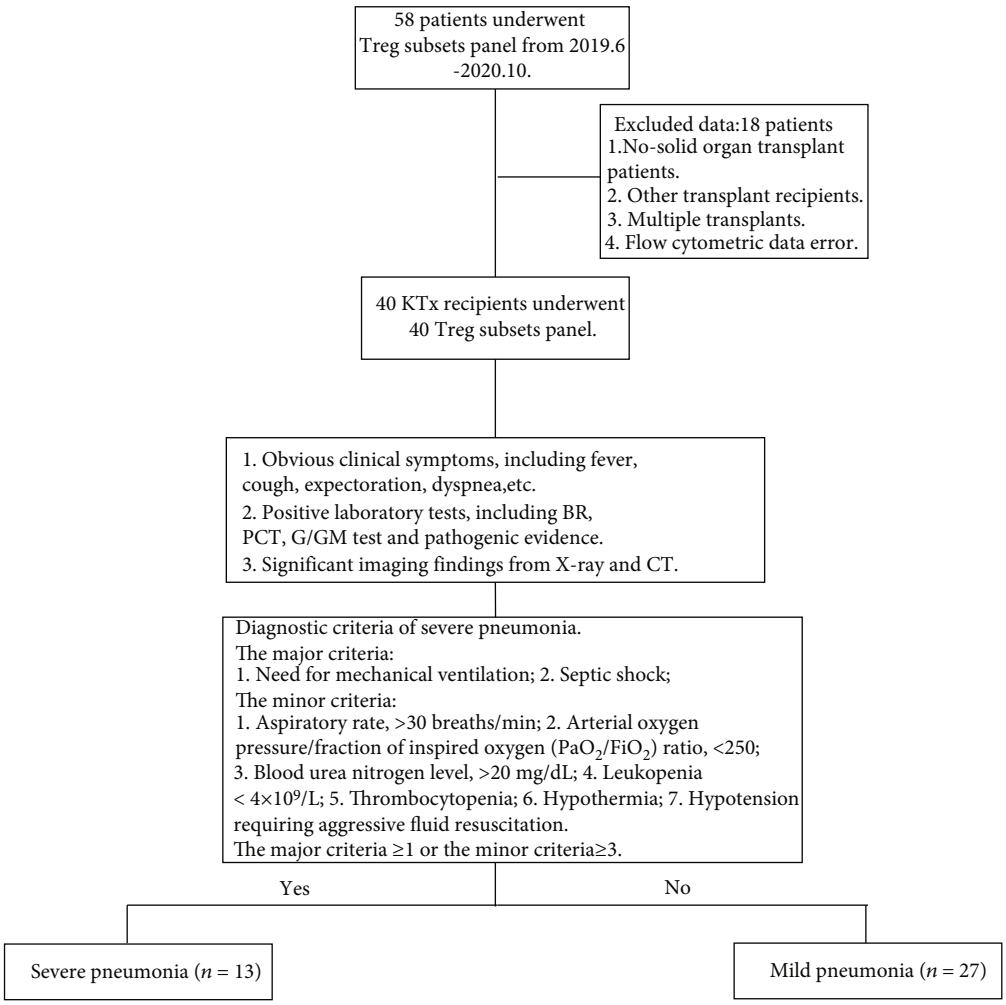

Figure 2: The study flowchart and exclusion criteria. 13 severe pneumonia and 27 mild pneumonia kidney transplant recipients were finally enrolled for analysis.

in the MP group (1671.00 ± 285.80 vs. 783.60 ± 184.60, P = 0.0329) (Table 3) (Figure 3).

3.3. Distribution and Counts of Treg Subsets. The Ab No. of $CD4^+CD25^+$ T cells was lower in SP patients compared to MP patients (40.48 ± 97.95/μL vs. 32.56 ± 34.53/μL, P = 0.0386). In the SP group, the percentage of total Treg ($CD4^+CD25^+FoxP3^+$) was significantly higher than that of the MP group (15.26 ± 0.97% vs. 25.94 ± 2.56%, P < 0.0001). The expression of Helios in Tregs could be used as a marker to distinguish natural Tregs from inducible Tregs in peripheral blood. The frequency and Ab No. of $Helios^+$ Treg in the SP group was significantly lower than that of the MP group (65.09 ± 4.43% vs. 30.25 ± 6.86%, P < 0.0001; 4.74 ± 9.93/μL vs. 1.07 ± 3.16/μL, P = 0.0127, respectively). Conversely, the percentage and counts of $Helios^-$ Treg in the SP group were significantly higher than that in the MP group (33.57 ± 4.47% vs. 69.42 ± 6.58%, P < 0.0001; 2.18 ± 2.64/μL vs. 4.73 ± 4.54/μL, P = 0.0308, respectively). The percentage of $CD39^+$ Tregs in the SP group was significantly higher than that in the MP group (26.74 ± 3.58 vs. 42.95 ± 5.81%, P = 0.0177), while the $CD39^-$ Treg percentage was significantly lower in the SP group than that in the MP group (71.38% ± 3.48 vs. 56.69 ± 5.81%, P = 0.0278). There were similar trends in the frequencies of $CD45RA^+$ (11.63 ± 8.09 vs. 27.27 ± 16.14, P = 0.0028) and $CD45RA^-$ (88.37 ± 8.16 vs. 72.73 ± 15.81, P = 0.0018) Tregs. Detailed information is presented in Table 4 and Figure 3.

3.4. Correlation Analysis of Treg Subsets with Clinical Information and Regular Immune Status. First, we analyzed the correlation between different Treg subpopulations and clinical information (Figure 4(a)). We found that the percentage of total Tregs was positively correlated with the BUN and Cr levels and HS periods (P < 0.001) and the CC (correlation coefficient) were 0.47, 0.52, and 0.62, respectively. The Ab No. of $CD39^+$ Treg was positively correlated with Cr levels (P < 0.01, CC = 0.50). Next, we analyzed the correlation between different Treg subpopulations and regular immune status (Figure 4(b)). We found that the Ab No. of $CD3^+CD8^+$ T cells were positively associated with the absolute counts of $CD4^+CD25^+$ T cells (CC = 0.48, P < 0.05) and $Helios^+$ (CC = 0.49, P < 0.05). The absolute counts of NK cells were also significantly positively correlated with

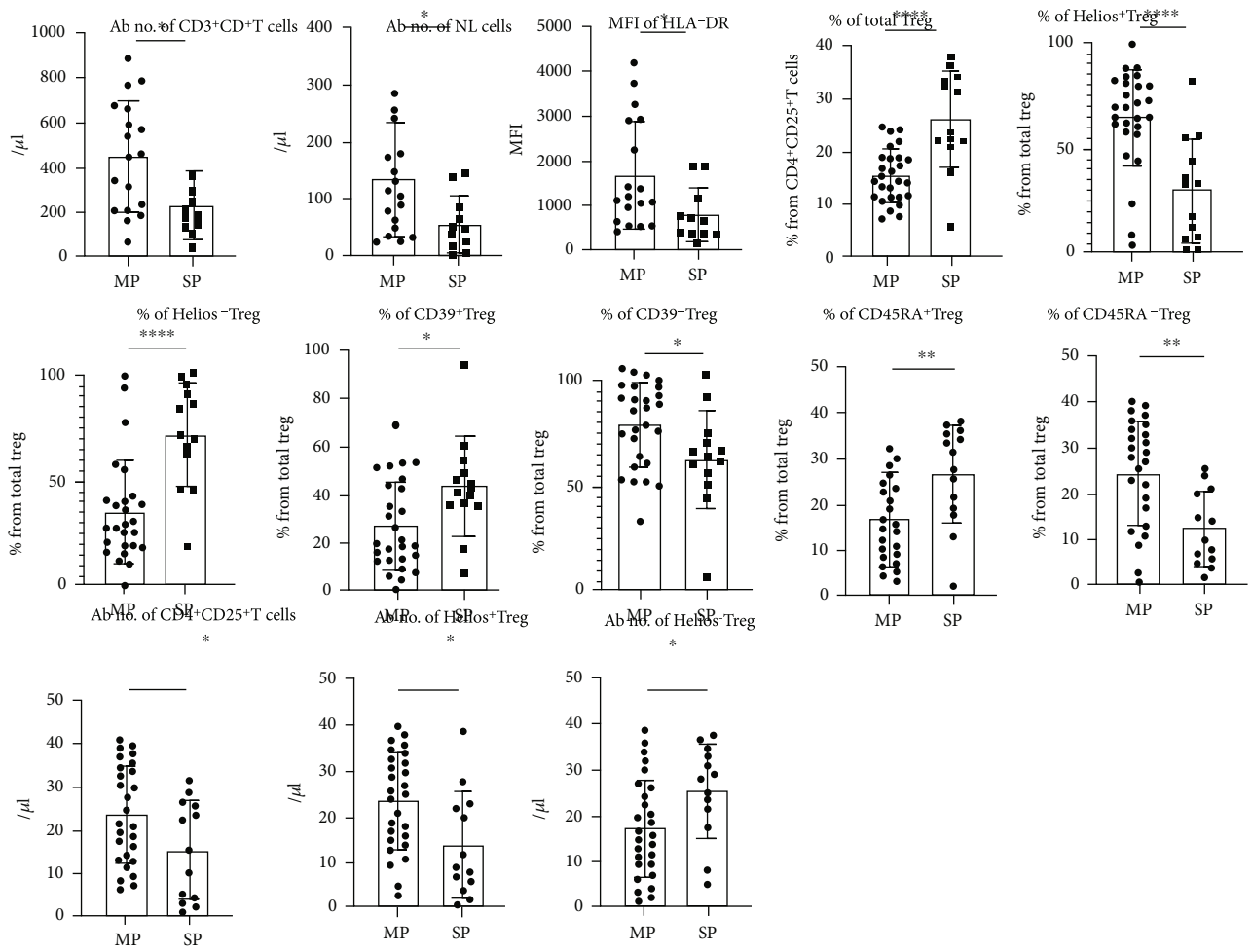

Figure 3: The distribution, Ab No., and MFI of regular immune indexes and Treg subpopulations in MP and SP patients. $****$ means $P < 0.001$, $**$ means $P < 0.05$, and $*$ means $P < 0.1$.

the absolute counts of $CD4^+CD25^+$ T cells (CC = 0.52, $P < 0.01$), $Helios^+$ (CC = 0.64, $P < 0.01$), $CD39^+$ (CC = 0.42, $P < 0.05$), and $CD45RA^-$ Tregs (CC = 0.41, $P < 0.05$). We discovered that the MFI of CD64 on neutrophils was negatively correlated with the absolute counts of $CD4^+CD25^+$ T cells (CC = −0.50, $P < 0.01$), $Helios^+$ (CC = −0.60, $P < 0.01$), $CD39^+$ (CC = −0.51, $P < 0.01$), and $CD45RA^-$ Tregs (CC = − 0.49, $P < 0.05$).

3.5. ROC and Cut-Off Values of Treg Subsets. We selected statistically significant indexes from the results 3.3 to discern patients with SP from MP patients. We analyzed the optimal cut-off values by ROC analysis, and the ROC curves are presented in Figure 5. The area under the curve (AUC) of all indicators was higher than 0.7. The optimal cut-off values were 15.62, 19.87, 56.91, 1.740, 42.06, and 2.835 for $CD4^+CD25^+$ T cells (/μL), total Treg (%), $Helios^+$ Treg (%), $Helios^+$ Treg (/μL), $Helios^-$ Treg (%), and $Helios^-$ Treg (/μL), respectively. The optimal cut-off values for $CD39^+$ Treg (%), $CD39^-$ Treg (%), $CD45RA^+$ Treg (%), and $CD45RA^-$ Treg (%) were 34.68, 67.84, 12.37, and 87.15, respectively. All AUC and cut-off values are displayed in Table 5.

3.6. The Independent Risk Factors. We aimed to foretell the independent risk factors of disease progression based on clinical descriptions and found that the levels of BUN, albumin, Cr, and HS periods were meaningfully related to disease progression by univariate logistic analysis. The multivariate logistic model of clinical information contained BUN and HS. A multivariate logistic analysis was used to show that the BUN (odds ratio (OR) = 1.24, $P = 0.01$) and HS (OR = 1.09, $P = 0.03$) were independent risk factors for disease progression (Table 6). In Table 7, the univariate logistic analysis suggested that the frequencies of total, $Helios^+$, $Helios^-$ Tregs, $CD39^+$, $CD39^-$, $CD45RA^+$, and $CD45RA^-$ Tregs were drastically associated with disease progression. The multivariate logistic model of Tregs contained the following determinants: the percentage of total Tregs and $Helios^-$ Tregs. Finally, a multivariate logistic analysis indicated that only the frequencies of total (OR = 1.24,

Table 4: Treg subset panel of the patients.

Parameters	All ($n = 40$)	Mild ($n = 27$)	Severe ($n = 13$)	P
$CD4^+CD25^+$ T cells, median ± IQR (%)	16.43 ± 11.43	17.54 ± 15.93	15.68 ± 8.84	0.3166#
$CD4^+CD25^+$ T cells, median ± IQR (/μL)	40.09 ± 56.26	40.48 ± 97.95	32.56 ± 34.53	0.0386#
Total Treg, mean ± SD (%)	18.73 ± 1.31	15.26 ± 0.97	25.94 ± 2.56	<0.0001
Total Treg, median ± IQR (/μL)	7.25 ± 11.82	7.21 ± 12.37	7.73 ± 8.27	0.4933#
$Helios^+$ Treg, mean ± SD (%)	53.77 ± 4.51	65.09 ± 4.43	30.25 ± 6.86	<0.0001
$Helios^+$ Treg, median ± IQR (/μL)	3.51 ± 9.38	4.74 ± 9.93	1.07 ± 3.16	0.0127#
$Helios^-$ Treg, mean ± SD (%)	45.22 ± 4.53	33.57 ± 4.47	69.42 ± 6.58	<0.0001
$Helios^-$ Treg, median ± IQR (/μL)	2.78 ± 4.48	2.18 ± 2.64	4.73 ± 4.54	0.0308#
$CD39^+$ Treg, mean ± SD (%)	32.01 ± 3.26	26.74 ± 3.58	42.95 ± 5.81	0.0177
$CD39^+$ T cell, median ± IQR (/μL)	1.68 ± 3.88	1.32 ± 3.20	1.79 ± 3.81	0.4133#
$CD39^-$ Treg, mean ± SD (%)	66.61 ± 3.17	71.38 ± 3.48	56.69 ± 5.81	0.0278
$CD39^-$ Treg, median ± IQR (/μL)	5.40 ± 7.56	6.43 ± 9.44	3.09 ± 5.12	0.1130#
$CD45RA^+$ Treg, median ± IQR (%)	13.98 ± 15.33	11.63 ± 8.09	27.27 ± 16.14	0.0028#
$CD45RA^+$ Treg, median ± IQR (/μL)	1.33 ± 1.42	1.17 ± 1.13	1.50 ± 1.70	0.2094#
$CD45RA^-$ Treg, median ± IQR (%)	85.37 ± 15.35	88.37 ± 8.16	72.73 ± 15.81	0.0018#
$CD45RA^-$ Treg, median ± IQR (/μL)	5.55 ± 10.63	5.55 ± 10.93	5.33 ± 5.42	0.2639#

#Tested by the Mann-Whitney U test; others were tested by the unpaired t-test; SD: standard deviation; IQR: interquartile range.

$P = 0.009$) and $Helios^-$ (OR = 1.06, $P = 0.008$) Tregs were independent risk factors for disease progression.

4. Discussion

This study successfully detailed the distribution and absolute counts of Treg subsets and demonstrated their significance in SP after KTx. We found that the frequencies of total and $Helios^-$ Tregs were independent risk factors for severe pneumonia progression after KTx. Therefore, the monitoring of Treg subpopulations and regular immune function may provide a full picture of the immune status for individualized prevention and therapy for severe pneumonia after KTx.

Pneumonia is a major threat to renal allograft recipients [35]. SP can lead to cellular immune disorders and pro- and anti-inflammatory cytokine imbalances [36]. Among the immune cells, NK cells, monocytes, and neutrophils in innate immune responses, as well as $CD4^+/CD8^+$ T cells and B cells in adaptive immune responses, play important roles in defending against the infectious pathogens. In our study, we found the expression of HLA-DR on monocytes and the Ab No. of $CD4^+$ T cells and NK cells were lower in SP patients than in MP patients. The decrease of immune cells caused the exacerbation of infection which was contributed to the progression of pneumonia. And the development of the pneumonia eventually led to a significant decrease in graft function. It can even lead to the death of the patients.

Tregs are a small subpopulation of T cells that inhibit effector/memory T cell proliferation and activation and have a dual effect on pneumonia by inhibiting the inflammatory response and promoting tissue repair. In inflammatory diseases, Tregs are involved in maintaining the immune homeostasis mainly by producing anti-inflammatory cytokines, such as IL-10, IL-35, and TGF-β [37]. A previous study has demonstrated that long-term use of immunosuppressants increased Tregs in PBMC of patients and mice with organ transplantation [38, 39]. Increased Tregs limited immune activation and prevented the development of graft rejection through secreting anti-inflammatory cytokines and inhibiting the activity of effector T cells [6]. So, patients with high levels of Tregs indicate great graft function and good prognosis. However, in patients with pneumonia, increased Tregs denoted to poor prognosis [40–42]. In our study, we found that the percentage of total Treg was higher in SP patients than in MP patients after KTx. High levels of Tregs prevented T cells from activation, and the maturation and the ability of antigen-presenting cells to activate effector T cells [6], which eventually increased the spread of infection and organ damage. The exacerbation of pneumonia ultimately would lead to decreased graft function in KTx patients [3]. In conclusion, monitoring of Tregs is of great significance for the occurrence and prognosis of infection in patients with KTx. The frequency of total Tregs was an independent risk factor for the development of pneumonia after KTx.

Helios has been reported to stabilize the immunosuppressive function of Tregs, which was also proposed to be a marker for discriminating natural from peripheral inducible Tregs. In our study, we found that the frequency and the Ab No. of $Helios^+$ Tregs were lower in SP patients than in MP patients. As the infection worsens, graft function and immune function of patients were gradually declined. Meanwhile, the frequency and Ab No. of $Helios^+$ Tregs were also decreased. The increased expression of $Helios^+$ Tregs indicated a favorable prognosis in pneumococcal infection and graft function [16, 17]. The decreased expression of $Helios^+$ Tregs indicated poor graft function and prognosis in KTx patients with pneumonia. Additionally, we found

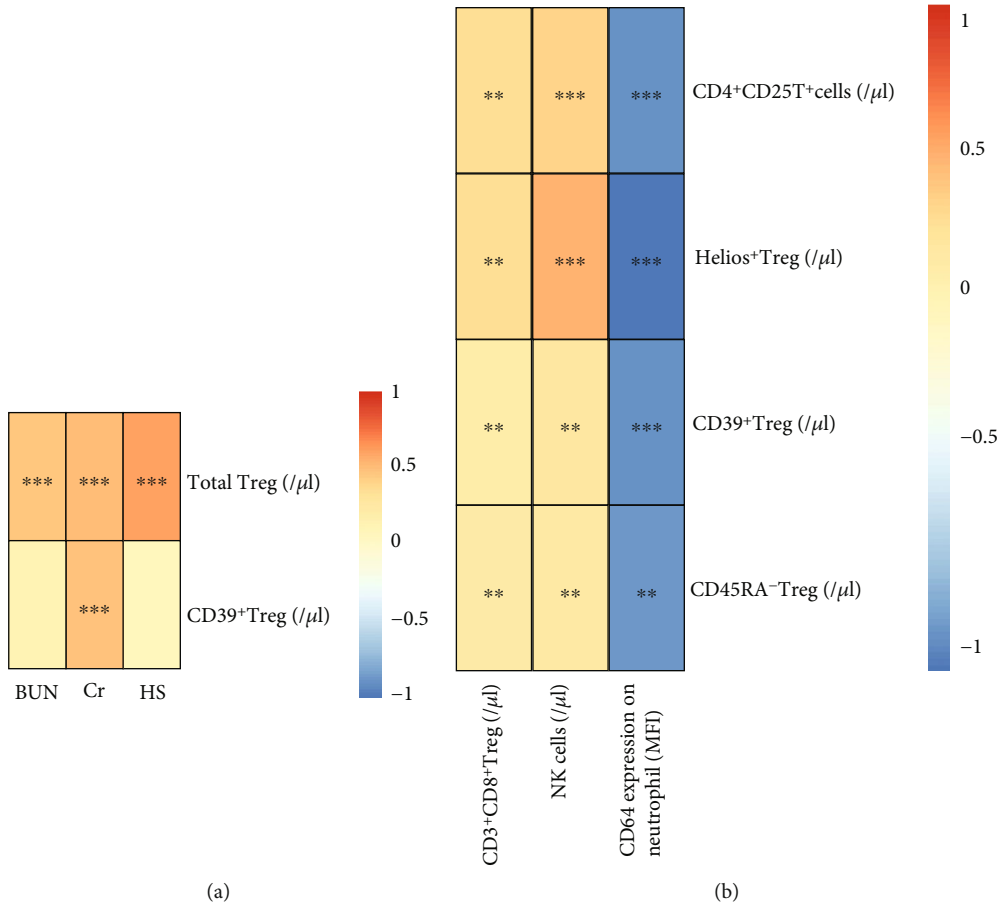

Figure 4: Correlation analysis of Treg subpopulations with clinical information and regular immune status. (a) The heatmap of the correlations between different Treg subpopulations and the clinical information of the patients. (b) The heatmap of the correlations between different Treg subpopulations and the regular immune indexes of the patients. HS: hospital stay period (days); BUN: blood urea nitrogen; Cr: serum creatinine. Red indicates positive correlations while blue indicates negative ones. $***$ means $P < 0.01$, $**$ means $P < 0.05$, and $*$ means $P < 0.1$.

that the increased frequency of Helios$^-$ Tregs was an independent risk factor for the development of pneumonia after KTx. Compared with Helios$^+$ Tregs, Helios$^-$ Tregs have a reduced suppressive capacity and secrete inflammatory factors [43]. In our research, we demonstrated that the frequency and the Ab No. of Helios$^-$ Tregs were higher in SP patients than in MP patients. The increased infiltration of Helios$^-$ Tregs could aggravate the progression of pneumonia and poor graft function in patients with KTx. Our study is the first to demonstrate that the frequency and Ab No. of Helios$^+$ Tregs are reduced in SP patients after KTx, which was tightly associated with disease progression.

CD39$^+$ Tregs demonstrated a stronger suppressive ability than CD39$^-$ Tregs. In our study, increased CD39$^+$ Tregs were observed in patients with SP after KTx, and the expression of CD39$^+$ Tregs was positively correlated to creatinine level. We showed that the high frequency of CD39$^+$ Tregs indicated a poor prognosis in pneumonia patients post KTx. A previous study has been proved that an increased CD39$^+$ Tregs in circulation was closely associated in patients with *mycobacterial* infection [44]. In addition, Huang et al. demonstrated that the level of circulating CD39$^+$ Tregs was significantly increased in sepsis patients, and a growing expression of CD39$^+$ Tregs was relevant to an unfavorable prognosis for sepsis patients [45]. The progression of infection significantly upregulated the frequency of CD39$^+$ Tregs in the whole blood of patients. Our research demonstrated that the frequency of CD39$^+$ Tregs was increased in SP patients after KTx, which was tightly associated with pneumonia progression.

Based on CD45RA expression, Tregs can be divided into two different subpopulations: (i) CD45RA$^-$ Treg (memory Treg (mTreg)) and (ii) CD45RA$^+$ Treg (resting Treg (rTreg)). A previous study demonstrated that mTregs were more suppressive than rTregs and were crucial for the maintenance of immune homeostasis. Meanwhile, increased mTregs are correlated with better transplant outcomes. Previous studies have demonstrated that reduced CD45RA$^-$ Tregs are correlated with both acute and chronic rejection in KTx recipients [30, 46]. Our study demonstrated a low frequency of CD45RA$^-$ Treg in SP after KTx, indicating poor pneumonia outcomes. In addition to the clustering method mentioned above, some researchers thought that CD45RA$^-$ Treg could be further divided into CD45RA$^-$Helios$^{+/-}$ Treg

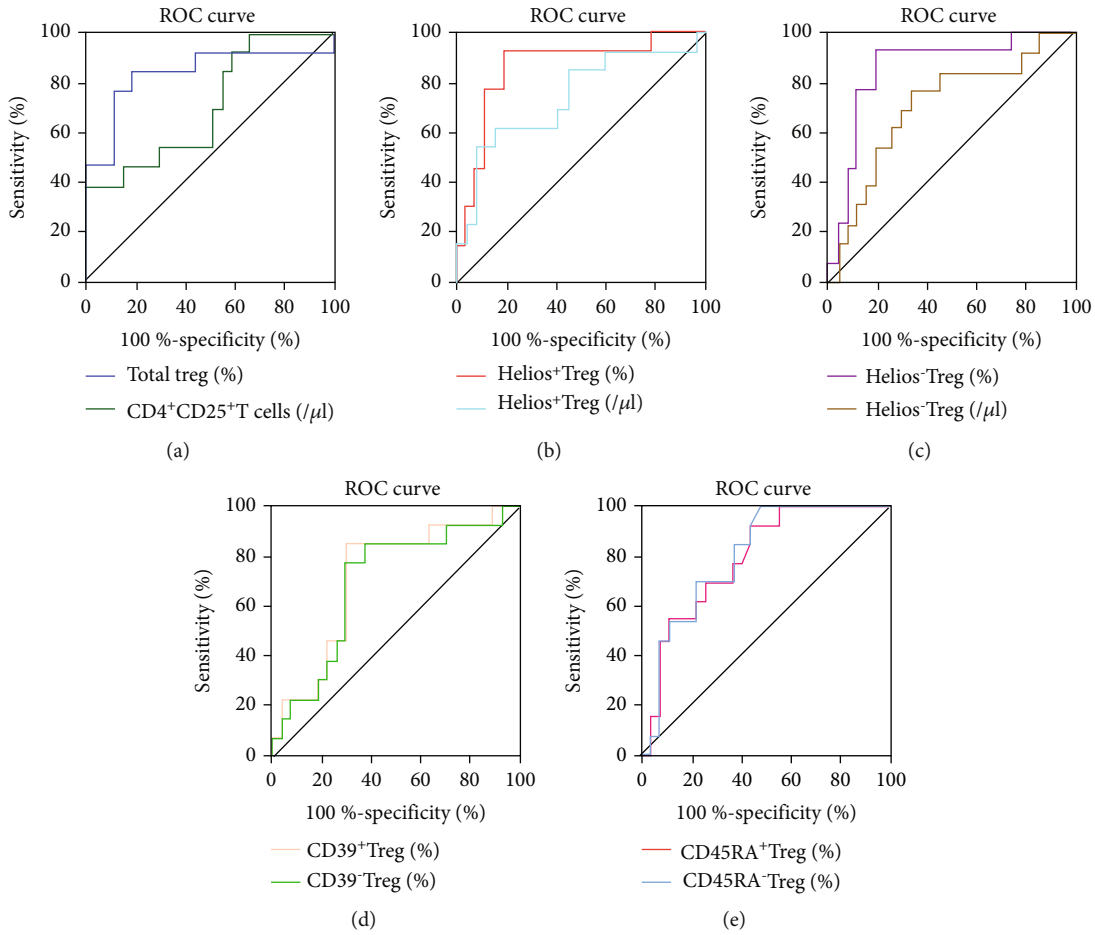

Figure 5: ROC curve of Treg subpopulations in MP and SP patients. (a) ROC curve of $CD4^+CD25^+$ T cells (Ab No.) and total Treg (%). (b) ROC curve of $Helios^+$ Treg (% and Ab No.). (c) ROC curve of $Helios^-$ Treg (% and Ab No.). (d) ROC curve of $CD39^+$ Treg (%) and $CD39^-$ Treg (%). (e) ROC curve of $CD45RA^+$ Treg (%) and $CD45RA^-$ Treg (%).

Table 5: Areas under the curve (AUC) and cut-off values of Treg subsets.

Test result variable(s)	Area	SEM	Asymptotic 95% confidence		Cut-off value	Sensitivity%	Specificity%
			Lower bound	Upper bound			
$CD4^+CD25^+$ T cells (/μL)	0.70	0.09	0.53	0.88	<15.62	38.46	100.00
Total Treg (%)	0.84	0.08	0.68	1.00	>19.87	84.62	81.48
$Helios^+$ Treg (%)	0.86	0.07	0.73	0.99	<56.91	92.31	81.48
$Helios^+$ Treg (/μL)	0.74	0.09	0.57	0.92	<1.740	61.54	85.19
$Helios^-$ Treg (%)	0.86	0.07	0.73	0.99	>42.06	92.31	81.48
$Helios^-$ Treg (/μL)	0.71	0.09	0.54	0.89	>2.835	76.92	66.67
$CD39^+$ Treg (%)	0.72	0.09	0.54	0.89	>34.68	84.62	70.37
$CD39^-$ Treg (%)	0.70	0.09	0.52	0.87	<67.84	84.62	62.96
$CD45RA^+$ Treg (%)	0.79	0.07	0.65	0.93	>12.37	92.31	55.56
$CD45RA^-$ Treg (%)	0.80	0.07	0.66	0.94	<87.15	100.00	51.85

SEM: standard error of mean.

and $CD45RA^-CD39^{+/-}$ Treg. We further discussed the association between different $CD45RA^-$ Treg subpopulations and the severity of pneumonia post renal transplantation. We found that the percentage and counts of $CD45RA^-Helios^+$ and $CD45RA^-CD39^-$ Tregs in the SP group were significantly lower than those in the MP group. However, the percentage and counts of $CD45RA^-Helios^-$ and $CD45RA^-CD39^+$ Tregs in the SP group were significantly

Table 6: Risk factors of clinical information for progression by logistic regression.

Variable	Univariate analysis OR (95% CI)	P	Multivariate analysis OR (95% CI)	P
Procalcitonin (ng/mL)	1.07 (0.98, 1.17)	0.11		
Albumin (g/L)	0.79 (0.67, 0.93)	0.0044**		
BUN (mmol/L)	1.24 (1.07, 1.44)	0.0046**	1.24 (1.05, 1.47)	0.01*
Cr admission (μmol/L)	1.01 (1.00, 1.02)	0.0373*		
Hospital stay period (days)	1.10 (1.03, 1.18)	0.0078**	1.09 (1.10, 1.18)	0.03*

OR: odds ratio; *<0.05, **<0.01, and ***<0.001.

Table 7: Risk factors of Treg subpopulations for progression by logistic regression.

Variable	Univariate analysis OR (95% CI)	P	Multivariate analysis OR (95% CI)	P
$CD4^+CD25^+$ T cells (/μL)	0.98 (0.95, 1.00)	0.08		
Total Treg (%)	1.24 (1.08, 1.43)	0.003**	1.24 (1.06, 1.45)	0.009**
$Helios^+$ Treg (%)	0.95 (0.92, 0.98)	0.0015**		
$Helios^+$ Treg (/μL)	0.90 (0.79, 1.03)	0.13		
$Helios^-$ Treg (%)	1.06 (1.02, 1.09)	0.0012**	1.06 (1.01, 1.10)	0.008**
$Helios^-$ Treg (/μL)	1.01 (0.94, 1.09)	0.77		
$CD39^+$ Treg (%)	1.04 (1.00, 1.09)	0.03*		
$CD39^-$ Treg (%)	0.96 (0.92, 1.00)	0.04*		
$CD45RA^+$ Treg (%)	1.07 (1.00, 1.15)	0.04*		
$CD45RA^-$ Treg (%)	0.93 (0.85, 0.99)	0.03*		

OR: odds ratio; *<0.05, **<0.01, and ***<0.001.

higher than those in the MP group. Detailed information was presented in supplementary Table 1 and Figure 1. We also analyzed the correlation between different $CD45RA^-$ Treg subpopulations and clinical information (Supplementary Figure 2A). We found that the percentage and counts of $CD45RA^-Helios^+$ and $CD45RA^-CD39^+$ Treg were significantly negatively correlated with the level of peripheral BUN and Cr. However, the percentage and counts of $CD45RA^-Helios^+$ and $CD45RA^-CD39^+$ Tregs were significantly positively correlated with the level of peripheral BUN and Cr. Next, we analyzed the correlation between different Treg subpopulations and regular immune status (Supplementary Figure 2B). We discovered that the MFI of CD64 on neutrophils was negatively correlated with the percentage and counts of $CD45RA^-Helios^+$ Treg but positively correlated with the percentage and counts of $CD45RA^-Helios^-$ Treg. Meanwhile, the counts of NK cells were negatively correlated with the percentage and counts of $CD45RA^-Helios^-$ Treg, yet positively correlated with the percentage and counts of $CD45RA^-Helios^+$ Treg. We analyzed the optimal cut-off values by ROC analysis, and the ROC curves were presented in Supplementary Figure 3. All the indices displayed a high AUC. All AUC and cut-off values were displayed in Supplementary Table 2. In Supplementary Table 3, the univariate logistic analysis suggested that the percentage and counts of $CD45RA^-Helios^+$, $CD45RA^-Helios^-$, $CD45RA^-CD39^+$, and $CD45RA^-CD39^-$ Tregs were drastically associated with disease progression. Therefore, indices of $CD45RA^-CD39^{+/-}$ and $CD45RA^-Helios^{+/-}$ Tregs showed good potential for the disease progression of pneumonia patients post KTx.

In the current study, we innovatively studied the distribution of different Treg subpopulations in whole blood of SP and MP patients post renal transplantation. A previous study showed that increased $Helios^+$ Treg, $CD39^+$ Treg, and $CD45RA^-$ Tregs were indicated a low rate of transplant rejection in different graft trials [16, 22, 29, 30]. In our research, increased $Helios^+$ Treg, decreased $CD39^+$ Tregs, and increased $CD45RA^-$ Tregs were observed in the MP group. Different from a previous study, our patients were in a state of pneumonia. In the next research, we will further study the relationship between different Treg subpopulations and rejection under a pneumonia state. Through ROC analysis, we found that the AUCs of all indicators were higher than 0.7. The AUC of the percentage of $Helios^{+/-}$ Treg was even higher than 0.85. We thought that $Helios^{+/-}$ Treg, $CD39^{+/-}$ Treg, and $CD45RA^{+/-}$ Treg could become the monitoring indicators for pneumonia patients after transplantation.

Finally, Tregs are known to engage in crosstalk with different immune cells, such as NK cells, monocytes, neutrophils, B cells, and other T cells. For example, NK cell counts are positively correlated with $Helios^+$ Tregs in transplant patients [47]. Furthermore, growing evidence

indicates that NK cells can modulate Treg responses in infections and inflammatory diseases [48]. Tregs can also suppress conventional T cells and B cells through cytokine secretion and cell-cell contact [49]. In our study, a close correlation was observed between different Treg subpopulations and regular immune cells. The MFI of HLA-DR on monocytes, and CD64 on neutrophils, is a common index to measure the infection of patients. As previous studies demonstrated that the expression of HLA-DR reflected the antigen presentation capacity of monocytes, low expression of HLA-DR indicates a poor prognosis in some infectious diseases like sepsis and virus B hepatitis [50, 51]. In our research, we found that the MFI of HLA-DR on monocytes was higher in the MP group. Our results were consistent with previous studies. Low expression of HLA-DR in monocytes symbolizes the poor prognosis of pneumonia after transplantation. In resting neutrophils, the levels of CD64 are very low. However, it is significantly increased in response to the infection in a very short time [52]. In our study, we found that high expression of CD64 had significantly negative correlation with part of Tregs which play an anti-inflammatory role in pneumonia. High CD64 expression means poor prognosis in infected patients, and this view has also been confirmed in our study.

To obtain a full picture of the immune status for guiding clinical treatment, multiple immune cell subsets need to be detailed. In our previous study, profiles of B cell and T cell subsets were detailed in immune-stable renal allograft recipients [34, 53]. Moreover, we applied machine learning models to determine the connection between immune monitoring and pneumonia in KTx patients, which can contribute to better-individualized therapy [4]. In this previous study, nonetheless, only a regular immune status panel (including TBNK panel, as well as HLA-DR, CD64) was used, and we paid more attention to the comparison between pneumonia and noninfected allograft renal recipients. In our current study, we mainly investigated the association between Treg subsets and the severity of pneumonia patients post kidney transplantation. Compared to the regular immune status panel, Treg subpopulations were also very important for the diagnosis and prognosis of pneumonia patients post kidney transplantation.

Additionally, our Treg panel was the commercial dry powder kit from Beckman Coulter, and each fluorochrome-conjugated antibody or channel was designed and fixed. And the protocol and flow strategy were all solid and fixed by Beckman Coulter. Every center using this commercial panel will do the same steps, not only the experimental protocol but the analyzing flow. For example, Holl et al. used this Treg panel to examine the tumor cellular immunome in cancer patients [54]. Therefore, this panel was designed to uniform the steps among different centers. Of course, in transplantation centers, this panel needs to be broadly applied. We will work to promote the One Study program in transplantation centers. Additionally, it is correct to figure out the association between Treg subsets and infection post KTx was very important and useful for subsequent tolerance induction.

There were some limitations to this study. The morbidity of pneumonia after transplantation is not high because of the gradual improvement of our diagnostic and therapeutic level, so our center collected only 40 valid samples in two years. Our study merely had a comparatively minor number of samples from a single center, which may have contributed to the bias of the data analysis. Meanwhile, our study failed to demonstrate the predicted efficacy for prognosis. Therefore, future large-scale, multicenter, controlled clinical studies are required to fully identify the mechanisms of Treg subpopulations in transplant infection and immunity. Secondly, due to the limitation of detection conditions, we failed to obtain the types of patient's pathogenic bacteria. Whether the distribution of different subpopulations of Tregs is affected by the types of pathogenic bacteria still needs further investigation. Thirdly, patients usually come to see a doctor after showing symptoms of pneumonia. Therefore, we did not get data on the patients' transplanted renal function prior to the onset of infection. We will timely supplement the research on this part in the future.

5. Conclusion

This study successfully detailed the distribution of Treg subsets and demonstrated that Treg subpopulations were closely associated with severe pneumonia progression after KTx. The frequencies of total and Helios$^-$ Tregs were independent risk factors for SP progression after KTx. Based on the monitoring of Treg subpopulations, better-individualized prevention and therapy might be achieved for patients with SP after KTx.

Data Availability

The raw data supporting the conclusions of this article will be made available by the authors upon request, without undue reservation.

Ethical Approval

The studies involving human participants were reviewed and approved by the Institutional Review Board (Ethics Committee) of the 3rd Xiangya Hospital, Central South University (No. 2018-S347). The study was in accordance with the principle of the Helsinki Declaration II.

Consent

The patients/participants provided written informed consent to participate in the study.

Conflicts of Interest

The authors declare that there is no conflict of interest regarding the publication of this paper.

Authors' Contributions

The study was conceived and designed by Q.Z. and YZ.M. Statistical analyses were performed by Q.Z. and HZ.C. Data

collection was performed by YL.L. Flow cytometry was performed by M.Y. and B.P. Tables and figures were made by Y.Z. The manuscript was written by Q.Z., M.Y., and HZ.C. All authors approved this study.

Acknowledgments

This study was supported by grants from the National Natural Science Foundation of China (81700658) and the Hunan Provincial Natural Science Foundation-Outstanding Youth Foundation (2020JJ3058).

Supplementary Materials

Supplementary Table 1: CD45RA$^-$ Treg subset panel of the patients. Supplementary Table 2: areas under the curve (AUC) and cut-off values of C45RA$^-$ Treg subsets. Supplementary Table 3: risk factors of Treg subpopulations for progression by logistic regression. Supplementary Figure 1: the distribution and Ab No. of CD45RA$^-$ Treg subpopulations in MP and SP patients. Supplementary Figure 2: correlation analysis of CD45RA$^-$ Treg subpopulations with clinical information and regular immune status. (A) The heatmap of the correlations between different CD45RA$^-$ Treg subpopulations and the clinical information of the patients. (B) The heatmap of the correlations between different CD45RA$^-$ Treg subpopulations and the regular immune indexes of the patients. BUN: blood urea nitrogen; Cr: serum creatinine. Red indicates positive correlations while blue indicates negative ones. $***$ means $P < 0.01$, $**$ means $P < 0.05$, and $*$ means $P < 0.1$. Supplementary Figure 3: ROC curve of CD45RA$^-$ Treg subpopulations in MP and SP patients. (A) ROC curve of CD45RA$^-$Helios$^+$ Treg (% and Ab No.). (B) ROC curve of CD45RA$^-$Helios$^-$ Treg (% and Ab No.). (C) ROC curve of CD45RA$^-$CD39$^+$ Treg (% and Ab No.). (D) ROC curve of CD45RA$^-$CD39$^-$ Treg (% and Ab No). *(Supplementary Materials)*

References

[1] R. A. Wolfe, E. C. Roys, and R. M. Merion, "Trends in organ donation and transplantation in the United States, 1999–2008," *American Journal of Transplantation*, vol. 10, no. 4p2, pp. 961–972, 2010.

[2] D. E. Dulek, N. J. Mueller, and on behalf of the AST Infectious Diseases Community of Practice, "Pneumonia in solid organ transplantation: guidelines from the American Society of Transplantation Infectious Diseases Community of Practice," *Clinical Transplantation*, vol. 33, no. 9, 2019.

[3] D. Wilmes, E. Coche, H. Rodriguez-Villalobos, and N. Kanaan, "Bacterial pneumonia in kidney transplant recipients," *Respiratory Medicine*, vol. 137, pp. 89–94, 2018.

[4] B. Peng, H. Gong, H. Tian et al., "The study of the association between immune monitoring and pneumonia in kidney transplant recipients through machine learning models," *Journal of Translational Medicine*, vol. 18, no. 1, 2020.

[5] J. H. Esensten, Y. D. Muller, J. A. Bluestone, and Q. Tang, "Regulatory T-cell therapy for autoimmune and autoinflammatory diseases: the next frontier," *Journal of Allergy and Clinical Immunology*, vol. 142, no. 6, pp. 1710–1718, 2018.

[6] P. L. Martin-Moreno, S. Tripathi, and A. Chandraker, "Regulatory T cells and kidney transplantation," *Clinical Journal of the American Society of Nephrology*, vol. 13, no. 11, pp. 1760–1764, 2018.

[7] L. E. Lucca and M. Dominguez-Villar, "Modulation of regulatory T cell function and stability by co-inhibitory receptors," *Nature Reviews. Immunology*, vol. 20, no. 11, pp. 680–693, 2020.

[8] S. Beissert, A. Schwarz, and T. Schwarz, "Regulatory T cells," *The Journal of Investigative Dermatology*, vol. 126, no. 1, pp. 15–24, 2006.

[9] M. Hu, Y. M. Wang, Y. Wang et al., "Regulatory T cells in kidney disease and transplantation," *Kidney International*, vol. 90, no. 3, pp. 502–514, 2016.

[10] C. Braudeau, M. Racape, M. Giral et al., "Variation in numbers of CD4+CD25highFOXP3+ T cells with normal immuno- regulatory properties in long-term graft outcome," *Transplant International*, vol. 20, no. 10, pp. 845–855, 2007.

[11] S. Brakemeier, A. Pfau, B. Zukunft, K. Budde, and P. Nickel, "Prophylaxis and treatment of *Pneumocystis jirovecii* pneumonia after solid organ transplantation," *Pharmacological Research*, vol. 134, pp. 61–67, 2018.

[12] L. McKinley, A. J. Logar, F. McAllister, M. Zheng, C. Steele, and J. K. Kolls, "Regulatory T cells dampen pulmonary inflammation and lung injury in an animal model of Pneumocystis pneumonia," *Journal of Immunology*, vol. 177, no. 9, pp. 6215–6226, 2006.

[13] J. Grzanka, D. Leveson-Gower, K. Golab et al., "FoxP3, Helios, and SATB1: roles and relationships in regulatory T cells," *International Immunopharmacology*, vol. 16, no. 3, pp. 343–347, 2013.

[14] H. Takatori, H. Kawashima, A. Matsuki et al., "Helios enhances Treg cell function in cooperation with FoxP3," *Arthritis & Rhematology*, vol. 67, no. 6, pp. 1491–1502, 2015.

[15] D. Getnet, J. F. Grosso, M. V. Goldberg et al., "A role for the transcription factor Helios in human CD4$^+$CD25$^+$ regulatory T cells," *Molecular Immunology*, vol. 47, no. 7-8, pp. 1595–1600, 2010.

[16] Y. B. Chen, Y. A. Efebera, L. Johnston et al., "Increased Foxp3$^+$ Helios$^+$ regulatory T cells and decreased acute graft-versus-host disease after allogeneic bone marrow transplantation in patients receiving sirolimus and RGI-2001, an activator of invariant natural killer T cells," *Biology of Blood and Marrow Transplantation*, vol. 23, 2017.

[17] D. R. Neill, V. E. Fernandes, L. Wisby et al., "T regulatory cells control susceptibility to invasive pneumococcal pneumonia in mice," *PLoS Pathogens*, vol. 8, no. 4, 2012.

[18] S. C. Robson, J. Sevigny, and H. Zimmermann, "The E-NTPDase family of ectonucleotidases: structure function relationships and pathophysiological significance," *Purinergic Signal*, vol. 2, 2006.

[19] F. Salcido-Ochoa, J. Tsang, P. Tam, K. Falk, and O. Rotzschke, "Regulatory T cells in transplantation: does extracellular adenosine triphosphate metabolism through CD39 play a crucial role?," *Transplantation Reviews*, vol. 24, no. 2, pp. 52–66, 2010.

[20] G. Borsellino, M. Kleinewietfeld, D. Di Mitri et al., "Expression of ectonucleotidase CD39 by Foxp3+ Treg cells: hydrolysis of extracellular ATP and immune suppression," *Blood*, vol. 110, no. 4, pp. 1225–1232, 2007.

[21] N. Cortez-Espinosa, J. D. Cortés-Garcia, E. Martínez-Leija et al., "CD39 expression on Treg and Th17 cells is associated

with metabolic factors in patients with type 2 diabetes," *Human Immunology*, vol. 76, no. 9, pp. 622–630, 2015.

[22] S. Deaglio, K. M. Dwyer, W. Gao et al., "Adenosine generation catalyzed by CD39 and CD73 expressed on regulatory T cells mediates immune suppression," *The Journal of Experimental Medicine*, vol. 204, no. 6, pp. 1257–1265, 2007.

[23] J. Gu, X. Ni, X. Pan et al., "Human CD39^{hi} regulatory T cells present stronger stability and function under inflammatory conditions," *Cellular & Molecular Immunology*, vol. 14, no. 6, pp. 521–528, 2017.

[24] M. F. Chevalier and L. Weiss, "The split personality of regulatory T cells in HIV infection," *Blood*, vol. 121, no. 1, pp. 29–37, 2013.

[25] Y. Tang, L. Jiang, Y. Zheng, B. Ni, and Y. Wu, "Expression of CD39 on FoxP3+ T regulatory cells correlates with progression of HBV infection," *BMC Immunology*, vol. 13, no. 1, 2012.

[26] P. Hoffmann, R. Eder, T. J. Boeld et al., "Only the CD45RA+ subpopulation of CD4+CD25high T cells gives rise to homogeneous regulatory T-cell lines upon in vitro expansion," *Blood*, vol. 108, no. 13, pp. 4260–4267, 2006.

[27] H. Nafady-Hego, Y. Li, H. Ohe et al., "The generation of donor-specific CD4+CD25++CD45RA+ naive regulatory T cells in operationally tolerant patients after pediatric living-donor liver transplantation," *Transplantation*, vol. 90, no. 12, pp. 1547–1555, 2010.

[28] M. Mirzakhani, M. Shahbazi, F. Oliaei, and M. Mohammadnia-Afrouzi, "Immunological biomarkers of tolerance in human kidney transplantation: an updated literature review," *Journal of Cellular Physiology*, vol. 234, no. 5, pp. 5762–5774, 2019.

[29] K. Wang, Z. L. Song, B. Wu, C. L. Zhou, W. Liu, and W. Gao, "Different phenotypes of CD4^{+}CD25^{+}Foxp3^{+} regulatory T cells in recipients post liver transplantation," *International Immunopharmacology*, vol. 69, pp. 194–201, 2019.

[30] F. Braza, E. Dugast, I. Panov et al., "Central role of CD45RA −Foxp3^{hi} memory regulatory T cells in clinical kidney transplantation tolerance," *Journal of the American Society of Nephrology*, vol. 26, no. 8, pp. 1795–1805, 2015.

[31] F. Simonetta, C. Lecuroux, I. Girault et al., "Early and long-lasting alteration of effector CD45RA^{-}Foxp3^{high} regulatory T-cell homeostasis during HIV infection," *The Journal of Infectious Diseases*, vol. 205, no. 10, pp. 1510–1519, 2012.

[32] Z. Li, Y. Ping, Z. Yu et al., "Dynamic changes in CD45RA^{-}Foxp3^{high} regulatory T-cells in chronic hepatitis C patients during antiviral therapy," *International Journal of Infectious Diseases: IJID: Official Publication of the International Society for Infectious Diseases*, vol. 45, pp. 5–12, 2016.

[33] L. A. Mandell, R. G. Wunderink, A. Anzueto et al., "Infectious Diseases Society of America/American Thoracic Society consensus guidelines on the management of community-acquired pneumonia in adults," *Clinical Infectious Diseases*, vol. 44, Supplement_2, pp. S27–S72, 2007.

[34] Q. Zhuang, B. Peng, W. Wei et al., "The detailed distribution of T cell subpopulations in immune-stable renal allograft recipients: a single center study," *PeerJ*, vol. 7, article e6417, 2019.

[35] K. R. Jackson, J. D. Motter, S. Bae et al., "Characterizing the landscape and impact of infections following kidney transplantation," *American Journal of Transplantation*, vol. 21, no. 1, pp. 198–207, 2021.

[36] M. Dukhinova, E. Kokinos, P. Kuchur, A. Komissarov, and A. Shtro, "Macrophage-derived cytokines in pneumonia: linking cellular immunology and genetics," *Cytokine & Growth Factor Reviews*, vol. 59, pp. 46–61, 2021.

[37] A. Sadeghi, S. Tahmasebi, A. Mahmood et al., "Th17 and Treg cells function in SARS-CoV2 patients compared with healthy controls," *Journal of Cellular Physiology*, vol. 236, no. 4, pp. 2829–2839, 2021.

[38] S. K. Lee, M. J. Park, J. Y. Jhun et al., "Combination treatment with metformin and tacrolimus improves systemic immune cellular homeostasis by modulating Treg and Th17 imbalance," *Frontiers in Immunology*, vol. 11, 2021.

[39] Q. Zeng, X. Y. Yuan, W. Li et al., "Effects of tacrolimus (FK506) and mycophenolate mofetil (MMF) on regulatory T cells and co-inhibitory receptors in the peripheral blood of human liver allograft patients," *Immunopharmacology and Immunotoxicology*, vol. 41, no. 3, pp. 380–385, 2019.

[40] Y. Liu, J. K. Sun, X. Qi et al., "Expression and significance of Th17 and Treg cells in pulmonary infections with gram-negative bacteria," *Immunological Investigations*, vol. 46, no. 7, pp. 730–741, 2017.

[41] S. O. Carrigan, Y. J. Yang, T. Issekutz et al., "Depletion of natural CD4^{+}CD25^{+} T regulatory cells with anti-CD25 antibody does not change the course of _Pseudomonas aeruginosa_ -induced acute lung infection in mice," *Immunobiology*, vol. 214, no. 3, pp. 211–222, 2009.

[42] J. L. Li, T. S. Chen, C. C. Yuan et al., "Regulatory T cell activity in immunosuppresive mice model of pseudomonas aeruginosa pneumonia," *Journal of Huazhong University of Science and Technology [Medical Sciences]*, vol. 37, no. 4, pp. 505–509, 2017.

[43] K. B. Dhuban, E. d'Hennezel, E. Nashi et al., "Coexpression of TIGIT and FCRL3 identifies Helios+ human memory regulatory T cells," *Journal of Immunology*, vol. 194, no. 8, pp. 3687–3696, 2015.

[44] M. C. Boer, K. E. van Meijgaarden, J. Bastid, T. H. Ottenhoff, and S. A. Joosten, "CD39 is involved in mediating suppression byMycobacterium bovisBCG-activated human CD8+CD39+ regulatory T cells," *European Journal of Immunology*, vol. 43, no. 7, pp. 1925–1932, 2013.

[45] H. Huang, R. Xu, F. Lin et al., "High circulating CD39^{+} regulatory T cells predict poor survival for sepsis patients," *International Journal of Infectious Diseases: IJID: Official Publication of the International Society for Infectious Diseases*, vol. 30, pp. 57–63, 2015.

[46] M. Mirzakhani, M. Shahbazi, R. Akbari et al., "Reduced CD4^{+} CD25^{++} CD45RA^{-} Foxp3^{hi} activated regulatory T cells and its association with acute rejection in patients with kidney transplantation," *Transplant Immunology*, vol. 60, article 101290, 2020.

[47] K. Trojan, L. Zhu, M. Aly et al., "Association of peripheral NK cell counts with Helios+IFN-γ– Tregs in patients with good long-term renal allograft function," *Clinical and Experimental Immunology*, vol. 188, no. 3, pp. 467–479, 2017.

[48] J. Li, X. Dong, L. Zhao et al., "Natural killer cells regulate Th1/Treg and Th17/Treg balance in chlamydial lung infection," *Journal of Cellular and Molecular Medicine*, vol. 20, no. 7, pp. 1339–1351, 2016.

[49] D. Calzada, S. Baos, L. Cremades-Jimeno, and B. Cardaba, "Immunological mechanisms in allergic diseases and allergen tolerance: the role of Treg cells," *Journal of Immunology Research*, vol. 2018, Article ID 6012053, 10 pages, 2018.

[50] Z. H. Yan, Y. Fan, X. H. Wang, Q. Mao, G. H. Deng, and Y. M. Wang, "Relationship betweenHLA-DRgene polymorphisms and outcomes of hepatitis B viral infections: a meta-analysis," *World Journal of Gastroenterology*, vol. 18, no. 24, 2012.

[51] I. Benlyamani, F. Venet, R. Coudereau, M. Gossez, and G. Monneret, "Monocyte HLA-DR measurement by flow cytometry in COVID-19 patients: an interim review," *Cytometry Part A*, vol. 97, no. 12, pp. 1217–1221, 2020.

[52] S. K. Hung, H. M. Lan, S. T. Han, C. C. Wu, and K. F. Chen, "Current evidence and limitation of biomarkers for detecting sepsis and systemic infection," *Biomedicines*, vol. 8, no. 11, 2020.

[53] Q. Zhuang, H. Li, M. Yu et al., "Profiles of B-cell subsets in immunologically stable renal allograft recipients and end-stage renal disease patients," *Transplant Immunology*, vol. 58, article 101249, 2020.

[54] E. K. Holl, V. N. Frazier, K. Landa, G. M. Beasley, E. S. Hwang, and S. K. Nair, "Examining peripheral and tumor cellular immunome in patients with cancer," *Frontiers in Immunology*, vol. 10, 2019.